LOAD DOCUMENT

DTIC ACCESSION NUMBER

LEVEL

INVENTORY

DOCUMENT IDENTIFICATION

DISTRIBUTION STATEMENT

H
A
N
D
L
E

W
I
T
H

C
A
R
E

ACCESSION FOR

NTIS	GRAAI	☐
DTIC	TRAC	☐
UNANNOUNCED		☐
JUSTIFICATION		

BY

DISTRIBUTION/

AVAILABILITY CODES

| DISTRIBUTION | AVAILABILITY AND/OR SPECIAL |
| | |

DISTRIBUTION STAMP

DATE ACCESSIONED

DATE RETURNED

20020129 173

DATE RECEIVED IN DTIC

REGISTERED OR CERTIFIED NUMBER

PHOTOGRAPH THIS SHEET AND RETURN TO DTIC-FDAC

DTIC FORM 70A
JUN 90

DOCUMENT PROCESSING SHEET

LOAN DOCUMENT

PREVIOUS EDITIONS MAY BE USED UNTIL
STOCK IS EXHAUSTED.

REPORT DOCUMENTATION PAGE

Form Approved OMB No. 0704-0188

1. AGENCY USE ONLY (Leave blank)	2. REPORT DATE 1956	3. REPORT TYPE AND DATES COVERED

4. TITLE AND SUBTITLE

Thermoelectric Properties of the Noble Metals and Their Alloys

5. FUNDING NUMBERS

5. AUTHOR(S)

Rudnitskii, Aleksandr Alekseevich

7. PERFORMING ORGANIZATION NAME(S) AND ADDRESS(ES)

Academy of Sciences, U.S.S.R
Moscow, USSR

8. PERFORMING ORGANIZATION REPORT NUMBER

9. SPONSORING/MONITORING AGENCY NAME(S) AND ADDRESS(ES)

United States Atomic Energy Commission
AEC Technical Services Extension
Oak Ridge, TN

10. SPONSORING/MONITORING AGENCY REPORT NUMBER

AEC-tr-3724

11. SUPPLEMENTARY NOTES

Translated from Russian by the U.S. Joint Publications Service, New York.

12a. DISTRIBUTION/AVAILABILITY STATEMENT

Public release; distribution unlimited.

12b. DISTRIBUTION CODE

A

12. ABSTRACT (Maximum 200 words)

13. SUBJECT TERMS

Russian Language, Translations

15. NUMBER OF PAGES

16. PRICE CODE

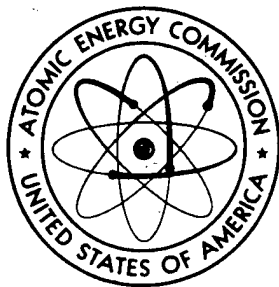| 17. SECURITY CLASSIFICATION OF REPORT Unclassified	18. SECURITY CLASSIFICATION OF THIS PAGE Unclassified	19. SECURITY CLASSIFICATION OF ABSTRACT Unclassified	

AEC-tr-3724

THERMOELECTRIC PROPERTIES OF THE NOBLE METALS AND THEIR ALLOYS

(Termoelektricheskie Svoistva Blagorodnykh
Metallov i ikh Splavov)

By
Aleksandr Alekseevich Rudnitskii

TABLE OF CONTENTS

FOREWORD

The physico-chemical analysis procedure, created by N. S. Kurnakov, has played a decisive role in the development of metallography.

Physical research methods are used more and more in the investigation of alloys. Only through the use of these metals has it been possible to explain the problems in the formation of chemical compounds and solid solutions, since methods of preparative chemistry were found to be utterly unusable in the case of alloys. However, the development of physico-chemical analysis, which has played a tremendous role in the theory of alloys at the beginning of the 20th century, was limited to an accumulation and generalization of experimental data and stood on the sidelines of modern theoretical physics of metals, which has in turn determined another path of development in this field.

Success in the theory of metals and alloys depends on how fast these two trends, merging into a single unit, will give a new spurt for further progress.

Naturally, theoretical science cannot develop apart from experiments, since experiment is the basis of recognition, the criterion of the true nature, and strict judge of the work of theoreticians.

In this work we consider thermoelectric phenomena in conjunction with the chemical nature of components and in some cases with the electrical and thermal properties of metals.

The thermoelectric method in its present form is a new method of physico-chemical analysis and makes it possible to determine the composition vs. temperature diagrams of phase transitions simultaneously with the plotting of the composition vs. property diagram.

The application of the thermoelectric method to the investigation of metals and alloys makes it possible to consider in principle the new problem of determining the difference in electric potentials between phases in equilibrium.

THERMOELECTRIC PROPERTIES OF NOBLE METALS AND THEIR
ALLOYS*

By A. A. Rudnitskiy

Academy of Sciences, USSR
Institute of Metallurgy imeni A. A. Baykov
Institute of General and Inorganic Chemistry
imeni N. S. Kurnakov

INTRODUCTION

The investigation of the thermoelectric properties of metals
and alloys is of great interest, since the phenomena of thermoelec-
tricity are extensively used in practice. Hardly any laboratory can
get along without the use of thermocouples. Factories having thermal
plants make extensive use of thermocouples to measure temperatures.
Thermoelectric phenomena are the basis of construction of many highly
sensitive instruments for the measurement of radiation in astronomy,
and in commercial practice of weak currents, high vacuum, and thermo-
electric-current sources.

A very large number of papers is devoted to problems of ther-
moelectricity. Many of these by now have only historic significance.
The measurement of thermoelectric properties of metals requires very
sensitive instruments, which were invented only by the end of the
past century.

The improvement in process of metallurgy has influenced the
investigation of thermoelectric properties of pure metals. Thus, a
modern laboratory can now have a large quantity of spectrally pure
metals. Their thermoelectric properties differ substantially from
the properties of metals containing even small amounts of impurities.
Thus, only recently have ideas been gained on the properties of pure
metals.

The investigation of alloys is also the subject of a large number of papers, particularly the study of solid solutions with an eye towards using them in thermocouples.

However, thanks to the high sensitivity of modern measuring instruments, the magnitude of the thermal emf plays a secondary role. The first place is occupied by the stability of the readings of the pyro-meter and the homogeneity of the thermocouple wire.

In this respect the Pt-(Pt + Rh) thermocouple is an unsur-passed instrument for the measurement of temperature.

An investigation of noble metals and their alloys plays a principal role in measurement technology, for only on the basis of these metals has it become possible to produce stable thermoelectric parameters for the measurement of high temperatures. While the thermoelectric properties of pure metals and of certain solid solutions are quite well investigated by now, relatively little attention was paid to the brittle metals and alloys which can be converted into long wires. This is probably due to the apparent difficulty in the experiments. There is therefore still not enough knowledge of the general laws that guide the thermoelectric phenomena as functions of the nature of the chemical interaction of metals.

Thermoelectric phenomena, discovered more than 100 years ago, represent a complicated picture of interaction of electric charges, placed in the crystal lattice of a metal. Modern theories attribute to the appearance of thermoelectricity to thermal diffusion of cur-rent carriers -- electrons -- in a non-uniformly heated metal from parts that are more highly heated towards the less heated ones. W. Thomson called this effect, which bears his name, the specific heat of electricity. However, current conductors have thermoelectric properties regardless of whether a temperature gradient exists. Thus, a certain difference of potentials is established between two adja-cent metals (the Peltier effect) even in the absence of any tempe-rature gradient.

Modern electron theory of metals is still unable to explain the quantitative aspect of thermoelectric phenomena, leading only to a correct order of magnitude of the thermal emf. Certain theo-reticians, for example, consider it unnecessary to compare their mathematical deductions with experiment. This is typical of modern bourgeois science.

In a considerably better status is the thermodynamic theory of thermoelectric phenomena, proposed by W. Thomson as early as in 1856.

The conclusions of W. Thomson have not lost their signifi-cance to this day and are fully **corroborated by experiment.**

A great role in the investigation of thermoelectric phenomena was played by the work of Russian scientists.

M. Avenarius, a professor of the Kiev Polytechnic Institute, has established experimentally the general temperature dependences of the variation of the thermal emf.

P. Bakhmet'yev in his extensive works has observed the influence of mechanical forces and of the magnetic field on the thermal emf of metals. He created his "thermoelectric system" and proved the periodicity of the thermoelectric properties of pure metals.

With the arrival of physico-chemical analysis, devised by N.S. Kurnakov, thermoelectric phenomena were applied to the analysis of metallic systems of alloys by N.N. Tuturin (1909), who uncovered all the various phenomena for various cases of chemical interactions.

Numerous investigations made by V. A. Nemilov on solid solutions of noble metals have produced alloys of practical importance. On the basis of these investigations it is possible to draw certain interesting theoretical conclusions.

The present work is devoted in a considerable portion to the development of an experimental procedure, accessible to any investigator. On the basis of this procedure a study is made of many pure metals and solid solutions, and great attention is devoted to an investigation of various types of transformations in metals and alloys.

Along with noble metals and their alloys, a study is also made of the iron groups.

This turns out to be essential for comparison of transformations that occur in iron, cobalt, nickel , and many investigated alloys.

The use of the method of thermoelectric phenomena in the investigation of transformations in metals and alloys has yielded exceedingly fruitful results. An entirely new and original method of the use of N. S. Kurnakov's pyrometer, a use proposed by the author, has simplified considerably the experimental procedure, shortening the time of experiments and refining the obtained results.

CHAPTER I

GENERAL INFORMATION ON THERMOELECTRIC PHENOMENA

According to modern concepts, thermoelectric phenomena which arise in metals are explained by thermal diffusion of the current carriers, the electrons.

The electron theory of the metallic state is at the present time incomplete, since it does not give a quantitative explanation of the phenomena and leads only to a correct order of magnitude of the thermal emf.

To interpret the entire variety of thermoelectric and galvano-magnetic phenomena it became necessary to assume the existence of positive current carriers -- "holes" -- along with negative electrons.

Thermoelectric phenomena arise not only in metals and alloys, but also in semiconductors, salts, and solutions of electrolytes. They are the external manifestation of the interaction between electric charges, regularly distributed and moving in a crystalline lattice or in a liquid current conductor.

In this chapter we explain, along with the general concepts of thermoelectricity, the thermodynamic theory of thermoelectric phenomena, which is in adequate rigorous agreement with experiment during the 100 years of its existence.

1. HISTORICAL INFORMATION ON THERMOELECTRIC PHENOMENA

The first experiments on thermoelectricity were carried out by the Russian academician Epinus $/ 1 /$. However, his investigations

were not widely known.

In 1796 Volta established that when two conductors come in contact they become electrified in different manners. Along with this, Volta found that in a closed loop, consisting only of first-class conductors (metals), the sum of the emf's is zero.

Seebeck $[2]$ showed in 1823 that Volta's law stops being true when the point of contact between different parts of the electric circuit are at different temperatures. The thermal emf arising in the conductors depends on the temperature and the nature of the metals.

In 1834, Peltier $[3]$ remarked that when a current passes through a junction of two metals there is a liberation or absorption of heat in an amount Q proportional to the current I:

$$Q = \pm \pi I,$$

where π is the Peltier coefficient, which depends on the nature of the contact-making metals and the temperature. This coefficient is called the Peltier emf.

Heat is liberated when π and I have opposite directions. If the directions of the current and of the Peltier coefficient are the same, the heat is absorbed.

W. Thomson $[4]$ has shown experimentally and theoretically that the individual portions of uniform metal, heated to different temperatures, can be considered as different bodies, between which an emf always arises. When current passes in a conductor, there is liberated, in addition to the Joule heat, a positive or negative amount of heat, caused by the difference of temperature at the terminals of the conductor:

$$q = \pm \sigma I,$$

where σ is the Thomson coefficient or voltage, arising in a conductor when the temperature difference at its terminals is 1° C.

The Peltier and Thomson effects are fully reversible. The coefficients π and σ can be expressed in volts or units of energy (Joules, calories, electron volts).

The total emf in a circuit consisting of two conductors a and b, the ends (junction) of which have different temperatures T_1 and T_2, is determined from the following equation

$$E = \pi_2 - \pi_1 - \int_{T_1}^{T_2} (\sigma_b - \sigma_a)\, dT,$$

where π_2 and π_1 are the Peltier voltages at the junctions of the conductors at temperatures T_2 and T_1; σ_b and σ_a are the Thomson emf's in conductors b and a.

The principal laws of thermoelectricity were established by Becquere $\underline{/\,5\,\underline{/}}$ and Magnus $\underline{/\,6\,\underline{/}}$.

1. In a circuit consisting of two metals, the thermal emf depends only on the temperatures of the junctions, and not on the temperature distribution along the conductors.

2. In a closed loop consisting of one metal, the total thermal emf equals zero at any temperature distribution.

The laws of Volta, Becquerel, and Magnus are the basis of thermoelectric phenomena and are in strict agreement with thermodynamic theory of Thomson.

Benedicks $\underline{/\,7\,\underline{/}}$ has attempted to refute the Magnus law. He stated that the thermal emf appears in a chemically homogeneous medium if the temperature gradient is not symmetrical (the Benedicks effect). However, it was impossible to derive any laws or interpretations from this phenomenon. The appearance of a thermoelectric current is actually observed in supposedly homogeneous conductors. The thermoelectric phenomena are exceedingly sensitive to the least irregularities of a metal. Parts of the same conductor differ from each other in structure, placement of grains, non-uniform degree of hardening and heat treatment.

The thermal emf changes under the influence of stretching and contraction and depends on the magnitude of the magnetic and electric field. The most homogeneous are well annealed wires made of pure metals, which have a cubic structure of the crystalline lattice, in which the anisotropy manifests itself least.

Such metals like zinc, bismuth or antimony are frequently inhomogeneous as a consequence of the considerable anisotropy of the crystals.

Impurities in pure metals, which range themselves irregularly between grains, are the sources of inhomogeneity of metals, which manifest themselves particularly strongly in alloys as a result of liquation.

The effect of temperature on the thermal emf was investigated in great detail by Avenarius [8]. He established that for many metals the thermal emf changes with the temperature in accordance with the parabolic law:

$$E = a + bt + ct^2.$$

The Avenarius formula is used to this day in the calibration of thermocouples.

Taking for the Thomson emf $\sigma = aT$, Tait [9] derived the Avenarius formula from the Thomson thermodynamic theory.

P. Bakhmet'yev [10,11] has established on the basis of his extensive research the periodicity of thermoelectric phenomena, comparing them with the atomic weights of metals. He has arranged the metals in a thermoelectric series, similar to the Volta series, in which, upon combining two metals, we find that the metal located high in the series is always negative and the lower metal is always positive.

Bakhmet'yev's thermoelectric series was later on modified by several investigators, since further improvement in metallurgical processes has made it possible to obtain metals of greater purity.

Many papers of Bakhmet'yev are devoted to the effect of tension and compression, and also to the effect of the magnetic field on the thermoelectric properties of metals [11,12].

At the present time these papers are only of historical value.

2. THEORY OF THERMOELECTRIC PHENOMENA

Based on the thermodynamic laws, W. Thomson [4,13] predicted the existence of an emf, which he called the specific heat of electricity, and later on proved experimentally the correctness of his conclusions.

Thomson's thermodynamic theory established the mutual relationship between the integral thermal emf and the Peltier and Thomson emf's.

A current I flows in a circuit consisting of two conductors (Fig. 1) with junction temperatures T_1 and T_2. A total of Q units of electricity have passed through the circuit. Assuming that the

current and the resistance are infinitesimally small, the Joule heat can be neglected.
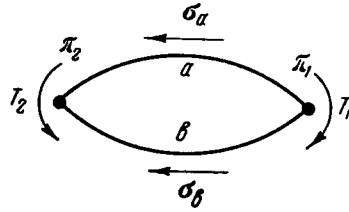
Fig. 1. Thermoelectric Effects in a Thermocouple.

We use the following symbols:

$q\pi_2$ -- heat absorbed in the hot junction.

$q\pi_1$ -- heat liberated in the cold junction.

$q\int_{T_1}^{T_2} \sigma_a dT$ -- heat absorbed in conductor a.

$q\int_{T_1}^{T_2} \sigma_b dT$ -- heat liberated in conductor b.

We then have from the first law of thermodynamics

$$qE = q\pi_2 - q\pi_1 - q\int_{T_1}^{T_2} (\sigma_b - \sigma_a)\, dT$$

or

$$E = \pi_2 - \pi_1 - \int_{T_1}^{T_2} (\sigma_b - \sigma_a)\, dT. \qquad (1)$$

Considering the process of the displacement of the heat as a circuital and reversible process, we can write, in accordance with the second law of thermodynamics

$$\frac{\pi_2}{T_2} - \frac{\pi_1}{T_1} - \int_{T_1}^{T_2} \left(\frac{\sigma_b}{T} - \frac{\sigma_a}{T}\right) dT = 0. \qquad (2)$$

Differentiating the last two equations, we get

$$\frac{dE}{dT} = \frac{d\pi}{dT} - (\sigma_b - \sigma_a),$$ (3)

$$\frac{d}{dT}\left(\frac{\pi}{T}\right) - \frac{\sigma_b - \sigma_a}{T} = 0$$

or

$$\frac{\pi}{T} = \frac{d\pi}{dT} - (\sigma_b - \sigma_a).$$ (4)

It follows from Eqs. (4) and (3) that

$$e = \frac{dE}{dT} = \frac{\pi}{T}$$ (5)

Differentiating this equation we get

$$\frac{d^2E}{dT^2} = \frac{1}{T}\frac{d\pi}{dT} - \frac{\pi}{T^2}.$$ (6)

From (4), (5), and (6) we find

$$\frac{d^2E}{dT^2} = \frac{\sigma_b - \sigma_a}{T}.$$ (7)

Thus, the principal conclusions of Thomson's thermodynamic theory can be expressed by the following two equations:

$$\frac{dE}{dT} = \frac{\pi}{T},$$ (8)

$$\frac{d^2E}{dT^2} = \frac{\sigma_b - \sigma_a}{T},$$ (9)

where T is the absolute temperature.

Boltzmann /14/ found Thomson's conclusions insufficiently rigorous and indicated the need for experimental verification. Thus, Thomson considers in his conclusions the reversible thermoelectric phenomena separately from the irreversible phenomena of heat conduction and electric conduction.

A. E. Gurevich [15] and S. R. Grot [16] have demonstrated the correctness of Thomson's theory, starting with the equations of thermodynamics of irreversible processes, based on the principle of symmetry of the Onsager kinetic coefficients [17].

Experimental verifications of Thomson's equations were made by many investigators by comparing the data obtained with electric and calorimetric measurements [18]

Nernst [19] proposed that the differential thermal emf

$$e = \frac{dE}{dT} \to 0 \ \text{и} \ \sigma \to 0,$$

when $T \to 0$.

Integrating Eqs. (9), Nernst obtained

$$e = \int_0^T \frac{\sigma_b}{T} dT - \int_0^T \frac{\sigma_a}{T} dT. \tag{10}$$

The correctness of the premises predicted by Nernst was confirmed by Keesom [20] and also by Borelius [18] on the basis of numerous investigations at temperatures close to absolute zero.

Thus, the differential thermal emf

$$e = \frac{dE}{dT}$$

represents the difference of the absolute thermal emf's of electrodes that make up the thermocouple:

$$e = \varepsilon_b - \varepsilon_a, \tag{11}$$

where

$$\varepsilon_b = \int_0 \frac{\sigma_b}{T} dT, \ \varepsilon_a = \int_0 \frac{\sigma_a}{T} dT.$$

Obviously, (11) is valid for all thermoelectric properties of any thermocouple.

$$E = E_b - E_a,$$
$$\pi = \pi_b - \pi_a,$$
$$\sigma = \sigma_b - \sigma_a.$$

Knowing the absolute values of the thermoelectric quantities of any given metal, which can serve as a comparison electrode, it is possible to determine these properties for any other metal from Eq. (11).

Lange and Hesse [21] verified experimentally the applicability of Thomson's equation to solutions of electrolytes.

Latimer [22], by comparing the values of the thermoelectric effect in metals, reached the conclusion that the Thomson heat is equivalent to the specific heat at constant volume. He therefore proposed the use of research on thermal emf as a method for determining the specific heats of metals. However, Latimer's data were not verified experimentally.

M. I. Temkin and A. V. Khoroshin [23], on the basis of thermodynamic conclusions, have shown that the absolute thermal emf is the entropy of the moving current carriers. They have started with the premise that the mechanism of occurrence of thermoelectric phenomena is that in each of two conductors, making up the thermocouple, there occurs thermal diffusion of current carriers as a result of the temperature gradient. This diffusion gives rise to a potential difference along the conductor, which combines with the potential jumps in the junctions of the thermocouple. The observed thermal emf is the result. According to A. Eastman [24] the entropy of the transfer of current carriers is

$$S_i^* = \frac{Q^*}{T},$$

where Q* is the heat of transfer and T the absolute temperature.

The entropy of the moving current carrier consists of the entropy at rest S_i and the transfer energy S_i*:

$$\overline{S}_i = S_i + S_i^*.$$

The authors have established that

$$\bar{\bar{S}}_i = -\int_0^T \frac{\sigma}{T}\, dT. \tag{12}$$

The (-) sign is used because the direction of motion of the electrons is opposite the direction of the current.

According to Eq. (12), the Thomson emf assumes the value of the specific heat of the current carriers:

$$\sigma = -c_p. \tag{13}$$

The authors have confirmed their conclusions using solutions of electrolytes [23].

The electron theory of thermoelectricity was first developed by H. A. Lorentz [25], who proposed that the electrons in metals behave like gas molecules, i.e., they participate in the thermal motion and have an average kinetic energy 3kT/2, where k is Boltzmann's constant and T is the absolute temperature.

In a metal in which there exists a temperature gradient, the electrons should diffuse from the hotter spot to the cooler one.

Starting with these basic premises, Lorentz calculated the Thomson emf for all metals:

$$\sigma = \frac{3}{2}\cdot\frac{k}{e} = -130 \text{ mcv/}^\circ\text{C}$$

where e is the electron charge.

The Lorentz theory was only a very rough approximation of the truth.

Applying the Fermi statistics to the calculation of thermoelectric effects in metals, more exact relationships were established by Sommerfeld [26], Wilson [27], Peierls [28], and Mott and Jones [29].

According to Sommerfeld the Thomson coefficient and the absolute thermal emf are

$$\sigma = e = \frac{\pi^2}{5}\cdot\frac{k}{e}\cdot\frac{kT}{E_0} = -170\,\frac{kT}{E_0}\,,$$

where E_0 is the average energy of the electrons at absolute zero.

The value obtained is closer in order of magnitude to the experimental data. However, it is impossible to indicate the conditions under which the Thomson emf would have a positive value.

To interpret the thermoelectric phenomena it became necessary to assume the existence of positive current carriers -- "holes" -- along with negative current carriers -- electrons.

Meisner [30] states in his survey that there exist no general laws whatever pertaining to thermoelectric phenomena in conductors.

All this shows that the aggregate of thermoelectric properties of conductors presents a very complicated picture.

When the temperature changes above the critical Debye temperature the absolute thermal emf of many conductors changes linearly. At low temperatures one observes more complicated laws.

To explain these anomalies, L. Gurevich [31] proposed that at different temperatures of the thermal emf is produced by different mechanisms. In the presence of a temperature gradient in the conductor, the conduction electrons and the vibrations of the crystalline lattice are distributed over the states not quite uniformly. The deviation of the electrons from equilibrium is explained by two causes: the direct action of the temperature gradient on the electrons, and the entrainment of the electrons by the flux of the lattice waves, or phonons, produced by the temperature gradient. Within a certain temperature interval, the second factor can prove to be predominant.

F. G. Serova [32], using this method, has calculated the Thomson coefficient for alkaline metals. She obtained results that are close to the experimental data. Thus, a characteristic of sodium is the predominance of the factor of the direct action of the temperature gradient on the electrons, while for lithium the entrainment of the electrons by the phonons is the decisive factor.

However, these are only the first attempts to obtain values close to the true ones, using the simplest examples.

3. TECHNICAL APPLICATION OF THERMOELECTRIC PHENOMENA

Thermoelectric phenomena find a technical application in the measurement of a temperature.

Ordinary thermoelectric parameters represent a thermocouple combined with a millivoltmeter, potentiometer, or another measuring instrument. The thermocouple should have the following principal properties:

(1) Stability of the thermal emf.
(2) Homogeneity of the wire.
(3) Regularly varying characteristic of the thermal emf vs. temperature.
(4) Sufficiently high thermal emf.

/33/.　Fig. 2 shows the thermal emf's of modern Soviet thermocouples
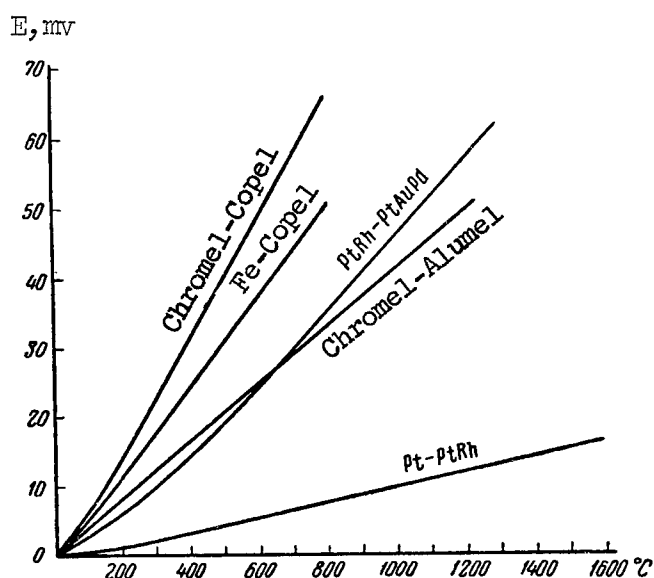
Fig. 2.　Thermal emf of Commercial Thermocouples.

In the Pt-(Pt + Rh) thermocouple, the positive electrode is an alloy of platinum with 10% of rhodium, while the negative electrode is platinum. The thermal emf of such a thermocouple is low and reaches 16.78 millivolts at 1600° C. The operating temperature of the thermocouple does not exceed 1300°C, since the stability of calibration and homogeneity of the thermocouple are disturbed above this temperature. This depends not only on the melting temperature, but also on other factors such as the evaporability of the metals, their ability of recrystallization, and the diffusion of metals in the hot junctions. The inhomogeneity of the wire should not exceed more than ± 10 microvolts. Consequently, the accuracy of measurement does not exceed ± 1°C. However, for thermocouple wires made of very pure

14

materials **and** correctly annealed, one can attain an inhomogeneity of $\pm$ 2 microvolts, i.e., a measurement accuracy of $\pm$ 0.2°C.

The thermocouple (Pt + Rh) -- (Pt + Au + Pd) has a high termal emf, reaching 50 microvolts per degree C. The positive electrode is an alloy of platinum with 10% of rhodium, and the **negative an alloy** of 60% gold, 30% palladium, and 10% platinum. The operating temperature of the thermocouple reaches 1200°C. Above this temperature the stability of calibration is greatly damaged by the intense evaporation of the gold.

The damage to homogeneity reaches $\pm$ 50 to 100 microvolts. Thus, the accuracy of measurement does not exceed $\pm$ 1 or 2°C. In spite of the high thermal emf, this thermocouple has no advantages over the platinum-platinum plus rhodium thermocouple.

Originally the (Pt + Rh)-(Pt + Au + Pd) thermocouple was produced in an effort to obtain a high thermal emf. This thermocouple was first proposed by Feussner /34/ and in the Soviet Union by G. P. Kul'bush /35/. Our latest investigators /116/ have shown that there is no need for platinum in the negative electrode, since it reduces the emf.

Thanks to the high emf and corrosion resistance, this thermocouple is very useful when operating with fused salts and organic substances, for in these cases no protective case is necessary. This circumstance facilitates greatly the operation and increases the sensitivity of the thermocouple, and reduces its inertia.

In chromel-alumel thermocouples the positive electrode is chromel, an alloy of 90%nickel and 10% chromium. The negative electrode is alumel, an alloy of 95% nickel, 2% aluminum, 2% manganese, and 1% silicon. The operating temperature of the thermocouple is not greater than 900-1100° C. The greatest advantage of this thermocouple is that its calibration characteristic is practically linear:

$$E_0^t = 40\, t\, \textbf{mcv}$$

However, the inhomogeneity of the chromel electrode sometimes $\pm$ 150 microvolts. This is why the measurement accuracy with a chromel-alumel thermocouple does not exceed $\pm$ 3° C.

Chromel-copel and iron-copel thermocouples have relatively high thermal emf. In either thermocouple the negative electrode is the copel, an alloy of 43% nickel and 57% copper. This alloy limits the application of the thermocouple to 600°C.

Modern technology imposes more and more stringent requirements on thermocouples. In connection with the rapid growth of measurement

apparatus the sensitivity of the measuring instruments has increased
and the magnitude of the thermally emf of the thermocouple becomes
secondary; the requirements concerning stability and temperature li-
mits of application of thermocouples are simultaneously increasing.

A. Metcalfe [36] has reduced the diffusion in the hot junction
by using a thermocouple (Pt + 1% Rh) - (Pt + 13% Rh). The thermal
emf of such a thermocouple was close to that of the Le Chatellier
Pt - (Pt + 10% Rh) thermocouple, but its stability was considerably
higher.

The use of platinum alloys containing more rhodium, namely
(Pt + 6% Rh) -- (Pt + 30% Rh) and (Pt + 20% Rh) -- (Pt + 40% Rh)
[37], has increased the stability of the thermal emf up to 1550° C
in prolonged measurements.

Goedecke [38] has used Pt -- (Pt + 8% Re) and Rh -- (Pt + 8%
Re) thermocouples. However, above 1300° C the alloys of aluminum
with ranium is insufficiently stable. More stable are the thermo-
couples Pt - (Pt + 4.5% Re + 5% Rh) and Rh -- (Rh + 8% Re).

High-melting point thermocouples were produced by Hoffmann
[39] (Ir -- (Ir + 10% Rh)),Feussner [40], (Ir -- (Ir + 60% Rh)), and
Schulze [41], ((Ir + 10% Ru) -- (Ir + 10% Rh)).

These thermocouples have high melting temperatures, but are
not sufficiently stable in air, owing to the volatility of the metals.

A great shortcoming are also the technological difficulties
in the manufacture of wires of these metals.

Morugina [42], Simons, Burton, and Hamstead [43], and Morgan
and Danforth [44] used thermocouple W -- Mo, W -- Ta, Mo -- Ta,
W -- (50% W + 50% Mo). Pirani and Wagenheim [45] used W -- (75% W
+ 25% Mo) while Troy and Stevens used W -- Ir.

The most widely used thermocouple is the tungsten-molybednum
one, because of its accessibility. However, Potter and Grant [47]
have shown that its thermal emf is unstable, having an inversion
point near 1250° C, a fact that introduces considerable inconven-
iences in operation.

4. CONCLUSIONS

In accordance with the thermodynamic theory, one can determine the absolute values of all thermoelectric quantities.

The relationships between the different thermoelectric properties are expressed by the following equations.

The absolute integral thermal emf

$$E = \pi_2 - \pi_1 - \int_{T_1}^{T_2} \sigma dT.$$

The absolute differential thermal emf

$$\varepsilon = \frac{dE}{dT}, \quad \varepsilon = \frac{\pi}{T}, \quad \varepsilon = \int_0^T \frac{\sigma}{T} dT.$$

The absolute thermoelectric potential

$$\pi = T\varepsilon.$$

The Thomson emf

$$\sigma = T \frac{d\varepsilon}{dT}.$$

Henceforth, for brevity, the author assumes the following symbols:

E -- integral thermal emf,
ε -- absolute thermal emf.
π -- thermoelectric potential.

The Thomson emf has the value of the specific heat of the moving carriers of the current:

$$\sigma = -c_p.$$

The absolute thermal emf has the value of the entropy:

$$\varepsilon = -\int_0^T \frac{\sigma}{T} dT$$

17

The thermoelectric potential then becomes the bound energy:

$$\pi = T\varepsilon = -ST.$$

For the enthalpy of the current carriers we obtain an equation

$$H = -\int_0^T \sigma\, dT$$

The integral thermal emf will represent the increment in the thermodynamic potential:

$$E = -T\Delta S + \Delta H = \Delta Z.$$

The thermodynamic deductions given in this chapter differ somewhat from the initial deductions of Thomson, who, as a result of his premises, obtained the following equations:

$$E = \pi_2 - \pi_1 + \int_{T_1}^{T_2} (\dot\sigma_b - \sigma_a)\, dT$$

and

$$\frac{d^2E}{dT^2} = -\frac{\sigma_b - \sigma_a}{T}.$$

Thus, according to Thomson, the absolute thermal emf and the Thomson emf have opposite signs:

$$\varepsilon = -\int \frac{\sigma}{T}\, dT.$$

This occurs because it has not been established sufficiently clearly what direction of the Thomson emf should be considered positive.

18

In the heated end of a conductor, the concentration of current carrier increases, and they diffuse towards the cold end, thus charging them with their charge and leaving the opposite charge on the hot end. Thus, the electronic conductors have a negative on the cold end and a positive charge on the hot one. Conductors with "hole" conductivity, to the contrary, have a negative charge on the hot end and a positive one on the cold one. In electronic conductors the Thomson emf is directed from the hot end towards the cold one and is considered negative, while in the case of conductors with "hole" conductivity the Thomson emf, which is directed from the cold end to the hot one, is considered positive.

The positive conductor is connected to the positive terminal of the measuring instrument.

According to Borelius /48/ the Thomson emf is considered positive when the current flowing through the conductor in the direction towards the decreasing temperature causes liberation of heat.

A. F. Ioffe /49/ considers that the sign of the thermal emf determines the sign of the current carriers. Thomson in his deductions has arbitrarily assumed the opposite, without paying due attention to this circumstance.

In our conclusions (see Fig. 1) we show the positive direction of σ for both conductors in accordance with the universally accepted definition. Therefore for thermoelectrically positive conductors all the quantities ε, π , and σ have a positive sign. According to Thomson, if ε and π are positive, σ is negative. This not only causes certain inconvenience in all the discussions, but also leads to incorrect conclusions.

It was shown in this chapter that the integral thermal emf represents the thermodynamic potential of the current carriers. If we take into account the combination of signs obtained by Thomson, we obtain

$$E = -(\Delta H + T \Delta S).$$

However, this equation makes no thermodynamic sense.

It is very interesting to establish whether the value of is really the absolute electric potential of the conductor (in the sense mentioned at the beginning of this section).

Let us assume that at absolute zero the conductor potentials are P_a and P_b. If π_a and π_b are the increments of the potential in the temperature range from absolute zero to the temperature T,

then at a temperature K the potentials of the conductors will be respectively

$$P_{aT} = P_a + \pi_a, \quad P_{bT} = P_b + \pi_b.$$

The potential difference between the conductors at a temperature T can be measured calorimetrically, and according to the Thomson-Nernst theorem it equals

$$\pi_b - \pi_a = T(\varepsilon_b - \varepsilon_a),$$

or

$$P_{bT} - P_{aT} = \pi_b - \pi_a.$$

However,

$$P_{bT} - P_{aT} = (P_b + \pi_b) - (P_a + \pi_a),$$

or

$$P_{bT} - P_{aT} = (P_b - P_a) + (\pi_b - \pi_a).$$

Then, $$P_b = P_a.$$

Consequently, the potentials of all conductors are equal to each other at absolute zero. However, as was shown experimentally by Borelius /18/, for superconductors the absolute thermal emf, and consequently the thermoelectric potential, vanish already near the absolute zero. But since the potentials of all conductors equal each other at absolute zero, therefore

$$P_b = P_a = \ldots = 0.$$

Thus, the thermoelectric potential of the conductor is

$$\pi = T\varepsilon$$

and is its absolute electric potential at a given temperature.

CHAPTER II

METHODS OF MEASURING THERMOELECTRIC PROPERTIES

1. INTRODUCTION. SURVEY OF MEASUREMENT METHODS

The thermoelectric properties of metals and alloys can interest the experimenter from various points of view.

The integral thermal emf is usually studied in a thermocouple with pure platinum or with a metal which henceforth will serve as one of the electrodes of the thermocouple.

To recognize the nature of transformations that take place in alloys, it is much more interesting to study either the differential thermal emf or the Thomson emf, since transformations manifest themselves much more clearly in these phenomena than in the integral thermal emf. The determination of the absolute values of the thermoelectric properties is of great interest, since in this case we obtain the thermoelectric effects of the investigated metal independently of the properties of the comparison electrode.

Thermoelectric properties of metals can be investigated by electric and calorimetric methods of measurement.

All thermoelectric properties of metals (integral thermal emf E, differential thermal emf ε , the Peltier emf π , and the Thomson emf σ) can be measured with great accuracy. However, these measurements are carried out only with relative respect to some other metal, the comparison electrode.

To determine the absolute values of the thermoelectric properties of the investigated metal it is necessary to exclude from the obtained values the thermoelectric properties of the comparison electrodes.

A direct measurement of the absolute values of the thermoelectric properties can be realized only by calorimetric means. The usual and only method is to determine the Thomson emf from absolute zero to a high temperature. One can then determine the function

$$\frac{\sigma}{T} = f(T),$$

geometric integration of which yields the value of the absolute thermal emf:

$$\varepsilon = \int_0^T \frac{\sigma}{T} \, dT.$$

At first glance this procedure appears complicated. It gives, however, very accurate results that are in good agreement with each other, in spite of the variety of measurement methods.

The method of measuring the Thomson emf was first described by Thomson /4/ , and was then perfected by Le Roux /50/ and used with slight modification by Berg /51/, Nettleton /52/, Young /53/, Smith /54/, Borelius /55,56,57/, Lander /58/, and Nystrom /59/.

The principle of the method consists of the following (Fig. 3). The end points of the investigated specimen are in metallic blocks having temperature T_1 and T_2. The current I passing through a conductor having a length of unity, a cross section q, and a specific resistivity ρ liberatures $\frac{\rho}{q} I^2$ as Joule heat and $\pm I\sigma\frac{dT}{dx}$ as Thomson heat, where dT/dx is the temperature gradient.
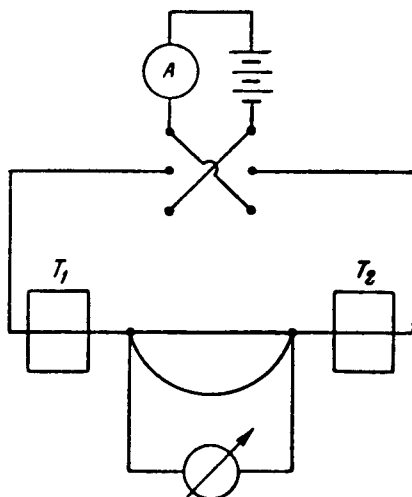
Fig. 3. Measurement of the Thomson effect.

In addition, a certain amount of Peltier effects may appear because the wire may be inhomogeneous, the value of the effect being πI . The net result is a certain amount of heat, causing a change in the temperature of the conductor

$$Q = \frac{\rho}{q} I^2 + I\pi - I\sigma \frac{dT}{dx} .$$

If we change the direction of the current, then π and σ reverse their signs and the wire will have a different temperature. Berg proposed to compensate for this difference in temperatures by the Joule heat. When the conductor temperature is maintained constant, the amount of heat will remain unchanged.

$$Q = \frac{\rho}{q} (I - \Delta I)^2 - (I - \Delta I)\left(\pi - \sigma \frac{dT}{dx}\right) .$$

Equating these two equations we get

$$\frac{\rho}{q} \Delta I = \sigma \frac{dT}{dx} - \pi.$$

To eliminate the Peltier effect, the measurement is repeated with an opposite direction of heat flux, at which

$$\frac{\rho}{q} \Delta I' = \sigma \frac{dT'}{dx} + \pi.$$

Summing these equations, we eliminate π and obtain an expression for the Thomson emf

$$\sigma = \frac{\rho}{q} \frac{\Delta I + \Delta I'}{\frac{dT}{dx} + \frac{dT'}{dx}} .$$

The above method for measuring the Thomson emf was proposed by Nystrom. His results are in good agreement with the data of the preceding authors.

Measurements of the Peltier effects can be carried out with respect to some standard metal. An absolute measurement of the thermoelectric potential is then possible.

The amount of heat liberated or absorbed in a junction of two metals a and b during a time t at a current strength I is

$$Q = \pm\, \pi I t.$$

The Peltier effect is fully reversible. Liberation of heat is observed when the direction of the current is opposite to the direction of the Peltier emf; when the current has the opposite direction, heat is absorbed. Measurement of the Peltier effect was performed by Edlund [60] with the aid of two differential calorimeters (Fig. 4). In one calorimeter the Peltier effect causes an increase in the temperature, and in the second one it causes a decrease in the temperature. The difference in temperatures is measured by a differential thermocouple. The Joule heat is eliminated by alternating the direction of the current. The calorimeters are two identical pieces of metal with known specific heat.
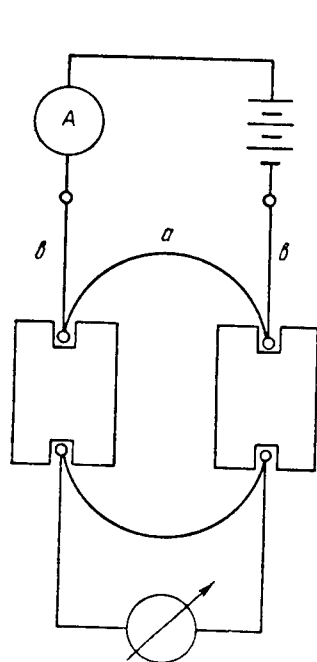
Fig. 4. Measurement of the   Fig. 5. Measurement of the
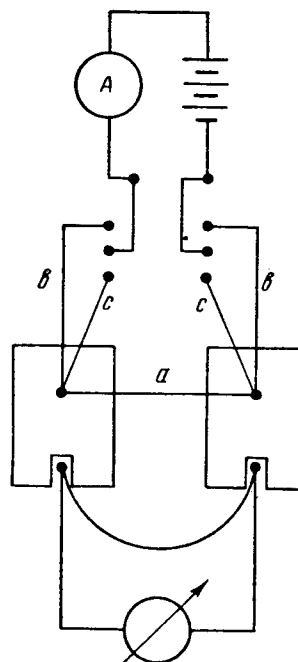   Peltier effect after   Peltier effect after
         Edlund.   Borelius.

The Peltier effect between conductors a and b is determined from the equation

$$\pi = \frac{c\Delta T}{2It},$$

where c is the specific heat of the calorimeter and ΔT is the temperature difference of the calorimeters, while t is the time during which the current I flows.

More accurate results were obtained by Borelius [61] by a differential method (Fig. 5). A direct current flows for a long time in the circuit b-a-b or c-a-c until complete equilibrium is reached.

In the first case we obtain a calorimeter temperature difference of ΔT_1, and in the second one we obtain ΔT_2. If the Peltier emf is known for the pair of metals ab, then the Peltier emf of the pair bc is determined by the following equation

$$\pi_{bc} = \frac{\Delta T_1}{\Delta T_1 - \Delta T_2} \pi_{ba}.$$

This method gives very accurate results. The influence of the Joule heat which is always superimposed on the process, is entirely eliminated.

The integral thermal emf is measured with a potentiometer or millivoltmeter. The cold junction is placed at a constant temperature, the hot junction is an oven of known temperature.

When measuring the differential thermal emf, the temperature of the cold junction is not maintained constant. The difference in temperature between the cold and hot junctions has a small value (approximately 5-30°C).

The differential thermal emf is determined from the equation

$$e = \frac{dE}{dT} \approx \frac{\Delta E}{\Delta T},$$

where ΔE is the thermal emf developed by the thermocouple at a temperature difference $\Delta T = T_2 - T_1$ at its ends.

Various versions of this method are described by Borelius [62], Burgess and Scott [63], Bidwell [64], and Durer [65].

This method, although less accurate as regards the relative error, has many advantages. It requires no long specimens, and the error due to the inhomogeneity of the investigated specimen is reduced to a minimum.

For electric methods of measuring the thermoelectric properties one must have stable and well calibrated thermocouples.

Since all the electric methods of measurements determine the thermoelectric properties when paired with a comparison electrode, it should be stable, homogeneous, and have well-known thermoelectric properties. Under these conditions the thermoelectric properties of the comparison electrode can be eliminated from the measured quantity and consequently one can obtain absolute values of the thermoelectric properties of the investigated specimen.

The measurement of absolute values of thermoelectric properties has that advantage, that the phenomena are characterized only by the properties of the given alloy, independently of the comparison electrode and its features. In addition, absolute values are readily compared with each other. Unfortunately, a large number of investigations carried out by the previous authors cannot be compared at all, since the investigated metals in alloys were compared with metals of unknown purity and properties. In the best case the comparison electrode used was platinum or copper. Sometime constantan, manganin, nichrome and other alloys with unknown properties were used.

In the present work we describe these electrical methods of measuring thermoelectric properties, which are the most accurate and accessible to the experimenter.

For all measurement methods it is necessary to have exactly calibrated thermocouples and a reliable comparison electrode for the calculation of the absolute values of the thermoelectric properties.

2. THERMOCOUPLES AND THEIR CALIBRATION

Thermocouples must meet many requirements, which are quite essential to attain suitable measurement accuracy.

Both wires of the thermocouple should be stable in the required temperature interval and as homogeneous as possible, since any deviation from homogeneity involves an error in the measurement of the temperature, and in the differential method the inhomogeneity of the thermocouples produces an error in the measured quantities.

The thermocouple wire was manufactured of spongy twice-refined platinum. Pure platinum and an alloy of platinum with 10% rhodium were melted in a high frequency furnace, forged in hot state, rolled in a hand rolling mill and drawn into wire 0.5 mm in diameter. During the treatment, the platinum was boiled in strong hydrochloric acid to free it of the iron that adheres to the surface of the metal from the hammer, anvil, and rolling mill.

The wire was annealed by heating with alternating current to 1300° C for two hours. The temperature was monitored with an optical pyrometer.

The annealed wire was checked for homogeneity with the aid of a potentiometer by passing it through a short furnace, as shown in Fig. 6. The appearance of an inhomogeneity of the wire in the zone of the maximum temperature gradient in the furnace produced a corresponding thermal emf. The inhomogeneity of pure platinum reached +2 microvolts, and that of the platinum-rhodium wire was up to +4 microvolts.

These wires were used to make up four thermocouples, each one meter long. The hot ends of the thermocouples were placed in thin porcelain capillary tubes, which were first heated in a furnace at a temperature of 900 to 1000° C for 30 minutes, to burn away any traces of organic substances in the tubes. The hot junction was fused with an electric arc.

The cold ends were placed in vinyl chloride tubes, twisted with copper wires and located in narrow glass test tubes with a small amount of Wood's alloy, which insured reliable contact and good heat conduction.
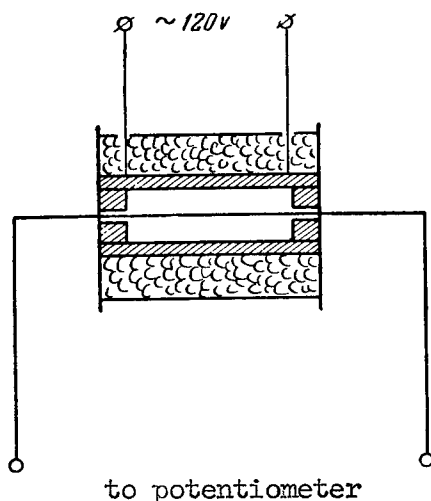
Fig. 6. Measurement of the homogeneity of the wire.
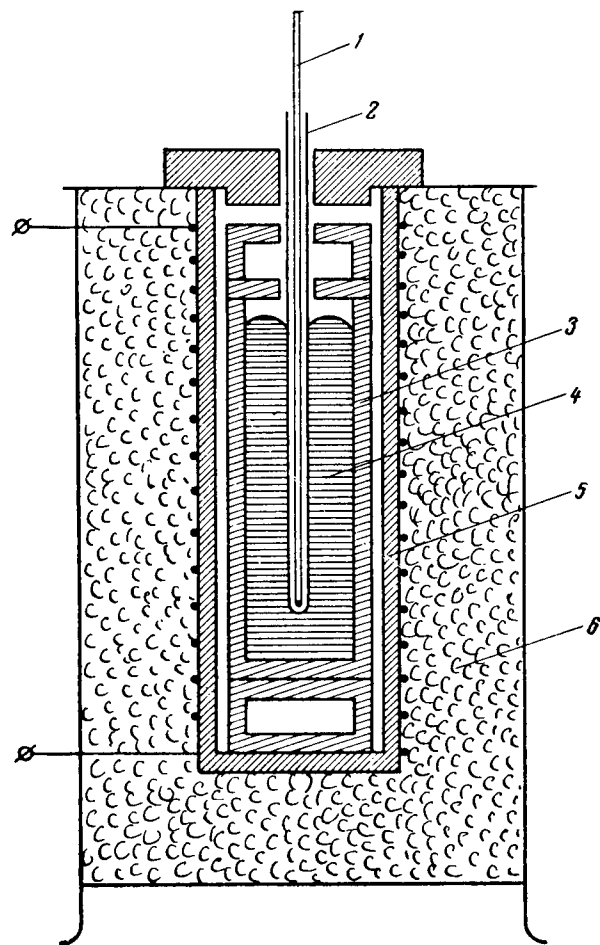
Fig. 7. Furnace for calibration of thermocouples.

1 -- thermocouples; 2 -- corundise cap; 3 -- graphite crucible; 4 -- metal; 5 -- porcelain cylinder;
6 -- asbestos.

The cold junctions of the thermocouples were placed in an ice-filled Dewar vessel at a depth of approximately 100 to 150 mm. A calibration of the thermocouple was carried out relative to the hardening point of the pure metals in accordance with the international standards, described by Roser and Wensel /66/, and also in accordance with the hardening point of naphthalene.

The naphthalene was first recrystallized from an alcohol solution to rid it of impurities, and then melted in a test tube

25 mm in diameter placed in hot water.

The hot junction of the thermocouple was introduced in the molten naphthalene without a cap to a depth of approximately 10 to 15 mm. The cooling curve was recorded with constant stirring of the naphthalene.

The thermal emf was measured with the aid of a low-resistance type PPTN potentiometer with an accuracy to 1 microvolt.

Metals for calibration were molten in graphite crucibles 100 mm high and 30 mm in diameter. The crucibles were installed in a deep muffle furnace with platinum winding (Fig. 7).

Table 1

Calibration of Thermocouples

Substance	Hardening Temperature, $^\circ C$	E, micro-volts	Probable error, microvolts
Naphthalene	80,1	502	±1
Tin	231,9	1746	±2
Lead	327,35	2643	±2
Zinc	419,48	3556	±1
Antimony	630,5	5776	±1
Copper	1083,0	11126	±1

A thermocouple in a protective cap made of porcelain or corundise was introduced into the furnace and centered by means of holes in the covers. Each of four thermocouples was calibrated twice: at a depth of immersion in the metal of 70 and 80 mm. Such a method of calibration insured a high degree of accuracy.

The values of the thermal emf of the thermocouple, obtained as the arithmetic mean of eight measurements for each point, are shown in Table 1.

The probable error in the measurement of the thermocouple reaches two microvolts. At low temperature it amounts to approximation $\pm 0.5^\circ$ C, and at high temperature it is approximation $\pm 0.2^\circ$ C.

From the data obtained we can write an equation for the emf.

At a temperature of 0-300° C

$$E = 5{,}406t + 0{,}0116t^2 - $$
$$- 0{,}00001053\ t^3\ \text{(microvolts)}$$

At a temperature above 300° C

$$E = -333{,}6 + 8{,}448t + 0{,}00197\,t^2\ \text{(microvolts)}$$
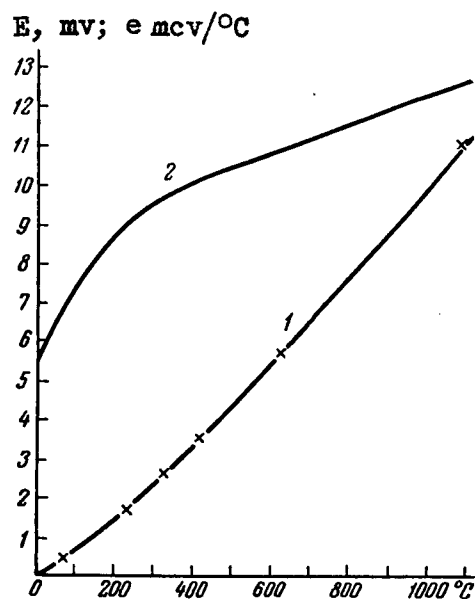
Fig. 8. Calibration Curve and its Derivative for a Platinum-Platinum Rhodium Thermocouple:

1 -- E, millivolts; 2 -- dE/dT, microvolt per degree C.

On the basis of numerous experiments, the thermal emf of the $\underline{/}$ Pt - (Pt + Rh) $\underline{/}$ thermocouple obeys a parabolic law in the range from 300 to 1200°C. Consequently, the last formula can serve for calculations up to 1200° C with sufficient practical accuracy.

To determine the differntial emf of the thermocouple, the resultant equations are differentiated.

30

However, in the range from 270 to 350° C it is necessary to resort to an intermediate formula:

At a temperature from 0 to 270° C

$$e = 5{,}406 + 0{,}0232\,t - 0{,}0000316\,t^2 \qquad (\text{microvolt}/^\circ\text{C})$$

At a temperature from 270 to 350° C

$$e = 7{,}811 + 0{,}00576\,t \quad (\text{microvolt}/^\circ\text{C})$$

At a temperature from 350 to 1200°C

$$e = 8{,}448 + 0{,}003939\,t \quad (\text{microvolt}/^\circ\text{C})$$

The entire variation from 0 to 1200°C cannot be covered by a single formula.

Table 2 and Fig. 8 show the calibration data for the thermocouple investigated by us.

Table 2

Thermal emf of a Pt - (Pt + Rh) Thermocouple

°C	E, micro-volts	e, microvolt/°C	°C	E, micro-volts	e, microvolt/°C
0	0	5,41	600	5 444	10,81
100	646	7,41	700	6 545	11,21
200	1 461	8,78	800	7 685	11,60
300	2 382	9,54	900	8 865	11,99
400	3 361	10,02	1 000	10 084	12,39
500	4 382	10,42	1 100	11 342	12,78

31

3. COMPARISON ELECTRODE

The comparison electrode employed can be a metal whose thermal emf is well known and stable within the required temperature range. The selected metal should have thermoelectric characteristics that vary smoothly with the temperature, should have no transformations in the given range of temperatures. Of all the known metals, the one investigated **in** greatest detail is copper.
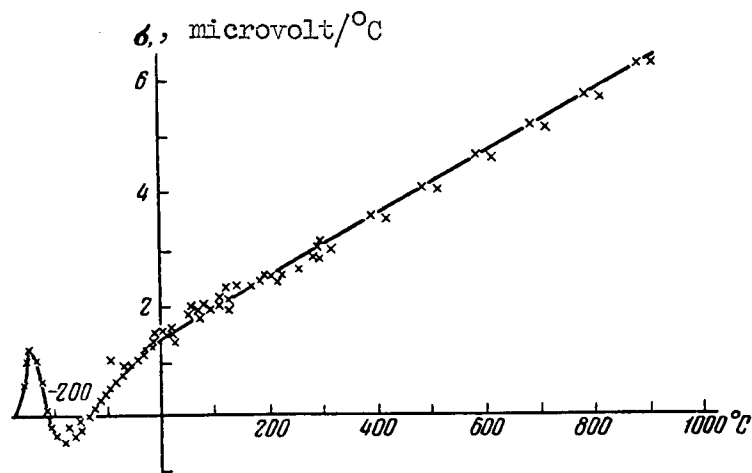
Fig. 9. Thomson emf of copper.

It is possible to derive with sufficient accuracy the temperature dependence of the absolute thermal emf of copper on the basis of the work by Berg $/51/$, Young $/53/$, Borelius $/55/$, Borelius and Gunneson $/56/$, Borelius, Keesom and Johansson $/57/$, Lander $/58/$ and Nystrom $/59/$.

Fig. 9 shows the Thomson emf of copper as a function of the temperature on the basis of the works of the above-mentioned authors. In spite of the great variety in the measurement methods and the differences in the copper specimens, all these data are in good agreement with each other. Obviously, a small amount of impurity does not exert a substantial effect on the thermoelectric properties of copper.

On the basis of investigations made by earlier authors and on the basis of his own investigations, Borelius $/48/$ plotted the curve for the absolute thermal emf of copper as a function of the tempera-

32
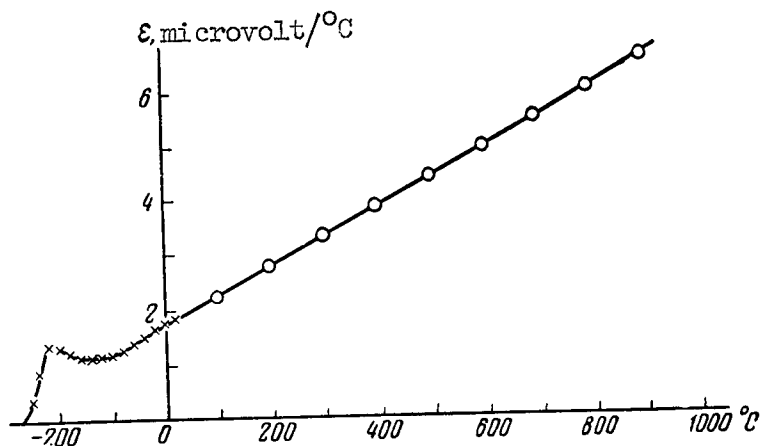
Fig. 10. Absolute thermal emf of copper.

ture from absolute 0 to 200° C. Nystrom [59] supplemented his data up to 900° C. Comparing all the above data, the author finds that the absolute thermal emf of copper as a function of temperature can be expressed by an equation valid from 0 to 900° C.

$$\varepsilon_{Cu} = 1{,}722 + 0{,}00534\,t \quad (\text{microvolt/°C}) \qquad (1)$$
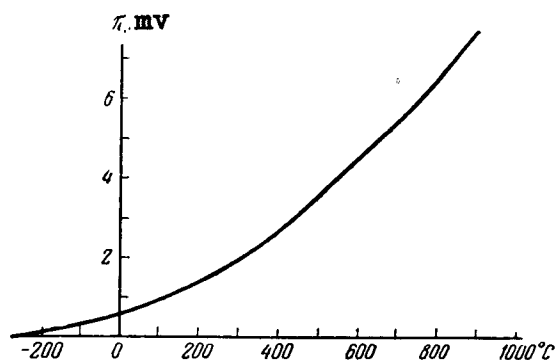
Fig. 11. Thermoelectric potential of copper.

Table 3 lists the values of the absolute thermal emf of copper, ε_{Cu}, according to data by Borelius [49], Nystrom [59], and cal-

culated from Eq. (1). The same table contains the values of the Thomson emf σ and the thermoelectric potential π, whown in Figs. 9, 10 and 11.

It would appear that copper is the most convenient comparison electrode, but after prolonged operation at temperatures above 300° it rapidly oxidizes and the electrode goes out of order.

A fully stable comparison electrode can be made of platinum, but its properties have been investigated in less detail in spite of the numerous experiments. Probably, even small impurities exert a considerably greater influence on the properties of platinum than on those of copper. Therefore, the primary comparison electrode was copper made by the Hilger Company, with a specific electric resistivity $\rho_0 = 1.56$ microhm-centimeter at 0°C, and $\rho_{100} = 2.235$ microhm-centimeter at 100°C.

The temperature coefficient of electric resistivity is

$$\rho_{100} : \rho_0 = 1{,}431.$$

The same value of temperature coefficient is given for the purest copper by Holborn /67/.

Thermocouple platinum, calibrated relative to copper, served as a constant comparison electrode for our experiments. To determine its absolute thermal emf, a thermocouple was made up of platinum and copper and the cold junction of this thermocouple was placed in a Dewar with ice.

The calibration was carried out against the hardening temperatures of pure metals as is found in the preceding section.

Table 4 gives the values of the thermal emf.

On the basis of the data obtained we compiled the following equations for the thermal emf:

At temperatures 0 to 300° C

$$E = 5{,}026t + 0{,}0214t^2 - 0{,}00001344t^3 \text{ (microvolt)}$$

Table 3

Thermoelectric Properties of Copper

T, °K	t, °C	ε_{Cu}, microvolt/°C			σ, microvolt/°C	π, mv
		Borelius	Nystrom	the author		
18,1	—255	0,34	—	—	0,50	0,006
33,1	—240	0,89	—	—	1,22	0,029
73,1	—200	1,37	—	—	—0,37	0,100
113,1	—160	1,15	—	—	—0,34	0,130
153,1	—120	1,15	—	—	0,28	0,176
193,1	— 80	1,30	—	—	0,91	0,263
233,1	— 40	1,51	—	—	1,24	0,351
273,1	0	1,73	—	1,72	1,46	0,470
373,1	100	2,23	—	2,26	1,99	0,84
473,1	200	2,75	2,77	2,79	2,53	1,32
573,1	300	—	3,31	3,32	3,06	1,91
673,1	400	(3,79)	3,85	3,86	3,59	2,60
773,1	500	—	4,39	4,39	4,13	3,39
873,1	600	(4,84)	4,93	4,93	4,66	4,30
973,1	700	—	5,47	5,46	5,20	5,31
1073,1	800	—	6,01	5,99	5,73	6,42
1173,1	900	—	6,55	6,53	6,26	7,65

Table 4

Calibration of Pt-Cu Thermocouple

Substance	Hardening Temperature, °C	E of thermocouple, microvolt
Naphthalene	80,1	533
Tin	231,9	2149
Lead	327,3	3467
Zinc	419,4	4915
Antimony	630,5	8869

At temperatures above 300° C

$$E = -317 + 8,314t + 0,00992t^2 \ (\text{microvolt})$$

The last equation can be extrapolated to 1200° C. Differentiating these equations and eliminating the absolute thermal emf of copper, we obtain equations for the absolute thermal emf of thermocouple platinum:

At temperatures from 0 to 300° C

$$\varepsilon_{Pt} = -3,30 - 0,0375t + 0,00000403t^2 \ (\text{microvolt}/°C)$$

At temperatures above 300° C

$$\varepsilon_{Pt} = -6,59 - 0,0145t \ (\text{microvolt}/°C)$$

The values of the absolute thermal emf of thermocouple platinum are given in Table 5 and in Fig. 12.
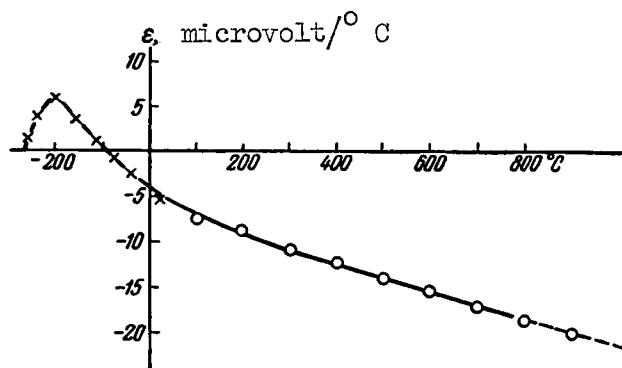
Fig. 12. Absolute thermal emf of thermocouple platinum.

These data were verified by the differential method, as described in Section 5 of this chapter and give good consistent results up to 1000° C. Fig. 12 shows the results compared with the data of Borelius and Nystrom.

Investigated specimen
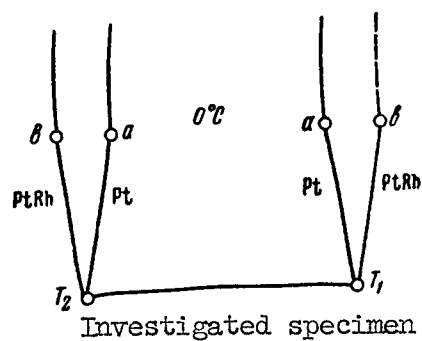
Fig. 13. Principal diagram of measurement of
differential thermal emf.

Table 5

Absolute Thermal emf of Thermocouple Platinum

t, °C	ε_{Pt}, mcv/°C	t, °C	ε_{Pt}, mcv/°C
0	— 3,30	700	—16,74
100	— 6,65	800	—18,19
200	— 9,20	900	—19,64
300	—10,94	1000	—21,09
400	—12,39	1100	—22,54
500	—13,84	1200	—23,99
600	—15,29	—	—

4. MEASUREMENT OF THE INTEGRAL THERMAL EMF

The determination of the integral thermal emf was carried out
by two methods. The first method -- using fixed points -- was al-
ready described in Section 2 of this chapter.

This method is applicable only if the emf vs. temperature
curve is unconditionally smooth and if the homogeneity of the wire
is high.

Another method, the comparison method, was used to investi-
gate solid solutions.

The investigated specimens were included in porcelain capillaries and were welded on one end to the hot junction of the thermocouple. The cold ends were connected to copper conductors by means of Wood's alloy and immersed in glass test tubes placed in a Dewar vessel with ice. The connection to the potentiometer was through a switch. The comparison electrode was thermocouple platinum, calibrated relative to copper.

The hot junction was placed in a quartz tube, sealed on one end, which was inserted as required inside a tubular furnace having a considerable temperature gradient. The furnace was heated to a maximum temperature in the central portion and was on all the time. Thus, a comparatively constant **temperature** was maintained in it at all times. The fluctuations of the temperature, resulting from the variations in line voltage, were quite slow, owing to the inertia of the oven and did not influence particularly the measurements.

By moving the quartz tube 10 or 15 mm along the axis of the oven the temperature of the hot junction was changed by 30 to 50° C. The temperature settled within 15 or 20 minutes. The thermal emf was read for several specimens, and the tube was placed further along the axis of the oven.

This method is sufficiently accurate and rapid, since it permits simultaneous measurement with several specimens (depending on the number of poles in the switch). The measurement errors were due to inaccuracy in reading, inhomogeneity of the wire, and a certain lack of constancy in the temperature; these were superimposed on the errors in calibration of the thermocouple and of the comparison electrode. Consequently this method is less accurate than the first one, but it makes it possible to obtain any number of readings for each specimen. The second method, like the first, gives very accurate results only in the case of smooth variation of the curve and of the thermal emf as functions of the temperature and requires long wires; consequently, it is applicable only to plastic alloys.

To determine the other thermoelectric properties, the integral thermal emf was plotted on graph paper as a function of the temperature on a large scale, and geometrical differentiation was used to determine the differential thermal emf:

$$e = \frac{dE}{dT}.$$

The absolute value of the differential thermal emf of the investigated specimen was found from the Thomson-Nernst equation

$$e = \varepsilon_x - \varepsilon_0,$$

where ε_0 is the absolute thermal emf of the comparison electrode (in our case platinum). This is given in Table 5 and in Fig. 12.

The thermoelectric potential of the investigated specimens was determined from the first Thomson equation

$$\pi = T\varepsilon_x,$$

where T is the absolute temperature. The Thomson emf was determined by a second graphic differentiation

$$\sigma = T\frac{d\varepsilon_x}{dT}.$$

The use of double graphic differentiation is possible only for metals and alloys which have no transformations in the investigated temperature interval, and requires great care in plotting the curves.

5. MEASUREMENT OF THE DIFFERENTIAL THERMAL EMF

The differential thermal emf can be measured using specimens of any shape.

Usually one uses in the experiments wire 20 to 40 mm long, rods drawn of molten metal into porcelain tubes, and pieces of metal of irregular shape. Two thermocouples are welded to the ends of the investigated specimens. The welding is with the aid of an electric arc. Borax is used to prevent oxidation of the metal during the welding.

The investigated specimen together with the thermocouples was inserted into a quartz tube sealed on one end, which was placed along the axis of the horizontal oven in which a certain temperature gradient was maintained.

To increase the temperature of the specimen, the quartz tube with the thermocouples and specimen were moved towards the center of the oven. The cold junctions of the thermocouple were placed in a Dewar vessel with melting ice. The principal diagram of the measurement of the differential thermal emf is shown in Fig. 13. Thermocouples were used to measure the temperatures of the ends of the specimen, T_1 and T_2. The measurement between points a and a correspond to the thermal emf ΔE_a , produced in the investigated speci-

men when coupled with platinum at a temperature difference ΔT = T_2 - T_1.

In this case the differential thermal emf was determined from the equation

$$e = \frac{\Delta E_a}{\Delta T}.$$

The determination of the temperature difference ΔT was by a differential method. For this purpose the potential difference ΔE_b was measured between b and b.

The difference in readings

$$\Delta E_c = \Delta E_b - \Delta E_a$$

is the thermal emf of the Ti - (Pt + Rh) thermocouple corresponding to the temperature difference ΔT, since in accordance with the Thomson-Nernst equation

$$\Delta E_a = \Delta E_{\mathrm{Pt}} - \Delta E_x,$$
$$\Delta E_b = \Delta E_{\mathrm{PtRh}} - \Delta E_x.$$

In these equations ΔE_{Pt} ΔE_{PtRh}, and ΔE_x are the absolute thermal emf's of platinum, platinum-rhodium, and the investigated specimen, corresponding to the temperature difference ΔT.

The differential thermal emf of the thermocouple (Table 2 and Fig. 8) is

$$e_c = \frac{\Delta E_c}{\Delta T}$$

and

$$\Delta T = \frac{\Delta E_c}{e_c}.$$

Thus, the differential thermal emf of the investigated specimen coupled with platinum is given by the equation

$$e_{Pt-x} = \frac{\Delta E_a}{\Delta E_b - \Delta E_a} \, e_c.$$

This formula serves as the principal equation for the calculation of the thermal emf. Its sign is determined by the sign of ΔE_a relative to platinum.

The absolute thermal emf was determined from the equation

$$\dot{\varepsilon}_x = \dot{e}_{Pt-x} + \varepsilon_{Pt},$$

where ε_{Pt} is the absolute thermal emf of platinum (given in Table 5 and in Fig. 12). The obtained values of ε_x were referred to the average temperature.

As indicated in the preceding section, the thermoelectric potential was calculated from the equation

$$\pi = T\varepsilon_x.$$

The Thomson emf was found from

$$\sigma = T\frac{d\varepsilon_x}{dT},$$

and the derivative $\frac{d\varepsilon_x}{dT}$ was found by geometric differentiation. In this case the differentiation gave sufficiently accurate results and could be used in the presence of any transformation occurring in the metals.

6. APPLICATION OF THE KURNAKOV PYROMETER TO THE MEASUREMENT OF THE THERMAL EMF

The use of a Kurnakov pyrometer for the investigation of thermoelectric properties of alloys gave quite fruitful results, particularly in those cases, when the alloys had transformations [69].

The short duration of the experiment (only 40 minutes) makes it possible to investigate alloys with non-noble metals, which are oxidized quite readily.

The use of the Kurnakov pyrometer excludes the possibility of accidental subjective measurement errors, although the accuracy of the pyrometer is so much lower than the accuracy of a potentiometer. The thermal emf curves are plotted with the aid of three mirror galvanometers. The principal diagram showing the connections to the galvanometers to the thermocouples and to the investigated specimens is shown in Fig. 14. Here galvanometer 1 indicates the temperature T_2, galvanometer 2 reads the thermal emf, ΔE_a, of the investigated specimen x coupled with the platinum, while galvanometer 3 reads the thermal emf ΔE_b of the investigated specimen coupled with a platinum-rhodium alloy, in the temerature range $\Delta T = T_2 - T_1$. In the diagram r_1, r_2 and r_3 are shunts for the galvanometers. The resistances of the shunts are somewhat greater than the critical resistances of the galvanometer. R_1, R_2 and R_3 are decade boxes used to regulate the deflections of the galvanometers.

The resistance R_1 was so chosen that at a temperature $T_2 = 1200^{\circ}C$, the "spot" of the galvanometer does not leave the limits of the drum, so that at a drum length of 240 mm a 1 mm deflection of the galvanometer corresponds approximate to $5^{\circ}C$.

The resistances R_2 and R_3 were chosen such that the both galvanometers had equal sensitivity:

$$\Delta E_a = aA_2; \quad \Delta E_b = aA_3,$$

where A_2 and A_3 are the deflections of galvanometers 2 and 3.

The proportionality coefficient a was exactly the same in both cases:

$$a = \frac{\Delta E_a}{A_2} = \frac{\Delta E_b}{A_3} .$$

In our case a = 10 microvolts per millimeter.

With such a ratio, the differential thermal emf coupled with platinum was determined from the equation

$$e_{Pt-x} = \frac{\Delta E_a}{\Delta E_b - \Delta E_a} e_c = \frac{A_2}{A_3 - A_2} e_c,$$

42
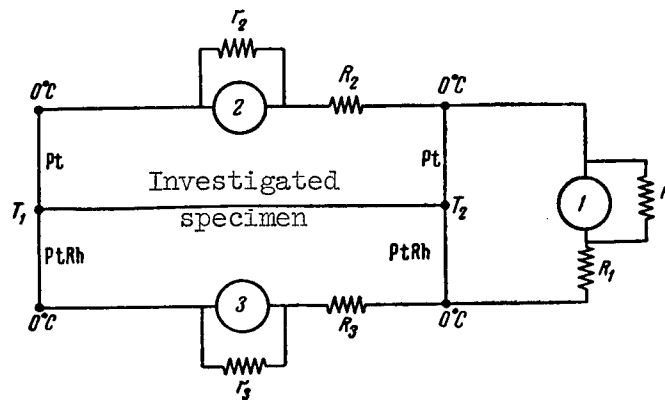
Fig. 14. Principal diagram for the measurement
of the thermal emf with the Kurnakov
Pyrometer.

where e_c is the differential thermal emf of the Pt - (Pt + Rh) thermocouple, given in Table 2. The temperature difference can be determined from the equation

$$\Delta T = \frac{\Delta E_b - \Delta E_a}{e_c} = \frac{a}{e_c}(A_3 - A_2).$$

The temperature of the cold junction is

$$T_1 = T_2 - \Delta T.$$

The null position of the galvanometer 1, which indicates the temperature, was set at the left side of the drum, and the pointers of galvanometers 2 and 3 were set at the center of the galvanometer. The null lines were recorded on each sheet, and the specimen together with the thermocouples was immersed in a Dewar flask with ice, where the cold junctions of the thermocouples were also placed. The null lines of galvanometers 2 and 3 are best superimposed.

Before proceeding to the measurement, the instrument was calibrated. For this purpose a specimen with the thermocouples welded to it was placed in an oven and kept there until its temperature became constant. The junction between the connection of the thermocouples to the potentiometer is shown in Fig. 15, which shows the connection diagram of the instruments. After a constant temperature was reached, the readings were taken with the potentiometer. Simultaneously, the drum was rotated for three to five minutes, and the illumination of the mirror galvanometers was turned on. The horizon-

43

tal lines ΔE_b and $\Delta E_{b'}$ corresponding to T_2, were recorded. Several calibration points were fixed on one sheet. Thus the thermocouple was calibrated and the accuracy of the ratio a = 10 microvolts per millimeter were simultaneously checked.

During the further course of the investigation, one calibration point was placed on each sheet and the zero lines was drawn. This verified the correctness and the constancy of the calibration.
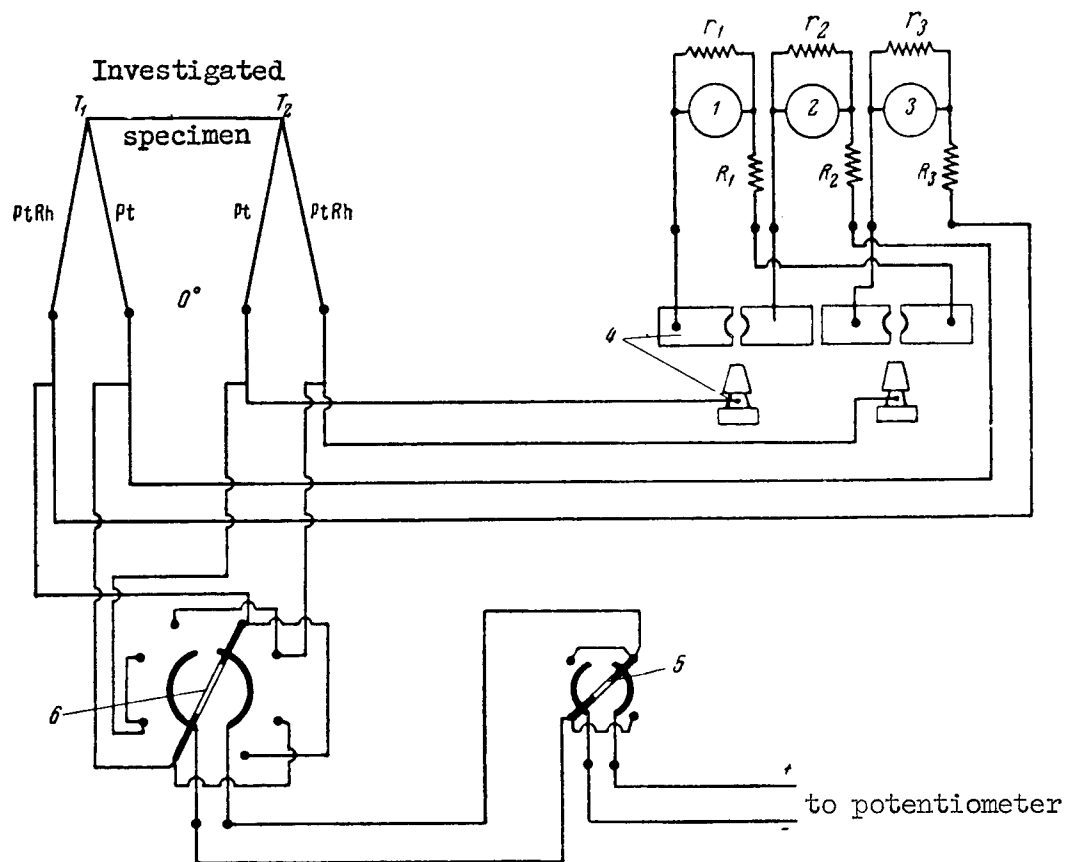
Fig. 15. Circuit for Measuring the Differential Thermal emf With a Kurnakov Pyrometer and a Potentiometer:

1, 2, 3 -- galvanometers; 4 -- plug disconnect; 5 -- reversing switch; 6 -- transfer switch.

The curves of the thermal emf were recorded while heating. For this purpose a special oven was constructed with two platinum windings. Such a construction of oven made it possible to regulate the temperature difference at the ends of the investigated specimens.

Fig. 16 shows a section through the oven, the placement of a specimen in it, and the connection diagram of the instruments. A rheostat was connected in parallel with the oven to regulate the temperature difference. The center tap of the furnace winding was connected to the slider of the rheostat. The furnace was supplied through a variac. At first approximately 40 or 50 volts were applied to the furnace. Then, the variac was rotated at uniform speed with the aid of a telechron motor with a reduction gear. The motor operated at a rate of 40 minutes for every revolution. Thus, by the end of the recording almost the total line voltage, approximately 100 volts, was applied to the furnace, at a current of 3 amperes. During this time the furnace was heated to 1200° C. After 40 minutes the drum of the parameter with the photographic paper had made one complete revolution. With this method of heating the temperature was increased very uniformly. The temperature difference between the end of the specimen increased from zero to a certain limit, which in our experiments amounted to 5 to 30° C.

The temperature difference was regulated in such a way, that the curves did not go beyond the limit of the sheet. Usually the position of the motion of the regulating rheostat was chosen beforehand and remained constant during the time of recording of the curve. If the deviations of the galvanometer were too small or too large, it became necessary to change the temperature difference, which was eliminated without affecting the accuracy of the measurement by shifting the slider of the rheostat into the necessary direction. After completing the recording, the illuminators of the galvanometers were turned off, the furnace current was reduced to 1.5 or 2 amperes, a constant temperature was established in the furnace, and then the reference point was recorded, verifying it with the potentiometer.

The experiment was repeated twice for each alloy at different directions of the heat flux. The first experiment was at $T_2 > T_1$, and the second at $T_2 < T_1$. In the first case the temperature, registered with galvanometer 1, corresponded to the hot junction $(T_2 > T_1)$, and in the second to the cold junction $(T_2 < T_1)$.

When the direction of the heat flux is reversed, the voltages ΔE_a and ΔE_b reverse their signs.

Typical diagrams of the records are shown in Figs. 17 to 21.

The diagrams were processed in the following manner: the reference points of the galvanometers were checked, and the points were marked on the temperature curve every 100° C. Then perpendiculars were drawn through these points to the zero lines. For each

temperature a measurement was made of the deflections of the galvano-
meters 2 and 3 (A_2 and A_3). The differential thermal emf of the in-
vestigated specimen coupled with the platinum were determined from
the formula

$$e_{\mathrm{Pt}-x} = \frac{A_2}{A_3 - A_2} e_{\mathrm{c}}.$$

The absolute thermal emf and other thermoelectric properties
were determined by the method indicated in Section 5 of this chapter.
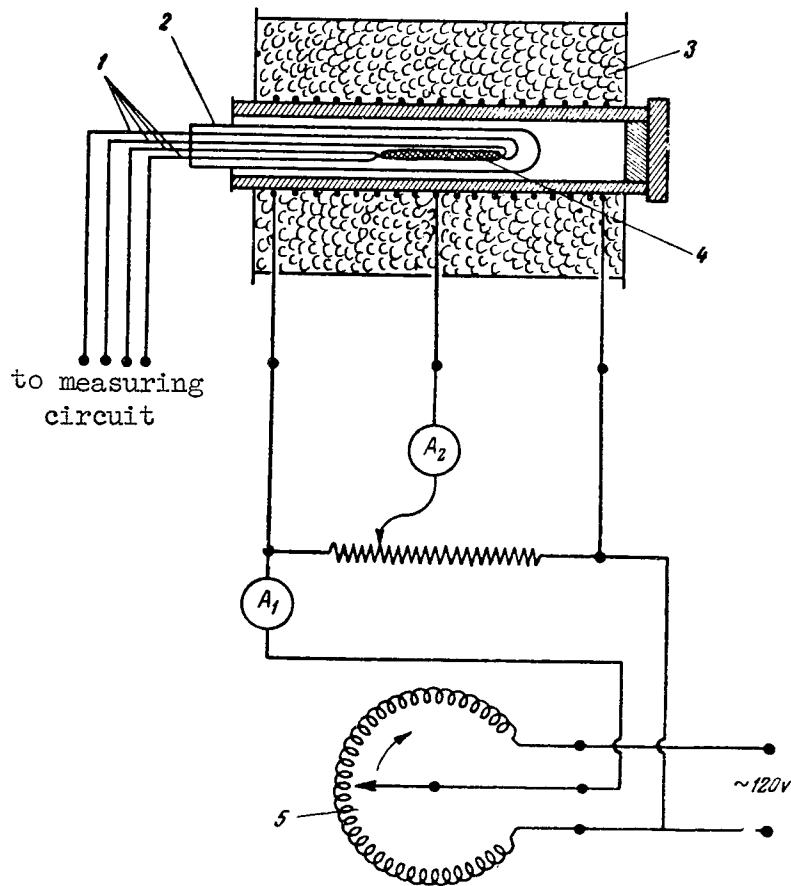
Fig. 16. Diagram of furnace used to measure the
differential thermal emf.

1 -- thermocouple; 2 -- quartz tube; 3 --
furnace; 4 -- investigated specimen; 5 --
variac.

The use of the Kurnakov pyrometer in the study of thermoelectric properties of alloys gives a rapid and accurate method of measurement, which makes it possible to investigate the alloys over a broad temperature interval.
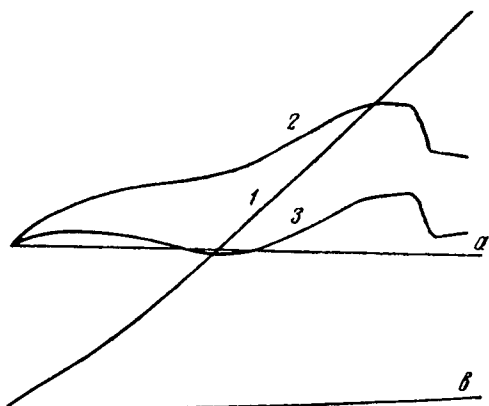
Fig. 17. Curves of the Thermal emf of Iron, Recorded With a Kurnakov Pyrometer: 1, 2, 3 -- Curves Corresponding to the Readings of the Galvanometers; a, b -- Zero Lines of the Galvanometers.
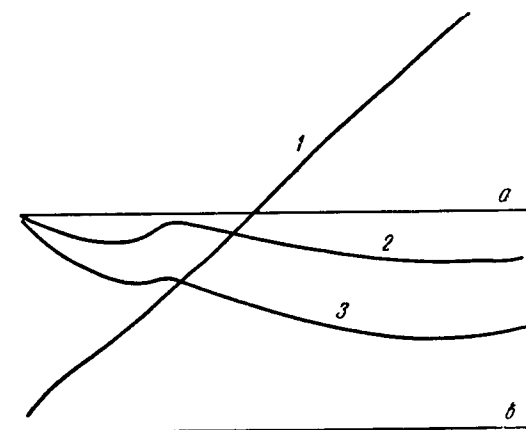
Fig. 18. Curves of the Thermal emf of Nickel, Recorded With a Kurnakov Pyrometer: 1, 2, 3 -- Curves Corresponding to Indications of the Galvanometers; a, b -- Zero Lines of the Galvanometers.
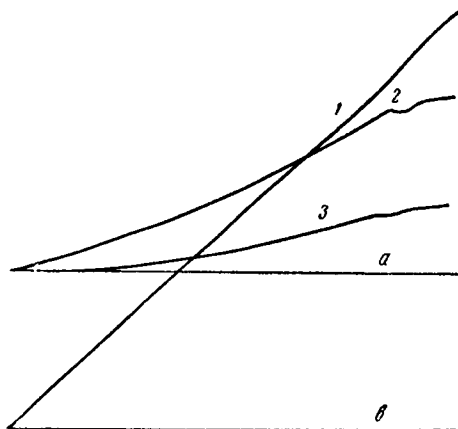
Fig. 19. Curves of the Thermal emf of Rhodium, Recorded With a Kurnakov Pyrometer: 1, 2, 3 -- Curves Corresponding to the Readings of the Galvanometer; a, b -- Zero Lines of the Galvanometers.
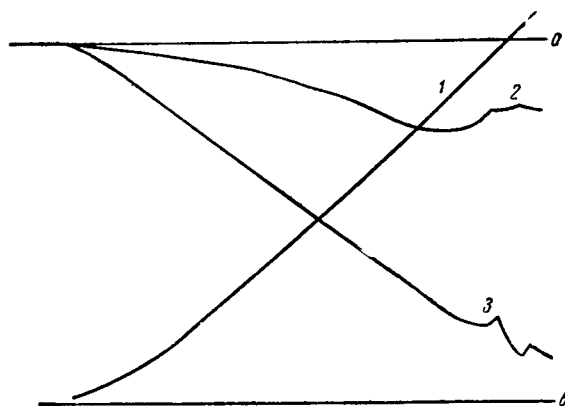
Fig. 20. Curves of the Thermal emf for a PtCu compound, Recorded With a Kurnakov Pyrometer: 1, 2, 3 -- Curves Corresponding to the Indications of the Galvanometer; a, b -- Zero Lines of the Galvanometers.
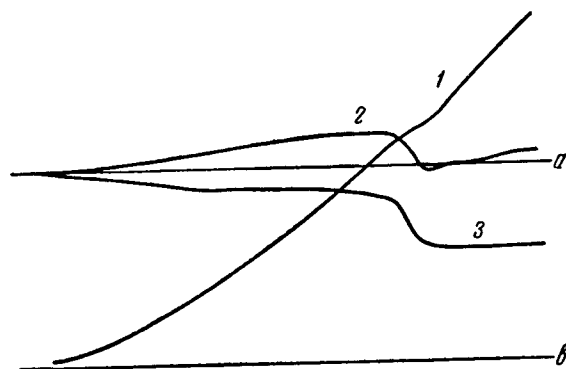
Fig. 21. Curves of the Compound PtCu₅,
Recorded With a Kurnakov Pyrometer.
1, 2, 3 -- Curves Corresponding to the
Readings of the Galvanometer; a, b -- Zero
Lines of the Galvanometers.

7. CONCLUSIONS

In this chapter we describe a generally accessible, very
simple and rapid method for the measurement of thermoelectric pro-
perties of metals and alloys. With the aid of this method one de-
termines the absolute values of the thermoelectric properties, which
have the greatest physical meaning. Only in such a case is it poss-
ible to compare and establish a connection between thermoelectric
properties of a metal and its other physical properties. In order
to eliminate the properties of the comparison electrode from the
obtained quantities, a detailed study was made of the thermal emf
of copper and platinum, relative to which the thermoelectric proper-
ties of the investigated specimens were determined.

In this chapter we describe in detail the method of measuring
the absolute thermal emf with the aid of a Kurnakov pyrometer.

A recording method employing photographic recording is supe-
rior to all other methods of measurement in that the readings of
the experimental data are objective. The continuity of the record
curve on photographic paper makes it possible to investigate the
process of heating or cooling of the metal in its completeness and
to obtain any number of experimental points. Finally, the record-
ing method makes it possible to carry out the process with any pre-
scribed speed.

48

As a preparatory stage for the method described above, we had to resort to a detailed development of an investigation method using a potentiometer. This method was used in all measurements and acts as control in individual cases; sometimes it serves as an independent method.

Particularly fruitful results were obtained using the Kurnakov pyrometer for metals and alloys in which transformations were observed.

This method is not only usable for measuring the thermal emf, but is also a unique method of differential thermal analysis.

The emf's of two differential thermocouples, platinum -- the investigated specimen -- platinum, and platinum-rhodium -- investigated specimen -- platinum-rhodium, were recorded on photographic paper. During the process of heating, the hot junction was first to go thru the transformation temperature, followed by the cold junctions of the differential thermocouples. Both points controlled each other.

One of the principal advantages of the described thermoelectric method is that the measured quantities are independent of the shape and dimensions of the investigated specimens.

CHAPTER III

INVESTIGATION OF THERMOELECTRIC PROPERTIES OF
PURE METALS

1.   INTRODUCTION

        Many investigations of pure metals, made in the 19th century
by Seebeck /2/, W. Thomson /4/, Mattiessen /70/, Avenarius /8/,
Bakhmet'yev /10,11/ and others are at the present time of only histo-
rical interest. Only by the end of the past century, after suffi-
ciently pure metals and accurate measuring instruments were avail-
able, were trustworthy papers published.

        A common shortcoming of many investigations is the fact that
the comparison electrode use was made of metal with unknown thermo-
electric properties. This shortcoming does not make it possible to
compare the results of the different authors and to calculate the
absolute values of the thermoelectric properties.

        However, many of the older works (by Holborn, Day and others),
were made with great accuracy, using very pure metals, and have a
practical value even now.

        Fig. 22 shows the integral thermal emf's of pure metals
coupled with platinum, according to Rohn /71/ and Pelabon /72/.

        Elements of the semiconductor type, such as silicon, have
very high positive thermal emf. On the other hand, bismuth has a
large negative thermal emf. Most metals are positive relative to
platinum. The highest emf is that of tungsten and molybdenum.

        The thermal emf of noble metals (Fig. 23), namely gold, sil-
ver, palladium, rhodium, and iridium, were investigated by Holborn
and Day /73,74/in 1900. The authors used very pure metals and made

the investigations very carefully. The subsequent investigations did not add substantially to their data. The polymorphism of rhodium is not reflected in the integral thermal emf.

Ruthenium was investigated by Jaeger and Rosenbohm /75/. The polymorphism of ruthenium is not reflected in the curve obtained by them for the integral thermal emf. Lander /58/ investigated the Thomson emf for gold, silver, copper, platinum, palladium, molybdenum, and tungsten. His data are shown in Fig. 24.

Of great interest is the investigation of thermoelectric properties of metals over a wide range of temperatures, in transitions from one aggregate state into another or from one modification into another.
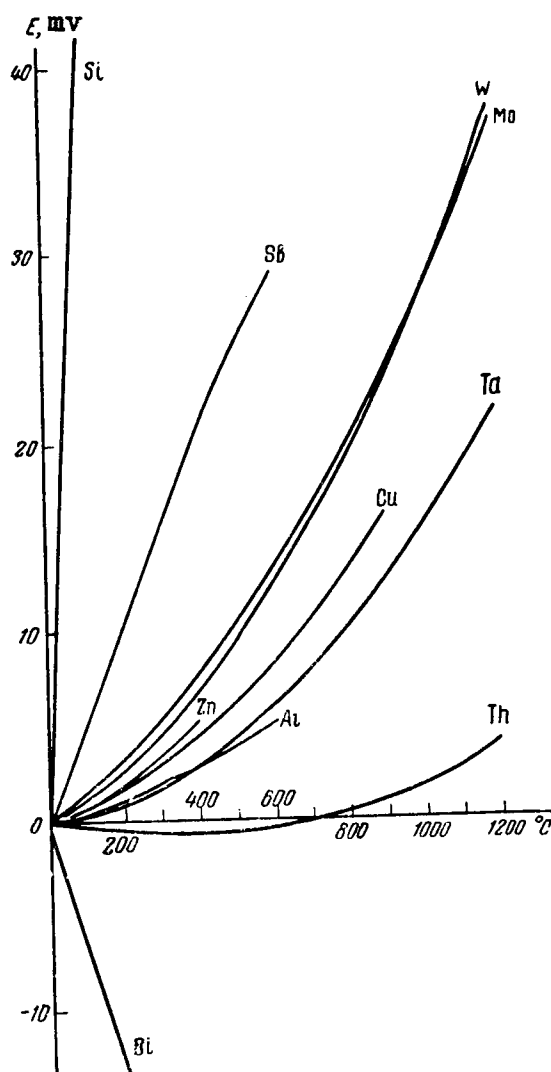
Fig. 22. Thermal emf of Pure Metals Coupled with Platinum.
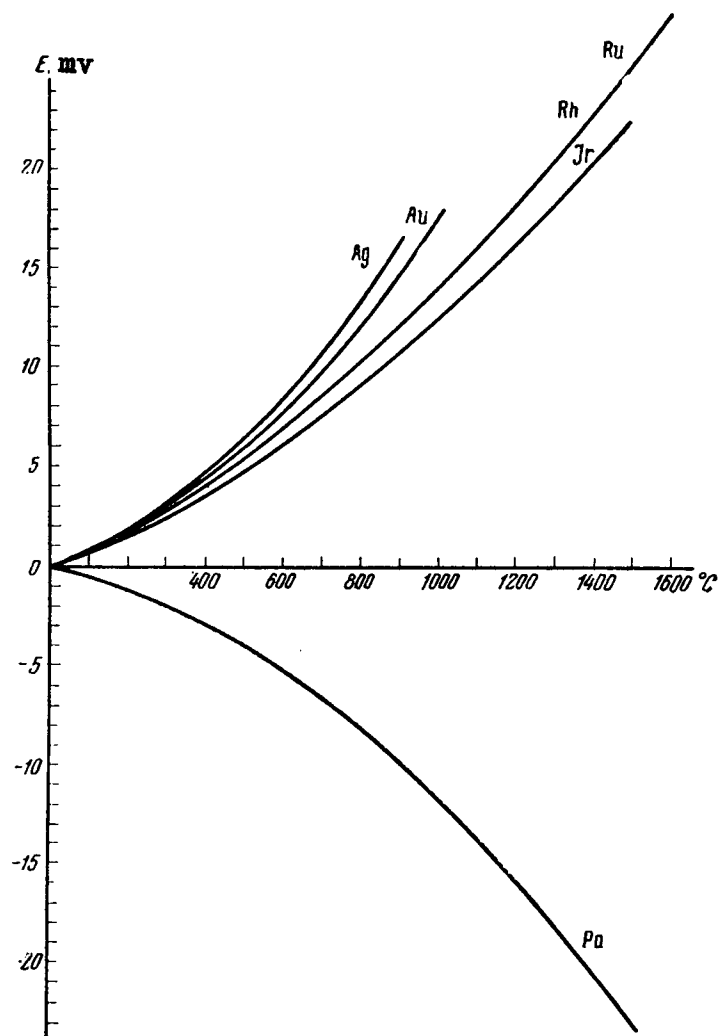
Fig. 23. Thermal emf of Noble Metals Coupled
with Platinum.
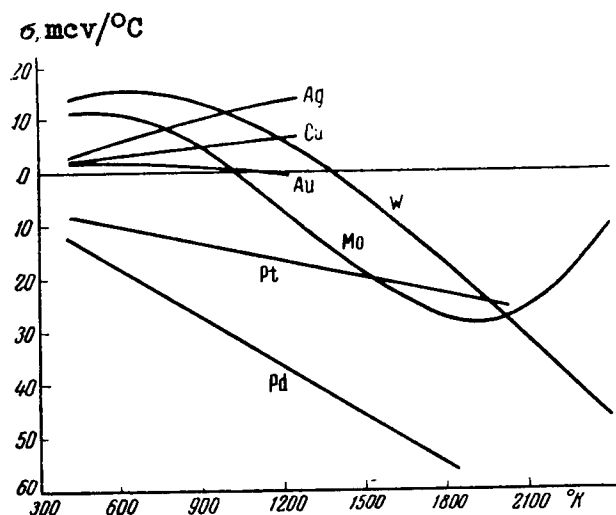
Fig. 24. Thomson emf of Pure Metals, after Lander.
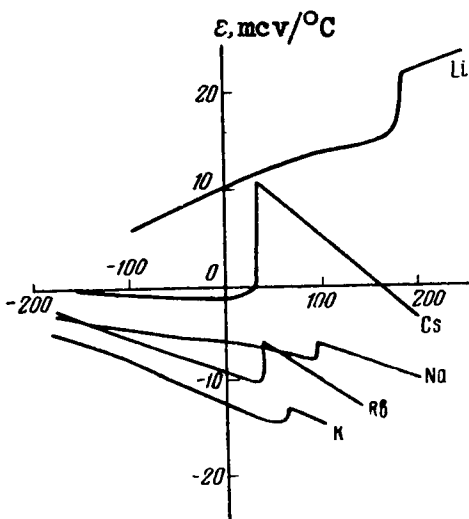
Fig. 25. Absolute Thermal emf's of Alkali Metals
after Bidwell.

To each phase state of a metal there corresponds a regular
variation of the thermoelectric properties as a function of the tem-
perature. When changing from one phase state to another, one ob-
serves corresponding changes in the thermoelectric properties.

The classical investigation of thermoelectric properties of

53

alkali metals, carried out by Bidwell /64/, has shown that at the melting point one observes a jump-like change in the differential thermal emf.

Fig. 25 shows curves of the absolute thermal emf of alkali metals, calculated from Bidwell's data. In changing over from the solid state to the liquid one, one observes a jump-like change in the absolute thermal emf. For cesium the jump reaches 12 microvolts per degree C, for potassium it is negligibly small, approximately 1 microvolt per degree C.

An investigation of the integral thermal emf does not give a clear picture of the transformations in metals. Fig. 26 shows curves for the integral thermal emf of iron, cobalt, and nickel coupled with platinum, plotted according to Rohn's data /71/. Here the polymorphism of the metals manifests itself in smooth inflections, and only approximate data can be obtained on the transformation temperature.

Of entirely different shape are the curves of the differential thermal emf of iron, shown in Fig. 27, coupled with platinum. These curves were plotted from the data of Burgess and Scott /63/, and on the data of Goetz /76/ for high temperatures.

Borelius, Keesom, Johansson, and Linde /57,77/ investigated noble metals at low temperatures, close to absolute zero. They have investigated in detail the absolute thermal emf of a normal silver electrode, containing 0.37 atomic percent gold. Such an alloy has a smoothly varying thermal emf at low temperatures. The authors have compared many metals against this alloy. This made it possible to determine their absolute thermal emf. They established a sufficiently complicated temperature relationship at low temperatures, the absence of thermoelectric phenomena in superconductors, and a jump-like change in the absolute thermal emf upon transition from the superconducting state into the conducting one.

In this chapter we describe investigations of thermoelectric properties of several pure metals, having a purity that is the maximum available to the author.

In addition to the investigations of noble metals (platinum, palladium, rhodium, gold, and silver), we describe also investigations of metals in the iron group, which are of great interest owing to the abundance and variety of their polymorphic transformations.

Fig. 26. Thermal emf of Iron, Cobalt, and Nickel
Coupled with Platinum.

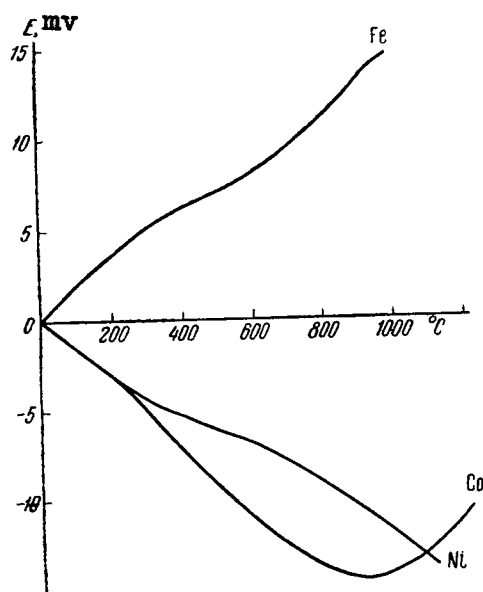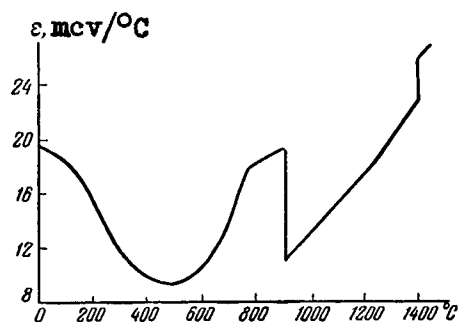Fig. 27. Differential Thermal emf of Iron, Coupled
with Platinum.

2. INVESTIGATION OF THERMOELECTRIC PROPERTIES OF METALS OF THE
IRON GROUP

The changes in the properties of iron, cobalt and nickel in
transition from modification into another has much in common with
the transformations in alloys.

55

The transition between various crystalline modifications (beta-Fe $\rightleftharpoons$ gamma-Fe) and (alpha-Co $\rightleftharpoons$ beta-Co) is carried out through first-order phase transitions, in which there occurs a jump-like rearrangement of the crystalline lattice. At the transition point, both modifications are in equilibrium. The change in the symmetry of the phases is not subject to any limitations. In first-order phase transitions the thermodynamic potentials of both phases are the same, the entropy changes jump-like, and the specific heat assumes an infinite value.

The theory of second-order phase transitions was developed by Landau and Lifshits /78/.

For ferromagnets at the Curie point one observes typical cases of phase transitions of the second kind, which is also characteristic in transition of metals into the superconducting state, the transition of liquid helium into the superfluid state, and is in certain cases characteristic of ordering of solid solutions.

V. K. Semenchenko /79/ includes among the second-order phase transitions also the critical phenomena that are observed upon transition of alloys from a heterogeneous mixture into a homogeneous solid solution.

Mutual transformations of two phases that differ from each other by some symmetry property, can proceed via a second-order phase transition, without necessarily changing the symmetry of the crystalline lattice.

At the curie points one observes no changes in the symmetry of arrangement of the atoms in the lattices of ferromagnets. It is therefore sometimes believed that α-iron and β-iron are not different phases. In this case we encounter changes in the symmetry of the arrangement of the elementary magnetic moments in the metal.

The states of both phases at the point of second-order transition are the same. The thermodynamic functions, the entropy, and the energy, all change without jump at the point of second-order transition. The specific heat experience a sharp increase with increasing temperature directly before the Curie point. At the point of transition one observes a jump-like decrease in the specific heat.

While the specific heat becomes infinite at a first-order transition point, in the case of a second-order phase transition the specific heat can have a finite value.

The thermoelectric properties of iron, cobalt, and nickel have been the subject of numerous investigations.

Thus, the differential thermal emf was investigated, as al-

ready mentioned, by Burgess and Scott [63] and Goetz [76]. Their data are shown in Fig. 27. A detailed investigation in the region of the α-iron $\longrightarrow$ β-iron transition was carried out by Ya. G. Dorfman, R. I. Yanus, K. V. Grigorov, and M. G. Chernikhovskiy [80], who found that a jump in the Thomson emf is observed at this point. However, the data of these authors are not comparable with those of the preceding investigations, since the comparison electrode used was nichrome, the thermoelectric properties of which are not known.

The differential thermal emf of cobalt was investigated by Schulze [81] who measured very few points, and therefore did not obtain the desired results at the α-cobalt $\longrightarrow$ β-cobalt transition point and at the point of magnetic transformation.

The thermoelectric properties of nickel were investigated many times. The most interesting data were obtained by Ya. G. Dorfman and R. I. Yanus [82], Ya. G. Dorfman and I. K. Kikoin [83], Grew [84], and Foster [85]. At the point of magnetic transformation there was established a jump-like change in the Thomson effect. Considering the value of the Thomson effect numerically equal to the specific heat of the atoms at the Curie point, the authors established the equality of these two quantities. It is therefore concluded that the conduction electrons are responsible for the ferromagnetism of nickel. However, after having investigated the Thomson effect for iron at the Curie point, the authors have refuted their views. [80]

Iron. Iron has four modifications.

α-iron has a space-centered cubic crystalline structure, stable to 768° C, and is ferromagnetic.

β-iron is stable in the temperature range from 768 to 910° C and has the same crystalline structure, but is non-magnetic.

γ-iron has a face-centered cubic lattice, is stable in the temperature interval from 910 to 1390° C.

δ-iron is stable in the temperature interval from 1390 to 1535° C (melting temperature), has the lattice of a space-centered cube, and is ferromagnetic, like α-iron.

We used in our investigations spectrally pure iron made by the Hilger Company. Specimens drawn into a wire 1 millimeter in diameter were welded to platinum thermocouples, placed in a furnace, and annealed at a temperature of 600°C. The thermal emf was determined with the aid of a Kurnakov pyrometer. The curve of a record made with a pyrometer is shown in Fig. 17. To verify the pyrometer, several points were monitored with the aid of a potentiometer.

Table 6 gives the values of the absolute thermal emf ε ,

the Thomson emf σ, and the thermoelectric potential π for iron.

Table 6

Thermoelectric Properties of Iron

Transformations	t, °C	ε, micro-volt/° C	σ, micro-volt/° C	π, mv
α	100	+6,3	—12,3	+2,31
	200	+3,1	—15,3	+1,46
	300	—0,2	—17,8	—0,12
	400	—2,8	—13,1	—1,88
	500	—3,8	—1,8	—2,94
	600	—3,4	+10,5	—2,97
	700	—1,7	+21,0	—1,66
	770	—0,1	+27,2	—0,10
β	770	—0,1	+7,3	—0,10
	800	+0,1	+7,5	+0,11
	900	+0,8	+8,2	+0,94
	910	+1,0	+8,3	+1,18
γ	910	—5,9	+7,1	—6,99
	950	—5,7	+7,4	—6,98
	1000	—5,4	+7,7	—6,88

The absolute thermal emf of iron (Fig. 28) is positive at a temperature from 0 to 300° C. Near 300° C the curve intersects the abscissa axis, assumed negative values and has a minimum near 500°C.

In the $\alpha\text{-Fe} \rightarrow \beta\text{-Fe}$ transition, the absolute thermal emf is close to zero and a kink is observed on the curve. In the region of existence of β-Fe one observes a linear increase in the absolute thermal emf. During the $\beta\text{-Fe} \rightarrow \gamma\text{-Fe}$ **transition,** the thermal emf of iron diminishes jumpwise. In the region of existence of the γ-Fe, one observes a linear increase in the thermal emf with increasing temperature.
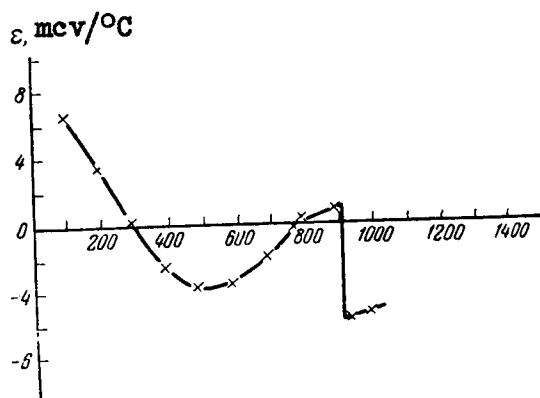
Fig. 28. Absolute Thermal emf of Iron.
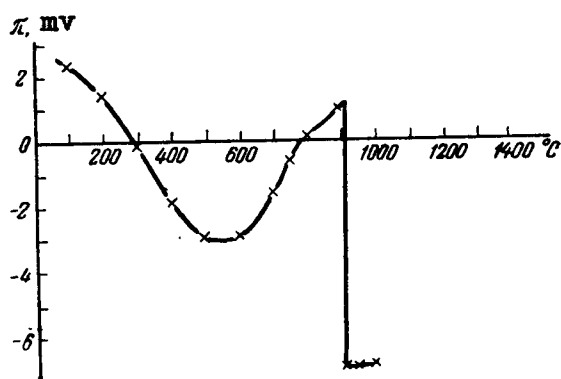
Fig. 29. Thermoelectric Potential of Iron.

The curve obtained by us for the absolute thermal emf of iron is quite similar to the curve of Burgess and Scott [63], but the numerical values are somewhat different. This is probably explained by the differences in the grades and properties of iron and platinum used as a comparison electrode.

Fig. 29 shows the curve of the thermoelectric potential, which differs in character very little from the curve of the absolute thermal emf. At the point of transition the potentials of α-Fe-iron and β-Fe-iron are the same. The jump in the potential occurring during the β-Fe→γ-Fe transition amounts to 8.17 millivolts and is the Peltier emf which arises at the point of contact between the β and γ phases at the transition temperature.

The Thomson emf is shown in Fig. 30. In the region from 0 to 300° C it diminishes smoothly and has a negative value. Nearing

59

300° one observes a smooth minimum, after which the Thomson emf increases rapidly to a maximum that takes place at 770° C. In the transition from the α- to the β- phase it diminishes jumpwise. In the region of existence of the β- phase one observes a linear change. The transition from the β- to the γ phase is accompanied by a break in the continuity of the curve, and the Thomson emf assumes a value of $-\infty$.
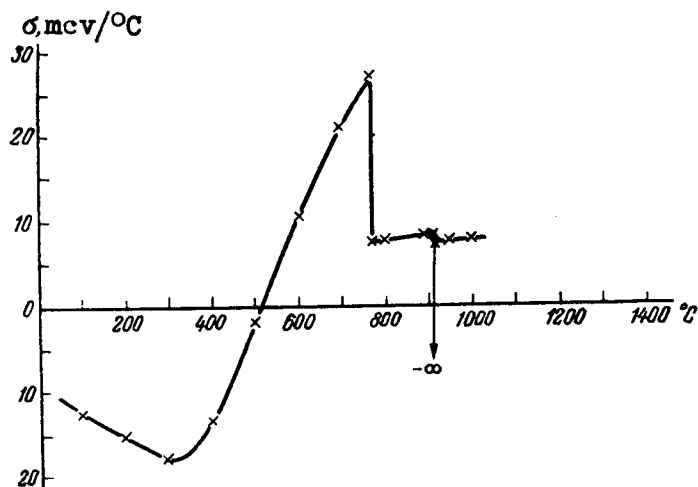
Fig. 30. Thomson emf of iron.

A comparison of the curves of the Thomson emf and of the atomic specific heat of iron [86], shown in Fig. 31, shows the analogy between these phenomena at the Curie point and in the transition from β-Fe $\rightarrow \gamma$-Fe.
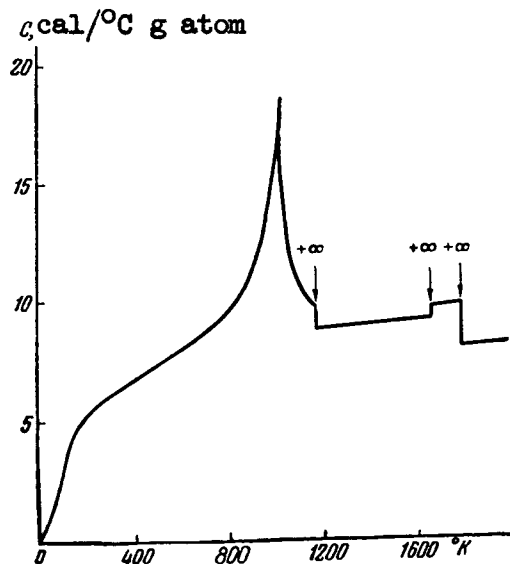
Fig. 31. Atomic specific heat of iron.

Up to the Curie point, in a second-order transition, the specific heat of the metal and the specific heat of the current carriers in the metal (Thomson emf) increase smoothly with increasing temperature until they reach a finite maximum, and diminish abruptly at the transition point.

In a first-order $\beta \to \gamma$ transition the specific heat of the metal assumes a value of $+\infty$, and the Thomson emf a value of $-\infty$.

In a $\gamma \to \delta$ transition the specific heat of the metal and of the carriers assume values of $+\infty$ (See Figs. 27 and 31).

Cobalt. Two known modifications of cobalt: α-Co -cobalt, which has a hexagonal structure with close packing, and β-Co, cobalt; which has a face-centered cubic lattice. The temperature of the α-Co $\rightleftarrows \beta$-Co transition and of the reverse transition, according to data of various authors, fluctuates between 360 and 492° C. According to our data /87/, obtained as the result of a differential thermal analysis, the temperature of the transition is near 390° C.

The magnetic transformation of cobalt occurs within the limits 1120-1200° C.

For the present investigation we use cobalt in cubical form produced by the Kallbaum Company. To prepare the specimens, the metal was molten in a high frequency furnace under borax and drawn into porcelain tubes 1.5 to 2.5 millimeters in diameter. The sticks were welded to thermocouples and annealed in the oven intended for the measurements at a temperature of 300° C.
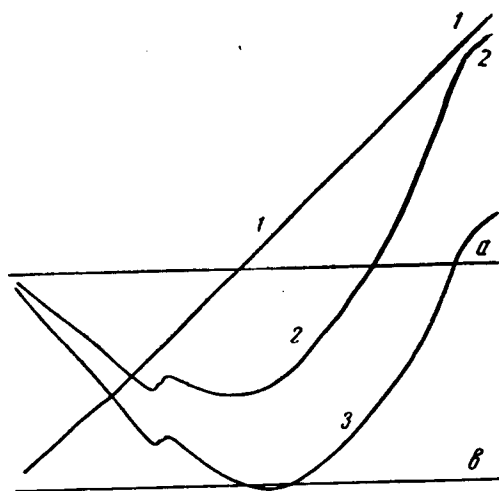
Fig. 32. Curves of the thermal emf of cobalt, recorded with a Kurnakov Pyrometer. 1,2,3 -- Curves corresponding to the galvanometer readings; a, b -- Zero lines of the galvanometers.

The thermal emf was recorded with a Kurnakov pyrometer. The curves were recorded during heating. A record is shown in Fig. 32.

From the data obtained we calculated the thermoelectric properties of cobalt, listed in Table 7.

Table 7

Thermoelectric Properties of Cobalt

Transformations	t, °C	ε, micro-volt/°C	σ, micro-volt/°C	π, mv
α	100	—17,0	—39,5	—6,34
	200	—26,0	—34,0	—12,3
	300	—31,6	—22,9	—18,1
	400	—34,3	—12,8	—23,1
	447	—35,1	—10,1	—25,3
β	447	—32,0	0	—23,1
	500	—32,0	0	—24,8
	600	—32,0	+3,5	—27,9
	700	—31,1	+16,5	—29,3
	800	—27,3	+36,5	—29,3
	900	—21,7	+62,2	—25,5
	1000	—15,6	+90,5	—19,9
	1085	— 8,8	+129,2	—11,9
Non-magnetic	1085	—8,8	+21,8	—11,9
	1100	—8,6	+22,0	—11,8
	1150	—7,7	+22,8	—11,0
	1200	—7,0	+23,6	—10,3

Fig. 33 shows the absolute thermal emf ε as a function of the temperature. For α-Co ε is negative and diminishes with increasing temperature. At a temperature of 447° C, α-Co changes into β-Co   . This transition is accompanied by a jump-like increase in the absolute thermal emf. In the region of existence of the β- phase there occurs a gradual increase in ε , at a temperature of 1085° C, at which cobalt has a magnetic transforma-

tion, one observes a kink in the curve.
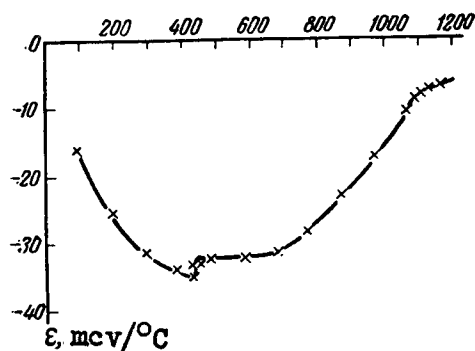
Fig. 33. Absolute thermal emf of cobalt.
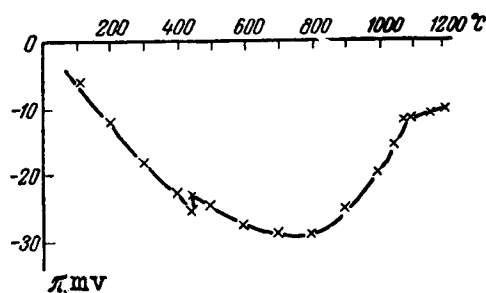
Fig. 34. Thermoelectric potential of Cobalt.

The absolute thermal emf of non-magnetic cobalt increases linearly as a function of the temperature.

As the temperature is increased, the thermoelectric potential π of cobalt (Fig. 34) diminishes smoothly to the transition point at 447° C. The difference in potential between the α- and β- phases amounts to 2.2 millivolts at this temperature. In the region of existence of β- cobalt one observes a change in the potential along a curve having a minimum. In the transition to the non-magnetic state, a kink is seen on the potential curve.

The Thomson emf σ (Fig. 35) for α-cobalt is negative and increases smoothly up to a temperature of 447° C, at which one observes a discontinuity in the curve, and the Thomson emf assumes the value of $+\infty$.

In the β-Co region the Thomson emf increases rapidly to a finite maximum at 1085° C.

At the point of magnetic transformation one observes a jump-like decrease in the Thomson emf. Non-magnetic cobalt has a Thomson emf that varies linearly with the temperature.
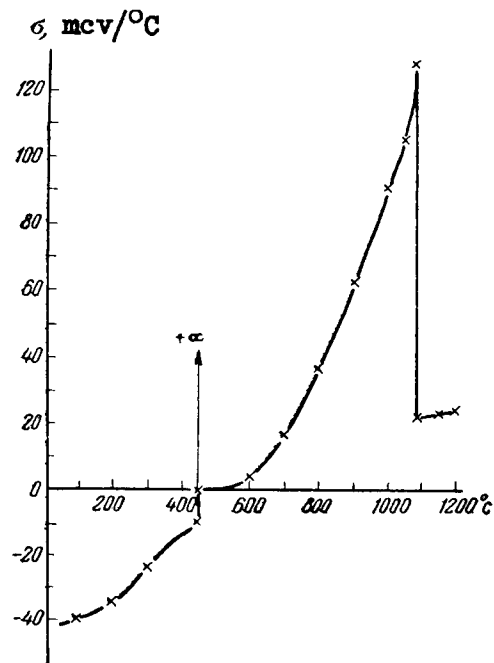
Fig. 35. Thomson emf of Cobalt.

The same as in the case of iron, the polymorphous transformation of cobalt, α-Co $\rightarrow \beta$-Co , is characterized by a jump-like change in the absolute thermal emf and in the thermoelectric potential, and represents a first-order transformation, at which the curve for the Thomson emf has a discontinuity and assumes an infinite value. The magnetic transformation of cobalt is a second-order transformation. It is characterized by a kink on the curves of the absolute thermal emf and of the thermoelectric potential. The Thomson emf changes jumpwise.

In the present investigation the α-Co$\rightarrow\beta$-Co transition point was obtained at 447° C. In reference 87, the value of 390° C which we have obtained is probably due to the presence of a large number of impurities in the metal.

Nickel. Nickel usually crystallizes in the form of a face-centered cube. By chemical means it is possible to obtain another version of nickel, which has a hexagonal structure.

Ordinary molten nickel, when serving as a component portion of

64

alloys, has a face-centered cubic lattice and only this modification of nickel is considered in the present work.

Nickel is magnetic at room temperature and becomes weakly paramagnetic at 360° C.

For a reliable investigation we used spectrally-pure nickel supplied by the Hilger Company. It was rolled and drawn into a wire 1 millimeter in diameter, welded to platinum thermocouples, and placed in an oven for annealing. To remove the case hardening the annealing was at 600° C for 15 minutes with subsequent slow cooling.

The thermal emf was recorded with a Kurnakov pyrometer. Fig. 18 shows the records of the thermal emf made with a pyrometer.

Table 8 lists the values of the absolute thermal emf ε , the thermoelectric potential π , and the Thomson emf σ .

Fig. 36 and 37 give the absolute thermal emf and the thermo-electric potential of nickel. At temperatures of 0 to 360° C their temperature curve has a minimum.

At the point of the magnetic transformation one observes a sharp maximum. In the region of existence of the non-magnetic nickel curves of the absolute thermal emf and of the thermoelectric potential are smoothly descending.

Table 8

Thermoelectric Properties of Nickel

Transformations	t, °C	ε, micro-volt/°C	σ, micro-volt/°C	π, mv
Magnetic	100	—10,0	—27,2	—3,73
	200	—15,8	—16,5	—7,47
	300	—16,9	+11,5	—9,68
	360	—11,8	+44,3	—7,47
Non-magnetic	360	—11,8	—18,4	— 7,47
	400	—14,2	—19,5	— 9,55
	500	—17,1	—22,4	—13,20
	600	—20,0	—25,3	—17,47
	700	—23,0	—27,2	—22,40
	800	—25,6	—26,8	— 27,45
	900	—27,8	—24,7	—32,60
	1000	—29,5	—19,1	—37,60

65

The Thomson emf (Fig. 38) for magnetic nickel increases rapidly, reaching a sharp maximum at 360° C. At the transition point one observes a jump on the curve, accompanied by a drop in the Thomson emf. In the region of existence of non-magnetic nickel, the Thomson emf changes along a curve with a gentle minimum.
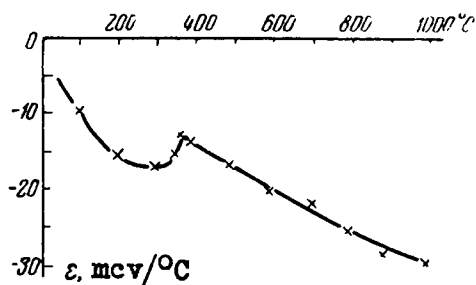
Fig. 36. Absolute Thermal emf of Nickel.
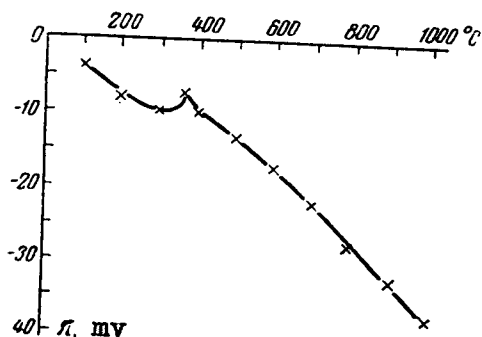
Fig. 37. Thermoelectric Potential of Nickel.

The magnetic transformation of nickel is a typical second-order transformation. The shape of the Thomson emf curve for nickel is analogous to the curves for iron and cobalt near the Curie points. Our data are similar to the data obtained by Grew /84/ and Foster /85/.

Fig. 39 shows a curve of the atomic specific heat of nickel as obtained by Foster /85/. As in the preceding case, one observes at the Curie point an analogy between the specific heat of the metal and the specific heat of the current carriers.

Investigations of the thermoelectric properties of iron, cobalt and nickel and their comparison with the specific heat have shown that the different transformations in these metals are accompanied by unique changes in the thermoelectric properties.

First-order transformations (γ-Fe $\to$ δ-Fe   and
α-Co $\to$ β-Co   ) are accompanied by a jump-like increase in the
absolute thermal emf (entropy of the current carriers), a jump-like
increase in the thermoelectric potential (bound energy of the current
carriers). The specific heat of the metal and the specific heat of
the current carriers assume values of plus infinity at the transition
point.

There is also another possible case of first-order transition.
In the point of transition from β-Fe $\to$ γ-Fe   one observes
a somewhat different phenomenon. All other conditions being equal,
this point is characterized by the fact that the β-Fe $\to$ γ-Fe
transition is accompanied by a jump-like decrease in the absolute
thermal emf (entropy of the carriers) and of the thermoelectric po-
tential (bound energy). At this point the Thomson emf (specific heat
of the carriers) assumes a value of $-\infty$. Thus, first-order trans-
formations can be of two types.
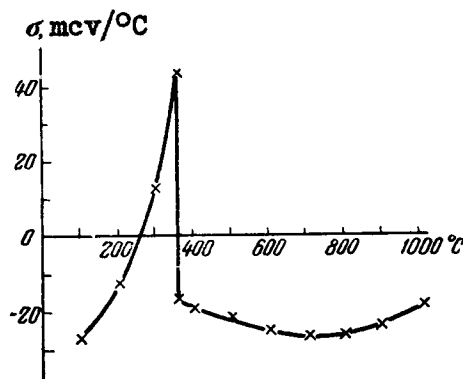
Fig. 38. Thomson emf of Nickel.
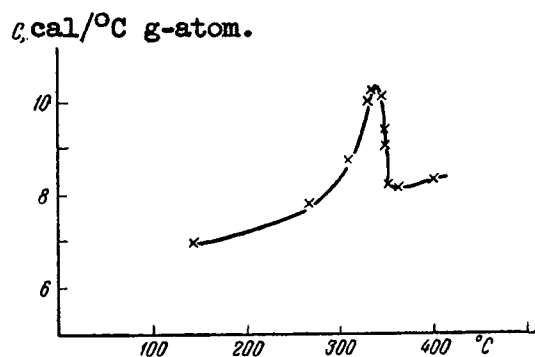
Fig. 39. Atomic specific heat of nickel.

Second-order transformations -- magnetic transformations of iron, cobalt, and nickel -- are accompanied by a jump-like decrease in the Thomson emf (specific heat of current carriers) like the specific heat of the metal. The absolute thermal emf's (carrier entropies) and thermoelectric potentials (bound energies) of both phases are equal to each other at the point of second-order transition.

3. INVESTIGATION OF THERMOELECTRIC PROPERTIES OF NOBLE METALS

The thermoelectric properties of noble metals have interested us primarily because these metals are the component parts of the alloys investigated by us. Particular attention was paid to the purity of the metals, since the electric and thermoelectric characteristics change considerably in the presence of even very small amounts of impurities. We also studied the specific electric resistivity and its temperature coefficient for these metals.

In the present work we used metals of highest purity.

Gold. The gold was subjected to refining. Commercial gold was dissolved in aqua regia. The solution was evaporated three times with sulfuric acid in a water bath to remove the oxides of nitrogen. The gold was reduced with sodium nitrate. The metal obtained was washed with water and boiled in strong nitric acid to remove traces of silver and was again washed with distilled water. The residue was dried, molten into ingots, which were forged, rolled and drawn into a wire 0.5 millimeter in diameter. During the process of treatment the gold was boiled in strong hydrochloric acid to remove the iron from its surface. Before the experiment the wire was annealed at 500° C for 30 minutes.

To establish the purity of the metal its specific electric resistivity was measured along with the temperature coefficient of the latter. These were found to have the following values:

Specific electric resistivity:

At 25° C

$$\rho_{25} = 2,191 \text{ microhm-cm,}$$

at 100° C

$$\rho_{100} = 2,857 \text{ microhm-cm.}$$

The temperature coefficient was

$$\alpha = 45{,}00 \times 10^{-4}.$$
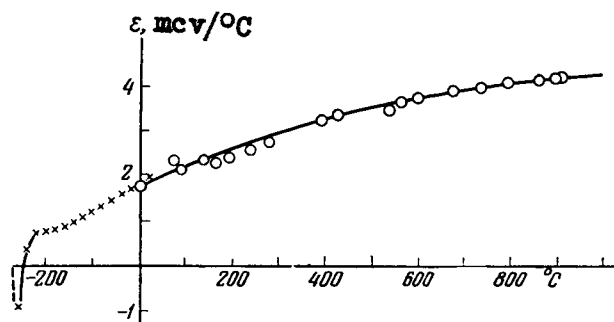
Fig. 40. Absolute Thermal emf of Gold:

O -- author's data; × -- Results of Borelius, Keesom, Johansson, and Linde.

The high temperature coefficient and the low specific resistivity are evidence of a high degree of purity of the gold.

The thermoelectric properties of gold were investigated by a differential method with the aid of a potentiometer.

The absolute thermal emf of gold can be expressed as the following function of temperature

$$\varepsilon = 1{,}72 + 0{,}0046\ t - 0{,}00000225\ t^2 \quad \text{(microvolt/}^\circ\text{C)}.$$

The Thomson emf is

$$\sigma = 1{,}26 + 0{,}0037\ t - 0{,}0000045\ t^2 \quad \text{(microvolt/}^\circ\text{C)}.$$
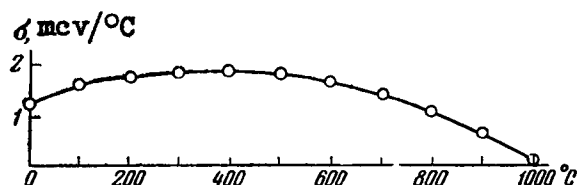
Fig. 41. Thomson emf of Gold.
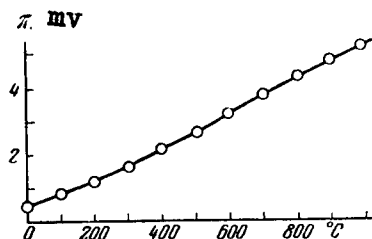
Fig. 42. Thermoelectric Potential of Gold.

Table 9 gives the values of ε, σ and π, which are plotted in Figs. 40-42.

The value of σ is in sufficiently good agreement with the data of Lander [58] in the temperature range from 0 to 400° C. At a higher temperature one observes a certain deviation from its data.

Fig. 40 shows our value of ε supplemented with the data of Borelius, Keesom, Johansson, and Linde [77].

Silver. To obtain pure silver, commercial silver was dissolved in nitric acid, and hydrochloric acid was used to precipitate silver chloride, which was washed with water and dissolved in ammonia. The ammonia complex was broken up with nitric acid. When this method is used, the palladium which is frequently present in silver remained in solution. Double precipitation from the ammonia solution was used. To reduce the silver, the silver chloride was mixed in a solution of caustic soda and glucose was added to the boiling mixture. The silver obtained was washed with water, dried, molten in corundise crucibles, forged, rolled and drawn into a wire 0.5 millimeter in diameter. Before the experiments the wire was annealed for 30 minutes at 400° C.

Table 9

Thermoelectric Properties of Gold

t, °C	T, °K	ε, micro-volt/°C	σ, micro-volt/°C	π, mv	t, °C	T, °K	ε, micro-volt/°C	σ, micro-volt/°C	π, mv
0	273,1	1,72	1,25	0,47	600	873,1	3,67	1,66	3,20
100	373,1	2,16	1,55	0,81	700	973,1	3,84	1,41	3,74
200	473,1	2,55	1,75	1,21	800	1 073,1	3,96	1,07	4,25
300	573,1	2,90	1,85	1,66	900	1 073,1	4,04	0,65	4,74
400	673,1	3,20	1,88	2,15	1000	1 273,1	4,07	0,13	5,18
500	773,1	3,46	1,82	2,67					
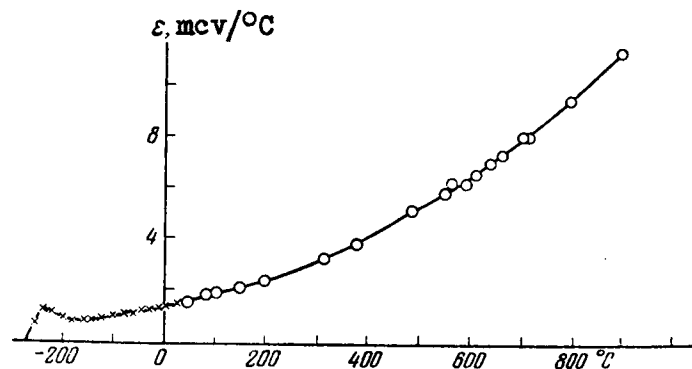
Fig. 43. Absolute Thermal emf of Silver:

O -- Our Data;   × -- Results of Borelius.

To establish the purity of the silver we measured the specific resistivity and its temperature coefficient, which were found to be the following:

Specific resistivity:

at 25° C, $\rho_{25} = 1,609$ microhm-cm,

at 100° C, $\rho_{100} = 2,051$ microhm-cm.

The temperature coefficient of electric resistivity is

$$\alpha = 40,33 \times 10^{-4}.$$

The data obtained are evidence of the high grade of the silver.

The investigation of the thermoelectric properties of silver was carried out by a differential method with the aid of a potentio-meter. Results of the measurements are given in Table 10 and in Figs. 43-45. The values obtained were supplemented by data of Borelius, Keesom, Johansson and Linde $\overline{/77/}$ down to absolute zero.

In the temperature range from 0 to 900° C, the absolute thermal emf of silver can be expressed by the following equation

$$\varepsilon = 1,42 + 0,00338t + 0,0000081t^2 \quad (\text{microvolt/°C}).$$

71

The Thomson emf is

$$\sigma = 0{,}924 + 0{,}078t + 0{,}0000162t^2 \quad (\text{microvolt}/^oC).$$

The values calculated from these formula are in very good agreement with the data of Lander $\underline{/58/}$ up to 500° C. At higher temperatures, deviations are observed.
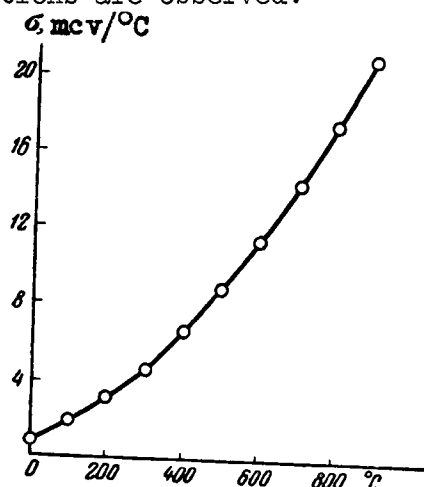
Fig. 44. Thomson emf of Silver.
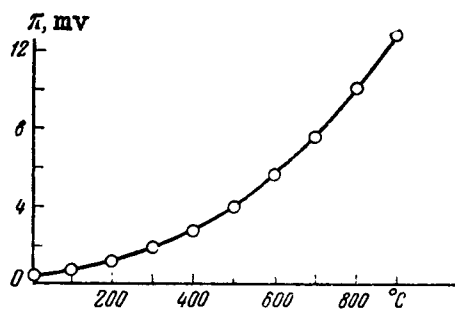
Fig. 45. Thermoelectric Potential of Silver.

Table 10

Thermoelectric Properties of Silver

t, °C	T, °K	ε,micro-volt/°C	σ,micro-volt/°C	π, mv	t, °C	T, °K	ε,micro-volt/°C	σ,micro-volt/°C	π, mv
0	273,1	1,42	0,922	0,39	500	773,1	5,13	8,87	3,96
100	373,1	1,84	1,86	0,69	600	873,1	6,37	11,44	5,56
200	473,1	2,42	3,13	1,15	700	973,1	7,75	14,33	7,54
300	573,1	3,16	4,72	1,81	800	1073,1	9,31	17,56	10,00
400	673,1	4,07	6,63	2,74	900	1173,1	11,02	21.07	12,90

Platinum /88/. The purest platinum is used principally for thermometric purposes in resistance thermometers and in thermocouples, thanks to the stability of the electric and thermoelectric character- istics at high temperatures and, as in the case of most pure metals, platinum has a considerable temperature coefficient of electric re- sistivity.

The high temperature coefficient of platinum is a criterion of the purity of the metal. The presence of spectral traces of im- purities in platinum are substantially reflected in the value of the temperature coefficient of electric resistivity.

At the present time it becomes possible to obtain platinum of very high purity. Spectral analysis cannot indicate even qualita- tively the presence of impurities in platinum.

Platinum, in which spectral analysis discloses no impurities, may have different physical properties, thus showing the presence of analytically indeterminable amounts of impurities in various speci- mens of the metal. Thus, physical methods of investigations are more sensitive methods for the determination of small amounts of im- purities in metal.

The maximum known value of temperature coefficient of elec- tric resistivity, obtained for spectrally-pure platinum, prepared at the Institute of General and Inorganic Chemistry imeni N. S. Kur- nakov, Academy of Sciences USSR, approaches a value R_{100}: R_0 = 1.3925/89/.

The first attempt at using physical methods of investigation for the determination of the purity of platinum was made in 1916 by S. F. Zhemchuzhnyy /90/, who studied the hardness, electric resis-

tivity, the temperature coefficient of electric resistivity, and the thermal emf of platinum and of its alloys with small amounts of impurities of palladium, iridium, and rhodium.

The physical properties of pure platinum was investigated by many workers: A. T. Grigor'yev /91/, N. S. Kurnakov and N. I. Podkopayev /92/, V. A. Nemilov and A. T. Grigor'yev /93/. According to their data, the Brinell hardness for purest specimens of platinum ranges from 24 to 28 kg/mm^2. The specific electric resistivity at 25° C amounts to approximately 10.88 microhm cm and the temperature coefficient of electric resistivity is 0.00392.

The absolute thermal emf of platinum was investigated by Borelius /48/ and Nystrom /59/.

For the present work, the author had spectrally pure platinum, obtained by the method proposed by I. I. Chernyayev and A. M. Rubinshteyn /94/. Several samples of platinum were used for the investigation:

Pt 1 - spectrally-pure platinum, molten in thorium-oxide crucibles (prepared by G. S. Muraveyskaya).

Pt 2 - spectrally-pure platinum prepared in the plant (batch #51), molten in thorium-oxide crucibles.

Pt 3 - the same platinum molten in zirconium-oxide crucibles.

Pt 4 - spectrally-pure platinum prepared by the plant (batch #50), molten in zirconium-oxide crucibles.

Pt 5 - high purity platinum, obtained by the method of Professor N. K. Pshenitsyn.

Pt 6 - commercially-pure platinum.

For all specimens of platinum, a study was made of the resistivity and its temperature coefficient. The thermal emf was studied in detail for the platinum specimen Pt 2.

To melt the platinum we used crucibles made of thorium-oxide and zirconium oxide, of Russian make. They were first treated with hot hydrochloric acid to remove the iron introduced by the presses, and the excess magnesium oxide, which is usually introduced in the manufacture of crucibles made of zirconium-oxide. The crucibles were washed with distilled water, dried, and heated at 1,000° C.

The platinum was not pressed before melting, to avoid contamination by the iron in the press. The melting was carried out in a high frequency furnace, and the metal, in spongy form, was added

gradually, as the melting proceeded.

In the hardening of spectrally-pure platinum no formation of a large amount of bubbles was observed, as usually occurs in the melting of ordinary pure platinum.

A bead of metal was forged at a temperature of 1000-1200° C. After each forging operation, the hot ingot was immersed in strong hydrochloric acid to remove the iron that fell from the hammer and from the anvil. A hand rolling mill was used. During the rolling process, after each passage of the roller, the metal was boiled in strong hydrochloric acid in order to remove the iron, introduced from the rollers on the surface of the metal. The wire was drawn through "pobedite" dies to a diameter of 0.5 mm.

To study the resistance, wires 200 mm long were used, and two ends of the same material were welded to the ends of this wire. The wire was wound on a porcelain tube, washed with hydrochloric acid, water, and alcohol. It was then annealed and copper wires were attached to the ends, after which it was again washed with alcohol. The electric resistivity was investigated at 0° C and at the boiling temperature of water, with allowance for atmospheric pressure. The measurements were carried out with a PPTN potentiometer with an accuracy up to 1 microvolt at currents of 30, 100 and 300 ma. The electric resistivity was compared with a resistance standard of 0.1 ohms. The resistance of the investigated wire was also approximately 0.1 ohm. The results of the measurements are given in Table 11.

Table 11

Electric Properties of Platinum

Metal	ρ_0, microhm-cm	ρ_{100}, microhm-cm	α	Metal	ρ_0, microhm-cm	ρ_{100}, microhm-cm	α
Pt1	9,2	12,9	1,3924	Pt4	9,3	12,9	1,3921
Pt2	9,6	13,4	1,3923	Pt5	9,6	13,2	1,3865
Pt3	9,4	13,1	1,3922	Pt6	10,2	14,0	1,3742

The temperature coefficient was determined from the formula

$$\alpha = \frac{R_{100}}{R_0} = \frac{\frac{R_t}{R_0} - 1}{t} \times 100 + 1,$$

where t is the temperature of boiling of water.

The absolute error in the determination of the temperature coefficient amounted on the average to approximately $\pm$ 0.0002. When measuring the specific electric resistivity, the error is considerably greater than $\pm$ 0.4 microhm-cm, as a result of the low accuracy of the measurement of the geometric dimensions of the specimen.

To study the absolute thermal emf of spectrally-pure platinum, a Pt 2 plus spectrally pure copper thermocouple was prepared.

The Pt 2-Cu thermocouple was calibrated against the melting points of pure metals (aluminum, antimony, zinc, lead, and tin), and also against the melting temperature of naphthalene. The cold junction of the thermocouple was kept at $0°$ C.

The results of the calibration are given in Table 12.

Table 12

Calibration of Thermocouples

Substance	Melting temperature, $°C$	E, microvolts	Substance	Melting temperature, $°C$	E, microvolts
Naphthalene	80,1	574	Zinc	419,4	4962
Tin	231,9	2194	Antimony	630,5	8904
Lead	327,3	3496	Aluminum	660,1	9509

The thermal emf of the Pt 2-Cu thermocouple can be expressed by the following equation, which is valid at temperatures from 300 to $1200°$ C.

$$E = -488 + 9{,}25t + 0{,}00893t^2 \quad \text{(microvolt)}.$$

Differentiating this equation and taking into account the absolute thermal emf of copper, we calculate the absolute thermal emf of platinum using the following equation

$$\varepsilon = -7,53 - 0,0125t \quad (\text{microvolt}/^\circ\text{C}).$$

The values of the thermal emf between 0 and 300° C were determined graphically.

Table 13

Thermoelectric Properties of Spectrally-Pure Platinum

°C	ε, micro-volt/°C	σ, micro-volt/°C	π mv	°C	ε, micro-volt/°C	σ, micro-volt/°C	π mv
0	— 3,50	—12,10	— 0,95	700	—16,29	—12,18	—15,85
100	— 7,10	—11,00	— 2,65	800	—17,54	—13,43	—18,82
200	— 9,56	— 9,70	— 4,52	900	—18,80	—14,70	—22,05
300	—11,28	— 8,19	— 6,47	1 000	—20,05	—15,94	—25,53
400	—12,54	— 8,43	— 8,44	1 100	—21,30	—17,20	—29,23
500	—13,79	— 9,97	—10,66	1 200	—22,55	—18,44	—33,20
600	—15,04	—10,92	—13,31	—	—	—	—

Fig. 46 shows the curve of the integral thermal emf of platinum coupled with copper. The same curve shows the points obtained from Rohn's data /71/.

The values of the thermoelectric properties of platinum are given in Table 13.

Fig. 47 shows the absolute thermal emf of spectrally-pure platinum. The same figure shows the data of Borelius /49/ and Nystrom /50/ for low and high temperatures. From 300° and above the absolute thermal emf changes linearly as a function of the temperature. This dependence can be extrapolated at least to 1200° C.

The thermoelectric potential (Fig. 48) of platinum changes according to a parabolic law above 300° C.

The Thomson emf of platinum is shown in Fig. 49. The same figure shows the data of Borelius, Keesom, Johansson, and Linde /77/ and Nystrom /59/.
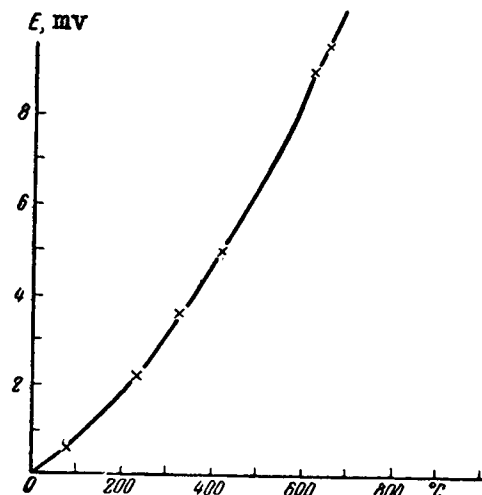
Fig. 46. Thermal emf of Platinum-Copper Thermocouples.

For spectrally-pure platinum the Thomson emf has a maximum in the vicinity of 300° C. Above this temperature σ changes linearly in accordance with the following equation

$$\sigma = -\, 0,0125T \quad (\text{microvolt}/^\circ\text{C}),$$

where T is the absolute temperature.

On Nystrom's curve the maximum is shifted somewhat towards the lower temperature.

The data of Borelius and Nystrom coincide with the values of the absolute thermal emf obtained by us for thermocouple platinum (see Chapter II).

All six specimens of platinum were compared with each other thermoelectrically, and for this purpose the following thermocouples were made: Pt 2 -- Pt 1, Pt 2 -- Pt 3, Pt 2 - Pt 4, Pt 2 -- Pt 5, Pt 2 -- Pt 6. The hot ends of the thermocouples were welded to a calibration thermocouple and placed in an oven, while the cold junctions of the thermocouples were placed in melting ice.

The results of the measurements are shown in Fig. 50. Pt 1 coupled with Pt 2 develops a negative emf. Pt 3 and Pt 2 are equivalent and the thermal emf between them is zero up to 1000° C. Pt 4 is thermoelectrically positive relative Pt 2. Pt 5 and Pt 6 develop a considerable positive thermal emf when coupled with Pt 2.

78
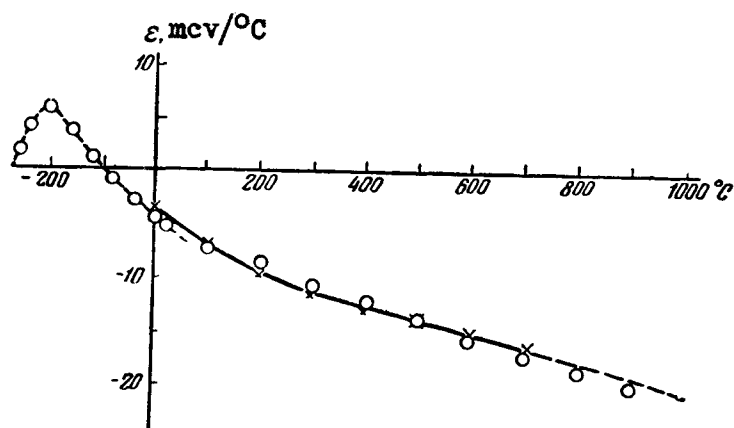
Fig. 47. Absolute Thermal emf of Spectrally-Pure Platinum.

O -- data of Borelius and Nystrom; × -- Spectrally-Pure Platinum.
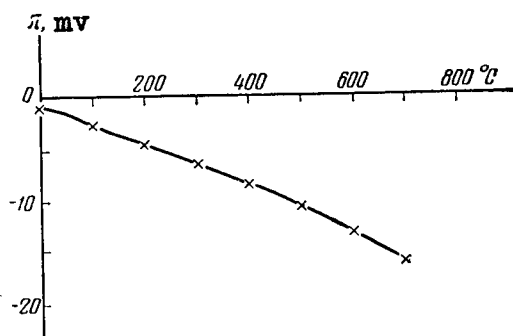
Fig. 48. Thermoelectric Potential of Spectrally-Pure
Platinum.

Fig. 50 shows also the curve of the thermal emf of thermocouple platinum (Chapter II) coupled with Pt 2. In this case, at a temperature of 0-30° C, one observes a sharp increase in the thermal emf towards the positive side and then the emf gradually rises to 800° C and again starts diminishing. The samples of the spectrally-pure platinum Pt 1, Pt 2, Pt 3, and Pt 4 which are used for the investigation are quite close to each other in their properties.

The absence of a thermal emf between the specimens Pt 2 and Pt 3 shows that the melting of platinum in crucibles made of thorium-oxide and zirconium-oxide is equivalent. Obviously, in the

selected method of melting and treatment of platinum no impurities
are introduced.

A study of the temperature coefficient of electric resistivity
and of the thermal emf has shown that the purest is Pt 1, since this
specimen has a maximum temperature coefficient and develops a nega-
tive thermal emf when coupled with its other specimens.

One can use as a criterion of the purity of platinum the
temperature coefficient of electric resistivity and the thermal emf.
In this case the purest platinum will have a maximum temperature co-
efficient and will be the most negative thermoelectrically.

Most metals (palladium, rhodium, iridium, ruthenium, copper,
and iron) produce with platinum alloys that are thermoelectrically
positive. Gold, to the contrary, produces a thermoelectrically nega-
tive alloy. When using the method of thermal emf to determine the
purity of platinum, we obtain a quite clear picture of the contamina-
tion of the metal, and the technique of the experiment is exceedingly
simple.
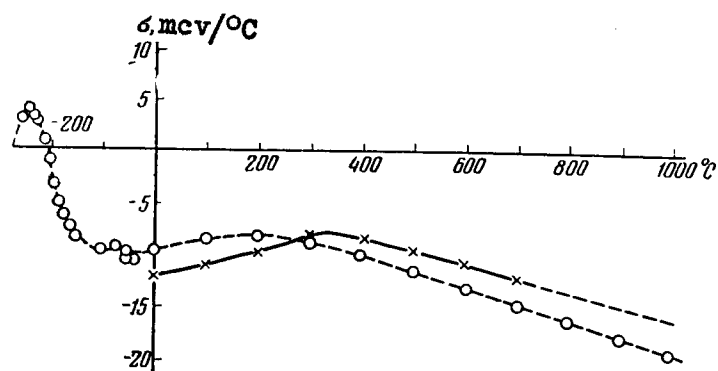
Fig. 49. Thomson emf of Spectrally-Pure Platinum:

X -- Spectrally-Pure Platinum;   O -- Data of
Borelius, Keesom, Johansson Linde, and Nystrom.

In determining the temperature coefficient of electric re-
sistivity, the experimental procedure is much more complicated and
requires greater skill. In this case the experimental error should
not exceed several tenths of a percent, since an experimental error
of 0.001% already is excessive.

For exact evaluation of the purity of spectrally-pure plati-
num it is necessary to use both methods of investigation. Corruccini
/95/ has established a graphical relationship between the temperature
coefficient and the thermal emf of pure platinum. Obviously, his

dependence holds only in that case, when the platinum is obtained from one source and when various grades of platinum contain the same impurities. Platinum obtained from concentrates usually contains traces of iridium, while platinum obtained by polymetallic ores contains palladium. For both grades of platinum it is possible to derive entirely different relationships. In any case, traces of gold violate the law obtained by Corruccini.
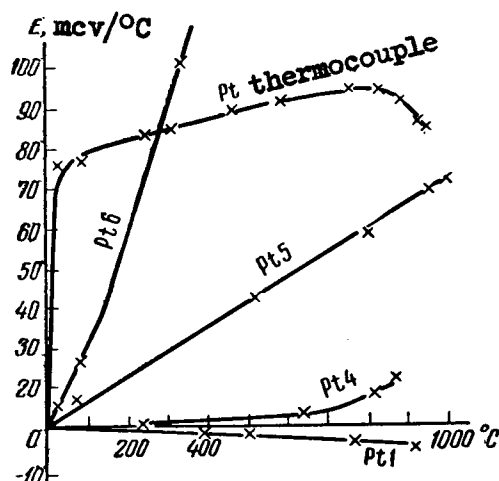
Fig. 50. Thermal emf of Various Specimens of Platinum
          Coupled with Pt 2.

Palladium $/96/$. The physical properties of pure palladium have been investigated many times by various authors, but in most cases there are no indications on whether the metal was sufficiently pure.

The specific electric resistivity of palladium was determined by V. A. Nemilov and A. T. Grigor'yev $/93/$, V. A. Nemilov, A. A. Rudnitskiy, and T. A. Vidusova $/97/$, Grube and Knabe $/98/$, Grube and Kastner $/99/$, and Connybear $/100/$. According to their data, the specific electric resistivity at $0°$ C fluctuates from 10 to 11 microhm-cm.

The temperature dependence of the electric resistivity for pure palladium, according to the data by the same authors, and also according to Schofield $/101/$ and Holborn $/102/$, fluctuates from 1.37 to 1.38.

Connybear has observed a considerable irreversible increase in the electric resistivity of palladium under prolonged annealing in the temperature range from 970 to 1000° C.

The Pd-Pt thermocouple was investigated by Holborn and Day

/74/. The absolute thermal emf of palladium at low temperatures and the Thomson emf were studied by Borelius /77/ and Lander /58/.

For the present investigation we used spectrally-pure spongy palladium, obtained by the method proposed by Professor A. M. Rubinshteyn. The palladium used was chosen from two batches refined, Pd 1 and Pd 2, which did not differ in principle from each other. For comparison we investigated commercial palladium, twice precipitated from an ammonia solution of palladozamine.

For melting the palladium we used corundise crucibles which were first boiled in strong hydrochloric acid, washed with distilled water, dried, and tempered at 1000° C.

The melting was in a high frequency furnace. In order not to contaminate the metal with iron, no pressing was used. The spongy palladium was added to the crucible as it melted.

The metal cooled as fast as possible, for in slow cooling and hardening there was observed formation of a large number of bubbles.

The molten palladium was forged at a temperature of $1100\text{-}1200^\circ$ C. At such a high forging temperature it became possible to forge out the bubles and weld them tight.

After each operation of forging, the hot metal was immersed in strong hydrochloric acid to remove from its surface the iron, which could be introduced by the hammer and anvil.

The thoroughly forged ingot of palladium was rolled in a hand rolling mill.

Table 14

Electrical Properties of Palladium

Palladium	ρ_0, microhm-cm	ρ_{100}, microhm-cm	α
Pd 1	9,2	12,7	1,3786
Pd 2	9,0	12,4	1,3793
Commercial	9,1	12,2	1,3416

To study the electric and thermoelectric properties, wires 0.5 mm in diameter were prepared. These wires were washed in alcohol to remove the grease from the surface of the metal and immersed in hot hydrochloric acid, and then washed with water. The annealing was at 800° C.

The measurement of the electric properties was carried out the same as for platinum. The results of the measurements are given in Table 14.

The thermoelectric properties of spectrally-pure palladium were studied using a specimen of Pd 1. Wire of 0.5 mm in diameter, washed with alcohol, hydrochloric acid, and distilled water, was annealed at a temperature of 800° C for 30 minutes. The annealed palladium wire was welded to a thermocouple with spectrally-pure platinum. The calibration of such a thermocouple was against the melting temperatures of pure metals (tin, lead, zinc, antimony, and aluminum), and also against the melting point of naphthalene. The temperature of the cold junction was maintained at 0° C.

The results of calibration of the thermocouple are given in Table 15 and in Fig. 51. In the Pt-Pd thermocouple, the negative electrode is the palladium.

Table 15

Calibration of Thermocouples

Substance	Melting Temperature, °C	E, microvolts
Naphthalene	80,1	451
Tin	231,9	1428
Lead	327,3	2150
Zinc	419,4	2962
Antimony	630,5	5352
Aluminum	660,1	5748

On the basis of the data obtained, the thermal emf of the Pt-Pd thermocouple can be expressed by the following equations:

at a temperature 0-300° C

$$E = 5,378t + 0,00304t^2 + 0,0000014t^3 \text{ (microvolts)},$$

83

at temperatures above 300°

$$E = 411 + 2{,}593t + 0{,}00832t^2 \quad \text{(microvolts)}.$$

The Pt-Pd thermocouple has the following values of thermal emf as a function of the temperature:

t, °C=	100;	200;	300;	400;	500;	600;	700
E, microvolts=	570;	1208;	1938;	2779;	3788;	4962;	6303

Fig. 51 shows, in addition to these values, also the data obtained by Holborn and Day [74].

To determine the absolute thermal emf of palladium, the comparison electrode used was of spectrally-pure copper.

The Cu-Pd thermocouple was calibrated the same as the Pt-Pd thermocouple. The results of the calibration are given in Table 16 and in Fig. 51.

It can be established from these data that the thermal emf of the Cu-Pd couple is given by the following equations:

at a temperature 0-300° C

$$E = 11{,}259t + 0{,}01942t^2 - 0{,}0000027t^3 \quad \text{(microvolts)},$$

At temperatures from 300° and above

$$E = -77 + 11{,}843t + 0{,}01725t^2 \quad \text{(microvolts)}.$$

Differentiating these equations and taking into account the absolute thermal emf of copper, we determine the equations for the absolute thermal emf of palladium:

at a temperature from 0 to 300° C

$$\varepsilon = -9{,}537 - 0{,}0335t + 0{,}0000081t^2 \quad \text{(microvolt/°C)},$$

84

At a temperature of 300° C

$$\varepsilon = -10,121 - 0,02926t \quad (\text{microvolt}/^{\circ}\text{C}).$$

Table 16

Thermal emf of a Pd-Cu Thermocouple
Results of Calibration

Material	^{t}Melting temperature, $^{\circ}$C	E, microvolts
Naphthalene	80,1	1025
Tin	231,9	3622
Lead	327,3	5647
Zinc	419,4	7925
Antimony	630,5	14245
Aluminum	660,1	15257
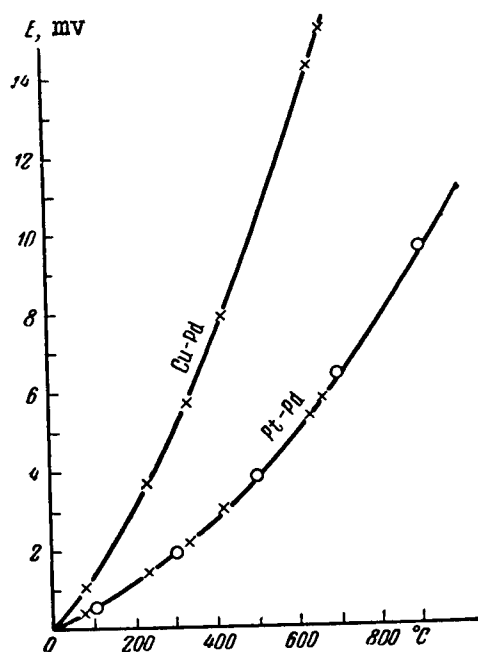
Fig. 51. Thermal emf of Pt-Pd and Cu-Pd Thermocouples:

O -- Holborn's data.

The results of the calculations based on these formulas are given in Table 17 and in Fig. 52. A portion of the curve from absolute 0 to 0° C is plotted using the data of Borelius /48/.

The thermal emf of spectrally-pure palladium was measured also by a differential method. The results of the measurements, obtained by both methods, are sufficiently close to each other.

Table 17

Thermoelectric Properties of Spectrally-Pure Palladium

t, °C	ε, micro-volts/°C	σ, micro-volts/°C	π, mv	t, °C	ε, micro-volts/°C	σ, micro-volts/°C	π, mv
0	— 9,54	— 9,15	— 2,61	700	—30,60	—28,47	—29,78
100	—12,81	—11,90	— 4,78	800	—33,53	—31,40	—35,98
200	—15,91	—14,33	— 7,53	900	—36,46	—34,40	—42,77
300	—18,90	—16,63	—10,83	1000	—39,38	—37,30	—50,14
400	—21,83	—19,71	—14,69	1100	—42,31	—40,15	—58,00
500	—24,75	—22,65	—19,13	1200	—45,23	—43,10	—66,65
600	—27,68	—25,60	—24,17	—	—	—	—

Fig. 53 shows the thermoelectric potential of palladium. The Thomson emf (Fig. 54) of palladium is negative and varies linearly with the temperature above 300° C.

Fig. 54 shows also the data of Lander /58/, which are somewhat lower than ours.

Specimens of palladium wires were welded at their ends to a calibrated Pt-Rh thermocouple and were placed in an oven to compare their thermoelectric properties. The free ends were immersed in a Dewar vessel with melting ice. The spectrally-pure palladium, Pd 1, was connected to the positive terminal of the potentiometer. We heated the ovens to various temperatures and read the thermal emf of Pd 1-Pd 2 and Pd 1 -Pd (commercial) thermocouples. The results of the measurements are given in Fig. 55.

Pd 2 coupled with Pd 1 develops a small thermal emf, not exceeding ± 5 microvolts. Probably these deviations are due to the inhomogeneity of the wires along their lengths.

Commercial palladium coupled with spectrally-pure palladium gives a considerable negative thermal emf.
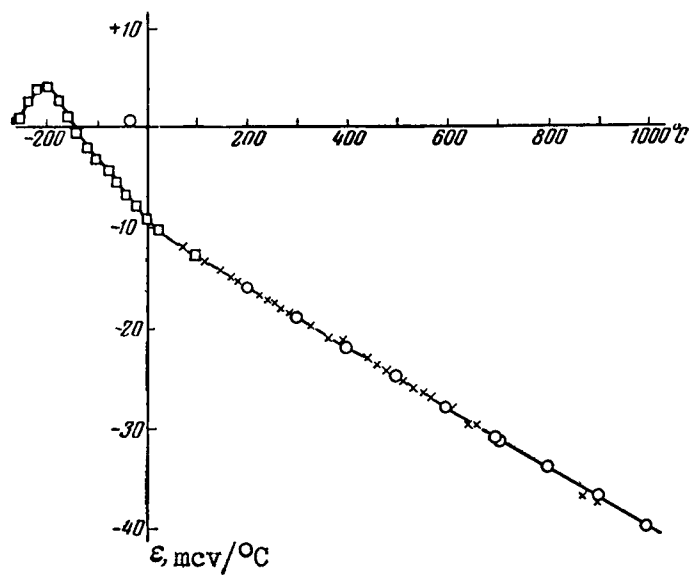
Fig. 52. Absolute Thermal emf of Spectrally-Pure
Palladium:

□ -- Data of Borelius;   ○ -- Integral Method;
× -- Differential Method.
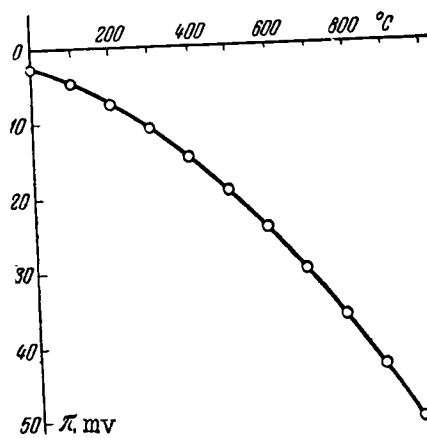
Fig. 53. Thermoelectric Potential of Spectrally-Pure
Palladium.
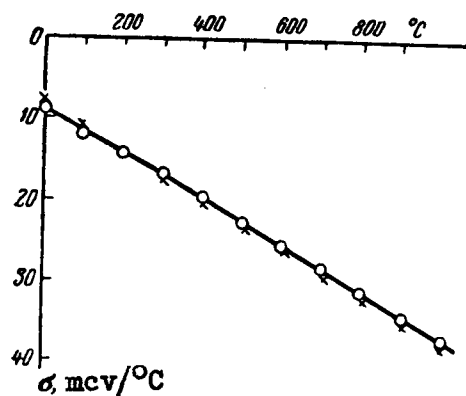
Fig. 54. Thomson emf of Spectrally-Pure Palladium:

× -- Data of Lander;   O -- Data of Rudnitskiy.
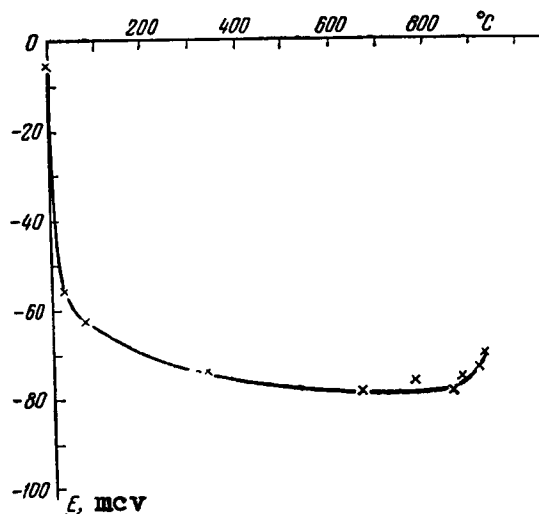
Fig. 55. Thermal emf of Commercial Palladium Copuled With Spectrally-Pure Palladium.

An investigation of two specimens of spectrally-pure palladium has shown that they are quite identical in their physical properties. The specific electric resistivity of spectrally-pure palladium amounts on the average to 9.1 microhm-centimeter at 0° C and 12.6 microhm-centimeters at 100° C.

These values are quite close to those obtained for commercial

palladium. The temperature coefficient of spectrally-pure palladium is

$$\alpha = R_{100} : R_0 = 1,3790.$$

This is approximately 3% higher than the temperature coefficient of commercial palladium. The thermoelectric properties of spectrally-pure palladium are substantially different from those of commercial ones.

The temperature coefficient of electric resistivity can be measured with an accuracy to hundredths of a percent; consequently, its high value, which approaches that given above, can be served as a criterion for the purity of the metal.

The thermal emf of the specimen of palladium containing impurities, coupled with spectrally-pure metal, gives a very clear picture of the contamination of palladium. However, it is dangerous to use only the thermoelectric method, since all metals, alloyed with palladium, cause a change in the thermoelectric properties towards the negative side. Thus, for example, gold, silver, or copper, when added to palladium in small amounts produce an alloy that is thermoelectrically negative relative to palladium, while platinum, rhodium, and tungsten produce a more positive alloy.

One cannot exclude the possibility that at a certain composition of different impurities there may be a mutual cancellation of their influence on the thermoelectric properties of the palladium.

Thus, to ascertain the purity of palladium one can recommend, as the simpler method, an investigation of the thermal emf of a thermocouple made up of the spectrally-pure palladium and the investigated metal. The presence of a considerable thermal emf is evidence of impurities in the metal. Its absence still does not indicate absolute purity of the metal. In this case it is necessary to measure accurately the temperature coefficient. A metal with a maximum temperature coefficient will be the purest.

Rhodium /69/. The first indications of the polymorphism of rhodium were given by Mendenhall and Ingersoll /103/ in 1908, as they observed the change in the light emission of rhodium at a temperature near 1050° C. Jaeger and Rosenbohm /75/ observed a maximum specific heat of rhodium in the interval of temperatures from 1100 to 1200° C. Dixon /104/ established a jump-like change in the electric resistivity and thermionic emission at a temperature near 1100° C. The x-ray research of Jaeger and Zanstra /105/ indicate the existence of two modifications of rhodium: α-rhodium, which is stable below 1200° C and has a simple cubic lattice, with a parameter 9.211 A, and β-rhodium, which is stable above 1200° C, has a

cubic face-centered lattice, with a parameter of 3.7957 A.

Booth and Dixon $\underline{/106/}$, investigating the thermal emf of rhodium coupled with platinum, have established the temperature of the polymorphous transformation as 1091° C. However, the method they used for the measurement of the integral thermal emf is not sufficiently accurate, since the change in the thermal emf at the transformation point of rhodium is quite small. Wensell and Tuckermann $\underline{/107/}$ have subjected to a correct critique the mathematical treatment of the results of Booth and Dixon, but have denied, without sufficient justification, the existence of polymorphous transformations of rhodium. The thermoelectric properties of rhodium were investigated by Holborn and Day $\underline{/74/}$. Their data do not give any indications of any polymorphism of rhodium.

For the present investigation we used commercial rhodium, containing not more than 0.02% of impurities.

The rhodium was molten in a high frequency furnace in a corundise crucible and **drawn** into a porcelain tube. The resultant stick of rhodium, approximately 20 mm long, was annealed at 100° C, and its thermoelectric properties were investigated with the aid of a Kurnakov pyrometer.

Fig. 19 shows curves of the thermal emf made with a pyrometer.

The temperature of the transformation $\alpha\text{-}Rh \rightleftarrows \beta\text{-}Rh$ is 1030° C.
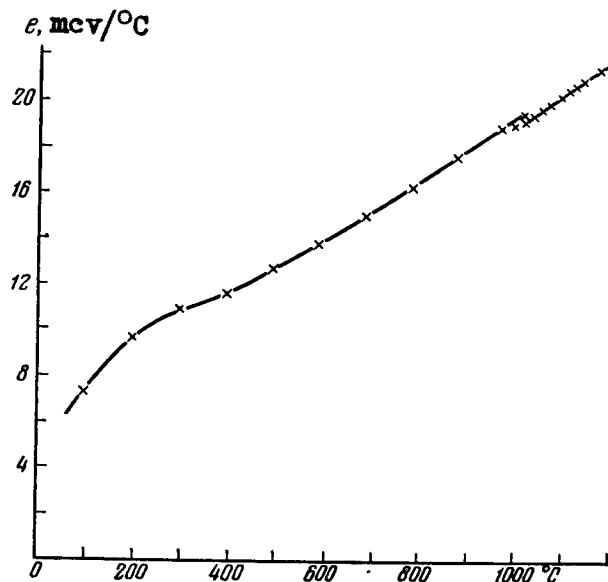
Fig. 56. Differential Thermal emf of Rhodium Coupled With Platinum.
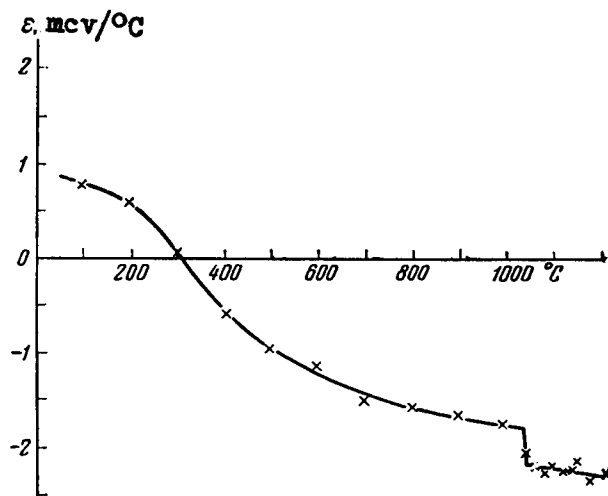
Fig. 57. Absolute Thermal emf of Rhodium.
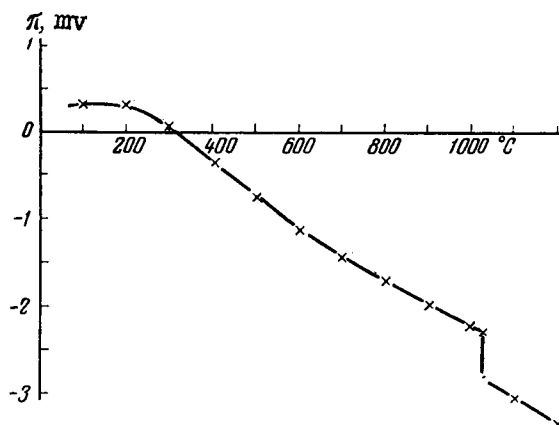
Fig. 58. Thermoelectric Potential of Rhodium.

The values of the differential thermal emf of rhodium coupled with platinum, obtained experimentally, are given in Table 18 and Fig. 56.

Rhodium coupled with platinum develops a positive thermal emf at temperatures from 0 to 1200° C.

Fig. 57 shows the curve of the absolute thermal emf of rhodium. At 0 to 300° C the thermal emf is positive. As the tempera-

ture rises its value diminishes smoothly, and at 1030° one observes
a jump-like change in the absolute thermal emf, connected with the
   α Rh→β-Rh   transition. The curve for thermoelectric potential
(Fig. 58) has a similar behavior.

The value of the thermoelectric properties of rhodium is given
in Table 19.

The Thomson emf (Fig. 59) is negative over the entire investi-
gated range of temperatures and has a minimum of 300° C. At the point
of polymorphous transformation, 1030° C, it assumes a values of $-\infty$.
The α-rhodium to β-rhodium transition represents a first-order
transformation and is similar in type to the β-iron to γ-iron
transition. It is accompanied by a jump-like reduction in the entropy
of the current carriers. The jumping potential is very small at the
transition point (0.53 millivolts).

Table 18

Differential Thermal emf of Rhodium

t, °C	e coupled with plati-num, micro-volt/°C	ε, microvolt/°C	t, °C	e coupled with plati num, micro volt/°C	ε, microvolt/°C
98	+ 7,38	+0,79	1029	+19,51	—2,00
196	+ 9,72	+0,60	1046	+19,60	—2,16
294	+10,94	+0,08	1064	+19,83	—2,19
393	+11,72	—0,57	1080	+20,11	—2,14
491	+12,77	—0,94	1104	+20,43	—2,17
588	+14,00	—1,12	1124	+20,75	—2,14
687	+15,07	—1,48	1129	+20,85	—2,11
784	+16,40	—1,56	1154	+21,05	—2,28
882	+17,74	—1,64	1189	+21,60	—2,23
980	+19,02	—1,72	—	—	—
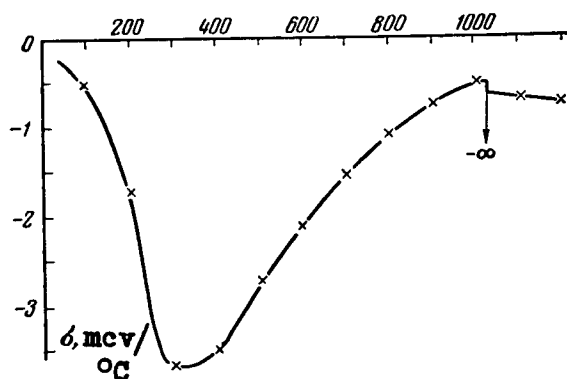
Fig. 59. Thomson emf of Rhodium.

Table 19

Thermoelectric Properties of Rhodium

°C	ε, micro-volt/°C	σ, micro-volt/°C	π, mv.	°C	ε, micro-volt/°C	σ, micro-volt/°C	π, mv.
100	+0,82	—0,49	+0,31	800	—1,58	—1,07	—1,70
200	+0,62	—1,70	+0,29	900	—1,66	—0,76	—1,95
300	+0,10	—1,36	+0,06	1000	—1,72	—0,51	—2,19
400	—0,56	—3,50	—0,38	1030	—1,74	—0,52	—2,27
500	—0,97	—2,70	—0,75	1030	—2,15	—0,65	—2,80
600	—1,27	—2,10	—1,11	1100	—2,18	—0,69	—3,00
700	—1,46	—1,56	—1,42	1200	—2,24	—0,74	—3,30

4. CONCLUSIONS

The thermoelectric properties have already been investigated for the majority of noble metals. Thus, it becomes possible to compare out data with those in the literature. Having on hand spec-trally-pure metals we obtained in this investigation the most reli-able results. Certain deviations from the literature data are ex-plained by the difference in the purity of the metal and of the com-parison electrodes, and also in the difference in the metals of in-vestigations.

We studied the metals in the first group of the periodic system of elements. Copper served as the primary comparison electrode, and its thermoelectric properties have been exactly established on the basis of extensive literature material. We studied similarly gold and silver. The metals of the first group are current conductors, in which the conductivity is essentially due to the positive carriers, namely "holes." This causes the positive thermal emf of copper, gold, and silver.

Of the metals of the eighth group of the periodic system of elements, we studied iron, cobalt, and nickel. For our investigations these metals are of interest because they are polymorphous transformations with many features in common with the transformation of the investigated alloy.

Of the noble metals of the eighth group, we investigated platinum, palladium, and rhodium.

We studied in great detail the thermoelectric properties of spectrally-pure palladium and platinum. These metals are typical electronic conductors, and have a negative thermal emf.

Having on hand several specimens of spectrally-pure platinum, the author has used the thermoelectric method to investigate the purity of the metal. Until now the measure of purity of platinum was a temperature coefficient of electric resistivity. The thermoelectric method is a more sensitive criterion of the purity of platinum for the establishment of spectrally indeterminable impurities. In addition, the thermoelectric method is readily realized technically.

An investigation of rhodium is of interest because its polymorphous transformations were not established with sufficient accuracy. A study of the thermoelectric properties of rhodium has shown that the point of polymorphous transformations of rhodium lies at 1030° C. Rhodium is a technically important component part of alloys, and a correct representation of its polymorphous transformations is very important. However, when alloys of rhodium are investigated, not enough due attention was paid to this problem.

In the present work the thermoelectric method was also used to investigate transformations in pure iron, cobalt, and nickel.

The thermoelectric properties, which depend on the properties of the current carriers and which are thermodynamic functions of the temperature, vary as the thermodynamic functions of the metal. Between these, naturally, there is close connection, but the exact mathematical relationship is unknown.

The thermoelectric method is applicable to the investigation of first-order transformations, occurring at a constant temperature.

In our experiments we studied the β-Fe$\rightarrow\gamma$-Fe, α-Co$\rightarrow\beta$-Co, and α-Rh$\rightarrow\beta$-Rh. transformations.

Along with these examples we also considered the γ-Fe$\rightarrow\delta$-Fe iron transition (according to data by Goetz).

Comparing the variations of the thermoelectric quantities and the thermodynamic functions of metals at the transition points, it is easy to note that first-order transitions, in two types. One of these is observed in the γ-Fe$\rightarrow\delta$-Fe and α-Co$\rightarrow\beta$-Co transitions and is accompanied, upon heating, by jump-like increases in the entropy of the metal and an increase in the absolute thermal emf (entropy of the current carriers). Here the specific heat of the metal and the Thomson emf (the specific heat of the carriers) assume values of

The second type of transformation, from β-Fe$\rightarrow\gamma$-Fe and from α-Rh$\rightarrow\beta$-Rh , is accompanied upon heating by jump-like increase in the entropy of the metal and a jump-like decrease in the absolute thermal emf. In this case the specific heat of the metal assumes a value of plus infinity while the Thomson emf equal minus infinity.

A clear example of both types of transformations is afforded by iron (Fig. 27). In the β-Fe$\rightarrow\gamma$-Fe transition one observes a transition from a space-centered cubic lattice into a face-centered cubic lattice. This transition is accompanied by a jump-like decrease in the absolute thermal emf. Upon further heating the crystal lattice again acquires a structure of a body-centered cube of iron. Accordingly, the γ-Fe$\rightarrow\delta$-Fe transition is accompanied by a jump-like increase in the absolute thermal emf.

If $\sigma = -\infty$ in the β-Fe$\rightarrow\gamma$-Fe transition, then the function

$$\Delta H = \int_{T_1}^{T_2} \sigma dT,$$

i.e., the enthalpy of the current carriers, experiences a discontinuity and its value decreases.

In the second case, in the γ-Fe$\rightarrow\delta$-Fe transition, we have, $\sigma = +\infty$ and the enthalpy of the current carriers has a discontinuity and increases its value.

Quantitatively these jumps are equal to the changes in the thermoelectric potential at the point of transition, since in this case the thermal emf (thermodynamic potential of the current carriers)

remains constant also at the point of transition:

$$\Delta E = \Delta \pi - \Delta H = 0.$$

The α-Co$\rightarrow\beta$-Co transition is accompanied by an increase in the enthalpy, while the α-Rh$\rightarrow\beta$-Rh transition is accompanied by a decrease in the enthalpy of the current carriers.

In our investigation we studied second-order transformations: the transition of iron, cobalt, and nickel into a non-magnetic state. The thermoelectric properties change also in these cases like the thermodynamic functions of the metal.

When heating, the specific heat of the metal and the Thomson emf increase rapidly and diminish jump-wise in the transition point.

The curve showing the variation of the thermal emf with the temperature exhibits a kink in the transition point, since the entropy of the metal and of the current carriers of both phases are the same at the point of second-order transition.

CHAPTER IV

INVESTIGATION OF THERMOELECTRIC PROPERTIES OF ALLOYS

1. INTRODUCTION

Before the development of physico-chemical analysis, the investigation of the thermoelectric properties of alloys did not bear a systematic character, and reduced to a study of the individual alloys for thermocouples or to the invention of thermocouple generators.

The first systematic investigation of various types of systems of alloys was carried by N. N. Tuturin /108/ in 1909. He investigated many systems that form eutectic mixtures: lead-tin, tin-aluminum, tin-zinc, tin-bismuth, lead-bismuth, and the following solutions: bismuth-antimony, silver-gold, and systems in which are formed chemical compounds: copper-antimony, copper-tin, copper-zinc, and copper-aluminum. It was established that in mechanical mixtures the thermal emf varies additively if the composition is expressed in atomic percent.

Kinks on the curves are formed on the boundaries of the phase regions and of the compositions of the chemical compounds.

The work of N. N. Tuturin was repeated by Rudolfi /109/, Haken /110/, and Broniewski /111/ in 1910. Solid solutions of alloys of noble metals were investigated by Geibel /112/ (palladium with gold, silver and platinum, partially platinum with iridium, gold, and silver).

Sedstrom /113/ investigated again several systems of alloys of noble metals in a narrow temperature interval (up to 100° C). In addition to the systems already studied by Geibel, Sedstrom investigated thermoelectric and other properties of gold-copper and palladium-copper alloys.

Norbury [114] investigated a large number of solid solutions of low concentrations and has shown that the thermal emf of copper, silver, gold, and iron decreases as small amounts of most metals are added to them. The author observed a similar phenomenon with palladium alloys. However, platinum increases the thermal emf of palladium. Small additions of metals, with the exception of gold, increased the thermal emf of platinum.

The extensive research of V. Ya. Nemilov and A. A. Rudnitskiy, T. A. Vidusova, and N. M. Voronova with their associates have extended considerably our ideas concerning the thermoelectric properties of solid solutions. They have studied in detail the alloys of platinum with rhodium [115], platinum with palladium and palladium with gold [116], and palladium and gold with silver [97].

A study was made of the variation of the thermal emf of platinum caused by small additions of silicon [117], ruthenium [118], iron and copper [119], tungsten [120], beryllium [121], rhenium [122], and also the effect of impurities of tungsten [123], rhodium [124], rhenium [125] and the properties of palladium.

The following triple solid solutions were studied: palladium-gold-silver [97], platinum-iron-copper [119], platinum-palladium-gold [116], and platinum-palladium-rhodium [126].

It is seen from the above investigations that in the formation of solid solutions the impurities sometimes increase and sometimes decrease the thermal emf of the metal.

Thus, for a continuous series of solid solutions, the isotherms of the thermal emf have either a maximum or a minimum.

First to be investigated systematically were triple solid solutions. The third component, introduced into the alloy increases the thermal emf in some systems and decreases it in others.

Chemical compounds are characterizied, on the diagram showing the composition vs. the thermal emf, by singular points that represent minima, maxima, or kinks on the isotherms. This phenomenon was first shown experimentally by N. N. Tuturin [108].

Chemical compounds, which have properties of semiconductors, have a very large thermal emf.

Fig. 60 shows a curve of thermal emf of alloys of antimony with zinc according to data of Ye. D. Devyatkova, Yu. P. Maslakovets, and L. S. Stil'bans [127]. The differential thermal emf of the alloy, corresponding in its to the chamical compound SbZn, coupled with lead, amounts to approximately 300 microvolt per degree C.
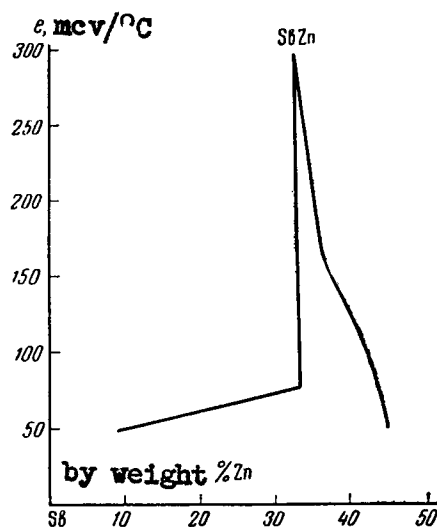
Fig. 60. Thermal emf of Antimony-Zinc Alloys.

The laws of variation of the Thomson emf in metallic alloys have not been discussed in the literature to date.

In this work we examine in detail the laws of variation of the thermoelectric properties of alloys for various cases of continuous series of solid solutions, give several versions of the limited solubility of components, and study in detail the diagrams of states in which there are cases of transformations connected with the formation of chemical compounds.

We use in this work the results of our previous works, and also obtain new data.

2. GOLD-SILVER /97/.

A considerable number of publications are devoted to the investigation of the gold-silver system and from these one can consider it rigorously established that the components are mutually totally soluble in the liquid and solid state. The diagram of states, investigated by Janecke /128/, Raydt /129/ and other authors /130/ is typical for a continuous series of solid solutions (Fig. 61).

Investigations of physical properties, carried out by Sedstrom /131/, Broniewsky and Weselowsky /132/ and Schimizu /133/ con-

99

firm the existence of a continuous series of solid solutions.
Olender /134/ has proposed, on the basis of electrochemical investigations, the possibility of the existence of new phases below 800° C
between 0-18 and 50-80 atomic percent gold.

X-ray investigations of the system, carried out by McKeehan
/135/, Weiss /136/, Young /137/, Holgersson /138/, Sacks and Weertd
/139/, and V. G. Kuznetsov /140/ have shown the presence of a cubic
face-centered lattice over the entire extent of the diagram.

The lattice parameter changes along the curve with a minimum,
which is an exception to the Vegard law.

Phragman /141/ has shown the absence of an ordered structure
in the alloys of gold with silver. Norman and Warren /142/ who
carried out an x-ray analysis of two alloys of the system, have
found superstructure lines on the x-ray patterns, indicating the presence of a near-order ordering, caused by the formation of chemical
compounds AuAg and $AuAg_3$. However, the conclusions of Normann and
Warren cannot be considered reliable, since the existence of these
chemical compounds have not been conformed by any other methods of
investigation.
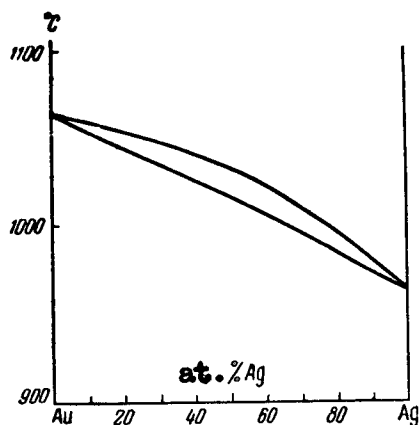
Fig. 61. Diagram of States of the Gold-Silver System.

The thermal emf of the alloys of gold with silver have been
investigated by N. N. Tuturin /108/, Rudolfi /109/ and Sedstrom
/113/.

Our own detailed investigation /97/ of the hardness, microstructure, electric resistivity, its temperature coefficient, tensile strength, elongation, and thermal emf over a wide range of temperatures have shown that the gold-silver alloys are a continuous
series of solid solutions.

To study the thermoelectric properties, the alloys were prepared in corundise crucibles in a high frequency furnace, forged, rolled, and drawn into a wire 0.5 mm in diameter. The wire was annealed at 500° C to remove the case hardening for five days and was cooled in the oven.

A potentiometer was used to study the integral thermal emf when coupled with platinum.

The results of the measurements are shown in Table 20 and in Fig. 62. The integral thermal emf of all the alloys of gold with silver is positive relative to platinum and increases smoothly with increasing temperature.

Table 20

Integral Thermal emf of Alloys of Gold with Silver
When Paired with Platinum, E, Millivolts

Ag		Temperature, °C								
atomic %	% by weight	100	200	300	400	500	600	700	800	900
10	5,70	0,601	1,455	2,501	3,795	5,298	6,813	8,569	10,423	12,527
20	12,00	0,523	1,252	2,228	3,392	4,742	6,035	7,760	9,450	11,407
30	18,99	0,509	1,222	2,104	3,212	4,512	5,804	7,353	8,956	10,830
40	26,70	0,466	1,169	1,997	3,024	4,278	5,520	7,006	8,558	10,378
50	35,36	0,438	1,111	1,915	2,905	4,105	5,313	6,760	8,280	10,083
60	45,07	0,405	1,145	1,938	2,952	3,880	4,895	6,905	8,327	9,895
70	56,07	0,423	1,090	1,885	2,050	3,970	5,139	6,662	8,327	10,003
80	68,63	0,433	1,135	1,953	2,962	4,072	5,252	6,920	8,719	10,512
90	83,12	0,482	1,238	2,141	3,279	4,468	5,767	7,923	9,779	11,805

Fig. 63 shows the isotherms of the integral thermal emf of alloys of gold with silver. They have a smooth minimum near approximately 60 to 70 atomic percent silver.

The values of the absolute thermal emf of alloys of gold with silver are shown in Table 21 and in Fig. 64. The absolute thermal emf of alloys in the vicinity of 10 to 50 atomic percent silver change with the temperature linearly. The thermal emf of the alloys containing 30, 60, and 70 atomic percent silver is practically constant as the temperature is increased. For alloys with 80 and 90 atomic percent silver the variation is represented by rising curves.
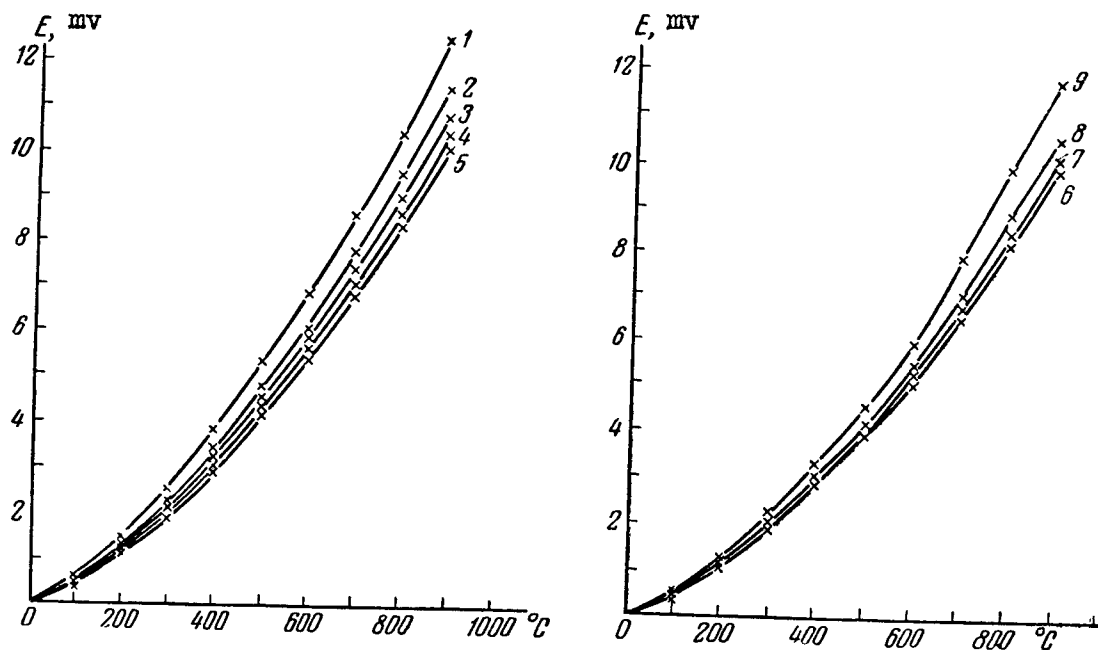
Fig. 62. Integral Thermal emf of Alloys of Gold with Silver Coupled
with Platinum:

1 -- 10% silver; 2 -- 20% silver; 3 -- 30% silver; 4 --
40% silver; 5 -- 50% silver; 6 -- 60% silver; 7 -- 70%
silver; 8 -- 80% silver; 9 -- 90%silver.

The isotherms of the composition vs the absolute thermal emf
of alloys of gold with silver are shown in Fig. 65.

Table 21

**Absolute Thermal emf of Alloys of Gold with
Silver ε, microvolt per degree C**

Ag atomic %	Temperature, degrees C									
	0	100	200	300	400	500	600	700	800	900
10	0,02	0,23	0,44	0,65	0,87	1,08	1,29	1,50	1,71	1,92
20	—0,88	—0,74	—0,60	—0,46	—0,32	—0,18	—0,05	+0,09	+0,23	+0,36
30	—1,00	—1,00	—1,00	—1,00	—1,00	—1,00	—1,00	—1,00	—1,00	—1,00
40	—1,14	—1,20	—1,26	—1,31	—1,36	—1,42	—1,48	—1,53	—1,59	—1,65
50	—1,50	—1,56	—1,62	—1,68	—1,74	—1,81	—1,87	—1,94	—2,00	—2,06
60	—1,84	—1,84	—1,84	—1,84	—1,84	—1,84	—1,84	—1,84	—1,84	—1,84
70	—1,60	—1,60	—1,60	—1,60	—1,60	—1,60	—1,60	—1,60	—1,60	—1,60
80	—1,60	—1,59	—1,58	—1,57	—1,52	—1,40	—1,20	—0,98	—0,67	—0,35
90	—1,14	—1,08	—1,00	—0,89	—0,68	—0,20	+0,70	+1,60	+2,50	+3,4

Depending on the composition, the curves of the absolute thermal emf are smooth and have gentle minima with slight negative values. As the temperature increases, the minimum shifts towards the center of the diagram.

Table 22

**Thermoelectric Potential of Alloys of Gold with
Silver, π , millivolts**

Ag atomic %	Temperature, degrees C									
	0	100	200	300	400	500	600	700	800	900
10	0,005	0,086	0,22	0,37	0,59	0,83	1,13	1,46	1,84	2,25
20	—0,24	—0,28	—0,28	—0,26	—0,22	—0,14	—0,04	+0,09	+0,25	+0,42
30	—0,27	—0,37	—0,47	—0,57	—0,67	—0,77	—0,87	—0,97	—1,07	—1,17
40	—0,31	—0,45	—0,60	—0,75	—0,91	—1,10	—1,29	—1,49	—1,71	—1,94
50	—0,41	—0,58	—0,77	—0,96	—1,17	—1,40	—1,63	—1,89	—2,15	—2,42
60	—0,50	—0,69	—0,87	—1,05	—1,24	—1,42	—1,61	—1,79	—1,97	—2,16
70	—0,44	—0,60	—0,76	—0,92	—1,08	—1,24	—1,40	—1,56	—1,72	—1,88
80	—0,44	—0,59	—0,75	—0,90	—1,02	—1,08	—1,05	—0,95	—0,72	—0,41
90	—0,31	—0,40	—0,47	—0,51	—0,46	—0,15	+0,61	+1,56	+2,68	+3,99

Table 22 and Fig. 66 and 67 show the values of the thermoelectric potential. Its variations with temperature and with the composition are analgous to the changes in the absolute thermal emf. Table 23 and Fig. 68 show the values of the Thomson emf as a function of the temperature. For alloys containing 30, 60 and 70 atomic percent of silver, the Thomson emf is zero, since the absolute thermal emf is constant. The Thomson emf of alloys with 80 and 90% atomic percent silver increases in a unique manner.
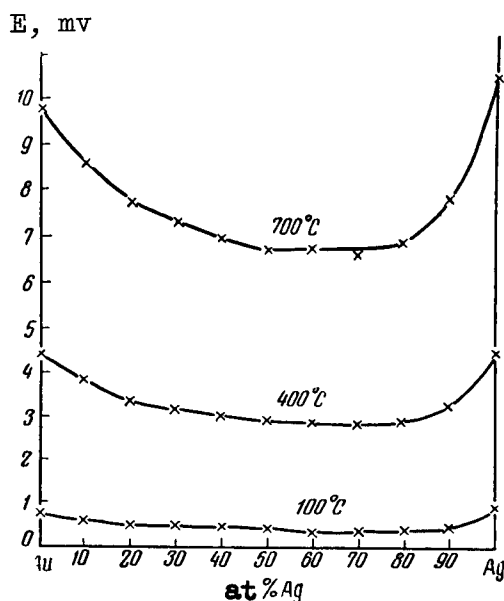
Fig. 63. Isotherms of Central Thermal emf of Alloys of Gold With Silver.

Table 23

Thomson emf of Alloys of Gold with Silver σ, per microvolt degree C

| Ag, atomic %	Temperature, degrees C									
	0	100	200	300	400	500	600	700	800	900
10	0,58	0,79	1,00	1,21	1,42	1,63	1,84	2,05	2,26	2,48
20	0,38	0,52	0,65	0,79	0,93	1,07	1,21	1,34	1,48	1,62
30	0	0	0	0	0	0	0	0	0	0
40	—0,15	—0,21	—0,27	—0,32	—0,38	—0,43	—0,49	—0,55	—0,60	—0,66
50	—0,17	—0,23	—0,29	—0,37	—0,42	—0,48	—0,54	—0,61	—0,68	—0,74
60	0	0	0	0	0	0	0	0	0	0
70	0	0	0	0	0	0	0	0	0	0
80	0,03	0,04	0,05	0,17	0,60	1,30	2,05	2,75	3,35	3,90
90	0,15	0,27	0,45	0,90	2,25	6,50	7,85	8,75	9,65	10,55
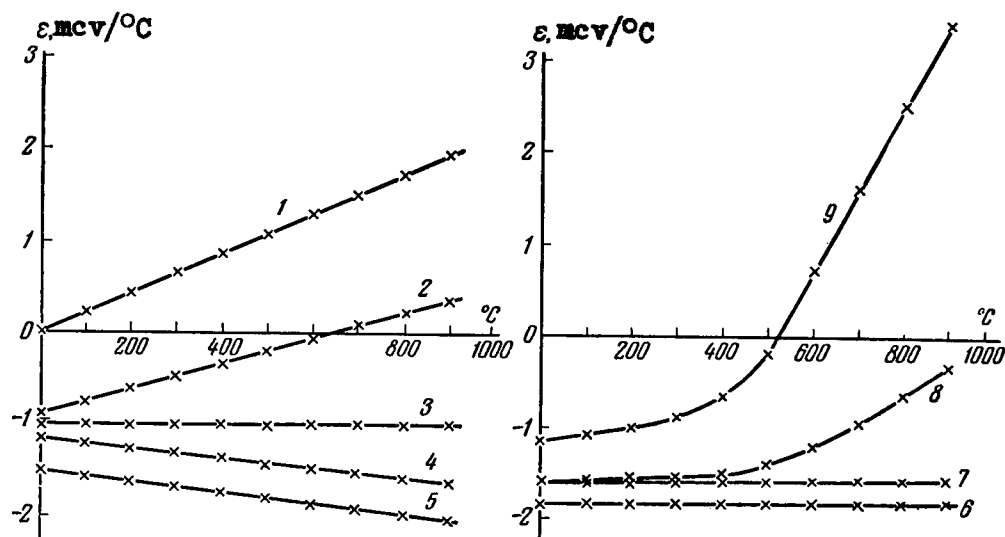
Fig. 64. Absolute Thermal emf of Alloys of Gold with Silver:

1 -- 10%silver; 2 -- 20% silver; 3 -- 30% silver;
4 -- 40% silver; 5 -- 50% silver; 6 -- 60% silver;
7 - 70% silver; 8 -- 80% silver; 9 - 90% silver.
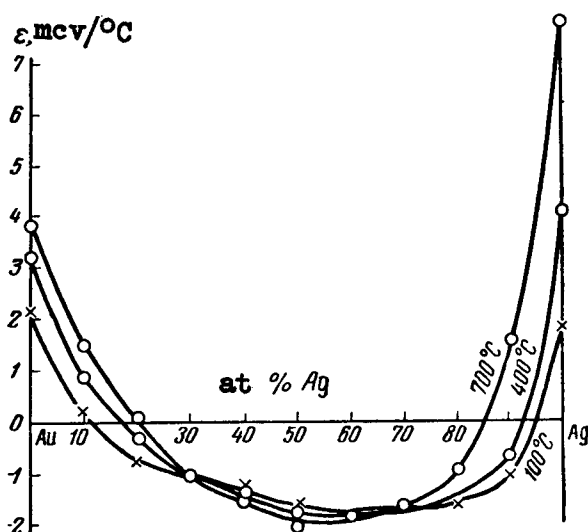
Fig. 65. Isotherms of the Absolute Thermal emf of Alloys
of Gold with Silver.

Fig. 69 shows isotherms of the Thomson emf as functions of
the composition. Up to 500° C they are smooth curves with a minimum

that has a slight negative value in the region of compositions from
30 to 70 atomic percent silver.
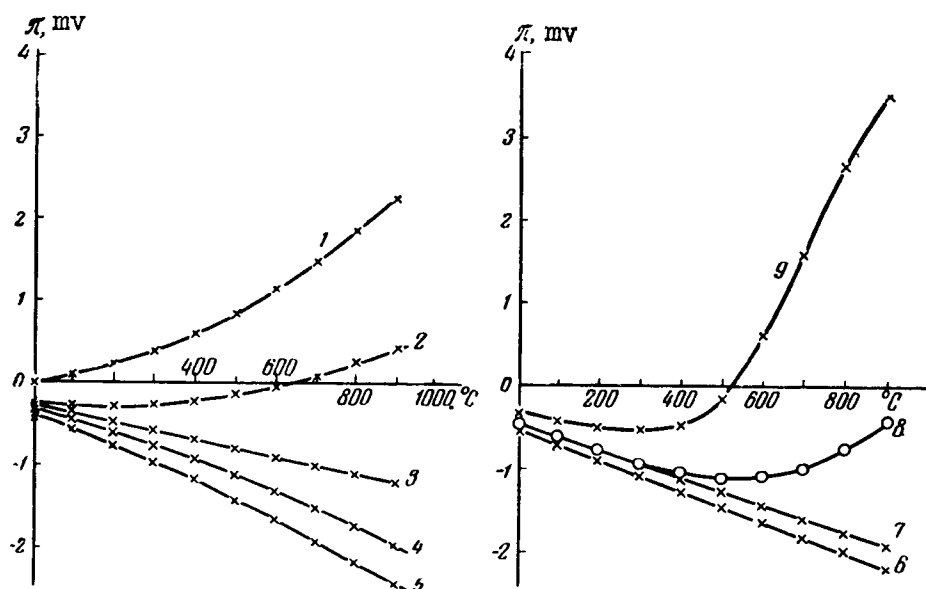
Fig. 66. Thermoelectric Potential of Alloys of Gold with
Silver:

1 -- 10% silver; 2 -- 20% silver; 3 -- 30% silver;
4 - 40% silver; 5 -- 50% silver; 6 -- 60% silver;
7 -- 70% silver; 8 -- 80% silver; 9 -- 90% silver.
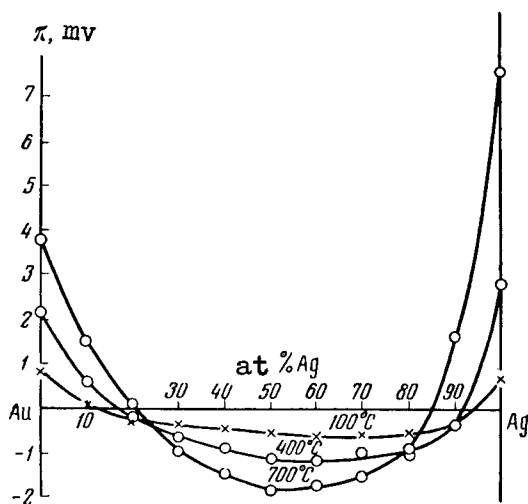
Fig. 67. Isotherms of Thermoelectric Potential of Alloys
of Gold with Silver.

At temperatures above 600° C and a composition of ten atomic percent silver one observes a small maximum, the formation of which is connected with the considerable drop in the Thomson emf of gold at high temperatures (Fig. 41).

For the sake of comparison, Figs. 70-72 show curves of the specific electric resistivity, its temperature coefficient, and the electric conductivity $\boxed{97}$.
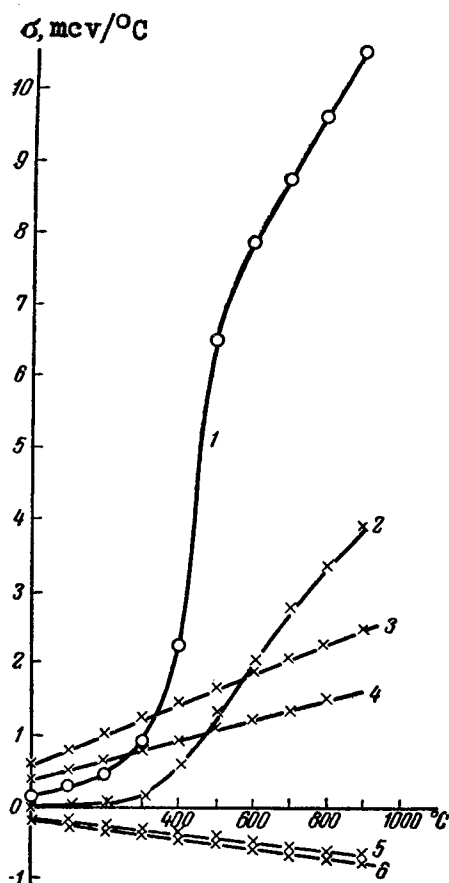
Fig. 68. Thomson emf of Alloys of Gold with Silver:

1 -- 90% silver; 2 -- 80% silver; 3 -- 10% silver;
4 -- 20% silver; 5 -- 40% silver; 6 -- 50% silver.
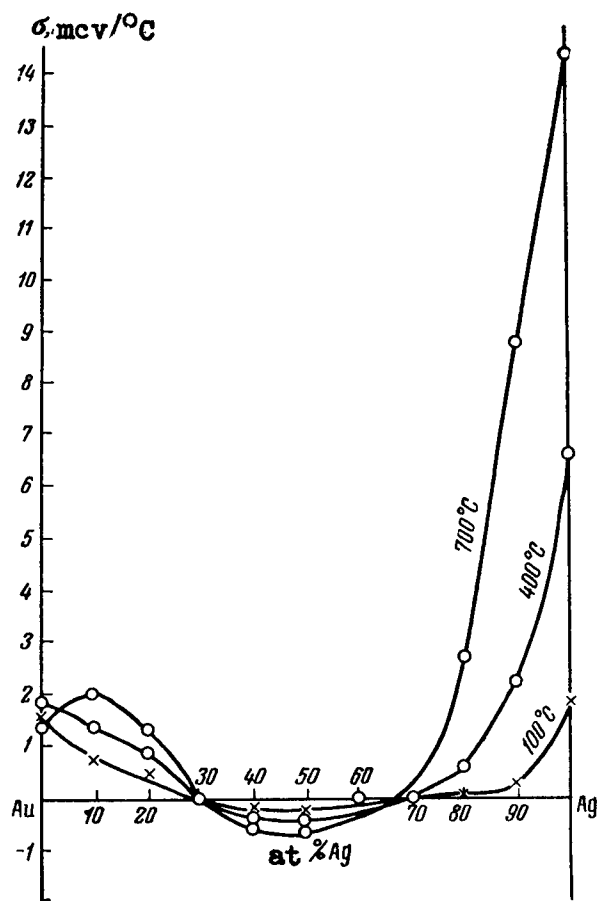
Fig. 69. Isotherms of the Thomson Thermal emf of
Alloys of Gold and Silver.
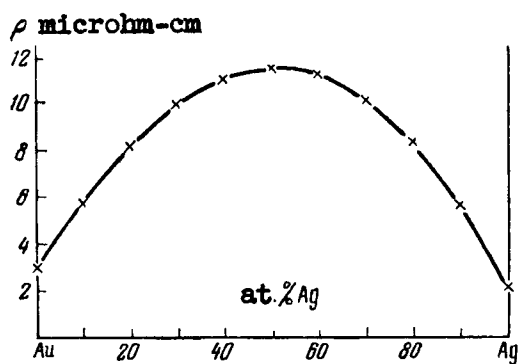
Fig. 70. Specific Electric Resistivity of Alloys of
Gold with Silver.
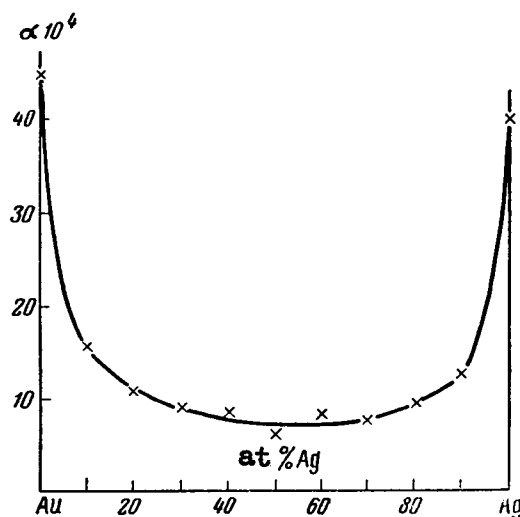
Fig. 71. Temperature Coefficient of Electric Resistivity of Alloys of Gold with Silver.

All the the thermoelectric and electric properties investigated by us for alloys of gold with silver vary along smooth curves which have no singular points and sharp bends. Thus, one can conclude that gold and silver form a continuous series of solid solutions. The possibility of formation of chemical compounds, established by Norman and Warren /142/ are not confirmed by our investigations.
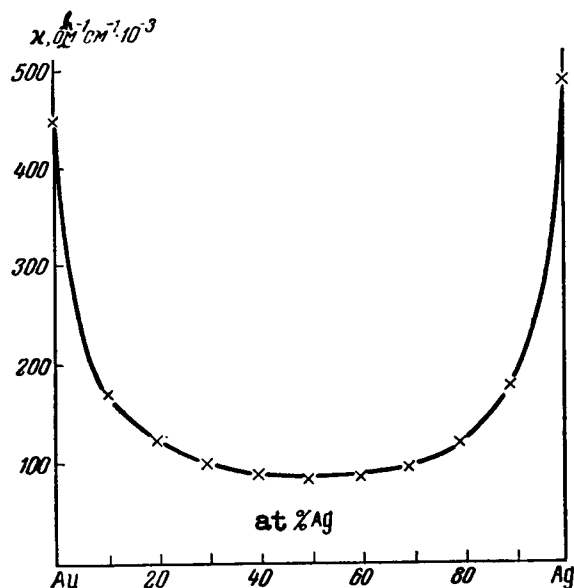
Fig. 72. Specific Electric Resistivity of Alloys of Gold with Silver.

The positive thermal emf of gold and silver indicates the presence of positive current carriers in these metals, along with electrons.

In the case of gold-silver alloys one observes a weak negative thermal emf. Consequently electron conductivity predominates there.

3. PLATINUM-PALLADIUM /116/

The melting temperatures of platinum with palladium have not been investigated to this day.

Investigations of the physical properties of alloys indicate the formation of a continuous series of solid solutions /143/. At first Rudolfi /109/ investigated the thermal emf of alloys. Alloys with palladium were examined in greater detail by Geibel /112/, who has established, on the basis of investigations of the electric resistivity, its temperature coefficient, the thermal emf, and tensile strength that the components have an unlimited solubility in each other.

Schulze /144/ and Van Liempt /145/ have investigated the heat conductivity.

Tamman and Rocha /146/, who investigated the hardness of alloys in quenched and annealed states, have reached the conclusion that transformations are possible in the solid state.

The investigations of Vogt /147/ and Schimizu /133/ on the magnetic susceptibility of the alloys have confirmed the presence of a continuous series of solid solutions in the palladium-platinum system.

Our own detailed investigations /116/ of the hardness, microstructure, electric resistivity, its temperature coefficient, and the thermal emf, carried out over a broad range of temperatures, tensile strength, and elongation have shown that there is a continuous series of solid solutions in the platinum-palladium.

To carry out the experiments, the alloys of platinum with palladium were molten in a high-frequency furnace, forged, rolled into a wire 0.5 mm in diameter, and annealed at a temperature of 1000° C for one hour. We studied the integral for the thermal emf of the alloys by comparison with the thermal emf of platinum with the aid of a potentiometer up to a temperature of 1400° C with the cold junction temperature being 0° C. The results of the measure-

110

ments are given in Table 24 and in Fig. 73. The curves of the integral thermal emf increase smoothly with increasing temperature. The thermal emf of the alloy 90% Pd + 10% Pt has a smooth maximum at 800° C.

Fig. 74 shows the isotherms of the integral thermal emf of platinum-palladium alloys coupled with platinum. The thermal emf increases rapidly from negative values, which occur for palladium, and assumes a positive value at approximately five atomic percent platinum.
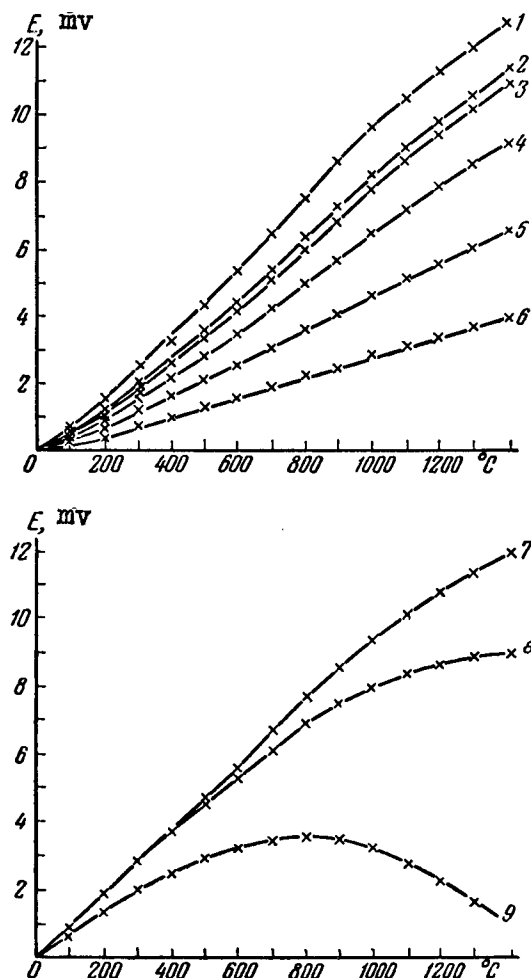
Fig. 73. Integral Thermal emf of Alloys of Platinum with Palladium, coupled with Platinum; Palladium Content: 1 -- 60%, 2 -- 50%, 3 -- 40%, 4 -- 30%, 5 -- 20%, 6 -- 10%, 7 -- 70%, 8 -- 80%, 9 -- 90%.

111
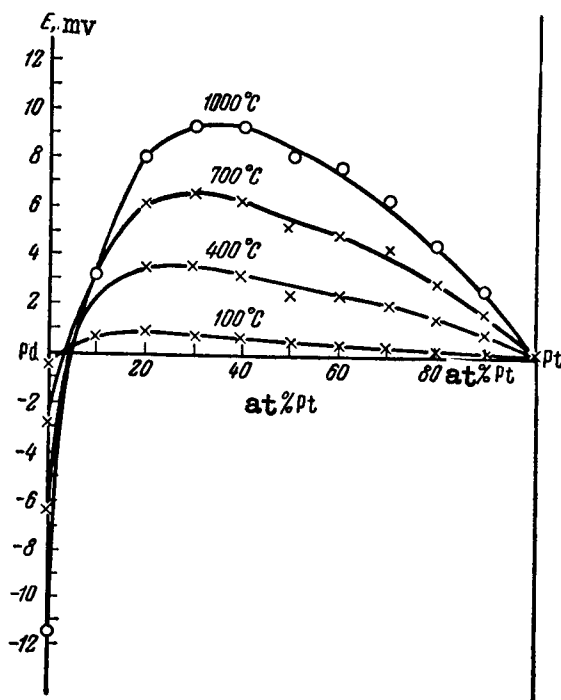
Fig. 74. Isotherms of the Spectral Thermal emf of Alloys
of Platinum with Palladium.

All curves exhibit smooth maxima that shift towards the pla-
timum side with increasing temperature. At 100° C the maximum lies
near 80 atomic percent palladium, and at 1000° C it shifts to 60
atomic percent palladium. The curves of the thermal emf over the
entire extent of the diagram change smoothly, without bends.

The values of the absolute thermal emf of alloys (Table 25
and Fig. 75) diminish smoothly with increasing temperature. Alloys
with 60 to 80 atomic percent palladium have small positive values
at temperatures from 0 to 200° C.

Table 24

Integral Thermal emf of Alloys of Platinum with Palladium, E, mv.

Pd atomic %	Pd % by weight	Temperature, degrees C 100	200	300	400	500	600	700	800	900	1000	1100	1200	1300	1400
10	5,73	0,14	0,36	0,71	0,94	1,24	1,51	1,87	2,19	2,51	2,82	3,10	3,40	3,66	3,93
20	12,02	0,25	0,64	1,18	1,55	2,10	2,45	3,04	3,56	4,06	4,58	5,05	5,53	5,98	6,42
30	18,98	0,38	0,91	1,65	2,12	2,79	3,41	4,24	4,96	5,65	6.39	7,07	7,74	8,37	9,01
40	26,71	0,44	1,08	1,94	2,50	3,30	4,06	5,06	5,93	6,77	7,65	8,46	9,28	9,97	10,72
50	35,34	0,52	1,22	2,06	2,60	3,54	4,36	5,29	6,25	7,15	8,08	8,87	9,60	10,35	11,19
60	45,05	0,69	1,56	2,59	3,24	4,30	5,29	6,37	7,41	8,43	9,44	10,30	11,11	11,81	12,59
70	56,05	0,79	1,75	2,85	3,55	4,62	5,61	6,65	7,67	8,57	9,40	10,15	10,82	11,34	11,90
80	68,62	0,84	1,80	2,86	3,50	4,51	5,29	6,11	6,91	7,49	8,01	8,38	8,63	8,82	8,93
90	83,11	0,66	1,34	2,02	2,39	2,88	3,21	3,43	3,50	3,40	3,14	2,74	2,16	1,61	—

Table 25

Absolute Thermal emf of Alloys of Platinum
with Palladium, ε , microvolt per degree C.

Pd atomic %	Temperature, degrees C						
	0	100	200	300	400	500	600
10	—3,5	—5,0	—6,5	—8,0	—9,5	—11,0	—12,5
20	—2,3	—3,8	—5,2	—6,6	—8,0	— 9,5	—10,9
30	—1,4	—2,1	—3,2	—4,7	—6,2	— 7,6	— 9,1
40	—0,9	—1,3	—2,2	—3,5	—4,9	— 6,3	— 7,7
50	—0,6	—1,0	—1,6	—2,6	—3,9	— 5,2	— 6,5
60	+1,2	+0,8	+0,2	—1,0	—2,4	— 3,9	— 5,4
70	+2,1	+1,7	+0,8	—0,5	—2,0	— 3,6	— 5,5
80	+2,5	+2,0	+1,2	—0,5	—2,6	— 4,8	— 7,0
90	0,0	—0,2	—1,7	—4,4	—7,2	—10,0	—12,8

Temperature, degrees C					
700	800	900	1000	1100	1200
—14,0	—15,5	—17,0	—18,5	—20,0	—21,5
—12,3	—13,7	—15,2	—16,5	—18,0	—19,4
—10,5	—12,0	—13,5	—14,9	—16,4	—17,9
— 9,0	—10,4	—11,8	—13,2	—14,6	—16,0
— 8,0	— 9,5	—11,2	—13,0	—14,9	—16,9
— 7,0	— 8,7	—10,5	—12,5	—14,6	—16,7
— 7,5	— 9,5	—11,5	—13,5	—15,5	—17,5
— 9,3	—11,8	—14,2	—16,6	—19,0	—21,4
—15,5	—18,4	—21,4	—24,0	—26,8	—29,7

Table 26

Thermoelectric Potential of Alloys of Platinum with
Palladium, π , millivolts

Pd atomic %	Temperature degrees C						
	0	100	200	300	400	500	600
10	—0,96	—1,86	—3,07	—4,58	—6,39	—8,50	—10,91
20	—0,64	—1,42	—2,46	—3,78	—5,38	—7,35	— 9,51
30	—0,38	—0,78	—1,51	—2,69	—4,17	—5,88	— 7,95
40	—0,25	—0,49	—1,04	—2,00	—3,30	—4,87	— 6,73
50	—0,16	—0,37	—0,76	—1,49	—2,62	—4,02	— 5,68
60	+0,33	+0,30	+0,09	—0,57	—1,62	—3,02	— 4,71
70	+0,57	+0,63	+0,38	—0,29	—1,35	—2,78	— 4,80
80	+0,68	+0,75	+0,57	--0,29	—1,75	—3,71	— 6,11
90	0	—0,075	—0,81	—2,52	—4,85	—7,73	—11,19

Temperature, degrees C

700	800	900	1000	1100	1200
—13,61	—16,65	—19,95	—23,59	—27,45	—31,67
—11,97	—14,71	—17,83	—21,00	—24,73	—28,60
—10,21	—12,89	—15,84	—18,98	—22,53	—26,38
— 8,75	—11,17	—13,84	—16,81	—20,03	—23,59
— 7,78	—10,20	—13,13	—16,56	—19,21	—24,92
— 6,81	— 9,34	—12,31	—15,91	—20,03	—24,60
— 7,30	—10,20	—13,50	—17,20	—21,27	—25,80
— 9,04	—12,68	—16,66	—21,15	—26,10	—31,55
—15,08	—19,76	—25,10	—30,59	—36,80	—43,80

Table 27

Thomsom emf of Alloys of Platinum with Palladium,
σ, microvolts per degree C

Pd, atomic %	Temperature degrees C											
	100	200	300	400	500	600	700	800	900	1000	1100	1200
10	—5,7	—7,1	— 8,5	—10,1	—11,6	—13,1	—14,6	—16,1	—17,6	—19,1	—20,6	—22,1
20	—5,3	—6,7	— 8,1	— 9,6	—11,0	—12,4	—13,8	—15,2	—16,7	—18,6	—19,5	—20,9
30	—3,4	—6,2	— 8,4	— 9,9	—11,4	—12,8	—14,3	—15,8	—17,5	—18,7	—20,2	—21,6
40	—2,4	—5,2	— 7,8	— 9,4	—10,7	—12,1	—13,5	—14,9	—16,3	—17,7	—19,1	—20,5
50	—1,6	—3,8	— 6,4	— 8,5	—10,6	—12,7	—16,2	—17,7	—20,4	—23,4	—26,6	—29,9
60	—1,6	—3,8	— 6,9	— 9,4	—11,6	—13,8	—16,3	—19,1	—22,0	—25,0	—28,2	—34,7
70	—2,4	—5,2	— 8,0	—10,9	—13,9	—17,0	—19,4	—21,4	—23,5	—35,5	—27,5	—29,5
80	—3,17	—6,72	— 10,6	—14,4	—17,6	—20,5	—23,4	—25,8	—28,2	—30,6	—33,0	—35,4
90	—3,9	—9,7	—15,5	—18,9	—21,7	—24,6	—27,4	—30,2	—33,0	—35,8	—38,6	—41,4

Fig. 76 shows the isotherms of the absolute thermal emf of alloys of platinum with palladium. The isotherms corresponding to 100° C has a smooth maximum at 80 atomic percent palladium in the positive region of values. As the temperature increases the maximum shifts towards the platinum side.
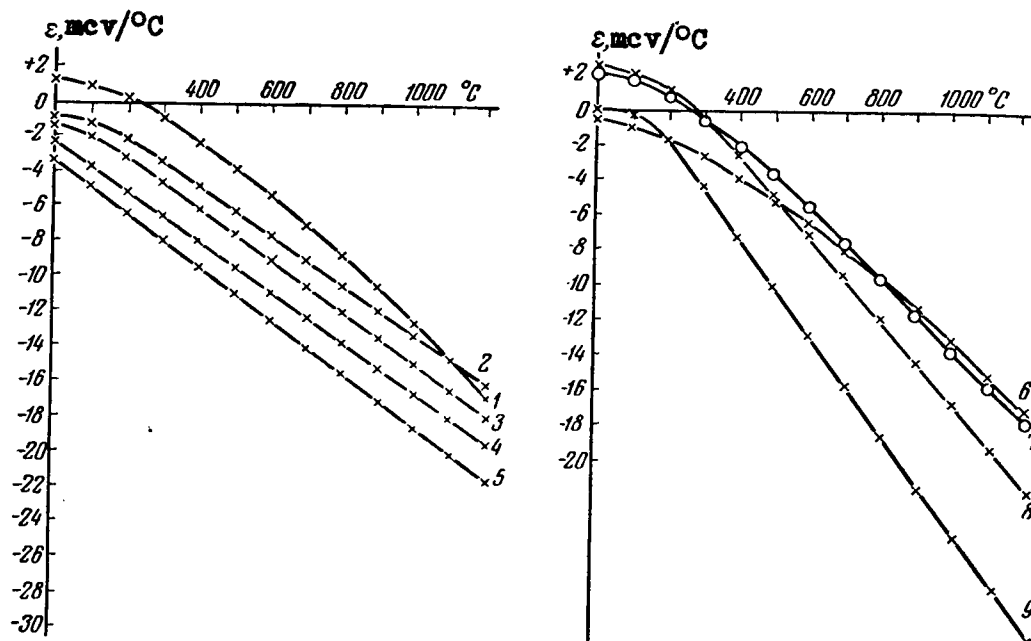
Fig. 75. Absolute Thermal emf of Alloys of Platinum with Palladium. Palladium content:

1 — 60%, 2 — 40%, 3 — 40%, 4 — 20%, 5 — 10%,
6 — 50%, 7 — 70%, 8 — 80%, 9 — 90%.
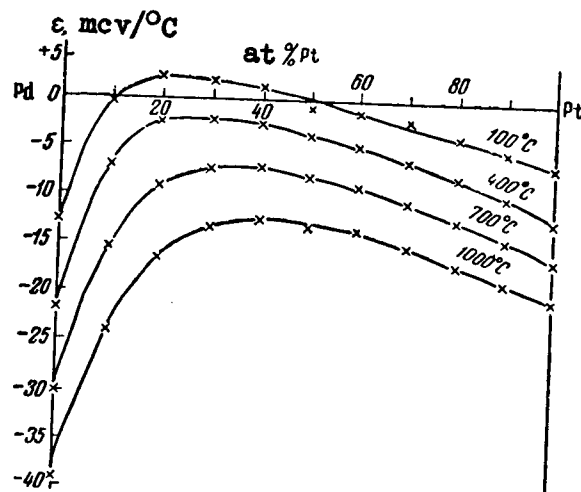
Fig. 76. Isotherms of Absolute Thermal emf of Alloys of Platinum with Palladium.

The thermoelectric potential (Table 26 of Figs. 77 and 78) changes with the temperature and with the composition, as does the absolute thermal emf, exhibiting a smooth maximum in the region of alloys with 60 to 80 atomic percent palladium. The values of the Thomson emf are given in Table 27 and in Figs. 79 and 80.

The Thomson emf for alloys of platinum with palladium is negative. The isotherms have a gentle maximum, which gradually becomes smoother with increasing temperature.

For the sake of comparison we show curves for the specific electric resistivity (Fig. 81) its temperature coefficient (Fig. 82), and the electric conductivity (Fig. 83) /116/.
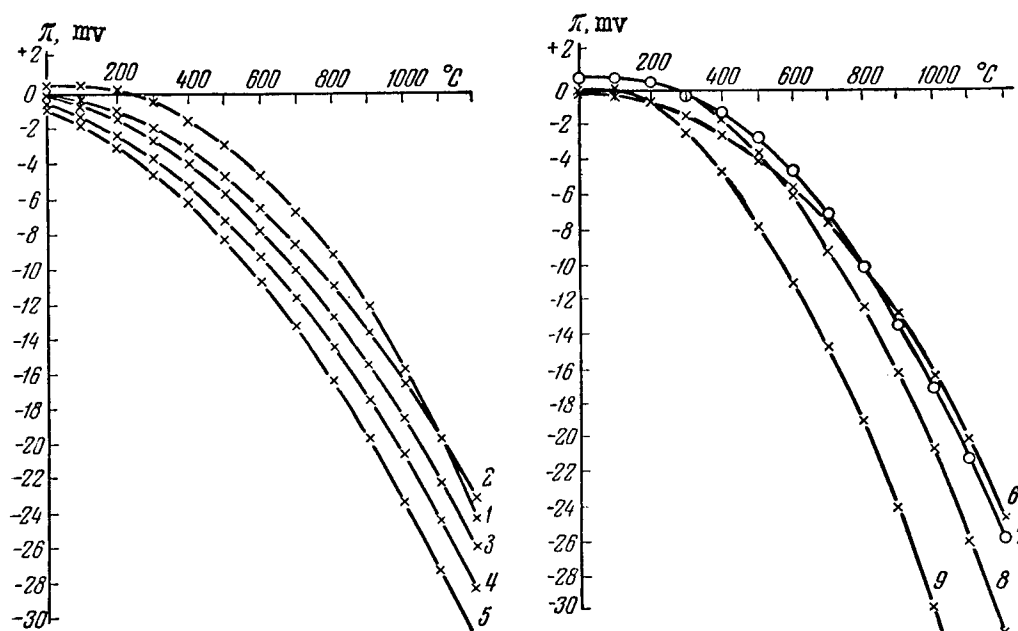
Fig. 77. Thermoelectric Potential of Alloys of Platinum with Palladium: Palladium Content:

1 -- 60%, 2 -- 40%, 3 -- 30%, 4 -- 20%, 5 -- 10%,
6 -- 50%, 7 -- 70%, 8 -- 80%, 9 -- 90%.
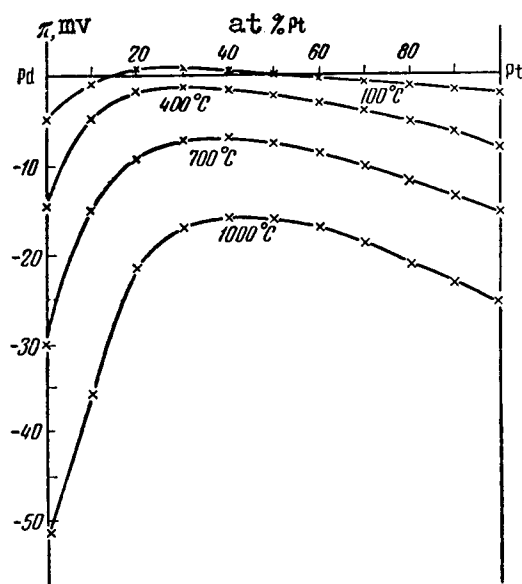
Fig. 78. Isotherms of the Thermoelectric Potential of
Alloys of Platinum with Palladium.
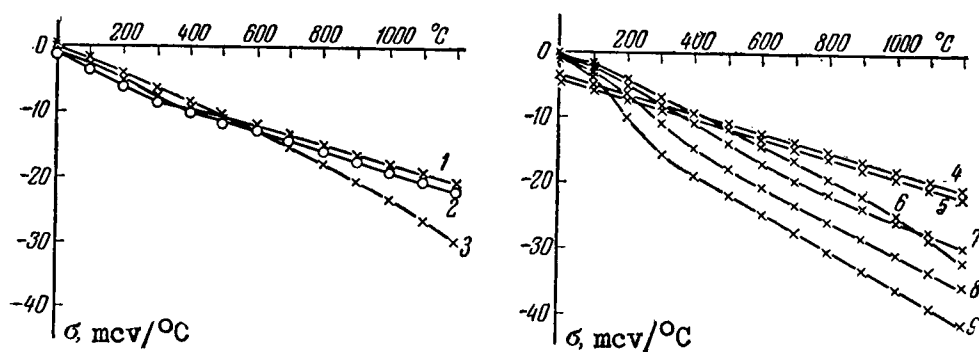
Fig. 79. Thomson emf of Alloys of Platinum with Palladium.
Palladium Content:

1 -- 40%, 2 -- 30%, 3 -- 50%, 4 -- 20%, 5 -- 10%,
6 -- 60%, 7 - 70%, 8 -- 80%, 9 -- 90%.
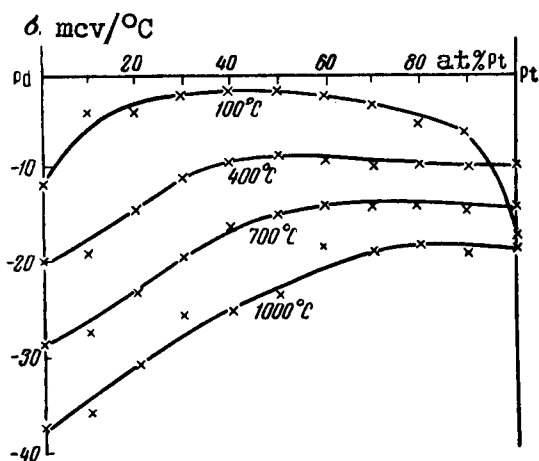
Fig. 80.   Isotherms of the Thomson emf of Alloys of
Platinum with Palladium.
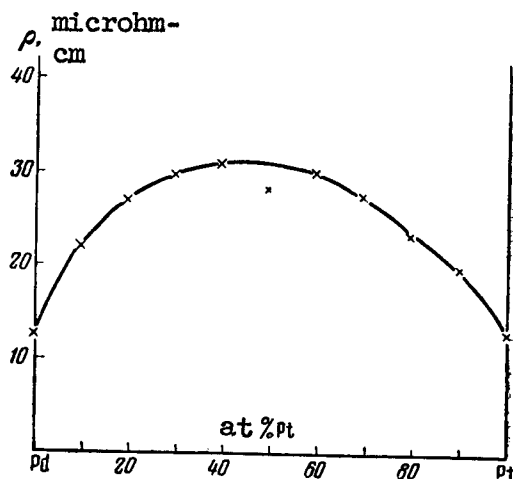
Fig. 81.   Specific Resistivity of Alloys of Platinum
With Palladium.
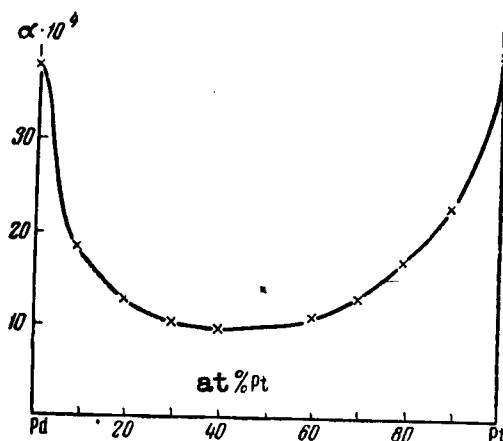
Fig. 82.   Temperature Coefficient of Electric Resistivity
of Alloys of Platinum with Palladium.
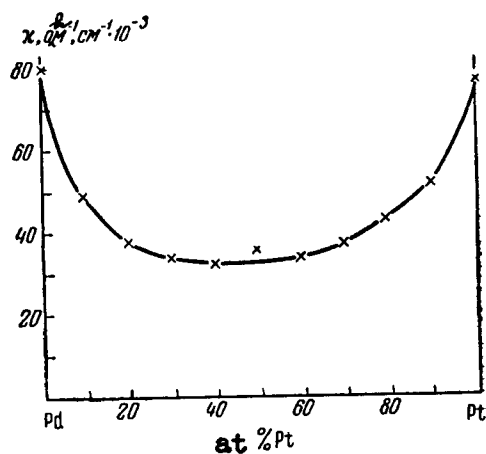
Fig. 83.   Specific Electric Conductivity of Alloys of
Platinum with Palladium.

All the thermoelectric and electric properties of alloys of platinum with palladium change along smooth curves, typical of a continuous series of solid solutions.

The absolute emf's of platinum and palladium are negative.

The components are typical electronic conductors, and the formation of solid solutions between them is characterized by the fact that the absolute thermal emf's of the alloys diminish in their absolute value and approach zero, while at low temperatures they

121

assume a small positive value. In this case, probably, a mixed conductivity appears.

4. PALLADIUM-GOLD /116/.

The diagram of states of palladium-gold system was first studied by Ruer /148/ and later on by Frenkel and Stern /149/ who, by carrying out a thermal analysis, have shown that the componeents form a continuous series of solid solutions. Detailed investigations of the physical properties /150/ have confirmed the result obtained by Ruer.

The x-ray analysis made by Holgersson and Sedstrom /151/, Stenzel and Weerts /152/, and V. G. Kuznetsov /140/ have shown that the alloys crystallize with formation of the continuous series of solid solutions, having a face-centered cubic lattice.

The thermoelectric properties were investigated by Geibel /112/, Borelius /153/ and Sedstrom /113/. It was shown by Schneidermann /154/ that the thermal emf of alloys is greatly changed by saturating them with hydrogen.
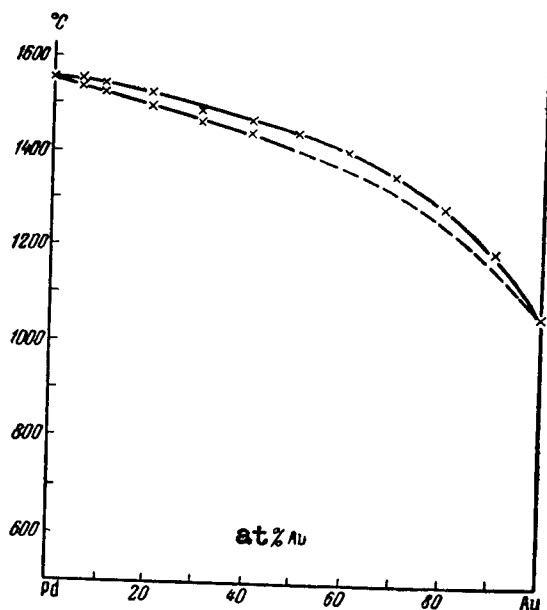
Fig. 84. Diagram of State of the Palladium-Gold
System.
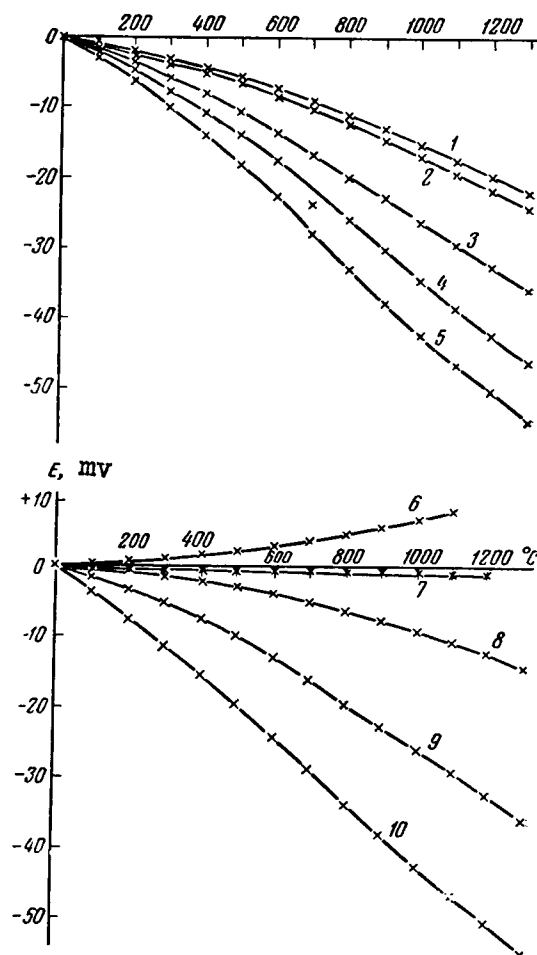
Fig. 85.   Integral Thermal emf of Alloys of Palladium with
Gold Coupled with Platinum.   Gold Content:

1 -- 5%, 2 -- 10%, 3 -- 20%, 4 -- 30%, 5 -- 40%,
6 -- 90%, 7 -- 80%, 8 -- 70%, 9 -- 60%, 10 -- 50%.

We have made /116/ a thermal analysis and studied the micro-
structure, hardness, tensile strength, elongation, electric resis-
tivity, its temperature coefficient, and the thermal emf over a wide
range of temperatures.

The diagram of state, drawn in accordance with our investiga-
tions, is shown in Fig. 84.

For the present investigation the alloys were prepared in a
high frequency furnace. They were welded to a wire 0.5 mm in dia-
meter. Before the investigations the alloys were annealed for seven

days at 1000° C. The integral thermal emf of the alloys was investigated by comparison with platinum, using a potentiometer.

The experimental data are given in Table 28 and in Fig. 85. An alloy containing 90 atomic percent gold is thermoelectrically positive relative to platinum, and all the remaining alloys when coupled with platinum are negative. Fig. 86 shows the isotherms of the integral thermal emf coupled with platinum. In the region of the diagram from 0 to 80 atomic percent gold, the thermal emf is negative relative to platinum. At 40 to 50 atomic percent gold there is a deep smooth minimum. At a contents of approximately 80 atomic percent gold, the isotherms intersect the abscissa axis and acquire positive values.

The data obtained were used to calculate the absolute thermal emf and the thermoelectric potential (Tables 29 and 30 and Figs. 87 and 88). For all the alloys, the values of ε and π are negative. The curves of the absolute thermal emf are convex downward, while the potential curves are convex upward, towards the temperature axis.
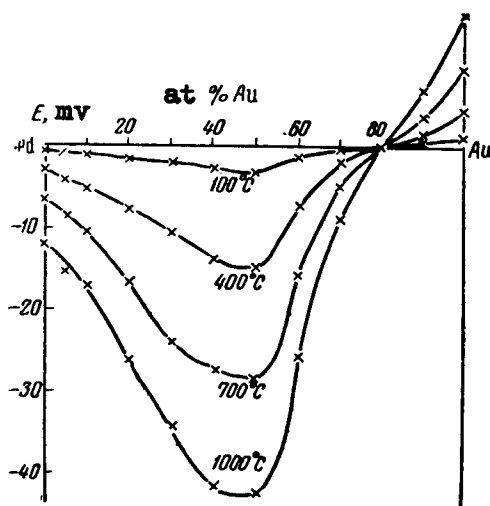
Fig. 86. Isotherms of the Integral emf of Alloys of Palladium with Gold.

Fig. 87.   Absolute Thermal emf of Alloys of Palladium
with Gold: Gold Content:

1 -- 5%, 2 -- 10%, 3 -- 20%, 4 -- 30%, 5 -- 40%,
6 -- 90%, 7 -- 80%, 8 -- 70%, 9 -- 60%, 10 -- 50%.

The absolute thermal emf and the thermoelectric potential vary analgously (Fig. 89 and 90). The isotherms display deep smooth minima in the region of 40 to 50 atomic percent gold. Upon further increase of the gold contents the isotherms of the properties experience an inflection. Approximately at a content of 97 atomic percent gold the curves intersect the abscissa axis and go into the positive region.

Table 31 gives the values of the Thomson emf, obtained by double differentiation, while Fig. 91 shows its curves as a function of a temperature. All the alloys have a negative

Alloys containing 70, 80, and 90 atomic percent gold have a straight-line characteristic. The Thomson-emf curves of alloys containing 10 to 60 atomic percent gold have minima that depend on the temperature.

The curves of the Thomson emf (Fig. 92) consist of several

Table 30

Thermoelectric Potential of Alloys of Palladium with Gold, π, millivolts

Au, atomic %	Temperature, degrees C						
	0	100	200	300	400	500	600
5	— 3,82	— 6,34	— 9,50	—13,30	—17,70	—22,75	—28,40
10	— 3,99	— 6,67	— 9,93	—13,87	—18,41	—23,73	—29,60
20	— 5,74	— 9,33	—13,76	—18,97	—25,00	—31,82	—39,10
30	— 6,80	—11,19	—16,70	—23,25	—30,80	—39,25	—48,0
40	— 8,47	—14,23	—21,10	—28,65	—36,45	—44,60	—53,30
50	—10,50	—16,40	—23,05	—30,07	—38,1	—45,6	—53,6
60	— 4,86	— 8,65	—13,32	—18,68	—24,75	—31,65	—39,10
70	— 2,29	— 4,25	— 6,71	— 9,73	—13,31	—17,46	—22,20
80	— 1,64	— 2,84	— 4,35	— 6,07	— 8,21	—10,60	—13,28
90	— 1,15	— 1,79	— 2,56	— 3,44	— 4,44	— 5,56	— 6,81

Temperature, degrees C					
700	800	900	1000	1100	1200
—34,60	—41,60	—48,50	—55,3	—62,1	—68,4
—36,20	—43,4	—50,7	—57,8	—64,3	—70,5
—46,60	—54,40	—61,00	—69,0	—75,9	—82,7
—56,2	—64,10	—71,60	—78,4	—84,9	—91,5
—61,80	—69,9	—77,4	—84,5	—91,6	—98,6
—61,30	—69,0	—76,3	—83,2	—90,1	—96,9
—46,60	—54,40	—61,8	—69,1	—75,9	—82,8
—27,55	—33,30	—39,8	—46,7	—54,4	—62,3
—16,33	—19,65	—23,25	—27,13	—31,3	—
— 8,16	— 9,67	—11,28	—12,99	—	—

Table 31

Thomson emf of Alloys of Palladium with Gold σ, microvolts per degree C

Au, atomic %	Temperature, degrees C											
	0	100	200	300	400	500	600	700	800	900	1000	1100
5	— 8,46	—11,57	—14,66	—17,77	—20,87	—23,97	—27,05	—30,20	—31,20	—28,20	—24,2	—20,6
10	— 8,80	—12,03	—15,25	—18,47	—21,70	—24,90	—28,1	—31,4	—33,3	—30,5	—22,9	—16,5
20	—11,05	—15,10	—19,5	—23,20	—27,2	—30,2	—29,7	—28,2	—24,7	—21,2	—16,6	—13,7
30	—14,3	—19,5	—24,7	—29,9	—35,2	—34,8	—31,2	—26,2	—19,3	—10,55	— 5,1	— 4,13
40	—20,8	—25,4	—28,4	—29,8	—29,6	—27,8	—24,4	—19,9	—13,95	— 7,05	— 5,1	— 4,13
50	—16,9	—19,0	—19,9	—20,0	—18,2	—16,2	—14,0	—11,7	— 8,6	— 5,86	— 3,82	— 2,75
60	—15,7	—19,8	—23,2	—25,2	—26,9	—27,8	—27,9	—27,2	—25,2	—22,9	—19,1	—15,1
70	— 7,73	—10,56	—13,39	—16,22	—19,05	—21,88	—24,71	—27,54	—30,37	—33,20	—36,03	—38,86
80	— 4,18	—· 5,71	— 7,24	— 8,77	—10,30	—11,83	—13,36	—14,89	—16,42	—17,95	—19,48	—21,01
90	— 1,64	— 2,24	— 2,84	— 3,44	— 4,04	— 4,64	— 5,24	— 5,84	— 6,44	— 7,04	— 7,64	—

The second branch is formed when gold is added to palladium and has a minimum at low temperatures. This minimum shifts with increasing temperature towards the palladium. Near 1000° the minimum vanishes. Between these two branches one observes a jump-like change in the properties. The jumps lie in the region of the diagram of 50 to 60 atomic percent gold and retain their position relative to composition with increasing temperature.
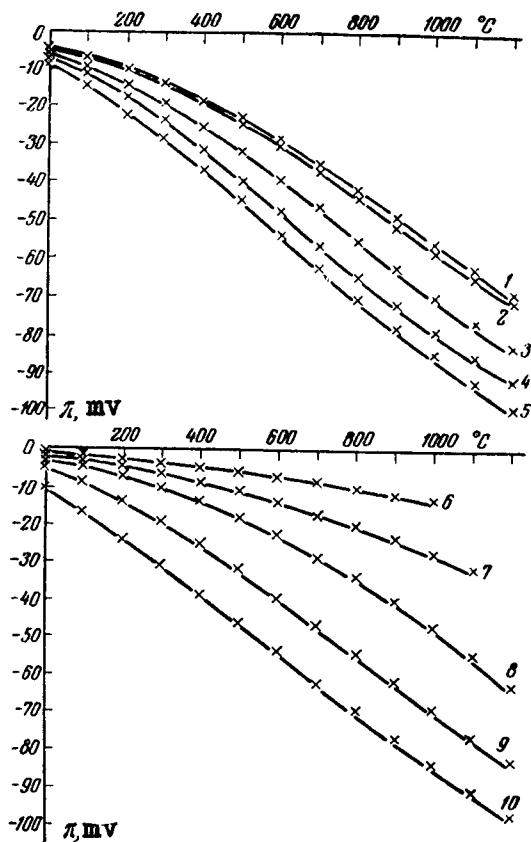
Fig. 88. Thermoelectric Potential of Alloys of Palladium with Gold. Gold Content:

1 -- 5%, 2 -- 10%, 3 -- 20%, 4 -- 30%, 5 -- 40%,
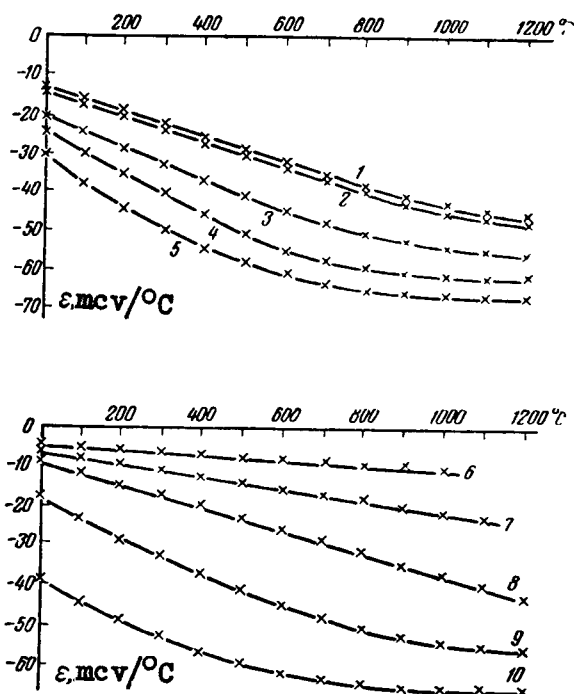6 -- 90%, 7 -- 80%, 8 -- 70%, 9 -- 60%, 10 -- 50%.
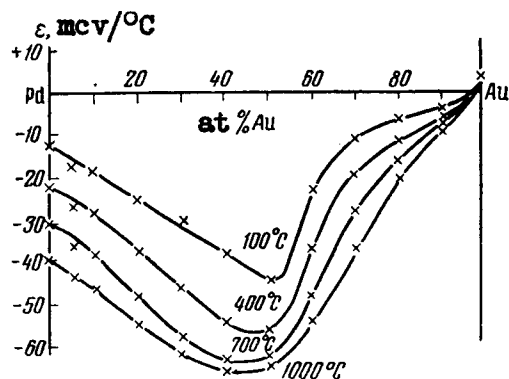
Fig. 89. Isotherms of the Absolute Thermal emf of Alloys of Palladium with Gold.
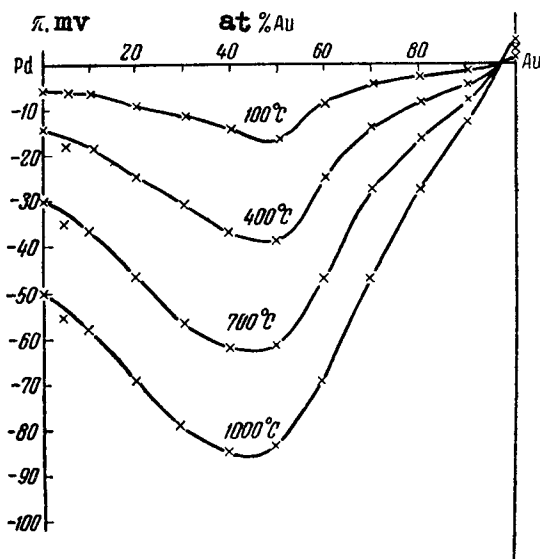
Fig. 90. Isotherms of Thermoelectric Potential of Alloys of Palladium with Gold.

Let us consider the curves of specific electric resistivity (Fig. 93), its temperature coefficient (Fig. 94) and the electric conductivity (Fig. 95).

On the curve of the specific electric resistivity there are no points of inflection that characterize a break in the continuity of the solid solutions. This curve is so to speak a mirror image of the curves of the absolute thermal emf and the thermoelectric potential.

The curve of the specific electric conductivity shows a hardly noticeable inflection in the region of 50 to 60 atomic percent gold. The curve of the temperature coefficient of electric resistivity shows quite clearly that the diagram consists of two parts and that in the region of 50 to 60 atomic percent gold one branch of the curve goes abruptly into the other. Investigations of the Thomson emf and of the temperature coefficient of electric resistivity of alloys of palladium with gold show that in the diagram of states there are two solid solutions, to which there belong two independent branches of the curves of the properties. At a content of approximately 50 atomic percent gold one observes, in a narrow range of concentrations, a sharp transition from one branch to another. Probably in this region there is a break in the continuity of the series of solid solutions.
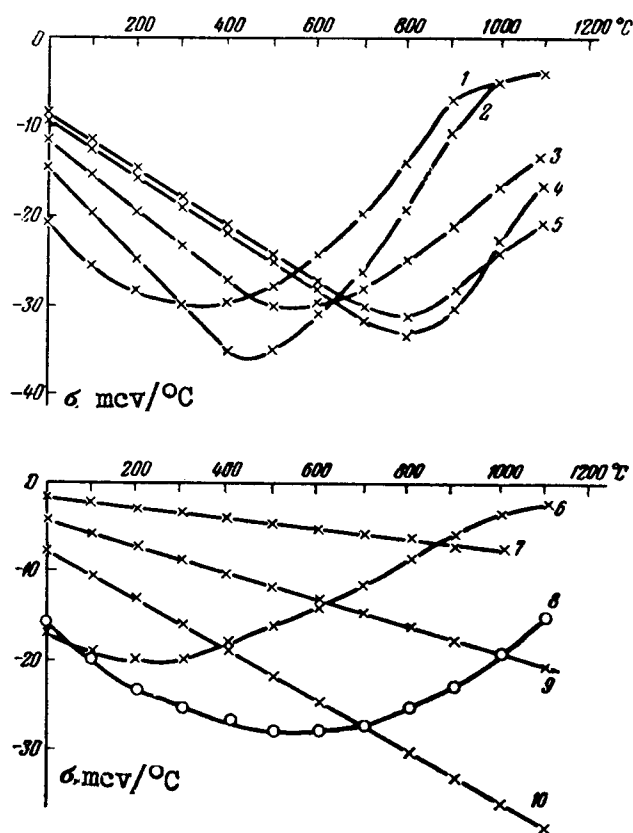
Fig. 91. Thomson emf of Alloys of Palladium with Gold. Gold Content:

1 -- 40%, 2 -- 30%, 3 -- 20%, 4 -- 10%, 5 -- 5%, 6 -- 50%, 7 -- 90%, 8 -- 60%, 9 -- 80%, 10 -- 70%.
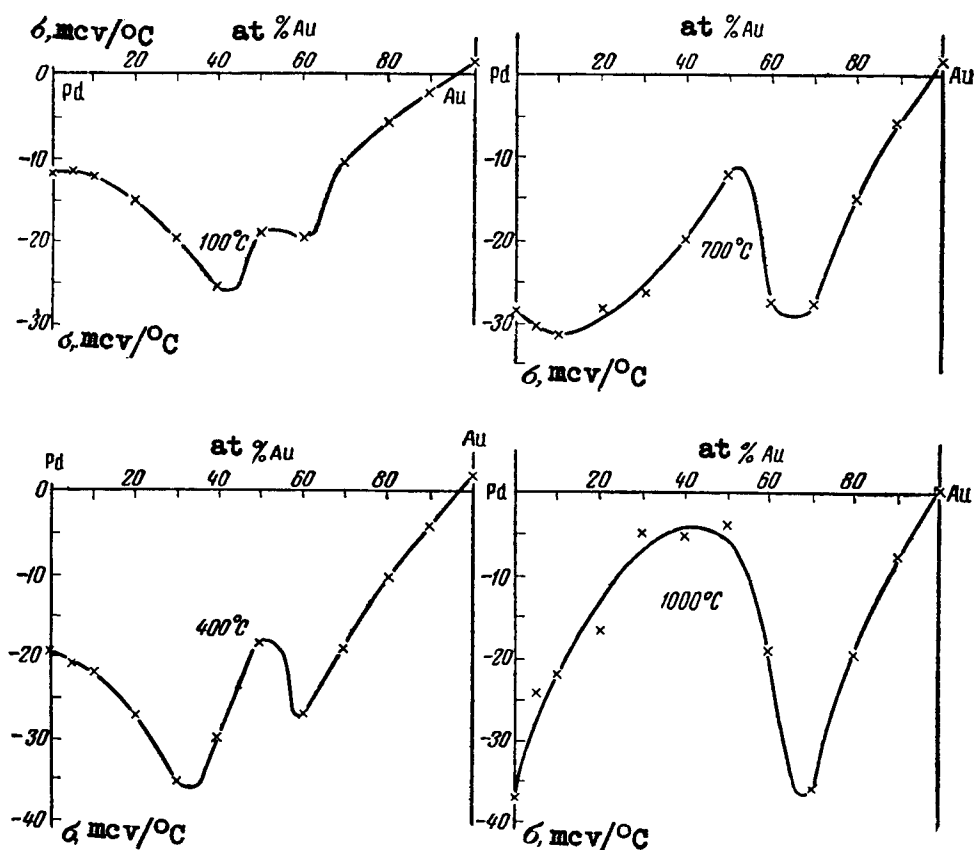
Fig. 92. Isotherms of the Thomson emf of Alloys of
Palladium with Gold.
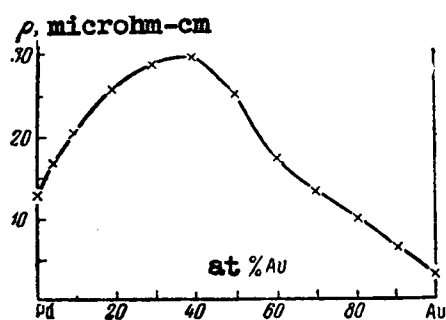
Fig. 93. Specific Electric Resistivity of Alloys of
Palladium With Gold.

133
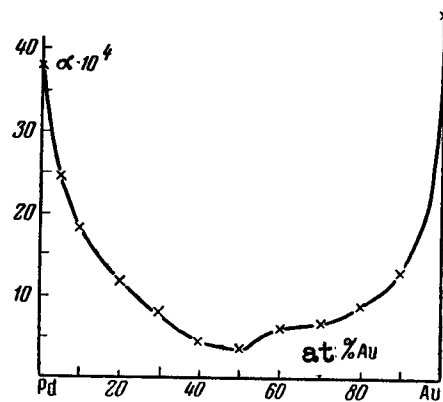
Fig. 94. Temperature Coefficient of Electric Resistivity
of Alloys of Palladium with Gold.
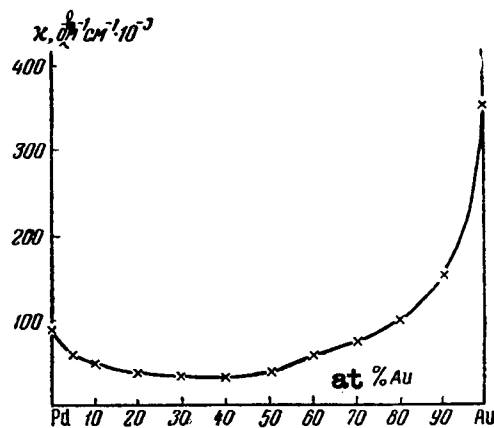
Fig. 95. Specific Electric Resistivity of Alloys of
Palladium with Gold.

The positive absolute thermal emf of gold indicates that
positive current carriers predominate in it. For palladium, to the
contrary, electron conductivity predominates. As a result of the
alloying of these metals we obtain alloys with electronic conduc-
tivity and with a large negative thermal emf.

5. PALLADIUM-SILVER /97/

In accordance with the thermal analysis carried out by Ruer

/155/ the diagram of state of palladium-silver represents a continuous series of solid solutions (Fig. 96). This result was confirmed by later investigations on the physical properties of the alloys /150/.

Ye. Ya. Rode /156/, who investigated the hardness and the microstructure of the alloys, has confirmed the results of the earlier workers and has shown that the physical properties depend on the composition of the gases absorbed by the alloys.

Investigations of the crystalline lattice structure, carried out by McKeehan /157/, Kruger and Sacklowski /158/, Stenzel and Weerts /152/, and V. G. Kuznetsov /140/ indicate the formation of a continuous series of solid solutions, which have a **face-centered** cubic lattice.

The thermoelectric properties of the alloys were studied by Geibel /112/, Borelius /153/ and Sedstrom /113/.

We have investigated /97/ the microstructure, hardness, electric resistivity, its temperature coefficient, tensile strength, elongation, and the thermal emf.

For these experiments the alloys were manufactured in a high frequency furnace. The alloys drawn into a wire 0.5 mm in diameter were annealed for seven days at a temperature of 700 to 800° C. We studied the integral thermal emf of the alloys when coupled with platinum at a cold-junction temperature of 0° C. (Table 32 and Fig. 97).
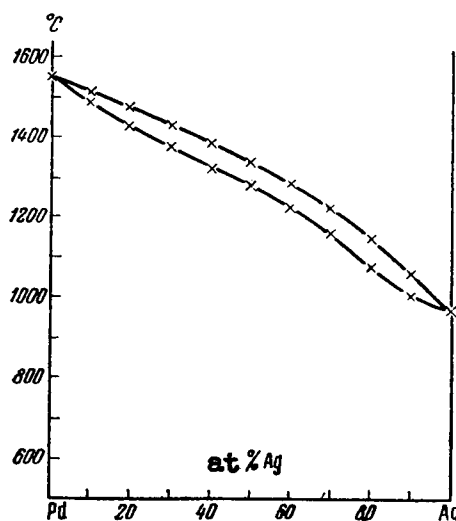
Fig. 96. Diagram of States of the Palladium-Silver System.
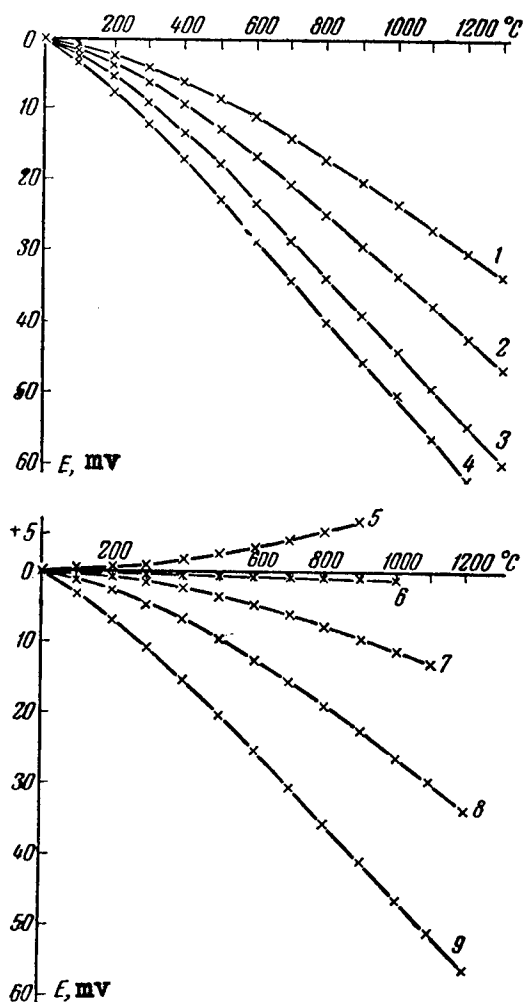
Fig. 97. Integral Thermal emf of Alloys of Palladium with Silver when Coupled with Platinum. Silver Content:

1 -- 10%, 2 -- 20%, 3 -- 30%, 4 -- 40%,
5 -- 90%, 6 -- 80%, 7 -- 70%, 8 -- 60%,
9 -- 50%.

The integral thermal emf of alloys of palladium with silver increases smoothly in absolute value with increasing temperature. An alloy containing 90 atomic percent silver is positive relative to platinum. All the other alloys are negative.

From the diagram of the integral thermal emf of alloys of palladium with silver, when coupled with platinum (Fig. 98) it follows that at a content from 0 to 80 atomic percent silver the thermal emf

136

is negative.
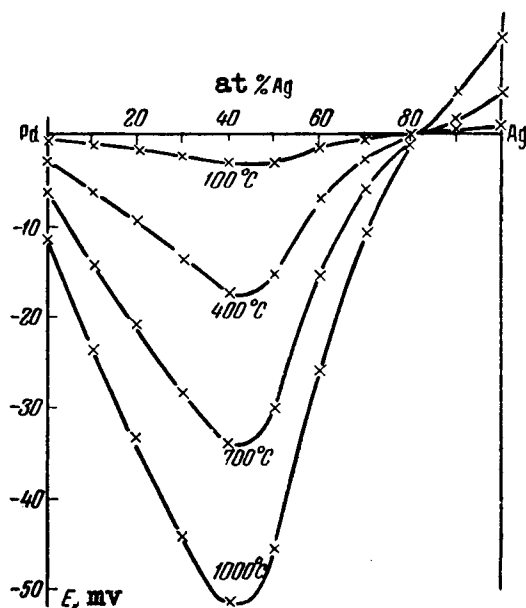
Fig. 98. Isotherms of the Integral Thermal emf
of Alloys of Palladium with Silver.

Table 32

Integral Thermal emf of Alloys of Palladium with Silver
when Coupled with Platinum, E, millivolts

Au		Temperature, degrees C						
atomic %	% by weight	100	200	300	400	500	600	700
10	10,10	—1,24	—2,66	— 4,33	— 6,36	— 8,73	—11,33	—14,26
20	20,18	—1,73	—3,60	— 6,34	— 9,52	—12,88	—16,73	—20,70
30	30,23	—2,47	—5,22	— 9,11	—13,54	—18,07	—23,18	—28,21
40	40,26	—3,34	—7,42	—12,07	—17,27	—22,93	—28,42	—34,08
50	50,28	—3,17	—6,80	—10,83	—15,29	—20,09	—25,00	—30,02
60	60,26	—1,24	—2,78	— 4,68	— 6,90	— 9,48	—12,35	—15,41
70	70,23	—0,43	—0,96	— 1,58	— 2,64	— 3,69	— 4,83	— 6,03
80	80,18	—0,17	—0,25	— 0,32	— 0,41	— 0,52	— 0,62	— 0,73
90	90,10	+0,12	+0,48	+ 0,91	+ 1,55	+ 2,35	+ 3,22	+ 4,28

800	900	1000	1100	1200	1300	1400
—17,33	—20,47	—23,48	—26,88	—30,39	—23,64	—
—25,11	—29,31	—33,48	—37,96	—42,43	—46,43	—
—33,72	—39,02	—44,24	—49,49	—52,69	—59,66	—
—40,02	—45,60	—51,43	—56,43	—62,20	—	—
—35,25	—40,23	—45,55	—50,15	—55,50	—	—
—18,81	—22,17	—25,89	—29,43	—33,48	—	—
— 7,84	— 9,17	—11,40	—12,72	—	—	—
— 0,86	— 0,97	— 0,14	—	—	—	—
+ 5,60	— 6,79	—	—	—	—	—

Table 33

Absolute Thermal emf of Alloys of Palladium with Silver, ε , microvolts per degree C

Ag atomic %	Temperature, degrees C						
	0	100	200	300	400	500	600
10	—15,2	—19,8	—24,8	—29,6	—34,5	—39,1	—43,3
20	—18,2	—26,3	—34,0	—40,7	—46,0	—50,6	—54,7
30	—24,0	—34,0	—43,8	—52,3	—58,2	—63,0	—66,7
40	—33,6	—44,6	—53,4	—60,5	—65,7	—69,5	—72,4
50	—29,4	—39,0	—47,3	—53,4	—58,7	—62,6	—65,3
60	—14,0	—20,7	—26,4	—31,6	—36,7	—41,2	—45,4
70	— 7,4	—11,8	—15,8	—19,5	—22,8	—25,8	—28,7
80	— 6,8	— 8,4	—10,0	—11,7	—13,3	—15,0	—16,6
90	— 4,6	— 4,8	— 4,9	— 5,0	— 5,2	— 5,4	— 5,5

Temperature, degrees C

700	800	900	1000	1100	1200
—46,8	—49,3	—51,3	—54,1	—56,2	—58,0
—58,2	—60,8	—62,8	—64,7	—66,3	—67,7
—69,6	—71,4	—72,7	—73,6	—74,5	—75,2
—74,8	—76,8	—78,2	—79,7	—80,8	—81,5
—67,3	—68,8	—70,0	—71,2	—72,3	—73,5
—49,4	—52,8	—56,0	—59,0	—62,0	—64,8
—31,3	—33,7	—36,0	—38,2	—40,2	—
—18,2	—19,8	—21,5	—23,2	—	—
— 5,6	— 5,7	— 5,9	—	—	—

The curves of composition vs. emf have a deep smooth minimum in the interval from 40 to 50 atomic percent silver. In the region of 80 to 85 atomic percent the curves intersect the abscissa axis, assume positive values, and rise smoothly to the right.

The absolute thermal emf of all alloys is negative (Table 33) and its curves are concave towards the temperature axis (Fig. 99).
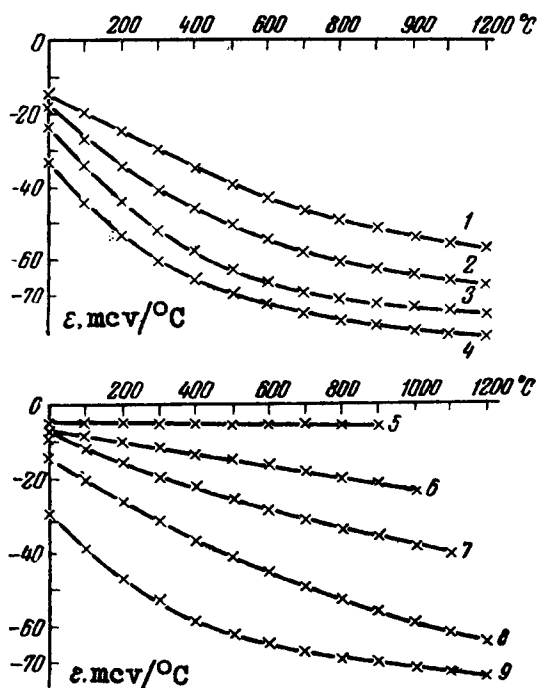
Fig. 99. Absolute Thermal emf of Alloys of
Palladium with Silver. Silver Content:

1 -- 10%, 2 -- 20%, 3 -- 30%, 4 -- 40%,
5 -- 90%, 6 -- 80%, 7 -- 70%, 8 -- 60%,
9 -- 50%.

The thermoelectric potential is also negative (Table 34) and its curves are convex towards the temperature axis (Fig. 100).

Figs. 101 and 102 show the isotherms of the absolute thermal emf and of the thermoelectric potential. The curves of the absolute thermal emf have a deep smooth minimum near a composition of 40 atomic percent silver plus 60 atomic percent palladium. In all isotherms there is one common intersection point (near 90 atomic percent silver); in the region of 94-98 atomic percent silver they intersect the abscissa axis.

The Thomson emf of the alloys of palladium with silver is

shown in Table 35 and Fig. 103.
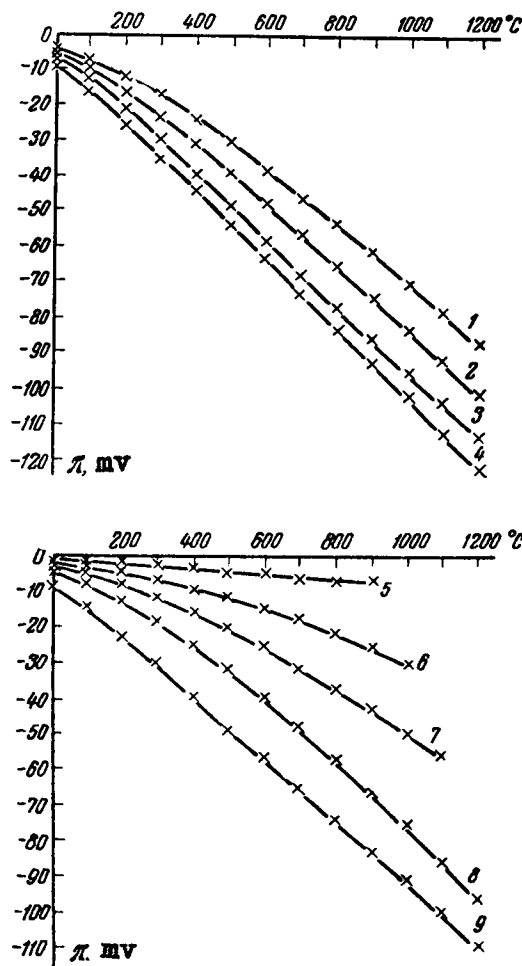
Fig. 100. Thermoelectric Potential of Alloys of
Palladium with Silver. Silver Content:

1 -- 10%, 2 -- 20%, 3 -- 30%, 4 -- 40%,
5 -- 90%, 6 -- 80%, 7 -- 70%, 8 -- 60%,
9 -- 50%.

For alloys containing 10 to 50 atomic percent silver, the
Thomson emf changes smoothly, has a minimum, and is negative. For
alloys containing 60 to 90 atomic percent silver, the curves of the
Thomson emf drop smoothly without inflection.

At 100° C the Thomson emf changes smoothly and has a deep
minimum near 30 to 40 atomic percent silver (Fig. 104). As the tem-
perature rises the curves form two minima. One of these lies near
60 atomic percent silver and retains its position with changing

composition. The second minimum, which lies in the region of alloys that have more palladium, shifts with increasing temperature towards the palladium, and vanishes at 800° C.

The isotherms of the Thomson emf above 400° C consist of two branches: one for 0 to 50 atomic percent silver and the other for 60 to 100 atomic percent silver. In the region of 50 to 60 atomic percent silver one branch changes abruptly into the other.
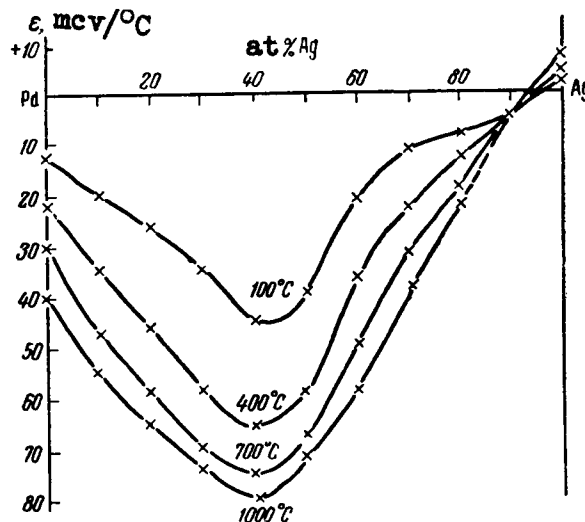
Fig. 101. Isotherms of the Absolute Thermal emf of Alloys of Palladium with Silver.
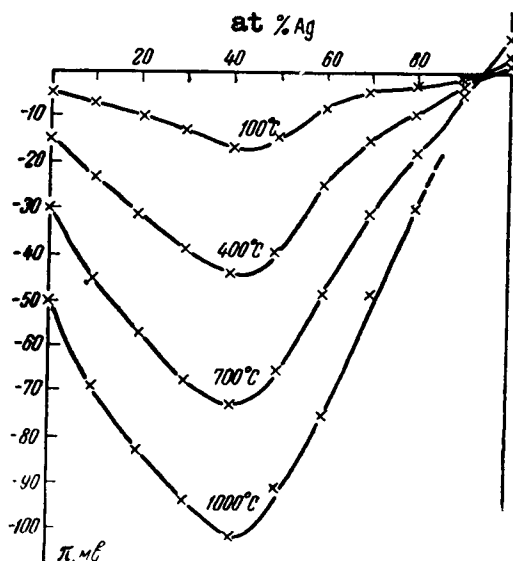
Fig. 102. Isotherms of the Thermoelectric Potential of Alloys of Palladium with Silver.

141
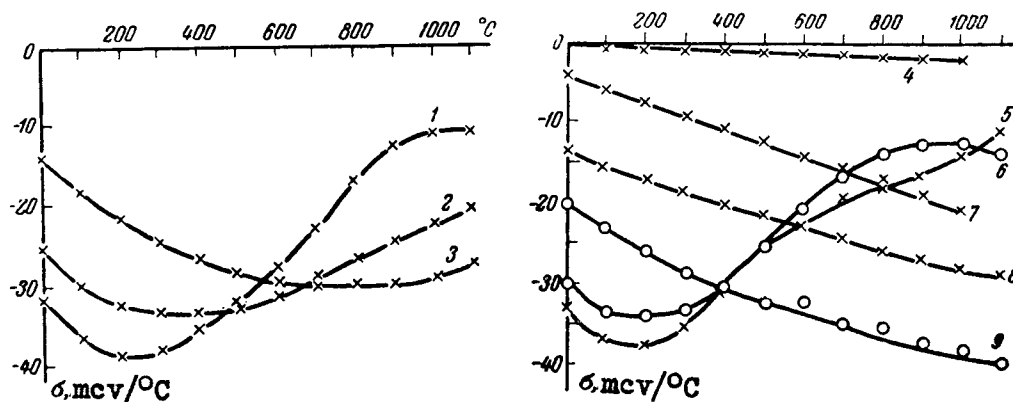
Fig. 103. Thomson emf of Alloys of Palladium with Silver. Silver Content: 1 -- 30%, 2 -- 20%, 3 -- 10%, 4 -- 90%, 5 -- 40%, 6 -- 50%, 7 -- 80%, 8 -- 70%, 9 -- 60%.

For comparison, we show the curves of the specific electric resistivity (Fig. 105), its temperature coefficient (Fig. 106), and the electric conductivity (Fig. 107).

The specific electric resistivity changes smoothly and has a maximum, while the specific electric resistivity changes smoothly and has a minimum.

The temperature coefficient of electric resistivity has two branches, one for 0 to 40 atomic percent silver, and the other for 60 to 100 atomic percent silver.

At 40 to 60 atomic percent one branch goes into the other.

Table 34

Thermoelectric Potential of Alloys of Palladium with Silver, π , millivolts

Ag atomic %	Temperature, degrees C							
	0	100	200	300	400	500	600	
10	—4,15	— 7,39	—11,73	—16,97	—23,2	—30,2	—37,8	
20	—4,97	— 9,81	—16,10	—23,35	—30,9	—39,1	—47,7	
30	—6,55	—12,69	—20,73	—30,00	—39,1	—48,2	—58,1	
40	—9,18	—16,64	—25,25	—34,60	—44,1	—53,7	—63,1	
50	—8,03	—14,55	—22,85	—30,60	—39,5	—48,4	—57,0	
60	—3,82	— 7,72	—12,50	—18,10	—24,6	—31,8	—39,6	
70	—2,02	— 4,40	— 7,47	—11,17	—15,3	—19,9	—25,0	
80	—1,83	— 3,13	— 4,73	— 6,70	— 8,94	—11,6	—14,5	
90	—1,26	— 1,79	— 2,32	— 2,85	— 3,50	— 4,17	— 4,80	

700	800	900	1000	1100	1200
—45,6	—53,0	—60,2	— 69,0	— 77,3	— 85,5
—56,6	—65,3	—73,7	— 82,4	— 91,0	— 99,8
—67,7	—76,6	—85,4	— 93,8	—102,4	—110,8
—72,8	—82,5	—91,8	—101,5	—111,0	—120,0
—65,5	—74,0	—82,1	— 90,6	— 99,4	—108,4
—48,1	—56,7	—65,8	— 75,2	— 85,2	— 99,5
—31,3	—36,2	—42,3	— 48,6	— 55,3	—
—17,7	—21,3	—25,22	— 29,5	—	—
— 5,45	— 6,12	— 6,93	—	—	—

Table 35

Thomson emf of Alloys of Palladium with Silver, σ, microvolts per degree C

Ag. atomic %	Temperature, degrees C						
	0	100	200	300	400	500	600
10	—13,93	—18,30	—21,75	—24,61	—26,92	—28,60	—29,70
20	—25,40	—30,20	—32,61	—33,20	—33,65	—33,20	—31,04
30	—31,70	—36,55	—38,80	—38,40	—35,65	—32,45	—27,90
40	—33,30	—36,90	—37,80	—35,50	—30,98	—25,50	—22,70
50	—30,00	—33,60	—34,01	—33,20	—30,25	—25,50	—20,95
60	—20,20	—23,10	—26,00	—28,60	—30,98	—32,41	—32,25
70	—13,65	—15,67	—17,50	—18,90	—20,25	—21,60	—22,65
80	— 4,48	— 6,12	— 7,76	— 9,40	—11,04	—12,68	—14,32
90	— 0,38	— 0,52	— 0,66	— 0,80	— 0,94	— 1,08	— 1,22

700	800	900	1000	1100
—30,18	—30,05	—30,50	—29,25	—27,70
—29,20	—26,90	—26,65	—22,93	—20,60
—23,38	—17,19	—12,90	—11,46	—11,00
—20,42	—18,25	—16,43	—14,00	—10,90
—16,54	—13,97	—12,90	—12,73	—13,73
—35,00	—35,41	—37,50	—38,20	—39,80
—24,32	—25,80	—27,00	—28,00	—28,85
—15,96	—17,60	—19,24	—20,88	—
— 1,36	— 1,50	— 1,64	—	—

The thermoelectric and electrical properties of alloys of palladium with silver are analogous to the thermoelectric and electric properties of alloys of palladium with gold. In both cases one observes, in the vicinity of 40 to 60 atomic percent, a jump-like change in the Thomson emf and in the temperature coefficient of electric resistivity. The break in the continuity on the curves of the temperature coefficient of electric resistivity and the Thomson emf as a function of the composition is probably due to a break in the continuity of the solubility in the palladium-silver system.
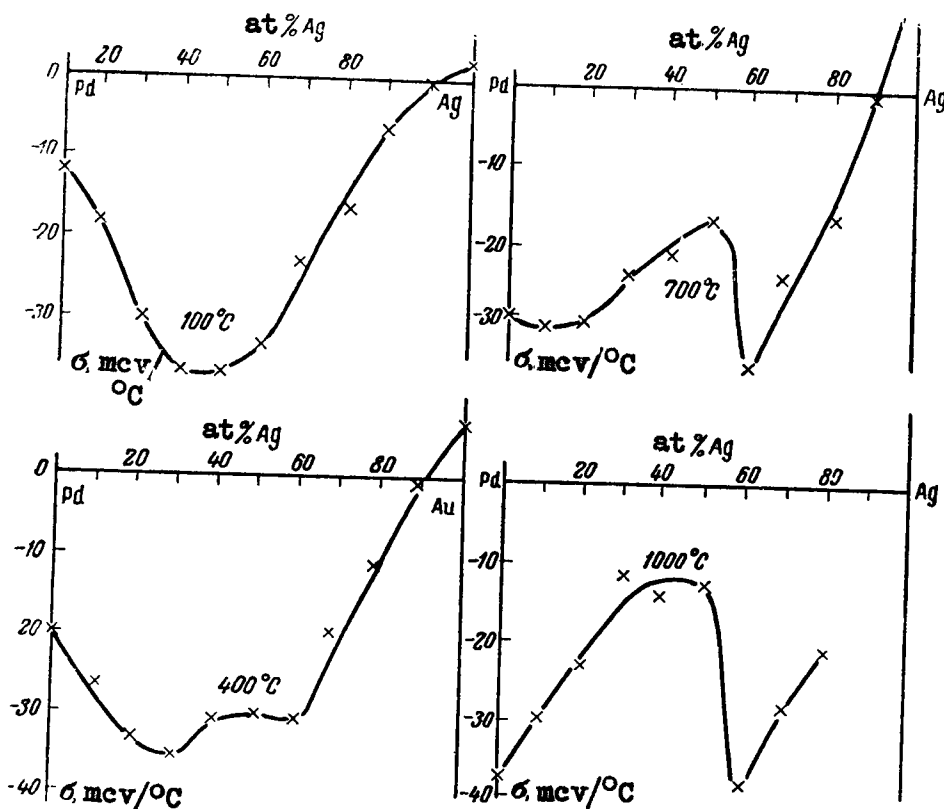
Fig. 104. Thomson Isotherms of Alloys of Palladium with Silver.

In this case the absolute thermal emf's of the components in alloys of palladium with silver have different signs.

In alloys one observes predominately electron conductivity, as can be ascertained from the negative absolute thermal emf.
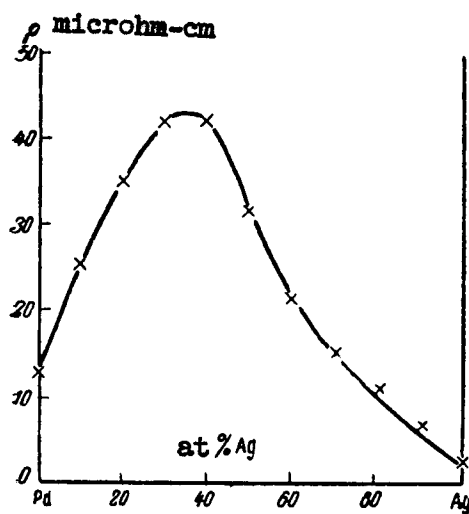
Fig. 105. Specific Electric Resistivity of Alloys
of Palladium with Silver.
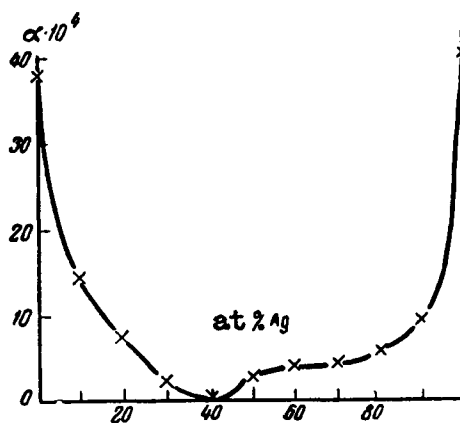
Fig. 106. Temperature Coefficient of Electric
Resistivity of Alloys of Palladium
with Silver.

145
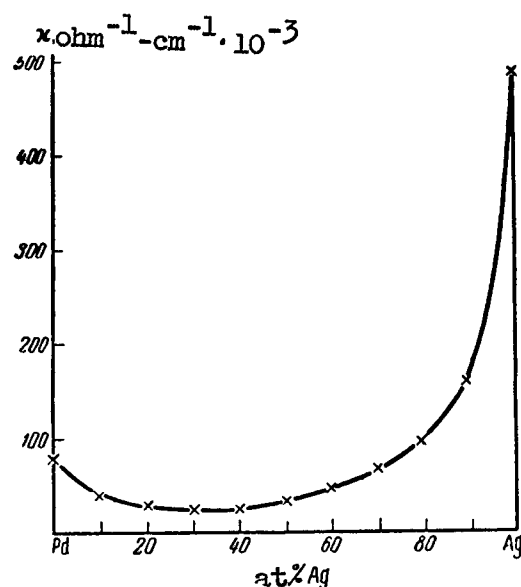
Fig. 107. Specific Electric Conductivity of Alloys of Palladium with Silver.

6. PLATINUM-GOLD

The first systematic investigation of alloys of gold with platinum was made by Erhard and Schartel /159/ who determined the temperatures of the start of the melting of the alloys from the change in the shape of specimens when heated. The authors have obtained a smooth curve that indicates the formation of a continuous series of solid solutions in the system. However, these data cannot be considered sufficiently reliable.

F. Doerinckel /160/, as a result of an investigation of the microstructure and of a thermal analysis of a portion of the system (0 to 60 percent platinum), reached the conclusion that there exists a continuous series of solid solutions.

Geibel /112/ who investigated the electric resistivity, its temperature coefficient, and the tensile resistance of alloys of gold with platinum, has established that at a content of up to 40% the platinum is fully soluble in gold. An investigation of the thermal emf did not give repeatable results, and consequently the author suggested the presence of a slow transformation.

Schulze /144/ considered the specific heat of alloys of gold with platinum and obtained data that are fully analogous to Geibel's.

146

A. T. Grigor'ev [161] investigated the gold-platinum system by thermal analysis, by the hardness method and by the microstructure method, established a peritectic reaction of 20-75% platinum at 1290° C. The author has tentatively determined the boundaries of the heterogeneous region in the solid state at 40 75% platinum.

Johansson and Line [162], in an investigation of alloys of gold with platinum by x-ray analysis methods and by measuring the electric resistivity, hardness, thermal emf, heat conduction, and magnetic permeability, have reached the conclusion that a continuous series of solid solutions is formed and these decompose upon cooling and form two solid solutions. In the opinion of these authors, there is no peritectic reaction in the gold-platinum system. However, x-ray pictures in the vicinity of 55 atomic percent platinum did not produce any clear lines. The boundaries of solubility in the solid states have been established from curves of the electric resistivity for alloys that are quenched at various temperatures.

Nowack [163] investigated aging processes by measuring the hardness of quenched and tempered alloys.

Stenzel and Weerts [164] again carried out an x-ray investigation of the solubility boundaries and observed in the vicinity of 40-65 atomic percent platinum a single phase structure in alloys quenched at 1160-1275° C, this being in contradiction to the data of Johansson and Linde.

Wictorin [165] repeated the investigations on electric resistivity and studied decomposition phenomena of solid solutions. In the region of 50-70 atomic percent platinum he obtained no reproducible results and proposed that the decomposition of solid solutions is so rapid that it is impossible to retain the single-phase state by quenching. Having determined the degree of variation of the electric resistivity with time and assuming it proportional to the degree of decomposition of the solid solution, Wictorin has established a metastable region of decomposition of the solid solution. This premise, as shown by N. V. Ageyev [166] is quite doubtful.

V. A. Nemilov, T. A. Vidusova, A. A. Rudnitskiy, and M. M. Putsykina [116], using the method of thermal analysis, hardness, and microstructure, confirmed the data of A.T. Grigor'yev and found that in the region of the diagram from 20 to 70 atomic percent platinum the peritectic reaction is observed at a temperature of approximately 1300° C. The limits of solubility of the components were established on the basis of investigations of the microstructure. The investigations of Grube, Schneider, and Esch [167], reproducible by the method of thermal analysis, have shown again the presence of a peritectic reaction in the region of 21-62 atomic percent platinum at a temperature of 1295-1301° C.

On the basis of x-ray investigations and of a study of the microstructure, the boundaries of the heterogeneous have been established.

A very detailed study of the alloys of platinum with gold was made by Darling, Mitern, and Chaston /168/ using methods of thermal analysis, microstructure, x-ray phase analysis, and electric resistivity. They established that the alloys crystallize with formation of a continuous series of solid solutions, which decompose into two phases as a result of further cooling. The thermal analysis was carried out only for the liquidus points. The solidus line was determined from the fussion of the specimens and from the microstructure. The peritectic line was not determined. The authors judge the limit of solubility from the shape of the curve of the electric resistivity as a function of temperature. In this case they assume, without any basis whatever, that the straight portion of the curve belongs to the solid solution and that in the two-phase region the electric resistivity varies according to some other curve. The intersection of these lines is assumed to be the solubility limit. There is no basis whatever for this opinion.

An x-ray phase analysis was carried out with great accuracy. However, in the region of 30 to 45% of gold by weight no single-phase alloys were observed.

The most correct results were obtained by the thermal analysis carried out by A. T. Grigor'yev /161/, V.A. Nemilov /116/, and G. Grube /167/, from which one can conclude that the alloys of gold with platinum form a diagram of states with a peritectic line.

A direct proof of this is afforded by the thermal pauses at a constant temperature 1280-1300° C, observed on the curves for the cooling of the alloys between the liquidus and solidus lines.

The authors who state that the solubility of gold with platinum is unlimited directly below the solidus line, base their conclusions on insufficiently reliable results, such as on the change in the variation of the curve for the temperature dependence of the electric resistivity. The peritectic line was not found by these authors, since it can be observed only by thermal analysis, which they did not perform.

For the present investigation the alloys were manufactured in a high frequency furnace. To investigate the electric properties, the alloys were drawn into porcelain tubes. The resultant sticks were rolled into rods of square cross section 1.2 mm on each side, with intermediate quenching at 900° C.

For the annealing, the alloys were heated to 900° C, and their temperature was then reduced to 600° C. The alloys were kept at this

temperature for seven days and were slowly cooled to room temperature within a week.
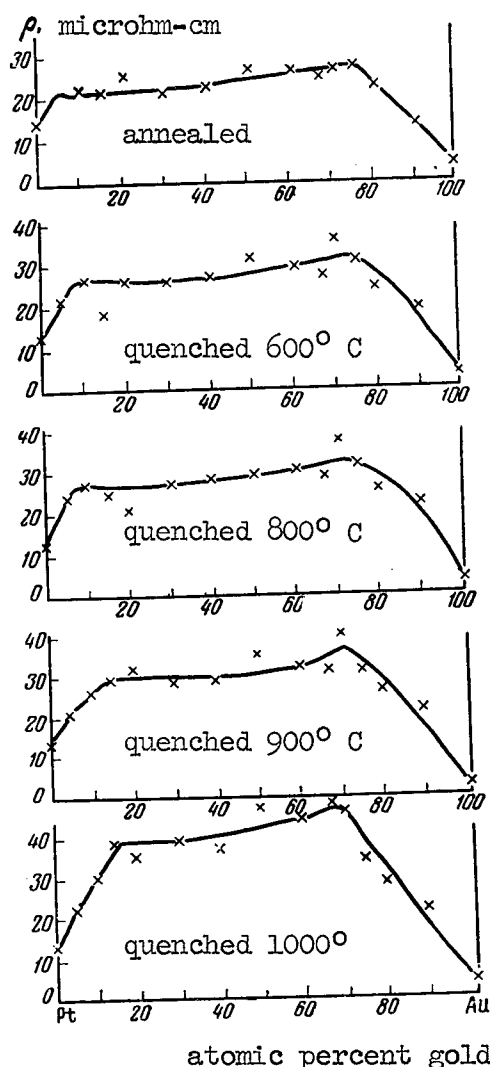
Fig. 108. Specific Electric Resistivity of
Alloys of Platinum with Gold.

To establish the solubility limit more accurately a study was made of the electric resistivity of the alloys. The electric resistivity was studied with the aid of a potentiometer. The measurements of the investigated specimen were carried at two temperatures, 25 and 100° C. For this purpose the alloys were placed in oil thermostat-controlled oil baths. The temperature coefficient of the electric resistivity was calculated from the following formula:

$$\alpha = \frac{\rho_{100} - \rho_{25}}{100\rho_{25} - 25\rho_{100}},$$

where ρ_{25} is the resistivity at 25° C in microhm-cm.
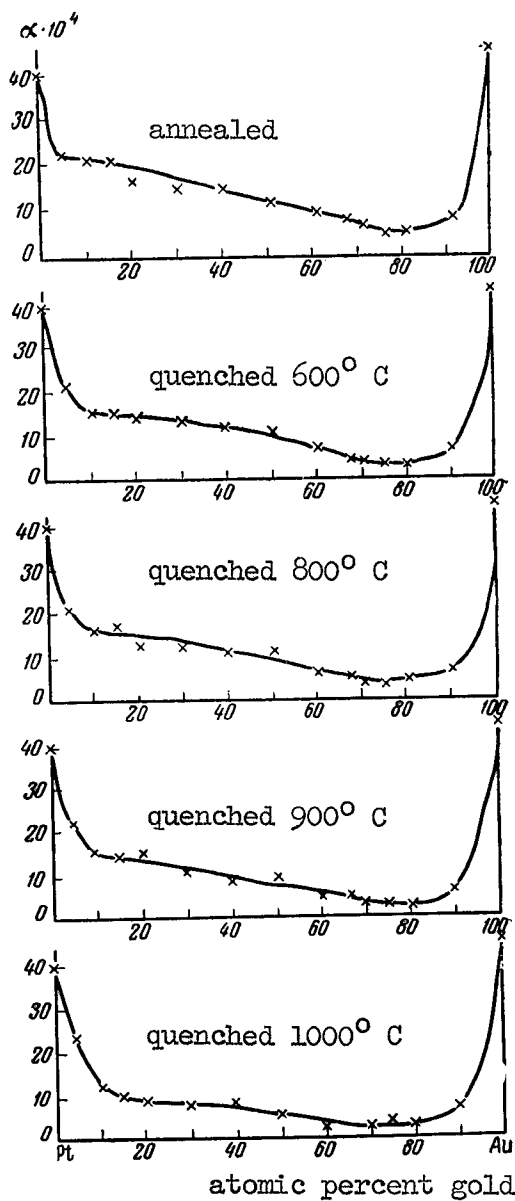
Fig. 109. Temperature Coefficient of Electric resistivity of Alloys of Platinum with Gold.

Electric Properties of Alloys of Platinum with Gold

Table 36

Au atomic %		5	10	15	20	30	40	50	60	66,67	70	75	80	90
percent by weight		5,05	10,09	15,07	20,16	30,21	40,24	50,26	60,24	66,89	70,21	75,19	80,16	90,09
ρ_{25} Microhm-cm	annealed	18,41	19,26	19,14	22,76	19,26	20,84	25,70	25,25	23,53	25,22	26,61	21,58	12,90
	quenched at 600°C	19,16	24,20	16,58	23,98	23,16	25,01	29,68	27,56	26,54	35,04	30,77	23,79	18,73
	800°C	20,95	24,38	22,39	19,44	25,08	26,61	29,02	29,35	27,84	36,71	31,01	25,11	21,07
	900°C	18,69	23,35	26,27	29,76	26,62	27,76	32,23	31,28	30,45	38,99	30,18	25,68	20,54
	1000°C	19,35	27,02	35,70	33,49	36,93	36,75	45,23	44,02	47,08	45,62	33,39	28,13	20,90
ρ_{100} Microhm-cm	annealed	21,29	22,17	21,89	25,41	21,34	23,05	26,68	26,84	24,88	26,48	27,55	22,41	13,63
	quenched at 600°C	22,14	26,95	18,46	26,41	25,34	27,12	31,99	29,02	27,46	36,17	31,48	24,42	19,57
	800°C	24,19	27,29	24,87	21,19	27,31	28,80	29,33	30,72	28,88	37,72	31,94	26,00	22,12
	900°C	21,71	26,00	29,05	32,35	28,80	29,63	36,48	32,42	31,79	40,13	31,04	26,12	21,54
	1000°C	22,56	29,91	38,38	35,58	39,08	37,46	47,56	44,78	48,04	46,29	34,31	28,95	21,92
$\alpha \times 10^4$	annealed	22,02	20,70	20,40	16,60	14,96	14,69	11,94	9,28	7,78	6,22	4,92	5,21	7,63
	quenched at 600°C	21,82	15,71	15,64	14,00	12,86	11,81	11,43	7,21	4,63	4,36	3,09	3,56	6,94
	800°C	21,20	16,55	17,62	12,44	12,24	11,31	11,27	6,38	5,08	3,73	3,87	4,81	6,82
	900°C	22,75	15,71	14,59	15,37	11,18	9,11	9,63	4,91	5,88	3,94	3,07	2,10	6,62
	1000°C	23,43	12,02	10,20	8,50	7,59	8,20	5,67	2,64	2,77	2,61	3,71	2,77	6,53

151

ρ_{100} is the specific resistivity at 100° C in microhm-cm.

Table 36 gives the results of the measurements of the specific electric resistivity ρ_{25} and ρ_{100} and its temperature coefficient α for annealed alloys, quenched at 600, 800, 900 and 1000° C.

An examination of the curves for the specific electric resistivity of the alloys of gold with platinum (Fig. 108) shows that the specific electric resistivity increases rapidly from pure metals in the vicinity of solid solutions, that at the solubility limit kinks are observed in the curves, and that in the heterogeneous region the electric-resistivity curves are slightly concave.

The curves showing the temperature coefficient of electric resistivity (Fig. 109) are the opposite of the curves of the specific electric resistivity. A sharp decrease in the temperature coefficient of electric resistivity is observed away from the pure metals. In the heterogeneous region the temperature coefficient curves are convex upward. However, on these curves the solubility limits are not as clearly seen as on the curves of the specific electric resistivity.

Table 37

Solubility of Gold in Platinum and of Platinum in Gold

$^{\circ}$C	Solubility of Gold in Platinum, Atomic Percent Gold	Solubility of Platinum in Gold, Atomic Percent Gold, Atomic Percent Platinum
100	5	25
600	7	27
800	10	28
900	14	30
1000	18	33

On the basis of the investigations of the electric resistivity we establish the solubility limits of the components (Table 37). According to data of A. T. Grigor'yev /161/, of the data of our preceding investigations /116/, and of the present work, we plotted the diagram of state of alloys of gold with platinum (Fig. 110).
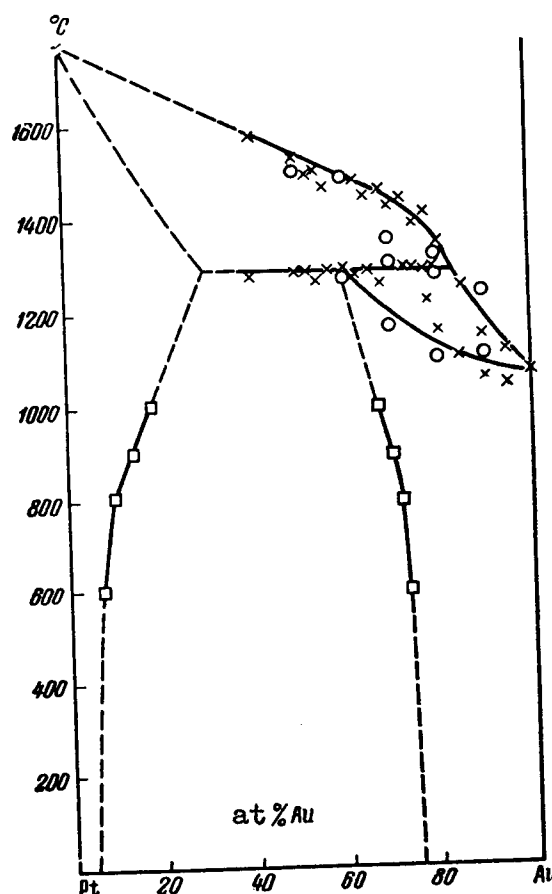
Fig. 110. Diagram of States of the System Platinum-
Gold:

× -- after A. T. Grigor'yev; ○ -- after
V. A. Nemilov; □ -- after A. A. Rudnits-
kiy.

The absolute thermal emf of the alloys of rolled and annealed
specimens was measured with a potentiometer. The results of the mea-
surements are shown in Table 38, and the dependence of the absolute
thermal emf on the temperature (Fig. 111) is represented by smooth
curves with a characteristic smooth point of inflection near 700-
800° C, which is particularly noticeable in the heterogeneous region
of the diagram (20-70 atomic percent gold). The inflection on the
curves of the absolute thermal emf of the alloys in this region is
due most readily to the considerable change in the properties of the
phases that enter into the composition of the mechanical mixture, to
the increase in temperature and solubility of the components, and
also to the insufficient equilibrium state of the alloys.

On the basis of the results obtained we plotted the isotherms of the absolute thermal emf of alloys of platinum with gold (Fig. 112). From these diagrams, plotted for temperatures of 100, 400, 700, and 1000° C it is seen that the absolute thermal emf diminishes smoothly starting with pure platinum and reaches a minimum in the vicinity of the solubility limit of platinum in gold. Then, in the solid-solution region that is rich in gold, the absolute thermal emf rapidly increases towards the pure gold. The solubility limit of gold in platinum is not noticeable on the isotherms of the absolute thermal emf.
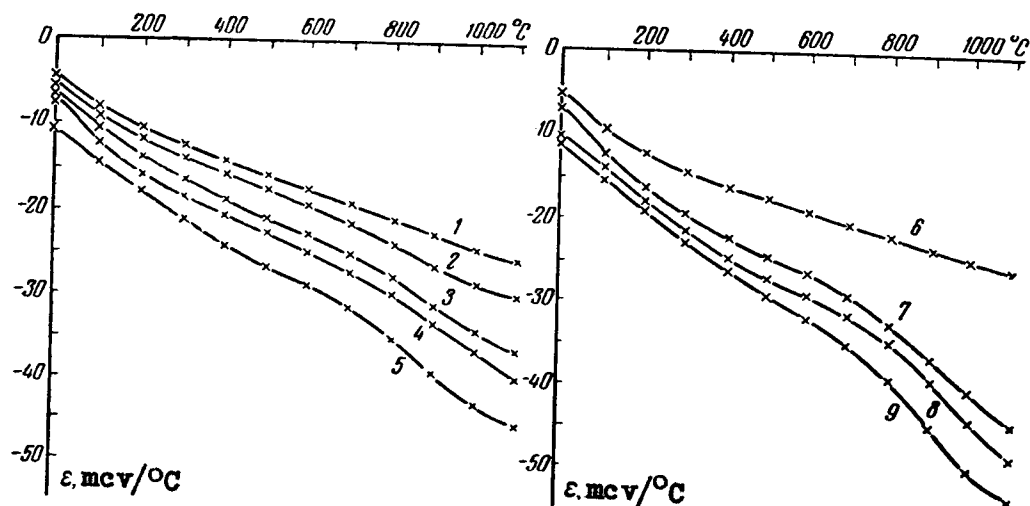
Fig. 111.   Absolute Thermal emf of Alloys of Platinum with
            Gold.   Gold content:

1 -- 10%, 2 -- 20%, 3 -- 30%, 4 -- 40%, 5 -- 80%,
6 -- 90%, 7 -- 50%, 8 -- 60%, 9 -- 70%.

Table 39 and Fig. 113 show the values of the thermoelectric potential while Fig. 114 shows the isotherms of the thermoelectric potential. This curve is quite to the curves of the absolute thermal emf.

The values of the Thomson emf are given in Table 14 and Fig. 115. In accordance with the curves of the absolute thermal emf, the Thomson emf varies with temperature in a unique manner and has a minimum near 800° C.

Table 38

Absolute Thermal emf of Alloys of Platinum with
Gold, ε , microvolts/degree C

Au		Temperature, degrees C									
atomic %	% by weight	100	200	300	400	500	600	700	800	900	1000
10	10,09	— 7,9	—10,4	—12,3	—14,0	—15,7	—17,4	—19,0	—20,8	—22,6	—24,2
20	20,16	— 8,9	—11,6	—13,8	—15,8	—17,6	—19,5	—21,6	—24,0	—26,4	—28,4
30	30,21	—10,4	—13,6	—16,2	—18,5	—20,7	—22,8	—25,0	—28,0	—31,6	—34,4
40	40,24	—12,0	—16,0	—18,4	—20,6	—22,8	—25,0	—27,5	—30,2	—33,6	—36,8
50	50,26	—12,3	—16,4	—19,5	—22,1	—24,4	—26,4	—29,5	—33,2	—37,5	—41,7
60	60,24	—14,0	—18,0	—21,6	—24,7	—27,1	—29,2	—31,9	—35,3	—40,1	—45,9
70	70,21	—15,1	—19,0	—22,7	—26,0	—29,2	—32,2	—35,4	—39,8	—45,8	—51,8
80	80,16	—14,1	—17,7	—21,2	—24,4	—26,8	—28,9	—31,4	—35,3	—39,8	—43,3
90	90,09	— 9,3	—12,0	—14,2	—16,1	—17,6	—19,1	—20,6	—22,1	—23,6	—25,1
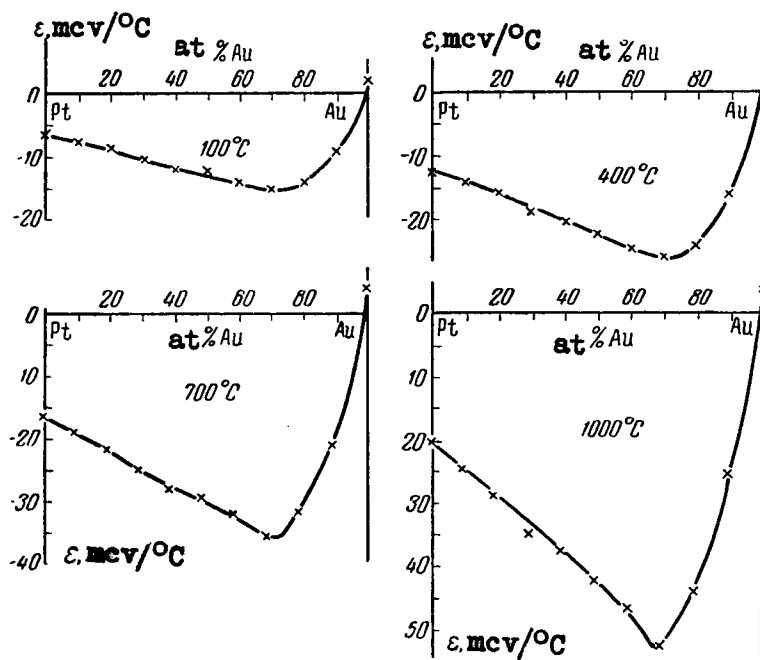
Fig. 112. Isotherms of the Absolute Thermal emf of
Alloys of Platinum with Gold.

Fig. 113. Thermoelectric Potential of Alloys of Platinum
with Gold. Gold content:

1 -- 10%, 2 -- 20%, 3 -- 30%, 4 - - 40%, 5 -- 50%,
6 -- 60%, 7 -- 90%, 8 -- 80%, 9 -- 70%.

Table 39

Thermoelectric Potential of Alloys of Platinum with
Gold, π , millivolts

Au, atomic %	Temperature, degrees C									
	100	200	300	400	500	600	700	800	900	1000
10	—2,94	—4,91	— 7,04	— 9,41	—12,10	—15,80	—18,47	—22,35	—36,50	—30,82
20	—3,32	—5,49	— 7,90	—10,62	—13,60	—17,00	—21,00	—25,80	—31,00	—36,20
30	—3,88	—6,44	— 9,28	—12,44	—15,99	—19,90	—24,30	—30,10	—37,10	—43,85
40	—4,48	—7,57	—10,53	—13,86	—17,60	—21,80	—26,75	—32,45	—39,40	—46,90
50	—4,59	—7,76	—11,17	—14,85	—18,85	—23,01	—28,70	—35,65	—44,00	—53,10
60	—5,22	—8,51	—12,38	—16,61	—20,93	—25,47	—31,00	—37,90	—47,10	—58,50
70	—5,63	—9,00	—13,00	—17,49	—22,55	—28,10	—34,40	—42,75	—53,80	—66,00
80	—5,25	—8,38	—12,14	—16,40	—20,67	—25,20	—30,52	—37,95	—46,70	—55,15
90	—3,47	—5,68	— 8,13	—10,81	—13,60	—16,65	—20,00	—23,75	—27,70	—32,00

The isotherms of the Thomson emf are shown in Fig. 116.

It can be seen from these curves that they have the same form as observed in the investigation of the absolute thermal emf. The Thomson emf varies smoothly and has a minimum in the vicinity of the solubility limit of platinum and gold. The solubility limit of gold in platinum is not identified by an inflection in the curve.

As in the case of palladium-gold and palladium-silver alloys, we find in any platinum-gold alloy two metals, one of which an electronic conductivity and the other one a "hole" conductivity. As in the preceding cases, one observes in the alloys a predominance of the electronic conductivity and the absolute thermal emf assumes a negative value.

In alloys of platinum with gold we observe a sufficiently broad heterogeneous region, at which the thermoelectric properties vary almost linearly.

For solid solutions rich in gold there is an independent branch of the curve for ε , π , and σ .
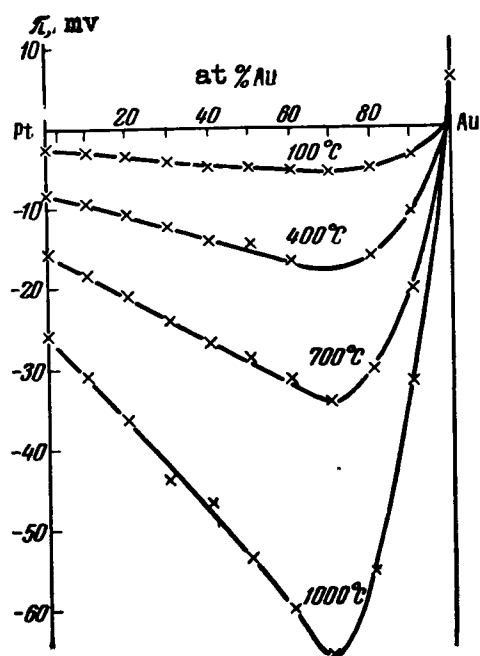
Fig.114. Isotherms of the Thermoelectric Potential of Alloys of Platinum with Gold.

157

The solubility limit of gold and platinum is not identified by any singular point on the isotherms of the thermoelectric properties.

What is striking is the unique shape of the curves of the absolute thermal emf and of the Thomson emf vs. the temperature. The curves of the absolute thermal emf (see Fig. 111) show an inflection in the vicinity of 700-900° C. The Thomson emf curves in the same region exhibit a minimum. This phenomenon may be caused by the non-equilibrium state of the alloys.

The scheme of the process is shown in Fig. 117. The equilibrium state of the alloy corresponds to the curve abc of the absolute thermal emf. However, at low temperatures there is practically no diffusion process. Therefore the absolute thermal emf varies along the curve ade, corresponding to the unchanged phase concentration. At the point d, when the temperature is sufficiently high, the phases begin to enter into equilibrium, and at the point b the speed of diffusion will be sufficiently high to make the equilibrium follow the temperature. Thus, the real curve of the absolute thermal emf will be of the form adbc with a corresponding inflection in the interval db.
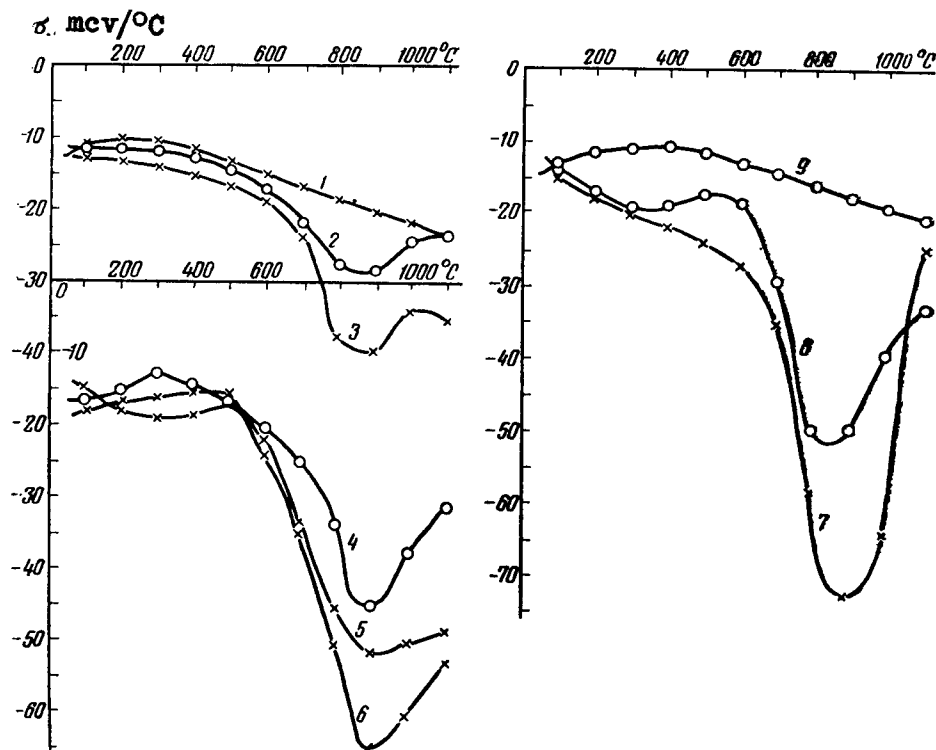
Fig. 115. Thomson emf of Alloys of Platinum with Gold.
Gold Content:
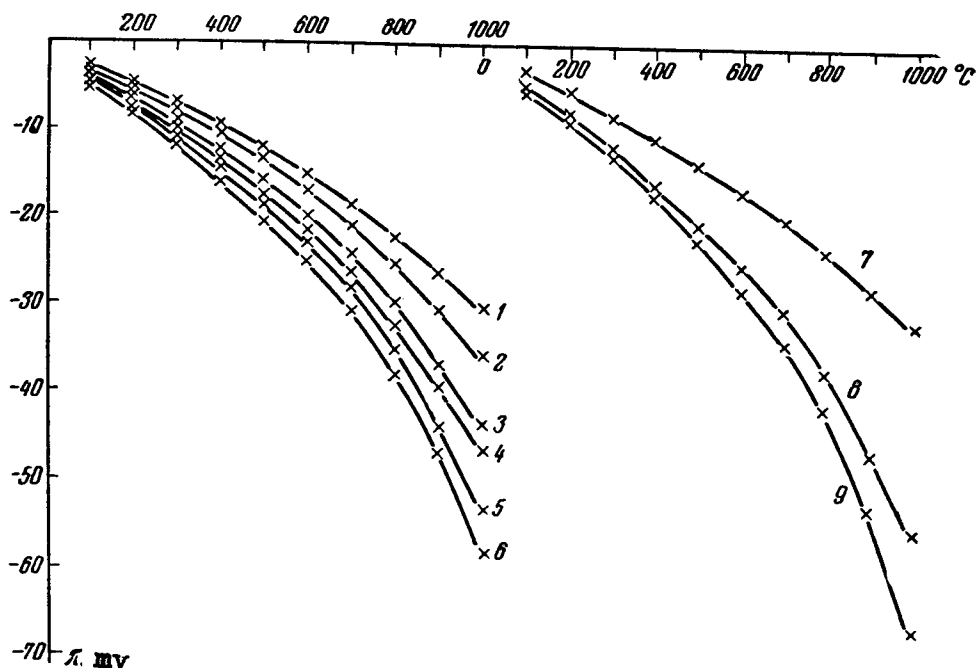1 -- 10%, 2 -- 20%, 3 -- 30%, 4 -- 40%,
5 -- 50%, 6 -- 60%, 7 -- 70%, 8 -- 80%, 9 -- 90%.
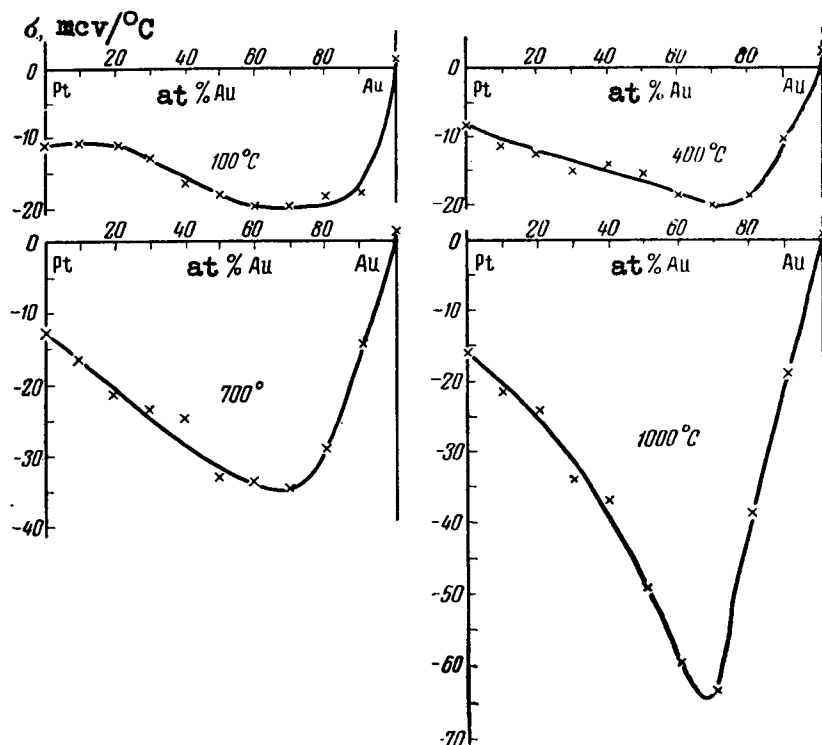
Fig. 116. Isotherms of the Thomson emf of Alloys of
Platinum with Gold.

Table 40

Thomson emf of Alloys of Platinum with Gold,
σ , microvolts/degree C.

Au		Temperature degrees C								
atomic %	% by weight	100	200	300	400	500	600	700	800	900	1000
10	10,09	—11,0	—10,4	—10,3	—11,4	—13,1	—14,8	—16,5	—18,3	—20,0	—21,6
20	20,16	—11,3	—11,4	—11,8	—12,5	—14,1	—17,3	—21,6	—27,2	—28,2	—24,0
30	30,21	—12,9	—13,5	—14,0	—14,9	—16,4	—18,5	—23,6	—37,6	—39,2	—33,9
40	40,24	—16,4	—15,1	—12,9	—14,3	—16,4	—20,2	—24,8	—33,3	—44,6	—37,0
50	50,26	—18,0	—17,0	—16,0	—15,6	—15,5	—21,8	—33,0	—45,1	—51,0	—49,7
60	60,24	—14,9	—18,0	—18,9	—18,6	—17,0	—24,0	—34,0	—50,0	—64,6	—59,9
70	70,21	—14,9	—18,0	—20,1	—21,4	—23,7	—27,1	—35,0	—58,0	—72,3	—63,7
80	80,16	—13,4	—17,0	—19,2	—18,8	—17,0	—18,8	—29,2	—49,4	—49,3	—38,9
91	90,09	—13,1	—11,4	—11,2	—10,8	—11,6	—13,1	—14,6	—16,1	—17,6	—19,1

159

The curve of the Thomson emf shows a minimum in this temperature interval.

A similar shape is seen also for the curves for platinum-gold alloys.

7. PLATINUM-SILVER

The first to investigate the diagram of state of platinum-silver was Doerinckel /160/ who, using methods of thermal analysis and microstructure, established the presence of a peritectic reaction in the system at 1184° C in the region of 31-80% platinum by weight.
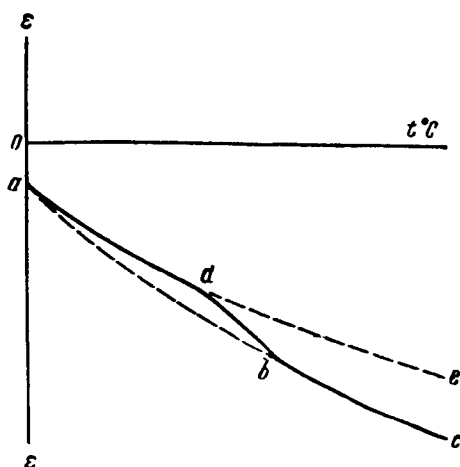
Fig. 117. **Variation of Thermal emf of Alloys of Gold with Platinum as function of the Temperature.**

N. S. Kurnakov and V. A. Nemilov /169/, in an investigation of the platinum-silver system by studying the hardness, microstructure, and electric resistivity. They also made use of the data of Doerinckel and established tentatively the solubility limits of the components.

The solubility limits of the components were determined more accurately by Johansson and Linde /170/ on the basis of data of electric resistivity and x-ray phase analysis of the alloys, quenched at various temperatures. From the shapes of the curves of the electric resistivity of the alloys the authors have established that in

the center portion of the diagram there is a two-phase region of
α-solid solutions, rich in silver, and of δ-solid solutions
rich in **platinum**.

At 750° C the authors have observed the formation of two new
phases: β, , corresponding PtAg in composition, and γ , corres-
ponding to Pt₃Ag. The presence of ordered phases, PtAg and Pt₃Ag,
was established also by x-ray analysis. The authors propose that
the γ phase goes into the γ' phase with increasing temperature.
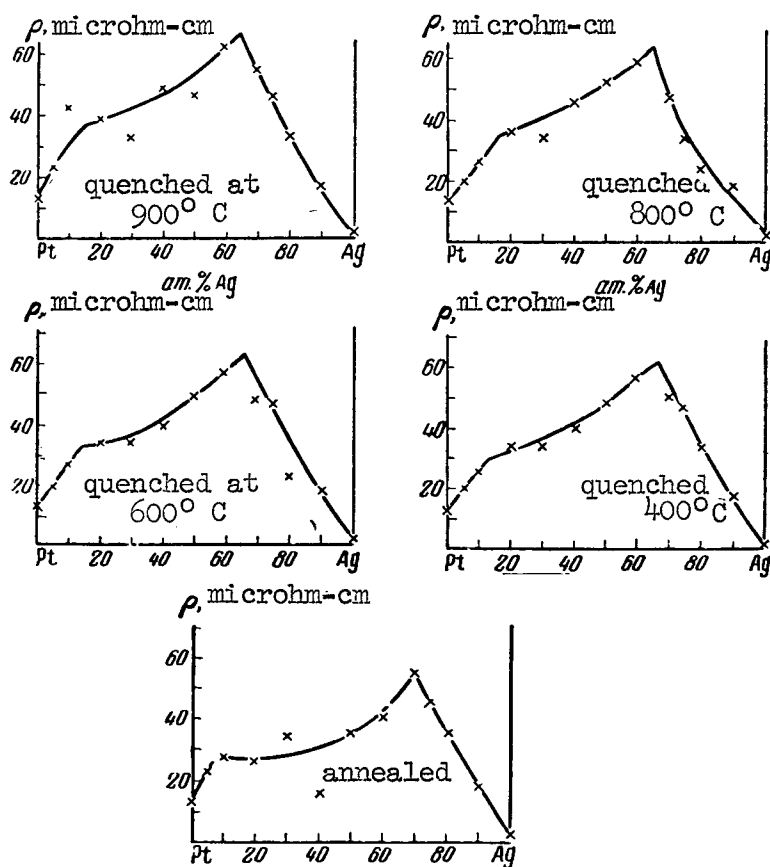
Fig. 118. Specific Electric Resistivity of
Alloys of Platinum with Silver.

No regularity whatever is observed in the change of the electric
resistivity in the heterogeneous region, probably due to the non-equi-
librium state of the alloys. It is impossible to prove the presence
of chemical compounds from these data. Nor is it known which experi-
ments have established the decomposition temperature of the chemical

compounds of 750° C. It is quite impossible to understand how super-structure lines can appear in the heterogeneous region of the diagram. The available x-ray analysis data are quite insufficient to establish homogeneous regions of the newly discovered phases.

Schneider and Esch [171] repeated the x-ray analysis with quenched alloys in the temperature region from 685 to 1130° C and have investigated the electric resistivity of five alloys at high temperatures. Their paper cites two microphotographs in the region of α-solid solutions, rich in silver. The authors indicate the existence of a $PtAg_3$ compound in the form of two modifications, α' and α'', a compound of PtAg with the β phase; a compound Pt_3Ag, which exists in two modifications, γ' and γ; and also a new phase in the vicinity of 90 atomic percent of platinum.

There is no experimental base for all the plots in the diagram below 685° C. The plotted diagrams at higher temperatures are not sufficiently well founded.

To determine more accurately the solubility limits we investigated the electric properties of the alloys. The alloys were manufactured in a high frequency furnace with corundise crucibles, drawn into porcelain tubes, and rolled into rods of square cross sections 1.2 mm on the side. The finished rods were subjected to heat treatment.

The alloys were annealed at 800° C for two days, and then the temperature was reduced to 600° C and the alloys were soaked for seven days and slowly cooled for an equal length of time. For quenching, the alloys were kept at the required temperature for two hours and quenched in cold water.

The electric resistivity of the alloys was investigated at two temperatures, 25 and 100° C. Alloys annealed and hardened at four temperatures, 900, 800, 600, and 400° C, were investigated.

The results of the measurements are given in Table 41. Fig. 118 shows the curves of the electric resistivity at 100° C. The electric resistivity rises rapidly from pure platinum to the solubility limit of silver in platinum. On the solubility limit we observe a kink in the curve. A further change in the electric resistivity with composition follows a smooth rising, but slightly sagging, curve.

On the limited solubility of platinum in silver one observes a maximum of electric resistivity, which is followed by a rapid reduction towards the pure silver.

The temperature coefficient of electric resistivity was calculated from the following formula:

$$\alpha = \frac{\rho_{100} - \rho_{25}}{100\rho_{25} - 25\rho_{100}}.$$

atomic percent silver
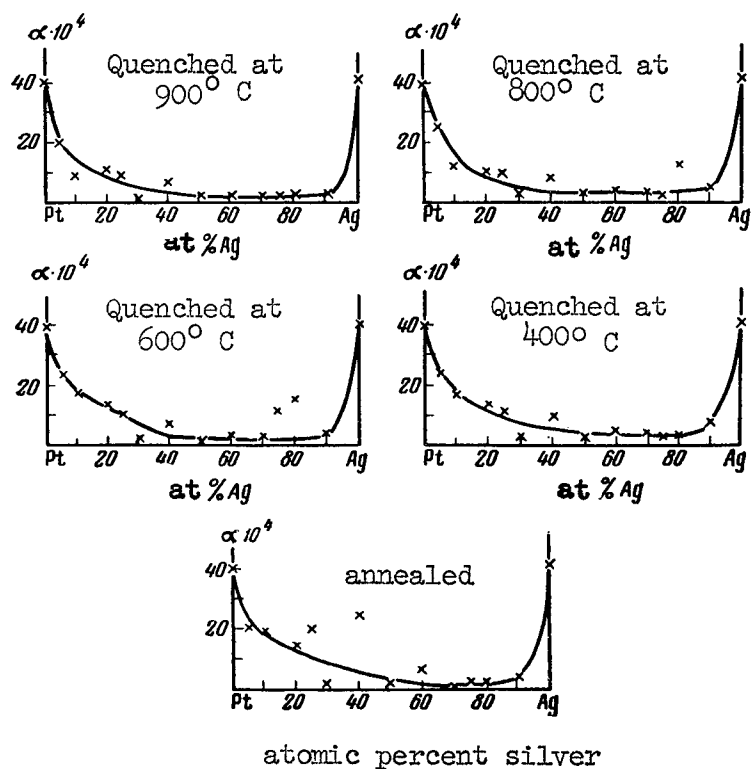
Fig. 119. Temperature Coefficient of Electric
Resistivity of Alloys of Platinum
with Silver.

The results of the calculations are given in Table 41 and
Fig. 119.

The temperature coefficient of electric resistivity of the
alloys of platinum with silver varies smoothly and has a gentle mini-
mum. The solubility limits of the components are not noticeable on
the curves of the temperature coefficient.

In the investigation of the electric properties of alloys one
observes also an irregular deviation of certain points from the
smooth variation of the properties. This is probably due to the
presence of bubbles in the alloys and to the incomplete equilibrium
of the alloys.

T a b l e 41

Electric Properties of Alloys of Platinum with Silver

Ag		5	10	20	30	40	50	60	70	75	80	90
atomic percent		5	10	20 ·	30	40	50	60	70	75	80	90
percent by weight		2,83	5,78	12,13	19,15	26,92	35,59	45,32	56,32	62,37	68,85	83,26
ρ₂₅ microhm-cm	annealed	20,3	24,8	23,1	33,6	13,2	34,4	38,1	54,1	44,1	34,1	17,3
	quenched at 400°C	17,2	23,4	30,3	33,4	36,6	47,5	54,5	48,6	45,0	32,8	16,3
	600°C	17,0	23,7	30,7	33,6	37,6	48,5	55,5	46,3	46,1	21,1	17,9
	800°C	16,8	23,7	33,1	33,0	42,4	50,2	56,5	45,5	33,2	20,4	17,9
	900°C	20,2	40,3	35,3	31,5	46,5	45,1	60,3	54,1	45,6	33,0	16,8
ρ₁₀₉ microhm. cm	annealed	23,3	27,2	25,7	34,3	15,6	35,0	40,1	54,5	44,9	34,8	17,9
	quenched at 400°C	20,2	25,2	33,2	34,0	39,0	48,2	56,2	49,7	46,7	33,4	17,1
	600°C	19,8	26,6	33,6	34,2	39,6	49,1	56,9	48,3	46,9	23,6	18,5
	800°C	19,7	26,4	35,6	33,6	45,0	51,0	57,9	46,4	33,6	23,4	18,4
	900°C	23,1	42,9	38,2	32,1	48,6	45,9	61,7	55,0	46,4	33,6	17,1
α·10⁴	annealed	20,8	19,6	15,6	2,4	25,0	2,26	7,38	0,84	2,22	2,46	4,15
	quenched at 400°C	23,9	16,7	13,3	2,51	9,34	2,11	4,21	3,15	2,33	2,40	6,60
	600°C	23,5	17,0	13,3	2,44	7,35	1,83	3,46	3,09	11,9	16,0	4,21
	800°C	24,6	12,0	10,6	2,65	8,30	2,19	3,16	2,60	1,61	2,04	3,88
	900°C	20,05	9,0	11,9	2,28	7,15	2,09	3,19	2,16	2,16	2,12	2,58

164

The investigations of Doerinckel /160/ and of N. S. Kurnakov and V. A. Nemilov /169/ have shown that the hardening of alloys of platinum with silver is accompanied by a peritectic reaction at 20-80 atomic percent silver and a temperature of 1184° C. The diagram of state is shown in Fig. 120.

Table 42

Solubility of Silver in Platinum and of Platinum in Silver

°C	Solubility of Silver, Atomic Percent Silver	Solubility of Platinum in Silver, Atomic Percent Platinum
100	10	30
400	12	33
600	14	34
800	15	35
900	16	36
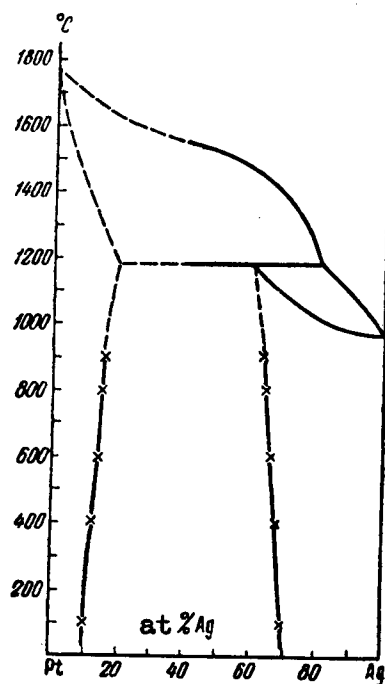
Fig. 120. Diagram of States of the Platinum-Silver System.

The solubility limits of the components are established most clearly by this research through the use of the curves of the specific electric resistivity as a function of the composition for alloys quenched from different temperatures.

Table 42 shows the values of the solubility of the components.

Table 43

Absolute Thermal emf of Alloys of Platinum with
Silver, ε , microvolt/degree C

Ag		Temperature, degrees C									
atomic %	% by weight	100	200	300	400	500	600	700	800	900	1000
5	2,83	—5,4	—8,0	—9,8	—10,6	—12,4	—14,1	—15,6	—17,1	—18,6	—20,0
10	5,78	—5,5	—8,1	—9,9	—11,0	—12,9	—14,5	—16,0	—17,4	—18,8	—20,2
20	12,13	—6,6	—9,4	—11,6	—13,3	—15,2	—17,4	—19,0	—20,6	—22,2	—23,5
25	15,56	—7,9	—10,0	—13,4	—15,4	—17,3	—19,7	—22,1	—24,0	—25,7	—27,2
30	19,15	—10,0	—13,5	—16,2	—18,2	—20,5	—23,5	—26,1	—28,4	—30,4	—32,0
40	26,92	—9,2	—12,7	—15,5	—17,6	—20,1	—23,3	—26,1	—28,4	—30,4	—32,1
50	35,59	—12,5	—16,2	—19,5	—22,1	—25,2	—28,0	—30,1	—33,6	—36,4	—38,8
60	45,32	—12,5	—16,5	—19,8	—22,5	—24,9	—27,9	—31,0	—34,4	—38,0	—41,8
70	56,32	—14,2	—18,3	—21,8	—24,6	—27,7	—31,0	—34,8	—38,7	—42,7	—46,9
80	68,85	—10,7	—14,1	—17,2	—20,1	—22,6	—24,9	—28,0	—31,5	—35,4	—40,2
90	83,26	—7,4	—9,7	—11,6	—13,0	—14,4	—16,2	—17,9	—19,7	—21,4	—23,2

Extrapolating the curves of solubility on the peritectic line, we find that at 1184° C approximately 20 atomic percent of silver is dissolved in platinum and approximately 40 atomic percent of platinum is dissolved in silver.

Our investigations show that there are no grounds for assuming that the platinum-silver diagram of state has any intermediate phases.

The thermoelectric properties of alloys were investigated using rolled and annealed specimens. The values of the absolute thermal emf are given in Table 43 and in Figs. 121 and 122.

The absolute thermal emf of the alloys of platinum with silver has a negative value over almost the entire extent of the diagram. This emf diminishes smoothly with increasing temperature. In the vicinity of 400-600° C one observes a small inflection.
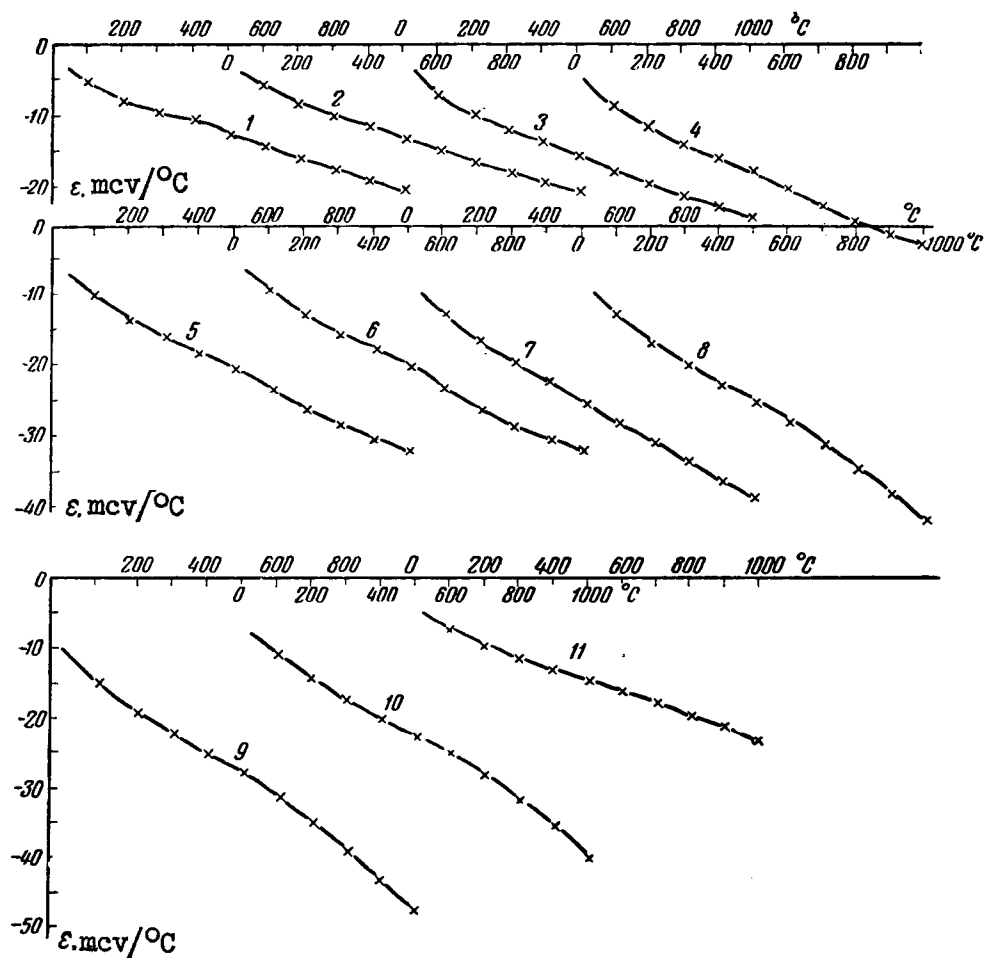
Fig. 121. Absolute Thermal emf of Alloys of Platinum
with Silver. Silver Content:

1 -- 5 atomic percent, 2 -- 10 atomic percent,
3 -- 20 atomic percent, 4 -- 25 atomic percent,
5 -- 30 atomic percent, 6 -- 40 atomic percent,
7 -- 50 atomic percent, 8 -- 60 atomic percent,
9 -- 70 atomic percent, 10 -- 80 atomic percent,
11 -- 90 atomic percent.

167
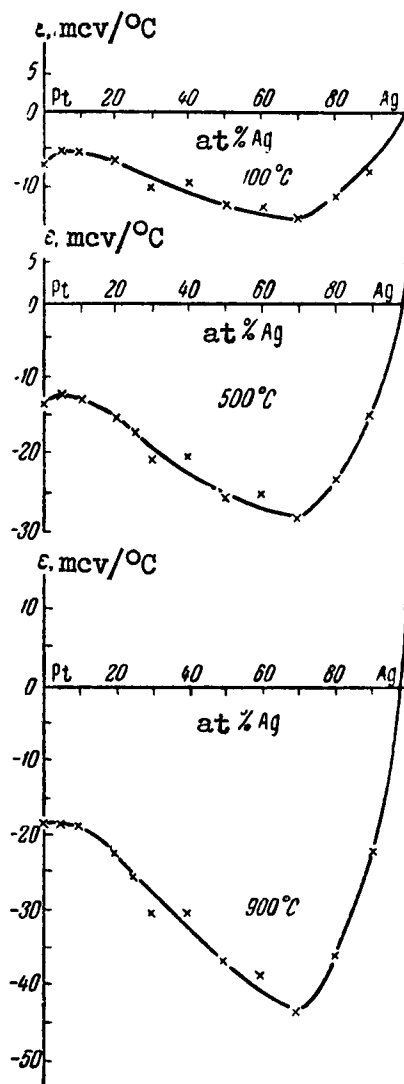
Fig. 122.   Isotherms of the Absolute
Thermal emf of Alloys of
Platinum with Silver.

The isotherms of the absolute thermal emf of alloys, shown in
Fig. 122, have a smooth maximum at the solubility limit of silver
and platinum and a deep maximum at the solubility limit of platinum
in silver.
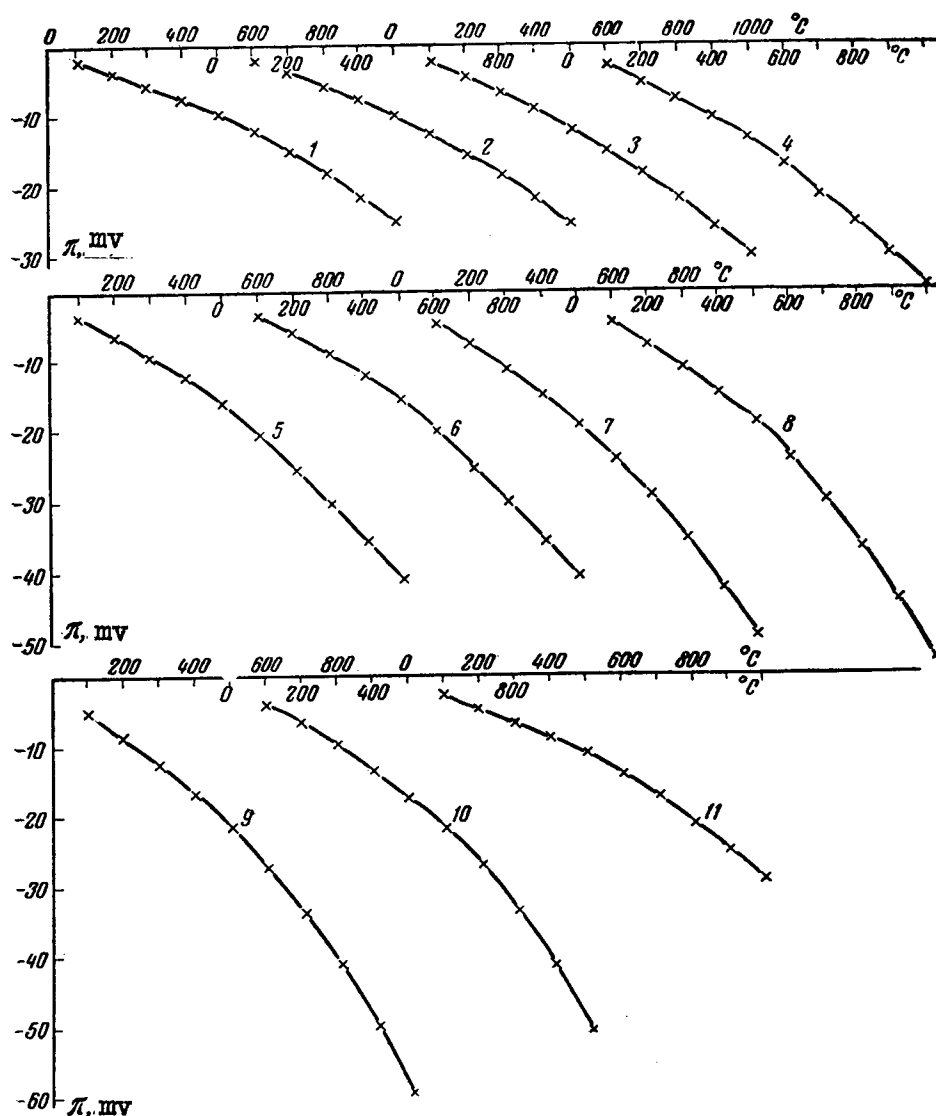
Fig. 123. Thermoelectric Potential of Alloys of
Platinum with Silver. Silver Content:

1 — 5%, 2 — 10%, 3 — 20%, 4 — 25%,
5 — 30%, 6 — 40%, 7 — 50%, 8 — 60%,
9 — 70%, 10 — 80%, 11 — 90%.

The values of the thermoelectric potential of alloys of
platinum with silver are given in Table 44 and are shown in Fig. 123.
The isotherms of the thermoelectric potential (Fig. 124) are similar
to the isotherms of the absolute thermal emf.

Table 44

Thermoelectric Potential of Alloys of Platinum with Silver, π, millivolts

Ag atomic %	Temperature, degrees C									
	100	200	300	400	500	600	700	800	900	1000
5	—2,01	—3,78	— 5,61	— 7,12	— 9,58	—12,30	—15,17	—18,37	—21,80	—25,46
10	—2,05	—3,83	— 5,66	— 7,4	— 9,96	—12,65	—15,66	—18,68	—22,05	—25,75
20	—2,46	—4,45	— 6,65	— 9,01	—11,74	—15,20	—18,49	—22,10	—26,05	—29,95
25	—2,94	—5,20	— 7,67	—10,35	—13,36	—17,20	—21,50	—25,80	—30,15	—34,61
30	—3,73	—6,39	— 9,29	—12,25	—15,84	—20,50	—25,40	—30,50	—35,70	—40,80
40	—3,43	—6,01	— 8,88	—11,85	—15,50	—20,35	—25,40	—30,05	—35,70	—40,90
50	—4,66	—7,66	—11,18	—14,90	—19,47	—24,45	—29,25	—36,05	—42,70	—49,45
60	—4,66	—7,80	—11,35	—15,13	—19,23	—24,37	—30,15	—36,90	—44,60	—53,30
70	—5,30	—8,65	—12,5	—16,55	—21,40	—27,05	—33,80	—41,50	—50,10	—59,70
80	—3,99	—6,66	— 9,85	—13,52	—17,47	—21,75	—27,20	—33,80	—41,90	—51,20
90	—2,76	—4,59	— 6,65	— 8,74	—11,11	—14,13	—17,40	—21,15	—25,10	—29,60

The Thomson emf (Table 43 and Fig. 125), when plotted against the temperature, has a curve with inflections in the vicinity of 400-600° C. These inflections are more clearly pronounced than in the case of the absolute thermal emf.
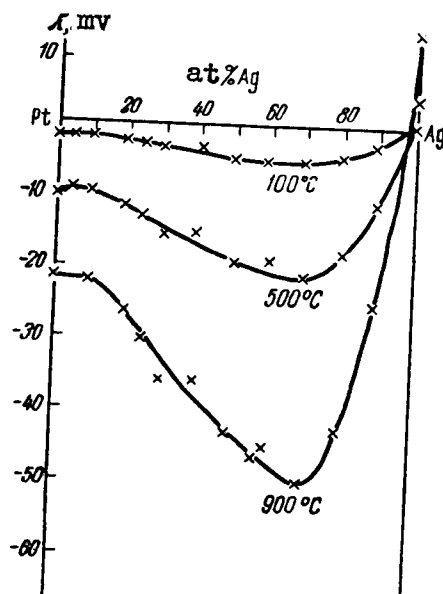
Fig. 124.   Isotherms of the Thermoelectric
Potential of Alloys of Platinum with
Silver.
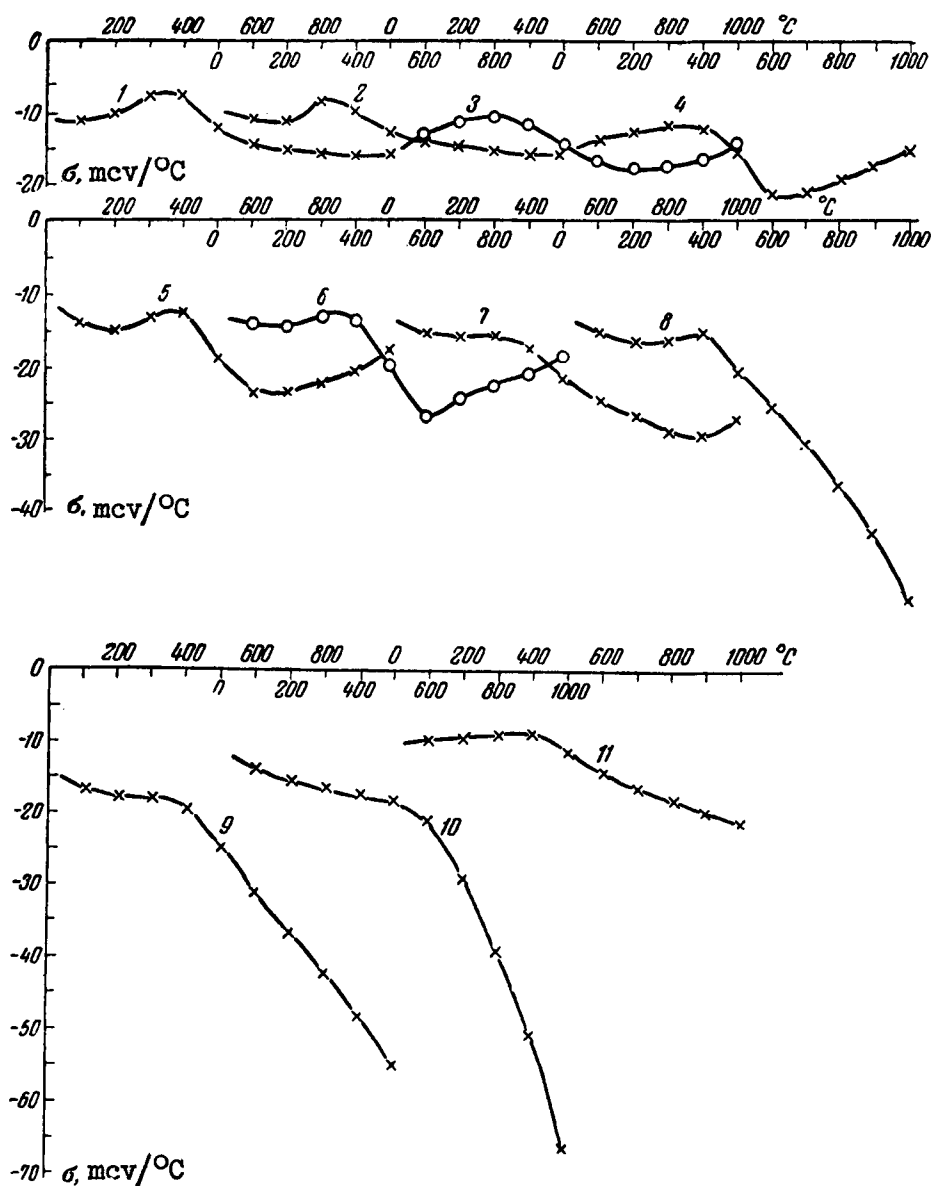
Fig. 125. Thomson emf of Alloys of Platinum with Silver.
Silver Contents, Atomic Percent:

1 -- 5%, 2 -- 10%, 3 -- 20%, 4 -- 25%,
5 -- 30%, 6 -- 40%, 7 -- 50%, 8 -- 60%,
9 -- 70%, 10 -- 80%, 11 -- 90%.

Table 45

Thomson emf of Alloys of Platinum with Silver, σ
microvolt/degree C

Ag, atomic %	Temperature, degrees C									
	100	200	300	400	500	600	700	800	900	1000
5	—11,2	—10,2	— 7,6	— 7,4	—12,4	—14,6	—15,2	—15,7	—16,0	—16,1
10	—11,0	—10,4	— 8,4	—10,1	—12,9	—13,9	—14,8	—15,5	—16,0	—16,3
20	—13,1	—11,5	—10,9	—12,1	—14,7	—17,1	—17,9	—17,8	—16,9	—14,8
25	—13,9	—13,2	—12,0	—12,8	—16,0	—22,2	—21,4	—19,9	—18,2	—15,9
30	—13,8	—15,2	—13,2	—12,8	—18,9	—23,7	—23,8	—22,0	—21,1	—17,8
40	— 14,6	—14,7	—13,5	—11,0	—20,0	—27,1	—24,3	—22,8	—21,2	—19,1
50	—15,6	—16,2	—16,0	—17,8	—22,0	—25,3	—27,2	—30,1	—30,5	—28,0
60	—15,8	—17,3	—17,2	—16,1	—21,6	—26,5	—31,7	—37,6	—44,0	—53,5
70	—16,6	—18,0	—17,8	—19,5	—24,7	—31,4	—37,0	—42,3	—48,5	—55,6
80	—13,5	—15,5	—16,9	—17,9	—18,5	—21,4	—29,5	—39,7	—51,5	—67,3
90	—10,1	—10,0	— 9,2	— 9,2	—12,1	—15,0	—16,9	—18,7	—20,4	—
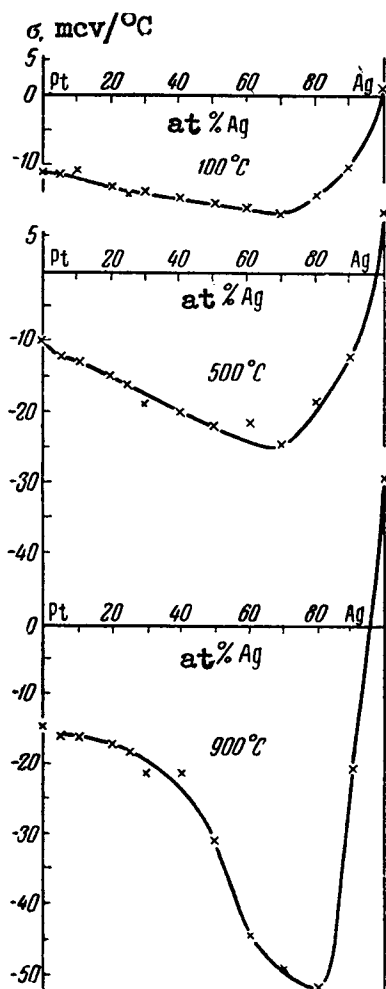
Fig. 126. Isotherms of the Thomson emf of Alloys of Platinum with Silver.

The isotherms of the Thomson emf (Fig. 126) vary with the composition smoothly and have a deep minimum in the vicinity of the solubility limit of platinum in silver.

The neat form of the curves of the absolute thermal emf and of the Thomson emf when plotted against temperature, for the case of alloys of platinum with silver, is explained by the insufficient equilibrium state of the alloys, as in the case of the alloys of platinum with gold.

An investigation of the thermoelectric properties of alloys of platinum with silver confirms our previous conclusion, made on the basis of the investigations of the electric resistivity, namely that the platinum-silver system has no intermediate phases at all.

In the heterogeneous region the absolute thermal emf and the Thomson emf vary with composition smoothly, but always additively.

The components in the platinum-silver system have different signs of absolute thermal emf. The alloys of platinum and silver have an electronic conductivity and a negative thermal emf, like alloys of platinum with gold.

## 8. PALLADIUM-RHODIUM $\underline{/172/}$

The first investigation of alloys of palladium with rhodium was made in 1931 by Tamman and Rocha $\underline{/146/}$ who, on the basis of data of microstructure and hardness, reached the conclusion that a continuous series of solid solutions is formed in this system. The investigations of V. A. Nemilov, A. A. Rudnitskii, and R.S. Polyakova $\underline{/173/}$ of the hardness, electric resistivity, and microstructure, all confirm the conclusions made by the earlier authors.

Palladium has a cubic face-centered lattice with a parameter 3.8825 A $\underline{/174/}$. Rhodium has two modifications: α-Rh , stable below 1030° C with a simple cubic lattice, the parameter of which is 9,211 A, and β-Rh , which is stable above 1030° C, and which has a face-centered cubic lattice with a parameter 3.7957 A $\underline{/105/}$.

The temperature of the α-Rh $\rightleftarrows \beta$-Rh transformation is 1030° C $\underline{/69/}$. The presence of a single crystalline lattice and nearly equal parameters for palladium and β-Rh causes the formation of the continuous series of solid solutions at a high temperature.

The substantial difference in the crystalline lattices of palladium and α-Rh gives grounds for assuming that there is a possible limited solubility of the metals below 1000 and 30° C, the point of polymorphous transformation of rhodium.

173

Table 46

Absolute Thermal emf of Alloys of Palladium with
Rhodium, ε , microvolt/degree C

Rh, % by weight	Temperature											
	100	200	300	400	500	600	700	800	900	1000	1100	1200
10	+5,2	+4,0	+2,5	+0,8	—1,1	—3,1	—5,3	—7,6	—9,9	—12,2	—14,5	—16,8
20	+8,0	+7,7	+7,3	+6,5	+3,4	+4,1	+2,5	+0,9	—0,8	—2,5	—4,2	—6,0
30	+7,9	+8,4	+8,6	+8,2	+7,5	+6,6	+5,7	+4,5	+3,1	+1,8	+0,7	—0,3
40	+7,6	+8,2	+8,5	+8,5	+8,3	+7,8	+7,1	+6,2	+4,6	+3,3	+3,4	+3,5
50	+6,2	+6,3	+6,3	+6,2	+6,0	+5,7	+5,2	+4,2	+3,3	+1,2	+1,6	+2,2
60	+5,0	+4,7	+4,4	+4,0	+3,8	+3,3	+2,7	+2,1	+1,3	+0,2	+0,5	+1,0
70	+4,3	+3,6	+3,0	+2,4	+1,9	+1,5	+1,0	+0,7	+0,5	—0,1	—0,6	—0,3
80	+4,2	+4,0	+3,9	+3,7	+3,5	+3,2	+2,8	+2,4	+2,0	+1,2	—0,8	—0,9
90	+2,9	+2,9	+2,8	+2,6	+2,3	+2,2	+1,7	+1,4	+0,8	—0,2	—1,8	—1,7

For the present investigation we used palladium made by cal-
cination of palladozamine, twice precipitated from ammonia solution,
and commercial rhodium, containing not more than 0.02% of impurities.

The alloys were molten in a high frequency furnace in corun-
dise crucibles and drawn into porcelain tubes. The resultant sticks
were annealed at 1000° C and then slowly cooled. Their absolute ther-
mal emf was investigated with the Kurnakov pyrometer. The results
of the measurements are given in Table 46 and Fig. 127.

The values of the absolute thermal emf diminish smoothly with
increasing temperature. For alloys containing 40-90% rhodium by
weight one observes a sharp kink in the curves at temperature near
900-1200° C.

Based on the data obtained we plotted isotherms of the absolute
thermal emf for the alloys of the palladium-rhodium systems, as shown
in Fig. 128.

The values of the absolute thermal emf of the alloys increase
rapidly from pure palladium and have a maximum which shifts with
increasing temperature from 20% rhodium by weight at 100° C to 40%
rhodium by weight at 1200° C.

The isotherms then diminish smoothly with increasing content
of rhodium, and at a content of approximately 17% rhodium by weight
one observes a minimum. In the region of 70-80% rhodium by weight,
the curves rapidly rise and then diminish again towards the pure

Fig. 127. Absolute Thermal emf of Alloys of Palladium-Rhodium. Rhodium Content:

1 -- 10%, 2 -- 20%, 3 -- 30%, 4 -- 40%, 5 -- 50%,
6 -- 60%, 7 -- 70%, 8 -- 80%, 9 -- 90%.

rhodium.
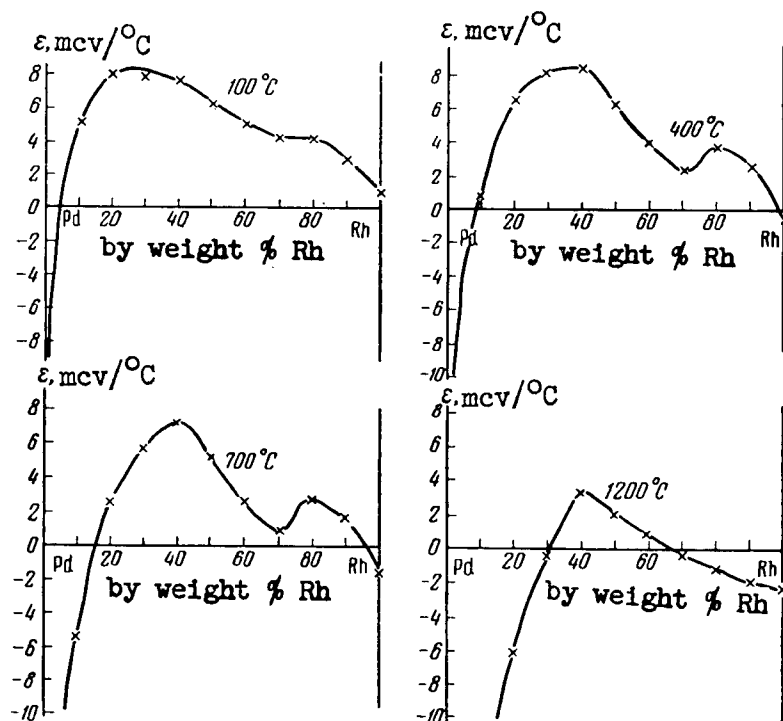
Fig. 128. Isotherms of the absolute thermal emf
of palladium-rhodium alloys.

The isotherm at 1200°C is a smooth curve with a maximum near 40% rhodium
by weight. Table 47 and Figures 129 and 130 show the values of the thermo-
electric potential of alloys of palladium with rhodium.

Table 47

Thermoelectric Potential of Alloys of Palladium
with Rhodium, π, Millivolts.

Rh % by weight	Temperature, °C											
	100	200	300	400	500	600	700	800	900	1000	1100	1200
10	+1,94	+1,89	+1,43	+0,54	—0,85	—2,71	—5,15	—8,16	—11,63	—15,53	—19,93	—24,90
20	+2,98	+3,64	+4,18	+4,37	+4,17	+3,58	+2,43	+0,97	—0,94	—3,19	—5,77	—8,85
30	+2,94	+3,97	+4,93	+5,51	+5,80	+5,75	+5,55	+4,83	+3,64	+2,29	+0,96	—0,44
40	+2,83	+3,88	+4,86	+5,71	+6,41	+6,81	+6,90	+6,65	+5,40	+4,21	+4,68	+5,16
50	+2,31	+2,98	+3,61	+4,17	+4,64	+4,97	+5,05	+4,51	+3,88	+1,53	+2,20	+3,24
60	+1,86	+2,22	+2,52	+2,69	+2,94	+2,88	+2,62	+2,26	+1,53	+0,25	+0,69	+1,47
70	+1,60	+1,70	+1,72	+1,61	+1,47	+1,31	+0,97	+0,75	+0,59	—0,13	—0,83	—0,44
80	+1,57	+1,89	+2,23	+2,49	+2,70	+2,79	+2,72	+2,58	+2,35	+1,53	—1,10	—1,33
90	+1,08	+1,37	+1,60	+1,75	+1,78	+1,92	+1,65	+1,50	+0,94	—0,25	—2,48	—2,50

176

The values of the Thomson emf are shown in Table 48 and Fig. 131.

The Thomson emf diminishes smoothly with rising temperature. For alloys in the vicinity of 30-90% rhodium by weight we observe critical points, near which the Thomson emf diminishes sharply and changes jump-like in the transition through the critical temperature, from negative values to positive ones.
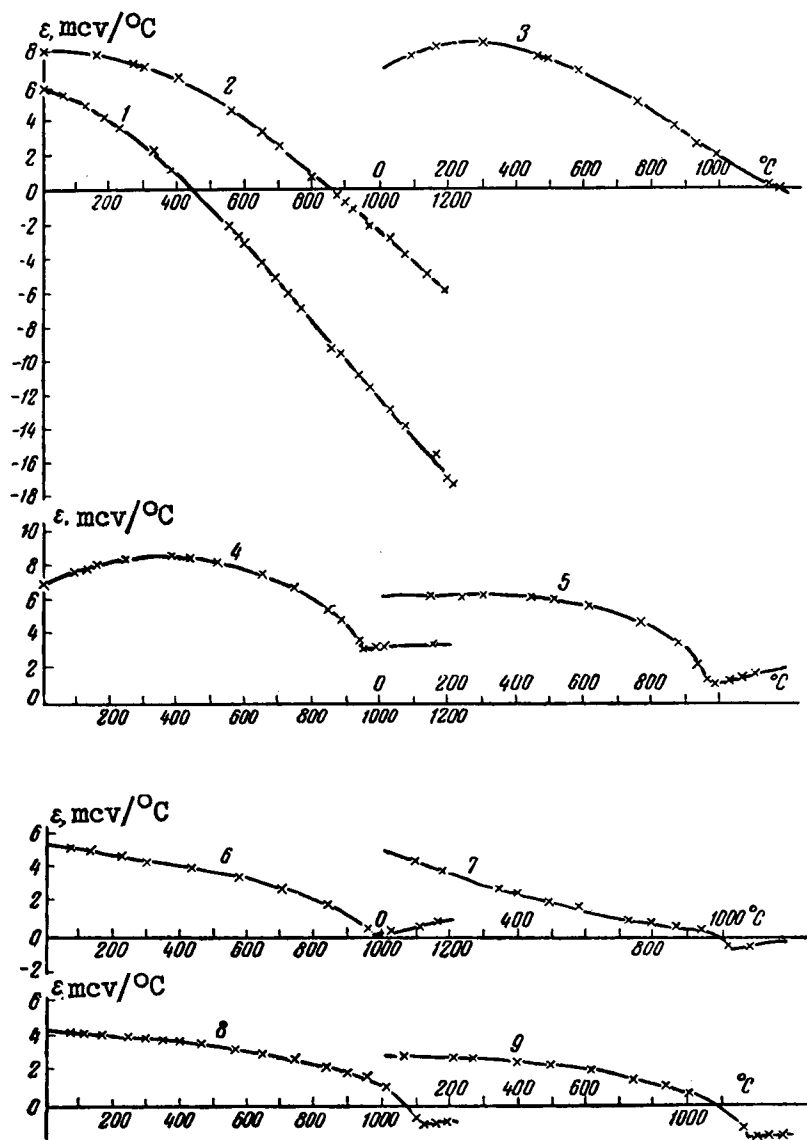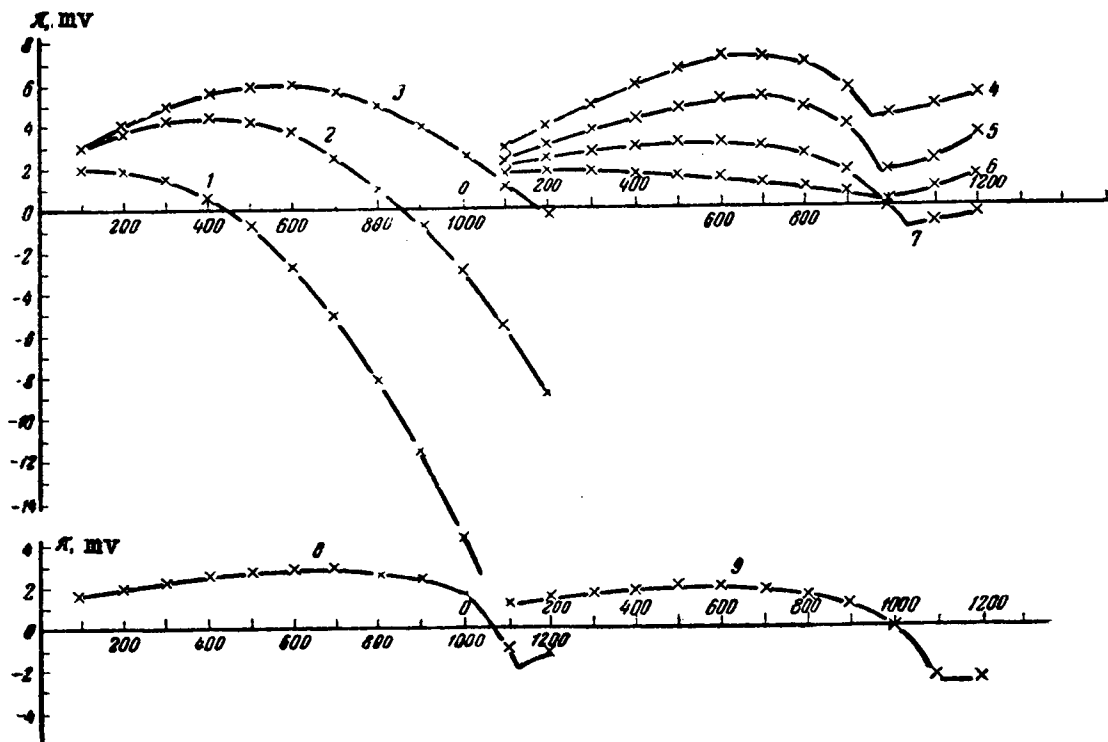

Fig. 129. Thermoelectric Potential of Palladium-Rhodium Alloys. Rhodium Content:

1 -- 10%, 2 -- 20%, 3 -- 30%, 4 -- 40%, 5 -- 50%,
6 -- 60%, 7 -- 70%, 8 -- 80%, 9 -- 90%.

Fig. 132 shows the isotherms of the Thomson emf. The isotherm at 1200° is a smooth curve having a maximum. At temperatures below the critical points we see wavy curves, which have points of inflections at the same places as the isotherms of the absolute thermal emf, i.e., in the region of 70-80% rhodium by weight.

177

Table 48

Thomson emf of Alloys of Palladium with Rhodium,
σ , microvolts/degree C

Rh, atomic %	Temperature, degrees C											
	100	200	300	400	500	600	700	800	900	1000	1100	1200
10	—3,4	—6,6	—9,2	—11,4	—15,5	—19,2	—22,4	—24,7	—27,0	—29,3	—31,6	—33,9
20	—0,8	—1,4	—3,7	—6,1	—9,7	—12,2	—16,1	—18,2	—20,0	—21,7	—23,4	—25,1
30	+3,0	+1,4	0	—4,0	—5,8	—7,4	—10,7	—13,4	—17,6	—14,6	—13,7	—14,0
40	+2,6	+2,4	+0,6	—1,0	—2,3	—5,2	—7,3	—11,8	—25,9	+1,3	+1,4	+1,5
50	+0,04	+0,05	0	—0,7	—2,3	—2,6	—5,8	- 9,7	—23,5	+5,7	+6,2	+6,6
60	—1,1	—1,4	—1,7	—2,2	—3,1	—4,1	—5,5	—6,8	—14,1	+5,6	+6,1	+6,5
70	—2,8	—3,2	—3,5	—3,8	—3,8	—3,5	—2,9	—2,2	—2,9	—21,0	+4,4	+4,7
80	—0,6	—0,7	—0,9	—1,0	—1,6	—2,3	—3,3	—4,3	—5,9	—13,0	—31,6	+4,1
90	0	—0,5	—0,9	—1,7	—1,9	—2,6	—2,9	—4,8	—8,2	—17,9	+1,4	+1,5
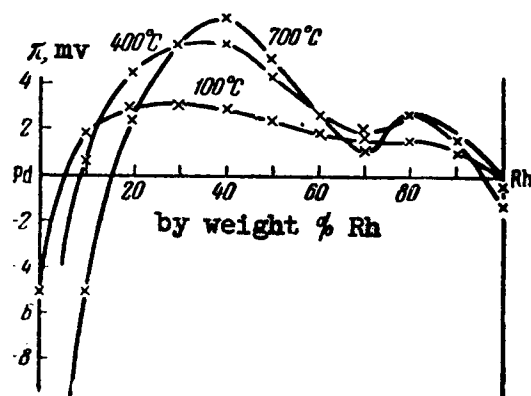
Fig. 130.   Isotherms of the Thermoelectric Potential
of Alloys of Palladium with Rhodium.

From the curves of the absolute thermal emf and the Thomson emf, plotted against the temperature, we have established the following critical points in the diagram of state of the palladium-rhodium system:

Rh, % by weight	30	40	50	60	70	80	90
t, °C....	920	955	970	980	1030	1120	1080
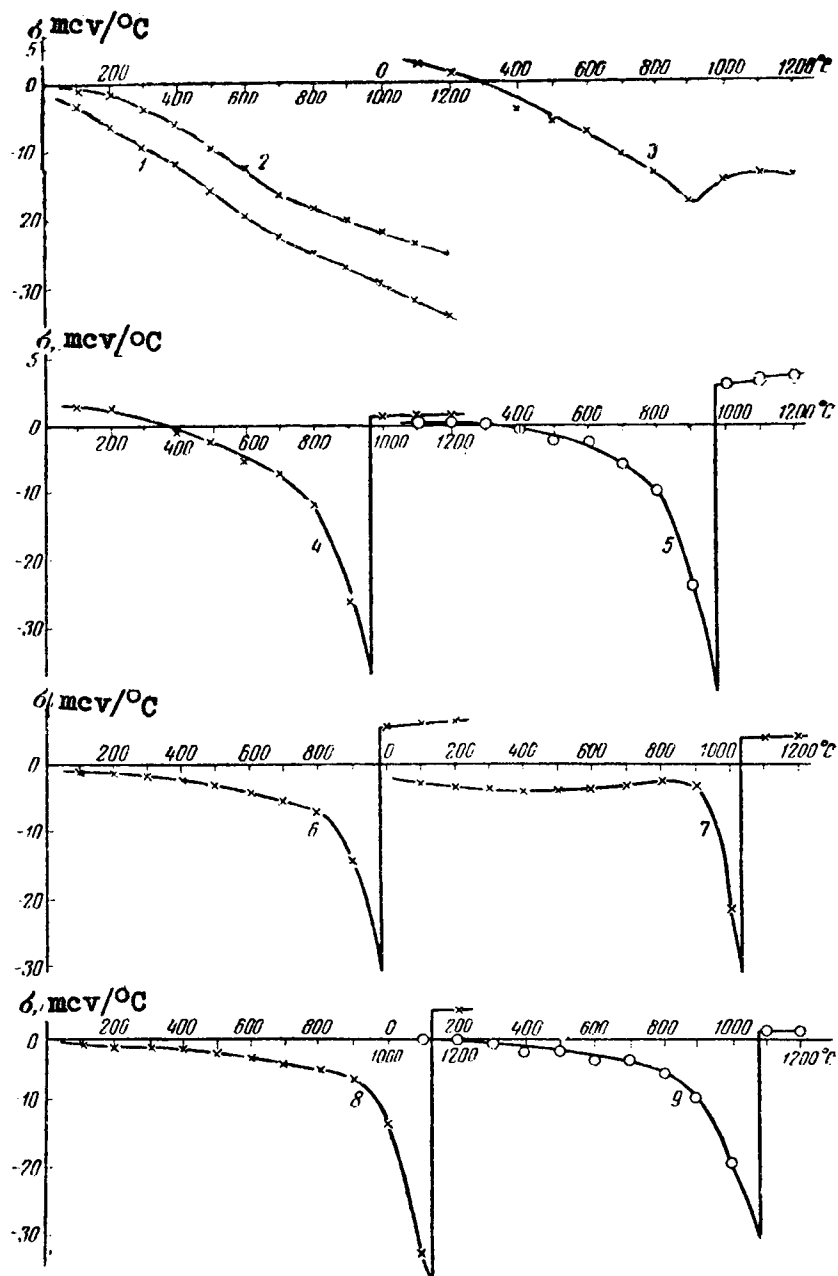
Fig. 131. Thomson emf of Alloys of Palladium with Rhodium.
Rhodium Content:
1 -- 10%, 2 -- 20%, 3 -- 30%, 4 -- 40%, 5 -- 50%,
6 -- 60%, 7 -- 70%, 8 -- 80%, 9 -- 90%.

179
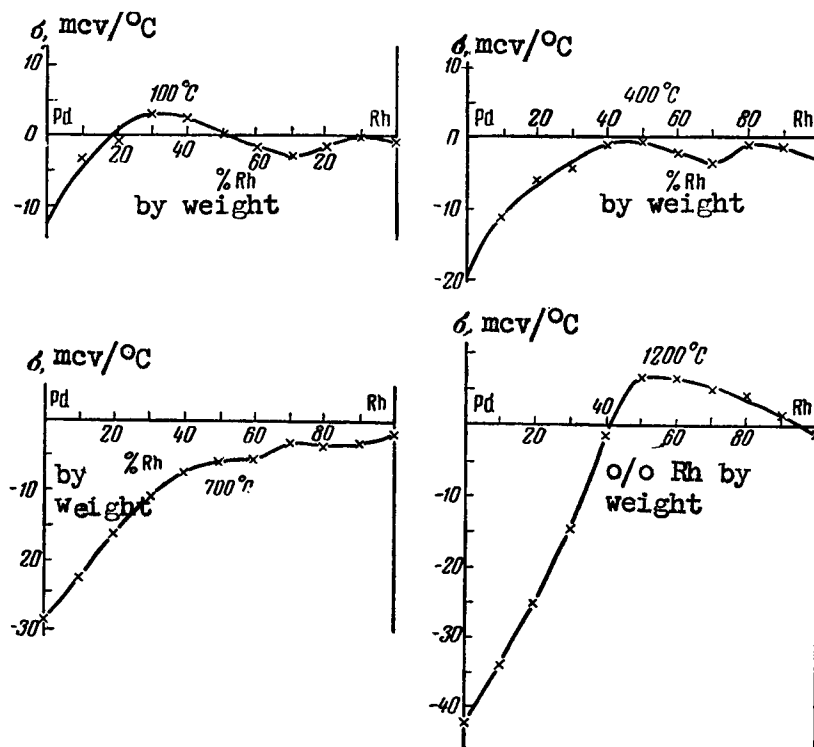
Fig. 132. Isotherms of the Thomson emf of Alloys of
Palladium with Rhodium.

Fig. 133 shows the diagram of state of the palladium-rhodium
system. The liquidus and solidus lines are plotted schematically.

A comparison of the thermoelectric properties with the data
of V. A. Nemilov, A.A. Rudnitskiy, and R.S. Polyakova /173/ shows
that the palladium forms a continuous series of solid solutions with
β-Rh . With decreasing temperature the β -solid solutions
goes into the α--solid solutions in the vicinity of 80-100% by
weight rhodium. In the vicinity of 30-80% rhodium by weight the so-
lid solution decomposes into two phases: the β- -solid solutions,
rich in palladium, and the α- -solid solution, rich in rhodium. The
region of the α--solid solution has a maximum near 80% rhodium by
weight.

The limit of homogeneity of the α- -solid solution ranges
from pure α-Rh to 20 or 30% palladium by weight at low tem-
perature. This is indicated by the bends on the isotherms on the ab-
solute thermal emf, and also the bends on the curves of the electric
resistivity, its temperature coefficient, the electric conductivity,

(Fig. 134), plotted from the data of V. A. Nemilov, A. A. Rudnitskiy, and R. S. Polyakova [173].

The solubility limit of rhodium in palladium is hardly noticeable. On the curves of the Thomson emf vs. the temperature (see Fig. 131) for an alloy containing 30% rhodium by weight there is clearly seen a critical point at 920° C. The maximum on the 100° C isotherm of the absolute thermal emf is located near the point corresponding to the contents of 20% rhodium by weight (Fig. 129).

As the temperature is increased this maximum shifts towards a point corresponding to a contents of 40% rhodium by weight at 400° C, and retains its position relative to composition all the way to the transition into a homogeneous solid solution.

The location of the maximum does not always correspond exactly to the solubility, owing to the incomplete equilibrium in the alloys. On the hardness curve (See Fig. 134) a change in the course of the curve is observed in an interval approximately between 30 and 40% rhodium by weight. The curves of the electric resistivity, its temperature coefficient, and the electric conductivity, and also the isotherms of the Thomson emf, disclose no characteristic bends in this region.

On the diagram of state (see Fig. 133) the limit of existence of homogeneous β- -solid solution below 900° C is located tentatively in the region of 20-30% rhodium by weight.

In the transition from the heterogeneous region towards the solid solutions, the curves of the temperature dependence of the absolute thermal emf have kinks at the critical points.

The Thomson emf changes near the points of transition from the heterogeneous region towards the homogeneous solid solutions in a manner similar to that observed for the specific heat in the region of second-order transformations. However, in the case of the specific heat a sharp maximum is observed, while in the case of the Thomson emf a minimum is observed for the investigated alloys.

The present investigation confirms the theoretical premises of V. K. Semenchenko /79/, who considers the transition from the heterogeneous region towards the homogeneous solid solution as a second-order transformation. A complete analogy is observed here between the specific heat and the Thomson emf.

The use of the thermoelectric method in the study of the palladium-rhodium diagram of state has made it possible for the author to determine the transformations that take place in the solid state.

181
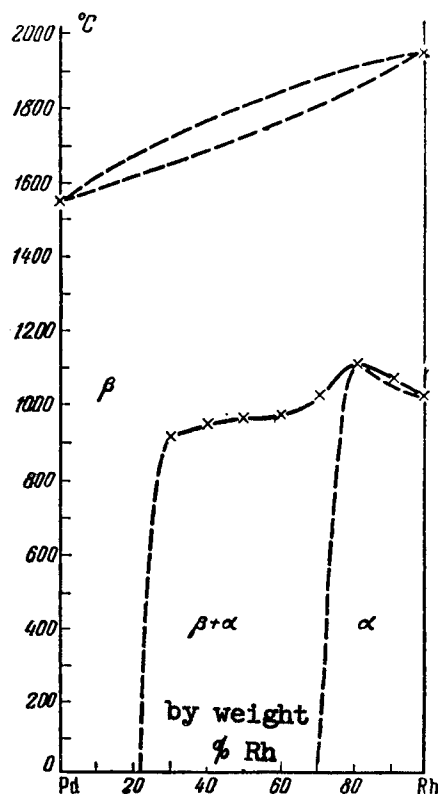
Fig. 133. Diagram of State of the
Palladium-Rhodium System.

An unlimited mutual solubility was found for palladium in
β-Rh . This is in complete agreement with the data of the
preceding authors.

Palladium and α-Rh have a limited solubility in each
other. The limit of the transition of the β-solid solution into
the α-solid solutions has been established, as well as the limit
of decomposition of the β-solid solution into two phases (see
Fig. 133).

At the temperatures below 900° C the palladium dissolves ap-
proximately 20 to 30% of rhodium by weight, while the α-Rh
dissolves approximately 20 to 30% of palladium by weight.

At high temperatures the rhodium is thermoelectrically nega-
tive, like the palladium. In the region of the β-solid solution
(see Fig. 128) there is observed on the isotherm at 1200° C a maxi-
mum that has a positive value. In this case the isotherms are

182

higher than the critical points and are similar to the isotherms of the absolute thermal emf of alloys of platinum with palladium.

At low temperatures the absolute thermal emf of rhodium becomes positive; the α-Rh forms limited solid solutions with palladium; the isotherms of the absolute thermal emf change in this case in a more complicated manner.
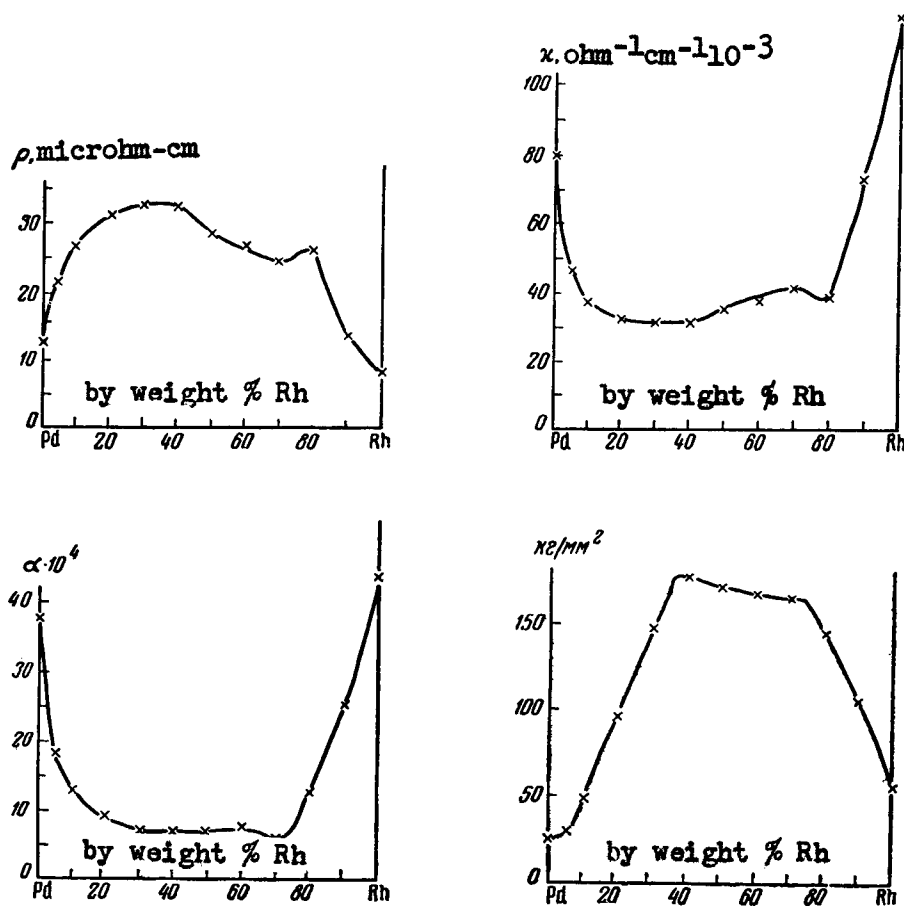
Fig. 134. Properties of Alloys of Palladium with Rhodium.

9. PALLADIUM-COPPER /68/.

The palladium-copper system was first investigated by Ruer /155/, who used thermal analysis and the microstructure method to establish that the components form a continuous series of solid so-

lutions.

In the region of 30-70% palladium by weight, the author has observed a needle-like structure, the origin of which is explained by the possibility of formation of an unstable modification of the solid solution.

Sedstrom [113] investigated the electric conductivity, the specific heat, and the thermal emf. On the curves of the properties the author has established singular points at 40 and 50 atomic percent palladium. The appearance of these points is explained by the formation of the chemical compounds Cu_3Pd_2 and $CuPd$.

Holgersson and Sedstrom [151], who carried an x-ray analysis of the systems, found in the alloys containing 39.7 and 49.8 atomic percent palladium a mixture of two cubic lattices: a volume-centered one and a face-centered one. The remaining alloys had a face-centered lattice. These results contradict the results of the preceding work by Sedstrom [113], although the authors have used this data in their experiments.

A study of the temperature coefficient of expansion, carried out by Johansson [175], did not help uncover any transformations in alloys in the solid state.

An x-ray investigation, carried out by Johansson and Linde [176], has shown in the region of 39.9 and 49.8 atomic percent palladium the presence of an ordered lattice of the cesium chloride type. In the alloy with 49.95 atomic percent palladium, there was found a cubic face-centered lattice with a statistical distribution of the atoms.

A more detailed investigation performed by the same authors [177] has established that in the quenched state all the alloys have a disordered face-centered cubic lattice. Upon annealing, an ordering of the lattice takes place in alloys with 10 to 28 atomic percent palladium, without a change in its symmetry. In alloys containing 37 to 49 atomic percent palladium there is formed an ordered volume-centered cubic lattice. The authors have found on the curve of the electric resistivity two gentle minima in the ordering regions.

Borelius, Johansson, and Linde [178] again investigated the electric resistivity and the lattice structure of palladium-copper alloys. On the curve of the electric resistivity of annealed alloys the authors have found two gentle minima in the regions corresponding to 10-25 and 40-50 atomic percent palladium. An investigation of the structure of the lattice has shown that the superstructure lines on the Debyegrams are hardly noticeable at 25 atomic percent palladium. They are strongest for an alloy with 17 atomic percent

palladium.

The authors use the formulas $PdCu_3$ and PdCu without sufficient justification. The compositions of these compounds are at the limit of the existence of ordered phases, as can be seen from the latest two works [177,178].

J. Linde [179], carrying out an investigation of the crystalline lattice, has confirmed the data of the earlier authors and indicated the existence of ordering regions at 10-25 and 38-50 atomic percent palladium. In the first case there is observed an ordered cubic structure with centered faces, and in the second that of a volume-centered cube.

The magnetic susceptibility was investigated by Svenssen [180], who showed that it varies smoothly with the composition. Such a result was obtained probably as a result of an incorrect heat treatment. Further investigations by Seemann [181] have shown that the magnetic susceptibility changes upon ordering of the $PdCu_3$. In the region of PdCu no changes were observed in the magnetic susceptibility.

Seemann's investigations of the electric resistivity [182] confirm the existence of singular minima at 20 and 37-43 atomic percent palladium. Taylor [183] studied the transformation temperatures, the electric resistivity, and the microstructure and found two maxima for the transformation temperature: near 20 and near 40 atomic percent palladium. These compositions correspond to the minima on the electric resistivity curve.

P. S. Belonogov [184] investigated the transformation temperatures, the hardness, the electric resistivity, and the microstructure and indicated maxima on the curves of the transformation temperatures and minima on the curves of the hardness and electric resistivity for compositions with 25 and 50 atomic percent palladium.

Belonogov's results contradict the x-ray-analysis data obtained by various authors.

A detailed x-ray-diffraction investigation, made by F. Jones and S. Sykes [185], has shown that in annealed alloys, containing ten to 18 atomic percent palladium, one observes a cubic face-centered ordered lattice. In alloys with 18-25 atomic percent palladium one observes a tetragonal ordered lattice. Alloys with 30-35 atomic percent palladium consist of a mixture of disordered face-centered and ordered volume-centered lattices. Alloys with 35-47 atomic percent palladium have an ordered volume-centered lattice. Alloys with 45-58 atomic percent palladium consist of a mixture of disordered face-centered and ordered volume-centered lattices. From the data of Jones and Sykes it is seen that the chemical compound

185

PdCu₃ corresponds to the limit of existence of the ordered phase, while the composition of the chemical compound PdCu corresponds to the two-phase region.
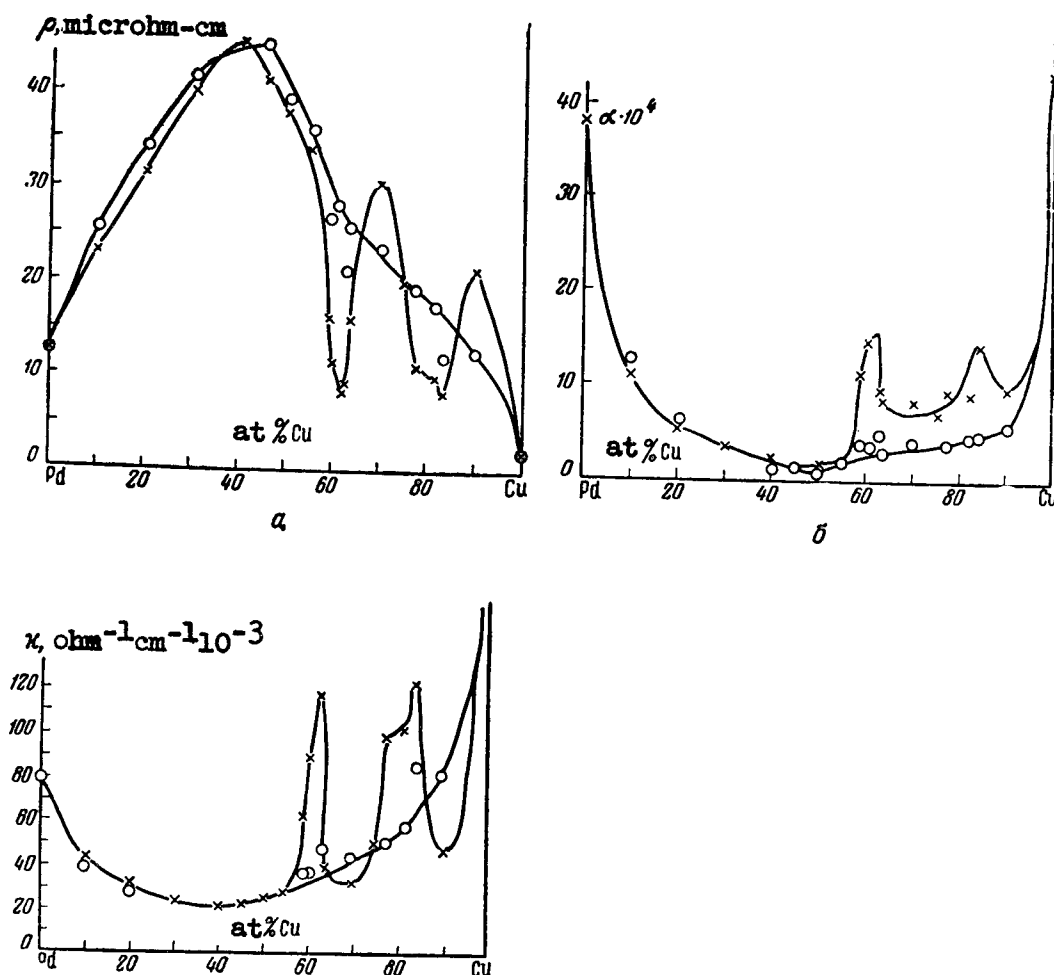
Fig. 135. Electric Properties of Alloys of Palladium with Copper:

× -- annealed;   O -- quenched.

Investigations made by Koster /186/ on the modulus of elasticity of an alloy with 25 atomic percent palladium, and those made by S. Sidorov /187/ on the Hall effect and on the electric resistivity of several alloys do not add anything new to the knowledge of the diagram of state.

A survey of the literature on the palladium-copper system shows that there are crystallized from the liquid state solid solu-

tions that have face-centered cubic lattices with statistically distributed atoms. Upon further cooling, an ordering of the crystal lattice occurs in the regions near 20 and 40 atomic percent palladium, followed by formation of chemical compounds whose composition has not been determined accurately.

The formulas PdCu₃ and PdCu, which are generally accepted at the present time for the chemical compounds, have been derived without sufficient foundation and are probably based on the analogy with the formulas AuCu₃ and AuCu.

Our own detailed investigation /188/, performed by the methods of differential thermal analysis, hardness, and electric resistivity with its temperature coefficient, has shown that the singular minimum points on the hardness and electric resistivity curves, and also the singular maximum points on the curve of the temperature coefficient of the electric resistivity and on the curve of the thermal analysis (Fig. 135) correspond to compositions PdCu₅ (16.67 atomic percent palladium) and Pd₃Cu₃ (37.5 atomic percent palladium). The results obtained are in good agreement with the investigations of the crystalline lattice of the alloys made by the earlier authors.

For the present investigation /68/ the author used alloys of an earlier work /188/.

The alloys located in the transformation regions were analyzed. Rolled and annealed wire was used in the experiments.

The absolute thermal emf was investigated with the aid of a potentiometer. The results of the measurements are shown in Table 49 and Fig. 136.

The curves showing the dependence of the absolute thermal emf on the temperature in the region of chemical compounds PdCu₅ and Pd₃Cu₅ consist of three branches each. One branch corresponds to a change in the thermal emf of the alloy, having an ordered crystalline structure. The second branch corresponds to the process of dissociation of the chemical compounds and is characterized by a sharp reduction in the thermal emf. The third branch, located in the region of high temperatures corresponding to the disordered state of the crystal lattice, varies smoothly towards a reduced absolute thermal emf. The curves exhibit sharp inflection points on the boundaries of the ordered and disordered states.

Fig. 137 shows two isotherms of the absolute thermal emf for alloys in the palladium-copper system. The isotherm corresponding to 700° C, which lies near the transformation points, has a deep smooth minimum at 55 atomic percent palladium in the region of disordered solid solution. The second isotherm, corresponding to a temperature of 300° C, lies below the transformation point and has

187

two singular maximum points, corresponding to the chemical compounds
PdCu₅ and Pd₃Cu₅.

Table 49

Absolute Thermal emf of Alloys of Copper with
Palladium, ε , microvolts/degree C

Pd		Temperature, degrees C						
atomic %	% by weight	100	200	300	400	500	600	700
0	0	+2,26	+2,79	+3,32	+3,86	+4,39	+4,93	+5,46
10,0	15,73	+1,8	+2,2	+2,5	—0,8	—4,5	—5,3	—5,7
15,93	24,12	+2,5	+3,1	+3,8	+2,9	—2,5	—7,5	—8,3
18,15	27,12	+0,5	+0,8	+2,0	+2,6	—5,0	—8,6	—10,2
22,73	33,05	0,0	—0,1	—0,5	+1,6	—7,3	—9,8	—12,2
25,0	35,87	—1,6	—2,1	—2,1	—3,0	—10,1	—12,6	—14,5
30,0	41,84	—4,8	—6,5	—8,1	—10,4	—14,0	—17,6	—21,0
36,59	49,20	—6,0	—8,6	—10,9	—13,6	—15,6	—22,6	—26,0
37,15	49,79	—3,7	—5,7	—7,7	—9,6	—12,5	—19,5	—27,2
39,81	52,62	—1,6	—3,3	—5,2	—7,5	—10,5	—14,8	—33,0
41,06	53,91	—3,1	—4,4	—5,9	—7,8	—10,5	—25,0	—30,6
45,0	57,87	—25,0	—30,7	—35,4	—39,1	—42,5	—45,6	—48,2
50,0	62,66	—28,6	—34,6	—39,8	—44,0	—47,7	—50,9	—53,7
55,0	67,25	—27,8	—35,0	—40,5	—44,8	—48,8	—52,2	—54,8
60,0	71,58	—23,8	—31,4	—36,9	—41,7	—45,7	—49,0	—52,0
70,0	79,67	—21,2	—28,2	—34,0	—39,1	—43,9	—47,9	—51,1
80,0	87,04	—17,7	—23,3	—28,0	—32,2	—36,4	—40,2	—43,5
90,0	93,79	—16,1	—20,7	—24,6	—28,5	—32,0	—35,5	—38,6
100	100	—12,81	—15,91	—18,90	—21,83	—24,75	—27,68	—30,60

Table 50 shows the temperatures of the beginning and end
of the transformations, and also the values of the thermal emf's at
these points.

Fig. 138 shows the diagram of state of the palladium-copper
system. The liquidus and solidus curves are plotted from Ruer's
data /155/. The transformation temperatures in the solid state are
taken from Table 50. These values differ somewhat from the values
obtained by V. A. Nemilov, A. A. Rudnitskiy, and R. S. Polyakova
/188/ from thermal-analysis data. The small difference in the values
is explained by the fact that the measurements of the thermal emf
were carried out in the equilibrium state of the alloys, while in
the earlier work the thermal-analysis was carried out during heating.
In the latter case it is possible for a certain lag in the ordering
of the crystal lattice to occur, and greater measurement errors are
probable.

Investigations of the thermoelectric properties of alloys of palladium with copper confirm fully the existence of these chemical compounds and are in full agreement with the x-ray investigations of Borelius, Johansson and Line /178/ and Jones and Sykes /185/.

The changeover from the ordered state $PdCu_5$ and Pd_3Cu_5 to the disordered solid solution proceeds at a constant temperature and is accompanied by a jump-like change in the absolute thermal emf. Thus, in both cases one observes typical first-order transitions.

The application of the thermal emf method to the study of the diagrams of state made it possible to fix more exactly the regions of ordered phases, which are the basis of the compounds $PdCu_5$ and Pd_3Cu_5.

At temperatures above the transformation point there is a region of a continuous series of solid solutions between components having thermoelectric properties of different signs, i.e., between the electronic conductor palladium and the copper, which has a "hole" conductivity. As in the preceding cases, the absolute thermal emf variation has a deep minimum in the palladium-gold and palladium-silver system.
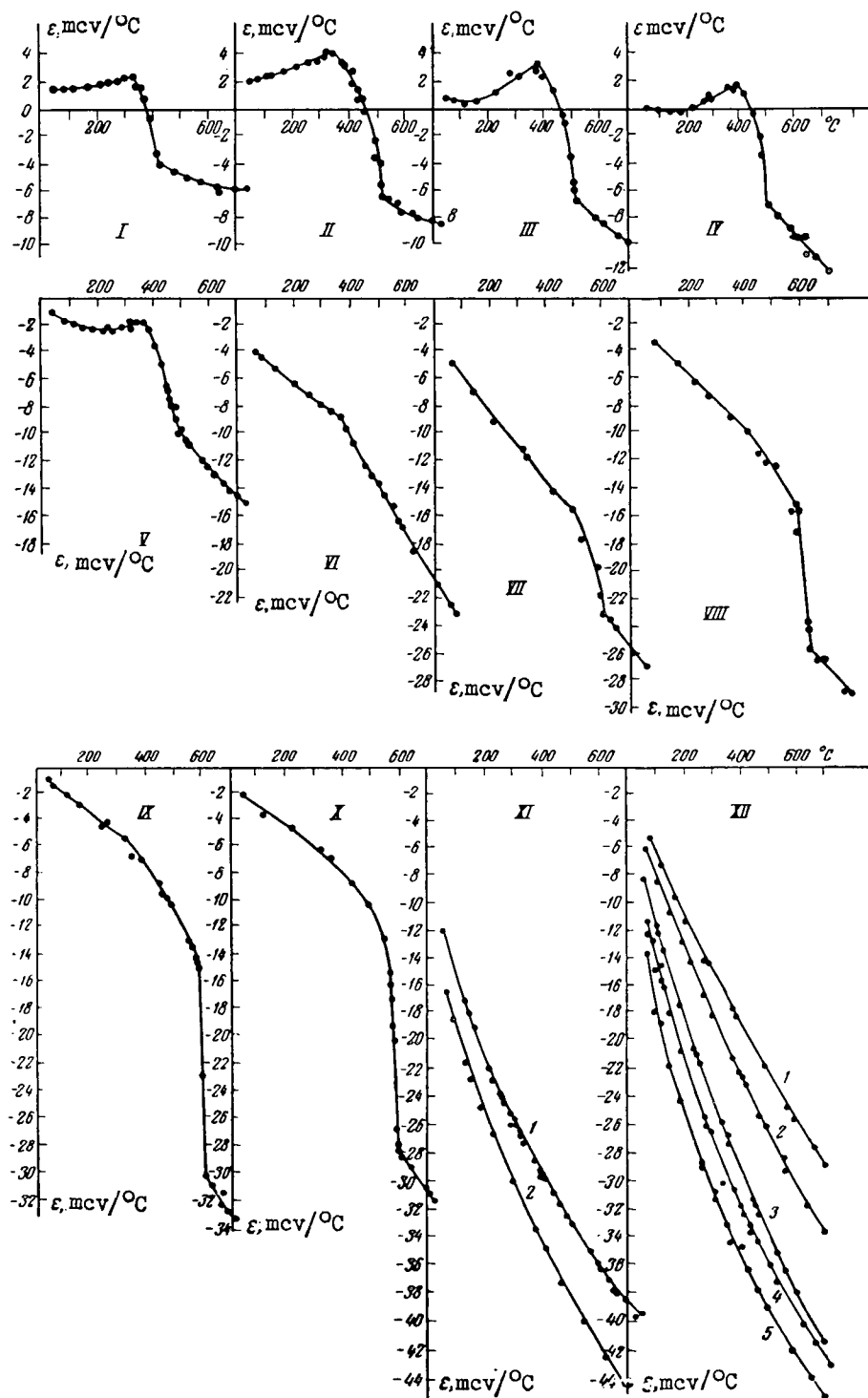
Fig. 136. Absolute Thermal emf of Alloys of Palladium
with Copper. Atomic Percentage of Palladium:

I -- 10%, II -- 15.96%, III -- 18.15%,
IV -- 22.73%, V -- 25%, VI -- 30%, VII -- 36.59%,
VIII -- 37.15%, IX -- 39.81%, X -- 41.06%, XI:
1 -- 45%, 2 -- 50%; XII: 1 -- 90%, 2 -- 80%,
3 -- 70%, 4 -- 60%, 5 -- 55%.

Table 50

Palladium, atomic %	Transformation temperature		ε during the transformation process, microvolts/degree C	
	start	finish	start	finish
10,0	425	330	— 2,7	+ 2,6
15,93	525	370	— 6,4	+ 4,2
18,15	515	385	— 6,8	+ 3,2
22,73	500	400	— 7,8	+ 1,6
25,0	490	365	—11,5	— 1,6
30,0	550	370	—15,3	— 9,1
36,59	600	495	—22,6	—15,5
37,15	630	580	—25,4	—15,2
39,81	625	600	—30,4	—14,8
41,06	610	570	—28,0	—13,5
45,0	405	320	—39,2	— 36,0
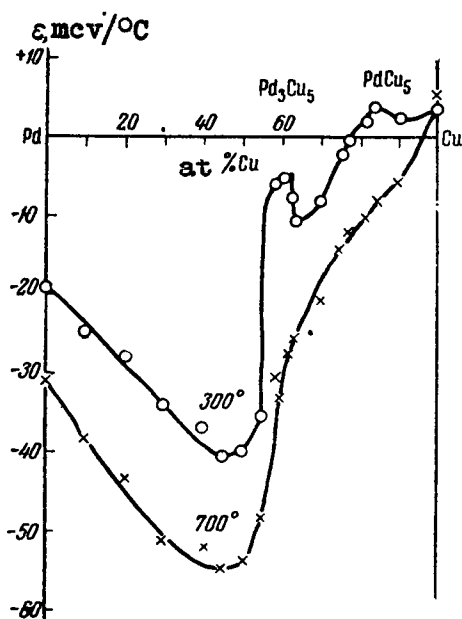
Fig. 137. Isotherms of the Absolute Thermal emf of Alloys of Palladium with Copper.
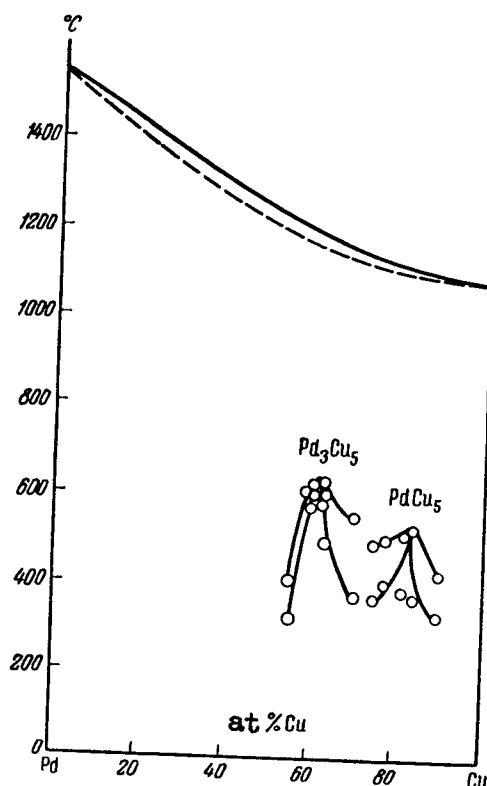
Fig. 138.   Diagram of State of the Palladium-
Copper System.

10. PLATINUM-COPPER

The first systematic investigation of alloys of platinum with
copper was made in 1907 by Doerinckel [160], who used the method of
thermal analysis and microstructure and concluded that there exists
a continuous series of solid solutions.

Sedstrom [113] investigated the electric conductivity, the
thermal conductivity, and the thermal emf of alloys of platinum
with copper and suggested that the conductivity of solid solutions
experiences an interruption at 10 to 20 atomic percent of platinum.

Johansson and Linde [177], who studied the electric resis-
tivity and the lattice structure of alloys of platinum with copper
have found that alloys quenched at a temperature close to the
melting point have a face-centered cubic structure with a statisti-
cal distribution of the atoms in the lattice. In the annealed state,

192

the authors found three different phases. In the vicinity of 10 to 26 atomic percent of platinum, a phase was found having a face-centered cubic lattice and an ordered arrangement of the atoms. In the region of 40 to 55 atomic percent of platinum, an ordered rhombohedric distorted lattice was established. In the vicinity near 60 to 80 atomic percent platinum the authors observed a cubic face-centered lattice with ordered arrangement with the atoms and double the lattice parameter of the pure metal. Although they carried out a detailed investigation, the authors drew no conclusions concerning the diagram of state.

N. S. Kurnakov and V. A. Nemilov $\underline{/189/}$ made a detailed investigation of the platinum-copper system by methods of thermal analysis, microstructure, hardness, electric resistivity and its temperature coefficient. On the basis of their investigations the authors have reached the conclusion that there exists a continuous series of solid solutions, formed when the alloys harden.

When the temperature drops to near 800° C, a chemical compound PtCu is formed. The authors indicate that there is a break in the continuity of the solid solutions in the region of 20 to 25 atomic percent platinum. Since the singular points on the curves for the electric resistivity, the temperature coefficient, and the hardness do not correspond to any composition of the form $PtCu_3$ or $PtCu_4$, the authors conclude that there are no compounds in this region.

Linde $\underline{/190/}$, after making an x-ray investigation of the platinum-copper system, found that in the vicinity of 25 atomic percent platinum there is observed an ordered phase $PtCu_3$, which has a same face-centered cubic lattice as $AuCu_3$. Two different structures have been established for the phase PtCu. In the vicinity of 40 go 63 atomic percent platinum there is located a trigonal phase, designated by the authors as PtCu I. Above 63 atomic percent platinum, new lines are added to the superstructure lines PtCu I. The authors ascribe these lines to the phase PtCu II and which they consider as a phase of PtCu I, in which a portion of the copper atoms is replaced by platinum atmos.

F. Weibke and H. Matthes $\underline{/191/}$ investigated in very great detail the emf of alloys in fused salts at high temperature. On the basis of their investigations, the authors have calculated the thermodynamic quantities and found the maximum of the heat of transformation for alloys with 50 and 20 atomic percent platinum. However it is quite difficult to draw any conclusion concerning the position of the singular points in the diagram, since no chemical analysis of the alloys was performed.

An x-ray investigation was made by Schneider and Esch $\underline{/192/}$, who also studied the electric resistivity of alloys at high tempera-

ture. On the electric-conductivity curves they observed sharp maximum at 22.5, 50, 72.5, 86 atomic percent platinum. They found the maximum of transformation temperatures at 20 and 50 atomic percent platinum. At 50 atomic percent platinum there was observed an ordered phase with a rhombohedrically distorted lattice, which gradually changed into a cubic face-centered lattice as the composition varied. With increase in content of platinum, the intensitivity of superstructural lines decreased. At 72.5 atomic percent platinum the intensitivity of the superstructure lines again increased and new lines appeared. At 86 atomic % platinum the superstructure lines were not observed. The authors have included from their investigations that at high temperatures one observes a continuous series of solid solutions. Considering the chemical compound $PtCu_3$ (25 atomic percent platinum), they observed a region of ordering with a maximum of ordering at 20 atomic percent platinum and temperatures below 645 degrees C. The transformation took place without changing the symmetry of the lattice. As they analyzed the composition of the compounds, the authors have encountered contradictions, although they do not mention these. In the region from 30 to 90 atomic percent platinum the maximum of the critical temperature lies at 812° C and composition of 50 atomic percent platinum. The transformation proceeds with a change in the type of the lattice. The authors propose the existence of a third chemical compound Pt_7Cu (87.5 atomic percent platinum), although no superstructure lines have been observed for this composition. Thus, the ideas concerning this chemical compound are not well founded.

No conclusions can be drawn concerning the exact position of the singular points on the diagram, since the authors did not carry out any chemical analysis.

Concerning the earlier works, it is possible to conclude that alloys of platinum with copper crystallize with formation of a continuous series of solid solutions and with a statistical arrangement of the atoms in a cubic face-centered lattice. During cooling there occurs a transformation that is accompanied by an ordering of the crystallized lattice and formation of the chemical compound PtCu, which has a rhombohedric distorted lattice. In the vicinity of 20 to 25 atomic percent platinum one observes a second transformation not connected with the change in the symmetry of the lattice. The face-centered cubic lattice with statistical distribution of the atoms goes into an ordered state without change in the symmetry of the lattice, with formation of a chemical compound whose composition is determined with insufficient accuracy. Although it is indicated in the works of the preceeding authors that the compound is $PtCu_3$, yet according to the data of Weibke and Matthes [191] and Schneider and Esch [192] one can suggest the existence of a compound $PtCu_4$.

In order to determine more accurately the nature of the chemical interaction of the component, we have studied the electrical

194

and thermodynamic properties of the alloys.

The alloys were prepared from spongy refined platinum and electrolytic copper.

The alloys were melted in a high-frequency furnace in corundise crucibles under a borax slag, were drawn into porcelain tubes, and were rolled in the quenched state at 900° C into a square wire 1.2 x 1.2 mm.

To investigate the electric resistivity and the thermal emf, the wires were annealed in vacuum at 600° C for seven days and were cooled gradually for an equal length of time.

All alloys were analyzed and the contents of the platinum was determined experimentally while the content of copper was calculated as the difference. The electric resistivity was measured with the aid of a potentiometer. The measurements were carried out at 25 and 100° C.
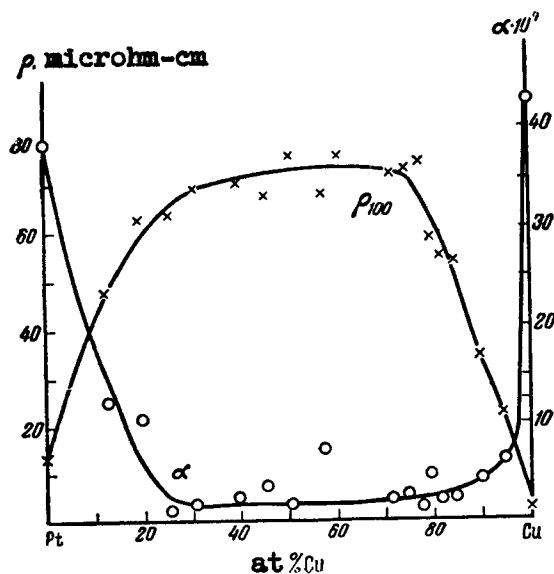
Fig. 139. Specific Resistivity and its temperature Coefficient for Hardened Alloys of Copper with Platinum.

The electrical properties were measured for alloys in the annealed and quenched state. The alloys were quenched from 900° C in cold water. The values of the specific electric resistivity, ρ, its temperature coefficient, $\alpha \times 10^4$, and of the specific electric resistivity $\times$ are given in Table 15 for alloys of platinum with copper.

195
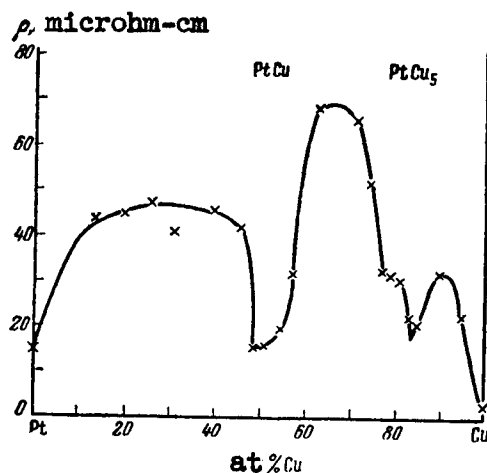
Fig. 140. Specific Electric Resistivity
of Annealed Alloys of Platinum
with Copper.

Fig. 139 shows curves of the specific electric resistivity
at 100° C and of the temperature coefficient for quenched alloys.
The curves are characteristic of a continuous series of solid solu-
tions. The specific-resistivity curve is smooth and has a gentle
maximum, while the temperature coefficient curve is smooth and has
a gentle minimum.

Fig. 140 shows the curve of the specific electric resistivity
of annealed alloys. It has three maxima and two minima. The minima
lie in the regions of the compositions of 50 and 67 atomic percent
platinum, and obviously correspond to the chemical compositions PtCu
and $PtCu_5$.

For the specific electricity resistivity of annealed alloys
we obtain an atribate curve (Fig. 141) with two singular maxima cor-
responding to the chemical compounds PtCu and $PtCu_5$.

The curves of the temperature coefficient of electric resis-
tivity, shown in Fig. 142, are similar to the curves of the electric
conductivity and have singular maximum corresponding to the chemical
compounds PtCu and $PtCu_5$.

An investigation of the absolute thermal emf was carried out
with the aid of the Kurnakov pyrometer. Sample curves recorded on
the pyrometer for the alloys PtCu and $PtCu_5$ are shown in Figs. 20
and 21. In order to check the obtained results, certain measurements
were monitored with the aid of a potentiometer. The results of both

196

methods are in agreement, with sufficient accuracy.

<div align="center">Table 51</div>

<div align="center">Electric Properties of Alloys of Platinum with Copper</div>

Pt, aт. %	Annealed					Quenched				
	ρ_{25}, microhm-cm	x_{25}, $\Omega^{-1}\text{cm}^{-1}$ $\times 10^{-3}$	ρ_{100}, microhm-cm	x_{100}, $\Omega^{-1}\text{cm}^{-1}$ $\times 10^{-3}$	$\alpha \times 10^4$	ρ_{25}, microhm-cm	x_{25}, $\Omega^{-1}\text{cm}^{-1}$ $\times 10^{-3}$	ρ_{100}, microhm-cm	x_{100}, $\Omega^{-1}\text{cm}^{-1}$ $\times 10^{-3}$	$\alpha \times 10^4$
5,39	22,04	45,4	22,82	43,8	4,81	21,10	47,4	22,36	44,3	6,35
10,62	31,08	32,2	32,30	31,0	5,79	32,97	30,35	33,99	29,42	4,45
15,45	19,12	52,3	20,08	49,8	6,82	52,75	18,97	53,84	18,6	2,50
17,21	20,76	51,8	21,86	45,8	7,51	—	—	—	—	—
18,81	28,01	35,7	30,00	33,3	7,56	53,38	18,76	54,28	18,42	2,26
20,17	30,01	33,3	31,78	31,5	7,87	56,53	17,67	58,22	17,19	4,81
22,70	30,67	32,6	31,98	31,3	5,74	72,75	13,75	73,43	13,64	1,23
25,20	49,96	20,03	51,69	19,33	3,43	71,41	14,02	72,42	13,83	2,64
28,61	65,23	15,33	65,34	15,3	0,23	70,37	14,22	71,24	14,04	2,31
37,95	66,94	14,95	68,71	14,55	1,50	—	—	—	—	—
42,99	30,40	32,9	31,81	31,4	4,98	66,21	15,1	67,21	14,9	7,08
45,39	18,34	54,5	19,27	51,95	10,13	—	—	—	—	—
49,72	14,24	70,2	15,61	64,0	13,35	74,24	13,47	75,22	13,30	1,74
51,83	13,68	73,1	15,09	66,4	18,50	—	—	—	—	—
54,22	39,71	25,2	41,79	23,95	6,79	65,20	15,34	67,08	14,90	3,89
60,44	44,17	22,65	45,96	21,80	5,49	69,15	14,45	69,96	14,30	2,49
69,60	39,30	25,45	40,86	24,5	5,48	68,13	14,67	68,98	14,5	1,64
74,35	45,62	21,9	47,06	21,23	4,43	63,57	15,71	63,77	15,69	0,72
80,17	42,87	23,3	44,40	22,57	4,76	56,95	17,6	62,65	15,97	10,85
87,26	41,73	24,0	43,48	23,02	5,68	44,10	22,7	48,04	20,8	12,44

The values of the absolute thermal emf are given in Table 52 and in Fig. 142.

From the curves, it is clear that the process of disordering is different for the chemical compounds PtCu and PtCu$_5$.

For the compound PtCu the disordering takes place within a certain temperature range and is accompanied by an increase in the absolute thermal emf. The beginning of a noticeable disordering lies approximately in the region of minimum of the curve of the absolute thermal emf vs. temperature. This minimum is at a constant tempera-

ture near 700° C for many alloys in the region from 43 to 52 atomic percent platinum.

The curves consist of two branches. In the region of the ordered phase the thermal emf diminishes gradually with increasing temperature, reaches a smooth minimum near 700° C, and then rises rapidly. At the point of complete disorder one observes a kink in the curve. Above this point the absolute thermal emf varies linearly.

The curves of the absolute thermal emf vs. temperature have a different character in the vicinity of the chemical compound $PtCu_5$. For alloys with 13 to 20 atomic percent platinum each curve consists of 4 branches. From room temperature to 450° C we have a curve corresponding to the stable state of the $PtCu_5$ compounds. At 450° C the curves have a kink, connected most probably with the transition of the compound into a different modification; with increasing temperature the curves have a second kink, connected with the transition of the chemical compound $PtCu_5$ into a disordered solid solution and accompanied by a jump-like decrease in the absolute thermal emf. At high temperatures the fourth branch of the curve corresponds to a disordered solid solution.

On the basis of the results obtained, we plotted the isotherms of the absolute thermal emf (Fig. 144). The isotherms of the absolute thermal emf increase from pure platinum, assume the form of an arch, and drop smoothly towards the chemical compound PtCu.
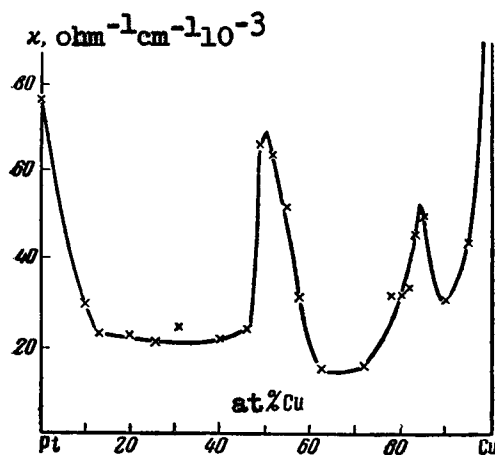
Fig. 141. Specific Electric Conductivity of Annealed Alloys of Platinum with copper.
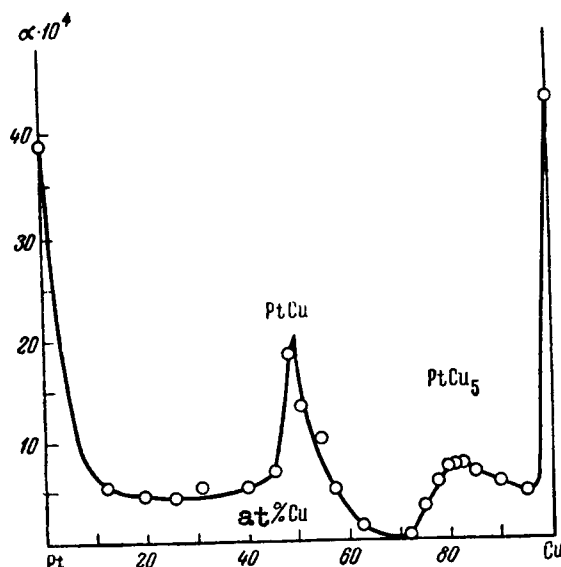
Fig. 142. Temperature Coefficient of Electric
Resistivity of Annealed Alloys of Platinum
with Copper.

A minimum is observed at the singular point corresponding to
the PtCu compound.

The boundaries of the existence of the PtCu phase are charac-
terized by bends on the isotherms (near 60 atomic percent copper)
which, passing through a smooth minimum, rise towards a chemical
compound PtCu$_5$.

A weak bending of the isotherms is observed at the singular
point of PtCu$_5$. The isotherms then rise to the limits of the ordered
phase.

The region between the ordered phase of PtCu$_5$ and the disor-
dered solid solution is characterized by a sharp decrease in the iso-
therms.

The sharp maximum of the isotherms of the absolute thermal
emf corresponds to the boundary of the ordered phase of PtCu$_5$, while
the sharp minimum corresponds to the boundary of the disordered solid
solution. The regions of the transion of the PtCu$_5$ phase into a dis-
ordered solid solution are marked on Fig. 144 by shaded rectangles.
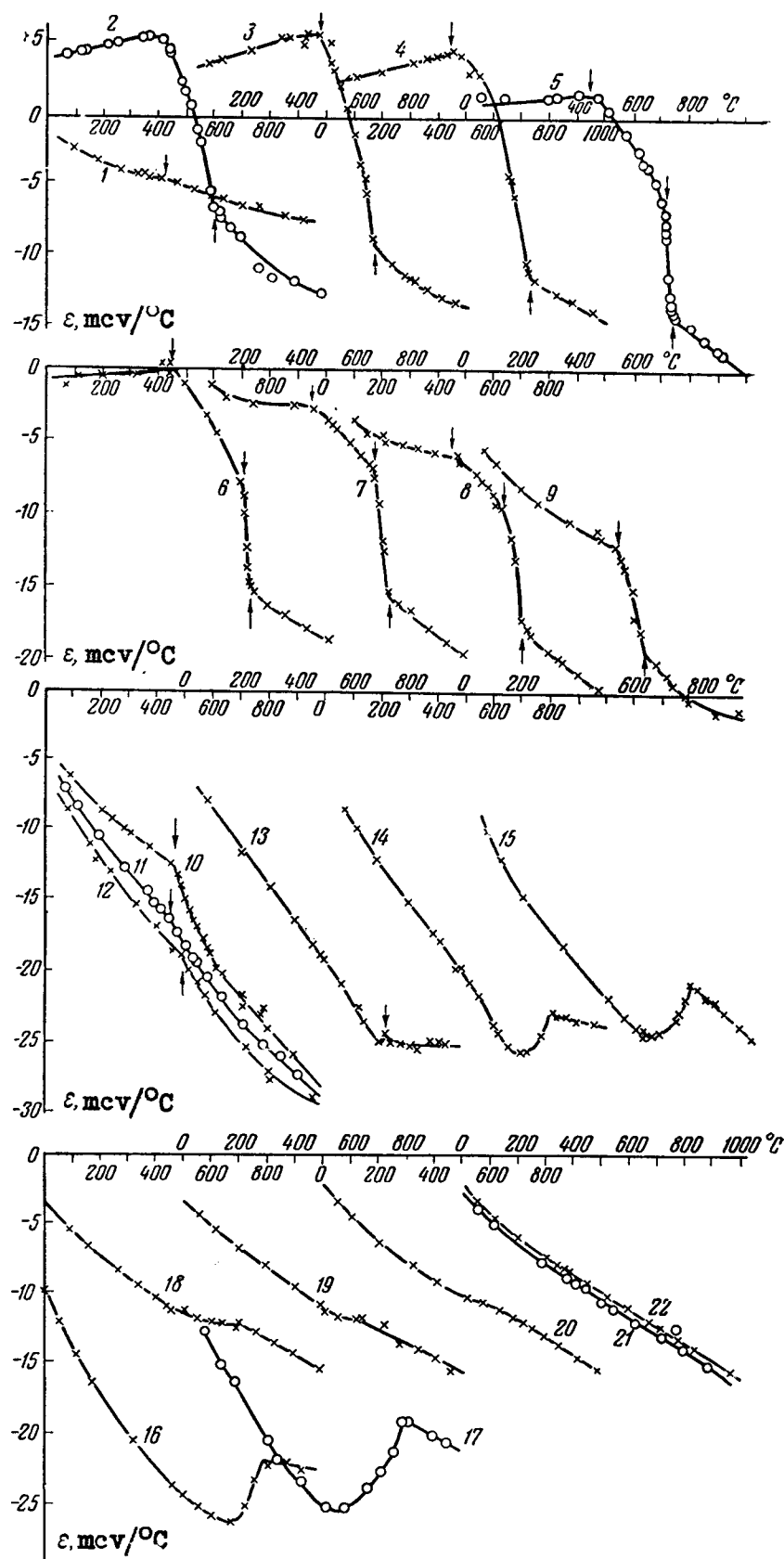
Fig. 143. Absolute Thermal emf of Alloys of Platinum with Copper.

(note: at. % = atomic %)

1 — 5,59 ar. % Pt; *2* — 8 ar. % Pt; *3* — 10,62 ar. % Pt; *4* — 13,09 ar. % Pt; *5* — 15,45 ar. % Pt;
6 — 17,21 ar. % Pt; *7* — 18,81 ar. % Pt; *8* — 20,17 ar. % Pt; *9* — 22,70 ar. % Pt; *10* —
25,20 ar. % Pt; *11* — 28,61 ar. % Pt; *12* — 37,95 ar. % Pt; *13* — 42,99 ar. % Pt; *14* — 45,39 ar. % Pt;
15 — 49,72 ar. % Pt; *16* — 51,83 ar. % Pt; *17* — 54,22 ar. % Pt; *18* — 60,44 ar. % Pt;
19 — 69,60 ar. % Pt; *20* — 74,35 ar. % Pt; *21* — 87,26 ar. % Pt; *22* — 80,17 ar. % Pt;

200

The isotherms at 1000° C correspond to a disordered solution and represent a smooth curve, recalling a sine wave with one maximum and one minimum. However, as the results of an insufficiently complete equilibrium and incomplete dissociation of the compounds in the region near 50 and 85 atomic percent copper, bends are observed near these regions.

Table 52

Absolute Thermal emf of Alloys of Platinum with Copper, ε, microvolt/°C.

Cu atomic %	% by weight	Temperature, °C
		100	200	300	400	500	600	700	800	900	1000
94,61	85,20	—2,7	—3,7	—4,3	—4,6	—5,2	—5,9	—6,4	—6,9	—7,3	—7,6
92,00	78,90	+4,2	+4,7	+5,2	+5,4	+1,6	—6,7	—8,8	—10,6	—12,0	—12,7
89,38	73,26	+3,5	+4,3	+5,1	+5,6	+4,8	—1,0	—10,4	—11,4	—12,5	—13,6
86,91	68,21	+2,7	+3,3	+3,8	+4,4	+4,4	+1,1	—8,5	—12,1	—13,0	—14,0
84,55	64,29	+1,2	+1,4	+1,6	+1,8	+1,0	—1,7	—5,7	—14,7	—16,1	—17,4
82,79	61,03	—0,4	—0,25	—0,15	0,0	—0,9	—4,0	—8,0	—16,2	—17,2	—18,2
81,19	58,43	—1,4	—2,0	—2,2	—2,4	—3,1	—4,8	—10,0	—16,3	—17,9	—19,4
79,83	56,31	—3,9	—4,4	—4,9	—5,4	—6,0	—8,2	—16,8	—19,0	—20,5	—22,0
77,30	52,69	—6,0	—7,8	—9,0	—10,2	—11,2	—15,6	—20,3	—22,0	—22,8	—23,4
74,80	49,15	—6,3	—8,5	—10,3	—11,8	—14,5	—18,6	—21,6	—23,7	—25,7	—27,9
71,39	44,83	—8,0	—10,5	—13,0	—15,3	—18,0	—20,8	—23,3	—25,2	—26,8	—28,4
62,05	34,74	—9,1	—12,0	—14,6	—17,0	—18,8	—22,4	—25,0	—26,8	—28,0	—28,9
57,01	30,16	—8,3	—11,0	—13,6	—16,2	—18,9	—21,8	—24,6	—24,8	—24,8	—24,8
54,61	28,15	—9,2	—12,2	—14,8	—17,0	—19,8	—22,7	—25,3	—23,0	—22,9	—23,4
50,28	24,77	—10,5	—13,8	—16,4	—18,8	—20,9	—23,0	—23,9	—21,5	—21,6	—23,4
48,17	23,25	—13,6	—16,6	—19,6	—22,0	—24,0	—25,5	—26,2	—22,4	—22,2	—22,6
45,78	21,56	—12,1	—15,7	—18,5	—20,9	—23,2	—23,8	—22,3	—18,8	—19,9	—21,0
39,56	17,57	—5,6	—7,4	—8,9	—10,2	—11,4	—12,1	—12,3	—13,2	—14,2	—15,4
30,40	12,45	—5,2	—6,7	—8,1	—9,5	—10,9	—11,8	—12,5	—13,4	—14,4	—15,4
25,65	10,10	—4,4	—6,2	—7,6	—8,9	—10,0	—10,6	—11,8	—12,9	—14,1	—15,3
19,83	7,45	—4,1	—5,8	—7,2	—8,4	—9,6	—10,8	—12,0	—13,2	—14,4	—15,6
12,74	4,53	—4,5	—6,2	—7,7	—8,9	—10,1	—11,4	—12,5	—13,7	—15,0	—16,4

From the absolute thermal emf vs. temperature curves we determine the regions of existence of the phases PtCu and PtCu$_5$.

Table 53 gives the temperatures of the transformations of the alloys and the corresponding values of the absolute thermal emf.

The diagram of state of platinum-copper is shown in Fig. 145. The solidus and liquidus curves are drawn from data of N. S. Kurnakov

and V. S. Nemilov [189].

Upon cooling of the solid solutions there is formed, in the region of the diagram corresponding to a content of 26 to 62 atomic percent copper, an ordered phase with a rhombohedric disorted lattice, according to Johansson and Linde [177], which is based on the chemical composition PtCu.

The existence of a chemical compound PtCu is proved by the presence of singular maximum points on the curves of the electric conductivity (Fig. 141) and of the temperature coefficient of electric resistivity (Fig. 142), and the presence of a singular minimum point on the curve of specific electric resistivity (see Fig. 140) and singular points on the isotherms of the absolute thermal emf (see Fig. 144).

Upon heating above 700° C, a noticeable disordering of the chemical compound PtCu begins. This process is accompanied by an increase in the absolute thermal emf (see Fig. 143). The temperature of complete disordering corresponds to the kink in the curves of the absolute thermal emf.

Thus, the process of disordering of the PtCu compound occurs within a certain temperature interval, and is therefore a second-order transition.

We calculated the Thomson emf for an alloy containing 49.72 atomic percent platinum. Its values as functions of the temperature are as follows:

t, °C.....100 200 300 400 500 600 700 750 800 900 1000

......−12,6 −14,4 −15,5 −15,9 −15,8 −14,8 0 +29,0 +80,0 +21,1 +22,9

σ , microvolt/°C

Fig. 146 shows the curve of the Thomson emf of the PtCu compound. It is obvious that for other alloys of this region one can obtain similar curves.

The shape of the Thomson emf curve, which recalls the Greek letter λ , is a characteristic of the specific heat in a second-ordered transition. Obviously the specific heat of the current carriers behaves like the specific heat of a metal in a second-order transition.

The region of the phase which is based on the chemical compound PtCu occupies the portion of the diagram corresponding to a content of 38 to 75 atomic percent platinum. The maximum the transformation temperature, 820° C, occurs for a composition with 50 atomic

percent platinum.
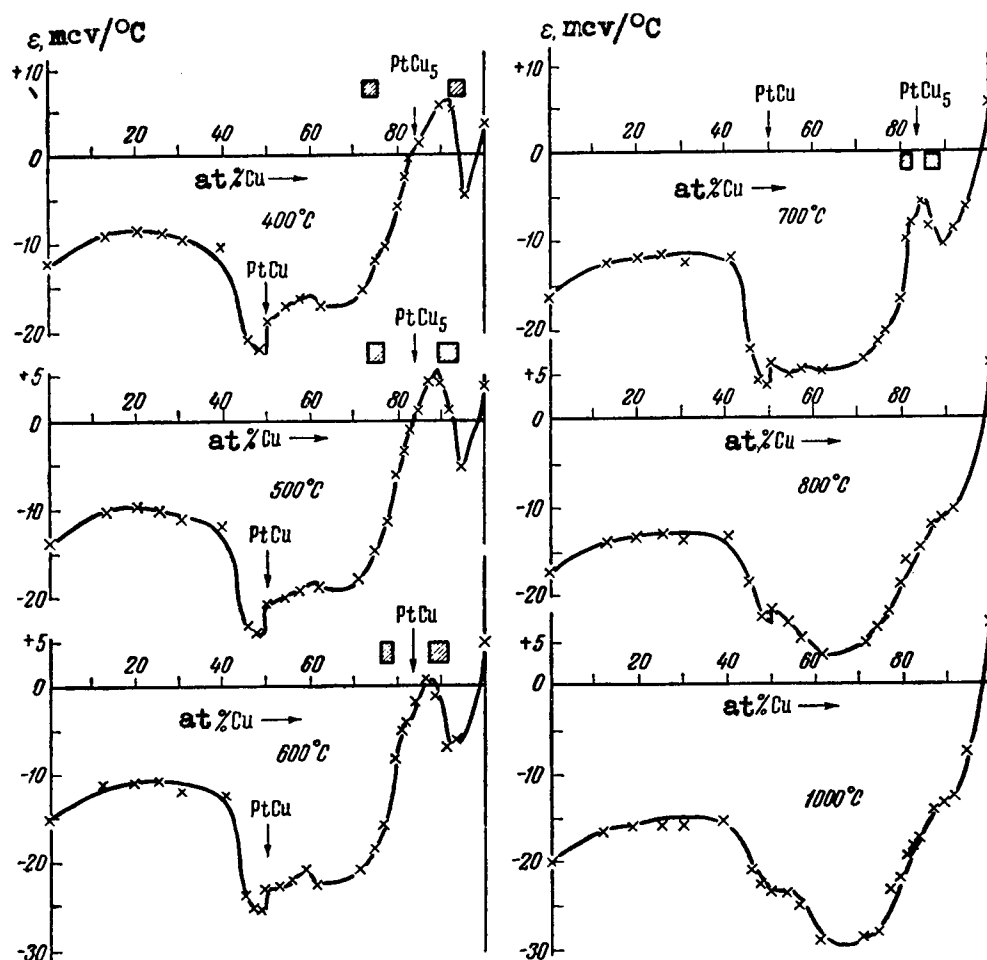
Fig. 144.   Isotherms of the Absolute Thermal emf of
Alloys of Platinum with Copper.

Upon cooling of solid solutions in the vicinity of the dia-
gram, corresponding to a content of 70 to 90 atomic percent copper,
an ordered phase is formed with a cubic face-centered lattice, ac-
cording to C. Johansson and J. Linde /177/. This phase is based on
the chemical compound PtCu$_5$, the existence of which is proved by the
presence of singular maximum points on the curves of electric con-
ductivity (see Fig. 141) and of the temperature coefficient of elec-
tric resistivity (see Fig. 142), and of a singular minimum point on
the curve of specific resistivity (see Fig. 140).

Table 53

Transformations in the Solid State of Platinum with
Copper

Pt, atomic %	First stage		Second stage		Third stage	
	t, °C	ε microvolt/°C	t, °C	ε microvolt/°C	t, °C	ε microvolt/°C
PtCu₅						
5,39	430	—4,7	—	—	—	—
8,00	600	—6,7	415	+5,3	—	—
10,62	675	—9,2	480	+5,6	—	—
13,09	728	—11,4	610	+0,5	450	+4,7
15,45	735	—13,4	715	—6,6	450	+1,8
17,21	730	—14,6	710	—8,4	450	0
18,81	720	—14,8	675	—6,4	450	—2,4
20,17	700	—16,8	635	—9,0	450	—5,6
22,70	620	—18,4	540	—11,6	—	—
25,20	470	—12,7	—	—	—	—
28,61	455	—16,4	—	—	—	—
PtCu						
37,95	505	—18,9	—	—	—	—
42,99	725	—24,6	700	—24,0	—	—
45,39	810	—22,4	700	—25,3	—	—
49,72	820	—20,2	700	—24,0	—	—
51,83	810	—21,9	700	—26,2	—	—
54,22	800	—18,8	570	—24,2	—	—
60,44	710	—12,2	—	—	—	—
69,60	630	—11,8	—	—	—	—
74,35	600	—10,6	—	—	—	—

On the isotherms of the absolute thermal emf the singular
point is then expressed by a change in the direction of the course
of the curves. Singular points of similar type were considered by
N. S. Kurnakov /193/, using as an example the isotherms of the in-
ternal friction is a water-acetic acid system.

As the temperature rises near 450° C there occurs in the alloys

of this region a transformation that is mostly likely connected with
transitions of the compound to a different modification. This trans-
formation is accompanied by a bend on the curve of the absolute ther-
mal emf vs. temperature (see Fig. 143). The process of disordering
of the chemical compound $PtCu_5$ occurs at a constant temperature and
is accompanied by a jumplike change in the absolute thermal emf.
For alloys that differ in composition from the chemical compound,
the disordering process occurs in the temperature interval which is
on the diagram of state (see Fig. 145) by the descending curves on
both sides of the chemical compound. The maximum of transformation
temperature, 736° C, belongs to the composition with 83.33 atomic
percent copper and 16.67 atomic percent platinum, corresponding to
the chemical $PtCu_5$.
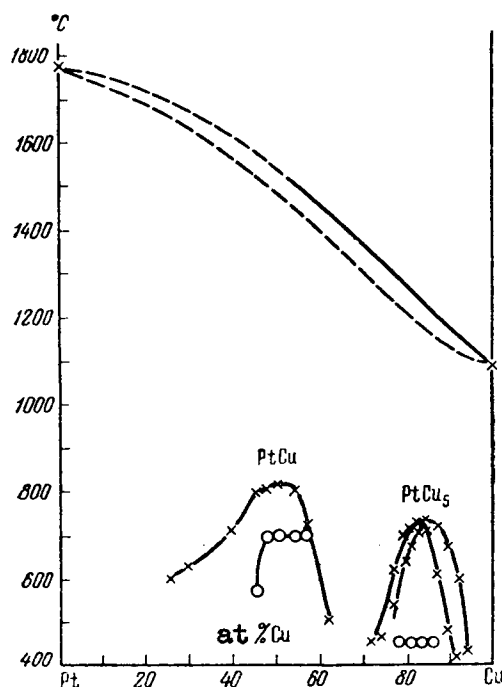
Fig. 145. State Diagram of the Platinum-
Copper System.

The Thomson emf was calculated for the alloy located in the
direct vicinity of the chemical compound (17.21 atomic percent pla-
tinum) and was found to have the following values as a function of
the temperature (Fig. 147):

t, °C . . .	100	200	300	400	500	600	700	800	900	1000
σ , micro-volts/°C..	0,37	0,47	0,57	0,67	—20,1	—30,5	—42,0	—12,9	—14,1	—15,3
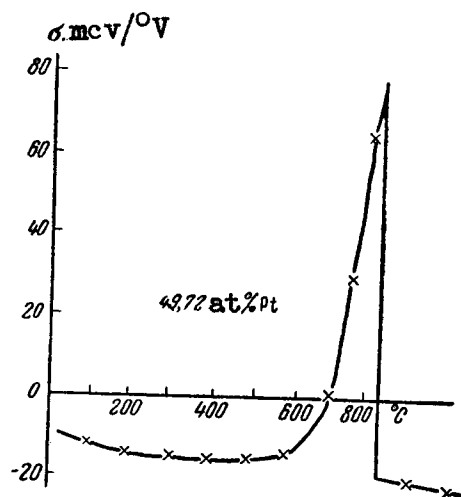
Fig. 146.   Thomson emf of the Compound
            PtCu.
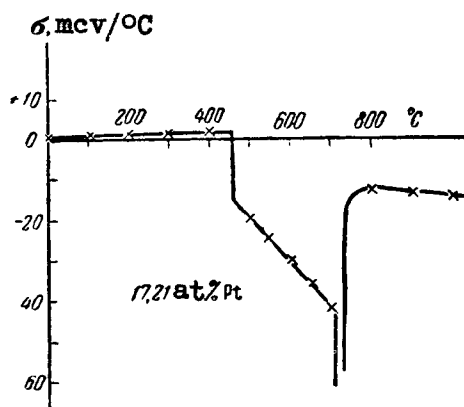
Fig. 147.   Thomson emf of the Compound
            PtCu₅.

At the 450° C transformation point the Thomson emf changes
abruptly. The process of disordering at 736° C, which occurs for
the chemical compound PtCu₅ at a constant temperature, is accompanied
by a discontinuity in the curve of the Thomson emf, which assumes
there a value of —∞ . The transformation occurs at a constant
temperature and is a typical first-order transformation.

An investigation of the electric and thermoelectric proper-

ties of alloys of platinum with copper has confirmed the formation of a continuous series of solid solutions in the platinum-copper system.

The chemical compound PtCu, established by N.S. Kurnakov and V.A. Nemilov /189/ is confirmed by the present investigation. The existence of the chemical compound $PtCu_5$ is proven for the first time.

The application of the thermoelectric method to an investigation of alloys has made it possible to determine the phase regions of the existence of the chemical compounds PtCu and $PtCu_5$ and to recognize the character of the disordering of the crystalline lattice. It was shown thereby that the disordering process of the chemical compound PtCu is a second-order transition, while the disordering of the chemical compound $PtCu_5$ is a first-order transition.

The existence of chemical compounds $PtCu_3$ and Pt_7Cu, established by Linde /190/ and Schneider and Esch /192/, has not been confirmed by our experiments.

In the region of the continuous series of solid solutions between the thermoelectrically negative platinum and the thermoelectrically positive copper (see Fig. 144, isotherm at 1000° C), the curve of the absolute thermal emf recalls a sine wave.

11. CONCLUSIONS

In this chapter we have considered nine binary alloys systems made up of metals that have an identical structure of the crystalline face-centered cubic lattice.

Continuous series of solid solutions are formed over the entire length of the diagram of state in the gold-silver and the platinum-palladium systems.

Up to recently it was believed that in palladium-silver and palladium-gold systems there are formed continuous series of solid solutions at all temperatures at which solid phases exist. However, an investigation of the Thomson emf and of the temperature coefficient has shown that the solid solutions cannot be considered continuous in these systems.

In the platinum-silver and platinum-gold systems the solubility of the components in the solid state is limited.

In the palladium-rhodium system the continuous series of solid solutions become discontinuous when the temperature is de-

creased as a result of a change in the structure of the crystalline lattice of rhodium.

In the palladium-copper and platinum-copper systems, the continuous series of solid solutions is disturbed by the formation of intermediate phases based on the chemical compounds Pd_3Cu_5, $PdCu_5$, $PtCu$, and $PtCu_5$.

Until recently it was impossible to establish the conditions that would be not only necessary but also sufficient for an unlimited mutual solubility of two metals.

On the basis of the experimental material, we have formulated the necessary but insufficient conditions for total mutual solubility of metals.

1. Continuous series of solid solutions are formed only as solutions of the substitution type between metals that have identical structures of the crystalline lattices.

2. The atomic radii should not differ by more than 10 to 15% according to B. Hume-Rothery /1947/ and by 8 to 10% according to I.I. Kornilov /1957/.

3. The electrochemical properties of the metals should be as nearly identical as possible.

The insufficiency of these conditions for the formation of continuous series of solid solutions is obvious from the examples considered.

The maximum difference in the atomic radii of the components in the systems we investigated amounts to 8.5% for alloys of platinum with copper.

Out of the nine systems that satisfy all three solubility conditions, only two (gold-silver and platinum-palladium) form continuous series of solid solutions over the entire extent of the compositions and temperatures at which the solid phases exist.

The metals that enter into the investigated systems can be divided into two classes: electronic conductors, which have a negative thermal emf (platinum and palladium), and conductors with positive current carriers (gold, silver and copper), which have a positive thermal emf.

Rhodium occupies an intermediate place. β-rhodium is thermoelectrically negative, while α-rhodium becomes thermoelectrically positive at low temperature.

Alloys of gold with silver consist of thermoelectrically positive components. The absolute thermal emf of the alloys changes along a smooth curve with a minimum (see Fig. 65).

Alloys of platinum with palladium and of palladium with β-rhodium consist of components which are thermoelectrically negative. The absolute thermal emf of alloys changes along a smooth curve with a maximum (see Fig. 76 and 128, isotherm for 1200° C).

In the palladium-rhodium system this law is violated at temperatures below the point of polymorphous transformation of rhodium.

The palladium-gold, palladium-silver, palladium-copper, and platinum-gold systems consist of components that have different signs of the thermal emf and different types of conductivity. In these systems one does not observe a complete solubility of components over the entire extent of the diagrams of state.

The absolute thermal emf curves have minima in all five cases.

In the palladium-copper system this law is violated at low temperatures, when intermediate phases are formed based on compounds Pd_3Cu_5 and $PdCu_5$.

In the platinum-silver and platinum-copper systems, which are also formed by components having different signs of the absolute thermal emf, one observes a sinusoidal variation with a maximum and minimum (see Figs. 122 and 144). From the above cases it is possible to deduce general laws for the variation of the absolute thermal emf in binary systems.

Upon formation of solid solutions in a binary system consisting of thermoelectrically-positive metals, the curves of the absolute thermal emf vs. composition is smooth and has a minimum (gold-silver).

Upon formation of solid solutions in a binary system consisting of thermoelectrically negative metals, the absolute thermal emf, depending on the composition, has a smooth curve with a maximum (platinum-palladium and platinum- β rhodium), i.e., when two metals having the same sign of the thermal emf are alloyed, one observes a reduced value in the absolute thermal emf.

When alloying metals with different signs of the absolute thermal emf, one observes two forms of curves. The isotherms of the absolute thermal emf have deep minima (palladium-gold, palladium-silver, platinum-gold, palladium-copper) or else a sinusoidal shape (platinum-copper, platinum-silver).

A feature common to all cases of alloy formation is the drop

in the positive absolute thermal emf of a pure metal that has a hole conductivity.

Actually, when other metals are added to the thermoelectrically positive copper, silver, or gold, one observes a drop in the absolute thermal emf. Instead of the hole conductivity of the pure metal there appears the electronic conductivity of the alloy.

In the cases we have considered, the unlimited solubility over the entire extent of the existence of the solid phase occurs only in those cases, when the metals have equal signs of the absolute thermal emf (gold-silver, platinum-palladium).

Naturally, the equality of the sign of the absolute thermal emf of the components still does not determine an unlimited solubility over the entire extent of the diagram of states. Thus, for example, silver and copper, which have positive signs of the absolute thermal emf, have a limited solubility in the solid state.

If the metals have different signs of absolute thermal emf, one can expect a discontinuity in the solid solutions. In the platinum-gold, platinum-silver, palladium-gold, and palladium-silver systems which we investigated discontinuities were observed in the solid solutions with formation of mechanical mixtures.

In the platinum-copper and palladium-copper systems the continuity of the solid solutions is disturbed by the appearance of new phases based on the chemical compounds.

The Thomson emf is a very sensitive property for the observation of transformations in alloys. With the aid of calculations of the Thomson emf it was possible to establish a discontinuity in the solid solutions in the palladium-gold and palladium-silver systems.

The Thomson emf, which is the specific heat of the current carriers, has much in common with the specific heat of the metal. Upon investigation of transformations in alloys we used this property to establish second-order transformations.

The use of the thermoelectric method in the investigation of transformations in alloys gave exceedingly fruitful results.

On the basis of combining the thermoelectric method with investigations of the electric resistivity and its temperature coefficient, we established the following new chemical compounds: Pd_3Cu_5, $PdCu_5$, and $PtCu_5$. We also confirmed the existence of the previously established chemical compound PtCu.

The formation of the chemical compounds PdCu, $PdCu_3$, and $PtCu_3$ was not confirmed by this investigation.

At the singular points, which correspond to the compounds, one can observe either maxima (Pd_3Cu_5 and $PdCu_5$), minima (PtCu) and kinks ($PtCu_5$) on the curves of the absolute thermal emf vs. the composition.

The processes of disordering of the crystal lattices of chemical compounds Pd_3Cu_5, $PdCu_5$, and $PtCu_5$ represent first-order transitions, which occur at a constant temperature and which are accompanied by a jump-like reduction in the absolute thermal emf, the thermoelectric potential, and the carrier enthalpy, similar to the β-iron to γ-iron transition.

The process of disordering of the crystal lattice of the chemical compound PtCu is a second-order transition, analogous to the magnetic transformations of iron, cobalt, and nickel. The Thomson emf (See Figs. 30, 35, 38 and 146) varies in this case the same as the specific heat of the metal in second-order transitions.

In our investigations we have considered transformations that are connected with the break-up of solid solutions into two phases in the palladium-rhodium system. A study of this type of transformation involves very great difficulties, since there is no thermal effect at all at the transition point. The process of the break-up of the solid solutions upon cooling and of the inverse transition to the solid solution is naturally accompanied by a thermal effect, but this effect is distributed over the entire range of temperatures at which the two phases exist. This is why V. K. Semenchenko [79] classified such transitions as phase transitions of second-order.

The thermoelectric method shows quite clearly the critical point of the transition from the heterogeneous region to the homogeneous solid solution. Here we observe a kink on the curve of the absolute thermal emf.

The Thomson emf varies in the same manner as in all other second-order transitions (see Fig. 131). In heating one observes a rapid decrease in the Thomson emf at the transition point -- a jump-like increase. Thus, we obtain in this case curves with a sharp minimum, while in the case of ferromagnets (see Fig. 30, 35, 38) and during the process of disordering of the compound PtCu, we had a sharp maximum (see Fig. 146).

An investigation of the thermoelectric properties of alloys makes it possible to determine the difference of electric potentials between phases that are in equilibrium in the heterogeneous region of the diagram. For this purpose it is necessary to determine the thermoelectric properties of saturated solid solutions from the isotherms of the properties.

In the platinum-gold system the absolute thermal emf and the thermoelectric potential of a saturated solid solution of platinum

in gold can be determined from the minima on the isotherms of these properties (see Fig. 112 and 114). The thermoelectric properties of saturated solid solutions of gold in platinum is determined by comparison of the solubility curve on the diagram of states (see Fi.g 110) with the isotherm of the properties.

The values of the thermoelectric properties of saturated solid solutions in the platinum-gold system are shown in Table 54.

Table 54

Thermoelectric Properties of Saturated Solid Solutions
of Alloys of Platinum with Gold

t, °C	ε_β, micro-volts/°C	ε_α, micro-volts/°C	$\varepsilon_\beta - \varepsilon_\alpha$, micro-volts/°C	π_β, mv	π_α, mv	$\pi_\beta - \pi_\alpha$, mv
100	—15,6	—7,4	8,2	—5,8	—2,8	3,0
200	—20,2	—9,8	10,4	—9,6	—4,6	5,0
300	—23,5	—11,8	11,7	—13,5	—6,8	6,7
400	—27,0	—13,2	13,8	—18,2	—8,8	9,3
500	—30,2	—14,9	15,3	—23,3	—11,5	11,8
600	—32,8	—16,8	16,0	—28,6	—14,7	13,9
700	—36,4	—18,8	17,6	—35,4	—18,3	17,1
800	—40,5	—21,2	19,3	—43,5	—22,8	20,7
900	—45,7	—24,2	21,5	—53,6	—28,4	25,2
1000	—52,5	—27,8	24,7	—66,9	—35,4	31,5

The difference of the ordinates on each of the isotherms gives the difference of the absolute thermal emf or the difference of the entropies and the difference of potential between the phases that are in equilibrium. The following equations hold in this case

$$\pi_\alpha = T\varepsilon_\alpha, \quad \pi_\beta = T\varepsilon_\beta,$$
$$\pi_\beta - \pi_\alpha = T\left(\varepsilon_\beta - \varepsilon_\alpha\right).$$

This difference of potentials remains constant over the entire extent of the heterogeneous region, since each of the phases retains its composition and properties at constant temperature over the entire extent of the discontinuity in the solid solutions. The composition and properties of saturated solid solutions are functions of the temperature.

The temperature dependence of the absolute thermal emf for each of the phases and their differences are shown in Fig. 148. In the given particular case one observes in first approximation a linear temperature dependence of the absolute thermal emf:

$$\varepsilon_\alpha = aT, \quad \varepsilon_\beta = bT,$$
$$\varepsilon_\beta - \varepsilon_\alpha = (b - a)\, T.$$

For the thermoelectric potential we obtain second-degree equations (Fig. 149):

$$\pi_\alpha = aT^2, \quad \pi_\beta = bT^2,$$
$$\pi_\beta - \pi_\alpha = (b - a)\, T^2.$$

For the platinum-silver system one determines in this same manner the thermoelectric properties of saturated solid solutions from the isotherms of the properties (see Fi.g 122 and 124). The properties of saturated α- -solid solution of silver in platinum were determined from the maxima on the isotherms, while the properties of β- -solid solutions of platinum in silver were determined from the minima on the same curves.
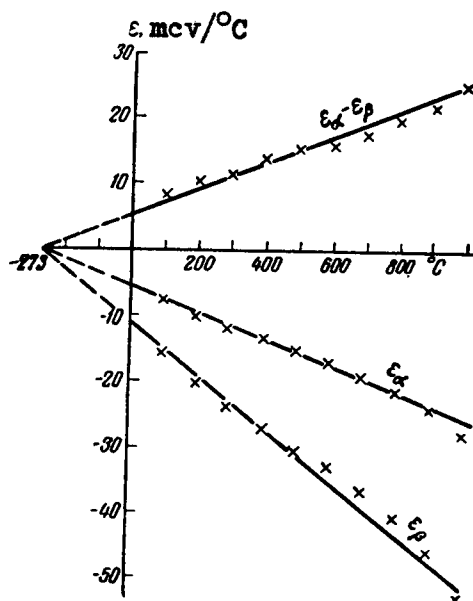

Fig. 148. Absolute Thermal emf of Saturated
Solid Solutions of the Platinum-Gold
System.

The values of the thermoelectric properties of saturated solid solutions of platinum-silver alloys are given in Table 55.

Figs. 150 and 151 show their temperature dependence. As can be seen from the curves of the absolute thermal emf, in this case one also observes a proportionality between the absolute thermal emf and the absolute temperature.
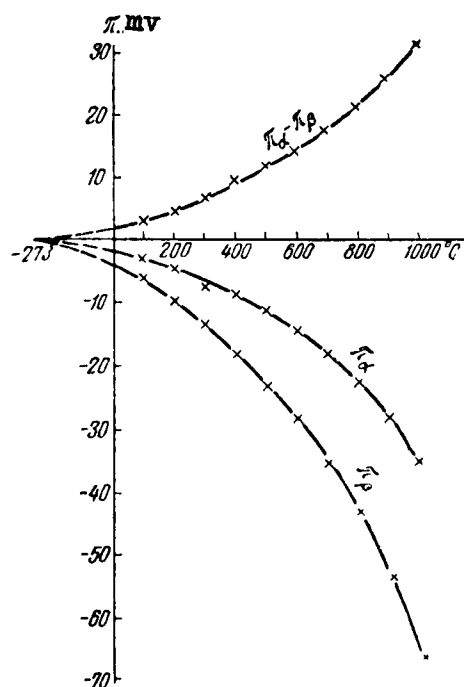

Fig. 149. Thermoelectric Potential of
Saturated Solid Solutions of the
Platinum-Gold System.

Thus, for the platinum-silver and platinum-gold systems, the absolute thermal emf of the saturated solid solutions change in proportion to the absolute temperature, while the thermoelectric potentials are proportional to the square of the absolute temperature.

The difference in the absolute thermal emf's of the phases that are in equilibrium will also change in proportion to the absolute temperature, while the difference in the electric potentials is proportional to the square of the absolute temperature.

It is obvious that such laws are applicable only to such solid solutions, that are far away from critical phenomena and have no tendency to form one solid solution at increased temperature.
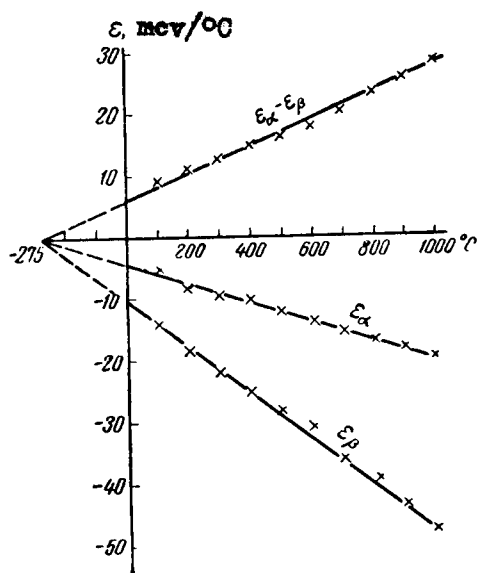
Fig. 150. Absolute Thermal emf of Saturated
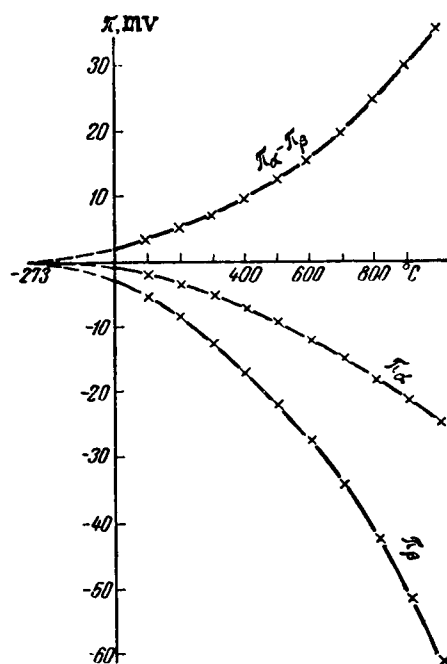Solid Solutions of a System Platinum-
Silver.

Fig. 151. Thermoelectric Potential of Satur-
ated Solid Solutions of the System
Platinum-Silver.

215

Table 55

Thermoelectric Properties of Saturated Solid Solutions
of Alloys of Platinum with Silver

t, °C	ε_β, micro-volts/°C	ε_α, micro-volts/°C	$\varepsilon_\beta-\varepsilon_\alpha$,	π_β, mv	π_α, mv	$\pi_\beta-\pi_\alpha$, mv
100	—14,2	—5,2	9,0	—5,3	— 1,9	3,4
200	—18,8	—8,0	10,8	—8,9	— 3,8	5,1
300	—22,2	—9,8	12,4	—12,7	— 5,6	7,1
400	—25,4	—10,6	14,8	—17,1	— 7,1	10,0
500	—28,4	—12,2	16,2	—21,9	— 9,4	12,5
600	—31,4	—14,0	17,4	—27,4	—12,2	15,2
700	—35,6	—15,6	20,0	—34,6	—15,2	19,4
800	—40,0	—17,0	23,0	—42,9	—18,3	24,6
900	—44,0	—18,6	25,4	—51,6	—21,8	29,8
1000	—47,8	—19,8	28,0	—61,0	—25,2	35,8

In fact, if both phases form one solid solution without reaching the melting temperature, as shown in Fig. 152, then the properties will be the same at the point of maximum C for both saturated solid solutions, and the potential difference will then be zero.

A similar situation arises in the system palladium-rhodium (see Fig. 133). The thermoelectric properties of the saturated β-solid solution were determined from the maxima on the isotherms (see Fig. 123 and 130), while those of the α-solid solution were determined from the minima.

The values of the thermoelectric properties of saturated solid solutions for alloys with palladium with rhodium are given in Table 56 and in Figs. 153 and 154.

As expected, we obtain in this case a more complicated dependence than in the cases of the platinum-gold and platinum-silver alloys. However, linear dependence is observed for the difference in the absolute thermal emf in the range from absolute zero to 200° C.
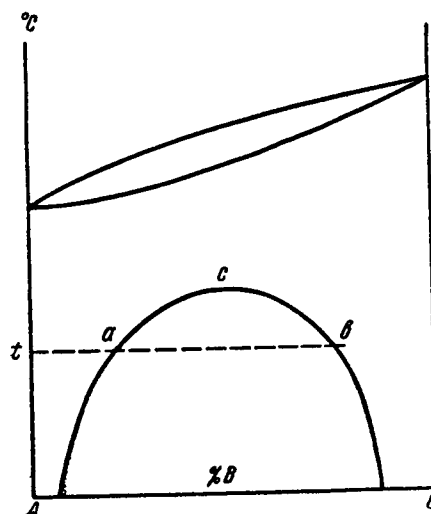
Fig. 152. Diagram of Phase Transitions with Decomposition of Solid Solutions.
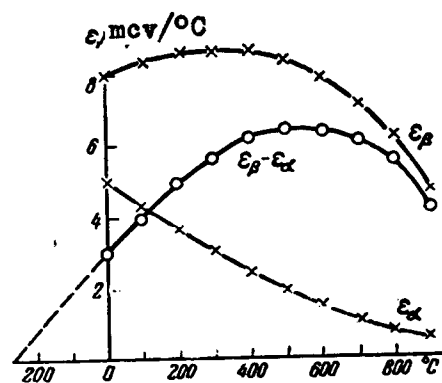

Fig. 153. Absolute Thermal emf of Saturated Solid Solutions of the Palladium-Rhodium System.
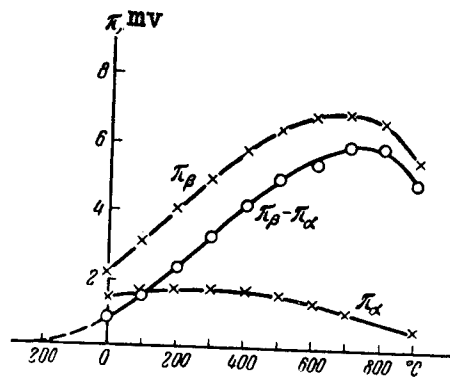
Fig. 154. Thermoelectric Potential of Saturated
Solid Solutions of the Palladium-
Rhodium System.

Table 56

Thermoelectric Properties of Saturated Solid Solutions
of Alloys of Palladium with Rhodium

t, °C	ε_β, micro-volts/°C	ε_α, micro-volts/°C	$\varepsilon_\beta-\varepsilon_\alpha$, micro-volts/°C	π_β, mv	π_α, mv	$\pi_\beta-\pi_\alpha$, mv
0	8,0	5,0	3,0	2,2	1,4	0,8
100	8,3	4,3	4,0	3,1	1,6	1,5
200	8,5	3,6	4,9	4,0	1,7	2,3
300	8,6	3,0	5,6	4,9	1,7	3,2
400	8,6	2,4	6,2	5,8	1,6	4,2
500	8,3	1,9	6,4	6,4	1,5	4,9
600	7,8	1,5	6,3	6,8	1,3	5,5
700	7,1	1,0	6,1	6,9	1,0	5,9
800	6,2	0,7	4,6	6,7	0,8	5,9
900	4,6	0,5	4,1	5,4	0,6	4,8

As the critical point is approached, the differences become
$\varepsilon_\beta - \varepsilon_\alpha \to 0$ and $\pi_\beta - \pi_\alpha \to 0$. They pass through a smooth maximum, and diminish rapidly.

CONCLUSION

The theoretical foundations of the present investigation are the Thomson-Nernst thermodynamic theory of thermoelectric phenomena, which establishes a connection between all the thermoelectric effects, and the Onsager theory, according to which the absolute thermal emf is the entropy while the Thomson effect is the specific heat of the moving current carriers. Thus, the thermoelectric effects are thermodynamic functions of the current carriers.

To investigate the thermoelectric effects we used different measurement methods: measurement of the integral thermal emf at constant points and comparison methods, measurement of the differential thermal emf with the aid of a potentiometer and the Kurnakov pyrometer.

The use of the Kurnakov pyrometer is in principle a new method for the investigation of thermoelectric phenomena. This method has advantages over other methods in its objectivity of reading. The continuous recording of a curve on photographic paper makes it possible to follow the process of variation of thermoelectric effect as a function of the temperature in its entirety, and simultaneously makes it possible to determine both the values of the thermal emf as well as the transformation temperatures.

In all the investigations the comparison electrode used was platinum with known thermoelectric properties. It was therefore possible to determine the absolute values of the thermoelectric quantities of the metals and alloys.

Using high-purity metals, we obtained the most reliable values of the absolute thermal emf for gold, silver, platinum, palladium, rhodium, and also for iron, cobalt, and nickel.

As a result of the use of the thermoelectric method for determination of the purity of platinum and palladium, it was possible to show that the thermal emf is quite sensitive to impurities that are not accessible to spectral analysis.

As a physico-chemical analysis method, the thermoelectric method is applicable to the following systems: gold-silver, platinum-palladium, palladium-gold, palladium-silver, platinum-gold, platinum-silver, palladium-rhodium, palladium-copper, and platinum-copper.

In the analysis of thermoelectric phenomena, we established for these systems the general laws of variation of the absolute thermal emf in binary systems. When fusing two metals that have the same signs of the thermal emf, one observes a reduction in the absolute value of the absolute thermal emf. If both components are thermoelectrically positive, the absolute thermal emf variation has a smooth minimum. If both components are thermoelectrically negative, the curve of the absolute thermal emf has a minimum.

When fusing metals that have absolute thermal emf's of different signs, the isotherms have deep minima (palladium-gold, palladium-silver, platinum-gold, palladium-copper), or else are sinusoidal curves (platinum-copper, platinum-silver).

In all cases, when any component is added to a thermoelectrically positive metal, a reduction is observed in the value of the absolute thermal emf. The hole conductivity of the pure metal is replaced by the electronic conductivity of the solid solution.

We have observed in our investigations an unlimited solubility over the entire extent of the diagram of state only for metals that have the same signs of absolute thermal emf. This premise is not a general law, for there are many exceptions.

In systems consisting of components with different signs of the absolute thermal emf, one can expect either a discontinuity in the solid solutions or the formation of intermediate phases.

An investigation of the Thomson emf of the palladium-silver and palladium-gold systems makes it possible to establish a discontinuity in the solid solutions in these diagrams over a narrow interval of compositions (near 40-60 atomic percent palladium). This is also confirmed by the character of the variation of the temperature coefficient of electric resistivity with a variation of composition.

An investigation of the thermoelectric properties of alloys of palladium with rhodium has made it possible to fix the region of limited solubility in this system.

The thermoelectric method jointly with other methods made it

possible to find new chemical compounds: Pd_3Cu_5, $PdCu_5$, and $PdCu_5$, and has also confirmed the existence of a PtCu compound.

On the basis of a detailed analysis of thermoelectric properties of the PtCu compounds it was shown that the ordering process in its crystalline lattice is a second-order transition.

The chemical compounds PdCu, $PdCu_3$, and $PtCu_3$, established by the earlier authors, were not confirmed by our experiments.

The isotherms of the absolute thermal emf have singular maximum points, corresponding to chemical compounds Pd_3Cu_5 and $PdCu_5$, and a minimum singular point for PtCu.

The chemical compound $PtCu_5$ corresponds to a kink on the absolute thermal emf isotherm.

An investigation of the thermoelectric properties of alloys over a wide range of temperatures had made it possible to determine the regions of existence of phases based on these compounds.

The method developed for the investigation of the thermoelectric properties with the aid of a pyrometer of N.S. Kurnakov has given exceedingly fruitful results in the investigation of transformations in alloys and metals.

It was established that first-order transformations come in two types.

1. Transformations accompanied by jump-like increase in the absolute thermal emf (entropy of the current carriers) and enthalpy of the current carriers. In this case the Thomson emf assumes a value of $+ \infty$ (γ-iron $\longrightarrow$ δ-iron, α-cobalt $\longrightarrow$ β-cobalt).

2. Transformations accompanied by a jump-like reduction in the absolute thermal emf and current-carrier enthalpy. Here the Thomson emf assumes a value of $- \infty$ (β-iron $\longrightarrow$ γ-iron, α-rhodium $\longrightarrow$ β-rhodium, disordering of the crystal lattice of chemical compounds Pd_3Cu_5, $PdCu_5$, and $PtCu_5$).

In first-order transitions the change in the enthalpy of the current carriers equals the change in the thermoelectric potential:

$$\Delta H = \Delta \pi.$$

In second-order transitions the thermoelectric properties change like the thermodynamic functions of the metal with the temperature.

The $\alpha\text{-}Fe \rightarrow \beta\text{-}Fe$ transformations, the losses in magnetic properties of cobalt and nickel, and the disordering of the crystal lattice of the chemical compound PtCu, being second-order transitions, are accompanied by an increase in the Thomson emf to a maximum and by a jump-like decrease at the Curie point.

Thus, the same change with temperature occurs in the Thomson emf as in the specific heat of the metal.

In the case of limited solubility of compounds in the solid state (in the palladium-rhodium system) one observes the same phenomena. In the transition from the heterogeneous mixture of the two phases to the homogeneous solid solution, the Thomson emf drops to a minimum and increases jump-like at the critical point. In this case we have an effect that has a sign opposite that of the specific heat.

An investigation of the **thermoelectric potential makes it possible** to determine the difference in the electric potentials between phases in equilibrium.

In first-order transitions the difference in electric potentials between phases in equilibrium is determined by the value of the jump in the thermoelectric potential at the point of transition and represents the Peltier emf, which arises upon contact between the two phases. This difference of potentials retains its value as long as the two phases exist in equilibrium.

The difference in electric potentials between phases in equilibrium is determined, in a binary diagram of state and in the case of limited solubility of components, from the isotherms of the thermoelectric potential.

It has been shown empirically that in particular cases of alloys of platinum with gold and with platinum with silver the thermoelectric potentials of saturated solid solutions change in proportion to the square of the absolute temperature:

$$\pi_\alpha = aT^2, \quad \pi_\beta = bT^2,$$
$$\pi_\beta - \pi_\alpha = (b - a)\, T^2,$$

where a and b are constants.

The absolute thermal emf's of saturated solid solutions change in proportion to the absolute temperature:

$$\varepsilon_\alpha = aT, \quad \varepsilon_\beta = bT,$$
$$\varepsilon_\beta - \varepsilon_\alpha = (b - a)\, T.$$

In the palladium-rhodium system this dependence is violated, since one observes with increasing temperature a change from a heterogeneous mixture of two phases to a homogeneous solid solution. Obviously, at the critical point the properties of both phases are the same and the difference of potentials is zero.

The difference in electric potentials between phases in equilibrium creates an additional factor that influences the equilibrium of the phases.

BIBLIOGRAPHY

1. K. M. Polivanov, Fizicheskiye osnovy elektrotekhniki /Physical Fundamentals of Electrical Engineering/ Moscow, Energoizdat, 1950, 159.

2. A. Seebeck. Cilb. Ann., 73 (1823), 115, 430.

3. J. C. Peltier. Ann. Chim. Physique, 56 (1834), 371.

4. W. Thomson. Phil. Trans., 3 (1856), 661.

5. E. Becquerel. Ann. Chim. Phys., 23 (1823), 135.

6. A. Magnus. Pogg. Ann., 83 (1851), 469; Ann. Chim. Phys., 34 (1855), 105.

7. C. Benedicks. Ann. Phys., 55 (1918), 1, 103.

8. M. Avenarius. O termoelektrichestve /On Thermoelectricity/ St. Petersburg (1864); Pogg. Ann. 119 (1863), 406; 122, (1864), 193; 149 (1873), 372.

9. P. G. Tait. Pogg. Ann., 152 (1874), 427.

10. P. Bakhmet'yev, ZhRFKho /Jl. of Russ. Phys. Chem. Soc./ 21 (1889), 264.

11. ___, ibid. 23 (1891), 220, 301, 430.

12. ___, ibid. 18 (1885), 47; 25 (1893), 256.

13. Lord Kelvin. Papers Cambridge, 1 (1882), 316.

14. L. Boltzmann. Ber. Wiener, Akad., 96 (1887), 1258.

15. A. E. Gurevich. Osnovy fizicheskoy kinetiki /Fundamentals of Physical Kinetics/ Gostekhizdat, 1840.

16. C. R. De Groot. Thermodynamics of irreversible processes. Amsterdam, 1951.

17. Onsager. Phys. Rev., 37 (1931), 405; 38 (1931), 2265.

18. G. Borelius. Physica, 19 (1953), 807.

19. W. Nernst, Theor. Chem., 1913. ___ Theoretical and Exper-
    imental Basis of a New Law of Heat (Russ. Transl.)
    GIZ, M-L, 1929.

20. W. H. Keesom. Comm. physic. Lab., Univ. Leiden., Suppl.,
    306 (1913), 1.

21. E. Lange u. T. Hesse. Z. Elektrochem., 38 (1933), 374.

22. W. Latimer. J. Amer. Chem. Soc., 44 (1922), 2136.

23. M. I. Temkin and A. V. Khoroshin, ZhFKh /Jl. of Phys.
    Chem./ 26 (1952) No 4, 500; No 6, 773.

24. A. Eastman. J. Amer. Chem. Soc., 48 (1926), 1482.

25. H. A. Lorentz. Proc. Acad. Amsterdam, 7 (1905), 438, 585,
    684.

26. A. Sommerfeld u. H. Bethe, Elektronentheorie der Metalle,
    Berlin, 1933; Russian translation, GONTI, 1938.

27. A. Wilson. Quantum Theory of Metals, Russian Transl. OGIZ,
    1941.

28. R. Peierls, Elektronentheorie der Metalle, Naturwissen-
    chaft, 11 (1932), 264. Russian Transl. GIIL, 1947.

29. N. F. Mott a. Jones. The Theory of the Properties of
    Metals and Alloys. Oxford, 1936

30. W. Meisner. Handbuch der Experimentalphys., 9 (1935), 1.

31. L. Gurevich, ZhETF /Jl. Experim. and Theoret. Phys./ 16
    (1946), 193.

32. F. G. Serova, ZhETF, 19 (1949), 460.

33. M. A. L'vov. Pribory dlya izmereniya temperatur v metal-
    lurgii /Instruments for the Measurement of Tempera-
    tures in Metallurgy/ (OST 40114). GONTI, 1944.

34. O. Feussner. Elektrotechn. Z., 48 (1927), 535.

35. G. P. Kul'bush. Elektricheskiye pirometry /Electrical
    pyrometers/ ONTI, 1932.

36. A. G. Metcalfe. Brit. J. Appl. Phys., 1 (1950), 256.

37. T. Land. Privat comm. E. J. Burton a. G. J. Weeks. J. Inst. Fuel, 26, No 154 (1953), 260; Arch. Techn. Mess., 205 (1953), 50.

38. W. Goedecke. Festschr. zum 50-jahr. Bestehen der Platin-schmelze, G. Siebert Hanau, 1931, 72.

39. F. Hoffmann. Ber. Ver. Feuerfest. Prod., 29 (1909), 45.

40. O. Feussner. Z. tech. Physik, 54 (1933), 155.

41. A. Schulze. Chemiker Ztg., 62 (1938), 308; J. Inst. of Fuel, 12 (1939), 541.

42. S. Morugina. Z. Techn. Physik, 7 (1927), 487.

43. J. P. Simons, E. J. Burton a. C. G. Hamstead. J. Iron a. Steel Inst., 175 (1953), 402.

44. F. Morgan a. W. Danforth. J. appl. Phys., 21 (1950), 112.

45. M. Pirani a. G. W. Wangenheim. Z techn. Physik, 6 (1925), 358.

46. W. C. Troy a. G. Stevens. Trans. Amer. Soc. Metals, 42 (1950), 1131.

47. R. D. Potter a. N. J. Grant. Iron Age, 31st March, 163 (1943), 65.

48. G. Borelius. Entsiklopediya metallofiziki /Encyclopedia of Metal Physics/ GONTI, 1937, 349.

49. A. F. Ioffe, Electronic Current Conductors. Jubilee Collection dedicated to the 30th anniversary of the Great October Socialist Revolution. Acad. Sci. USSR, 1947, 305.

50. E. P. Le Roux. Ann. Chim. Physique, 10 (1867), 201, 257.

51. O. Berg. Ann. Physik, 32 (1910), 477.

52. R. Nettleton. Proc. Phys. Soc., 34 (1922), 77.

53. J. Young. Proc. Phys. Soc., 37 (1925), 145.

54. H. E. Smith. Proc. Phys. Soc., 38 (1925), 1.

55. G. Borelius. Ann. Phys., 63 (1920), 845.

56. G. Borelius. F. Gunnesson. Ann. Physik, 65, (1921), 520.

57. G. Borelius. W. H. Keesom, C. H. Johansson. Comm. Phys. Lab. Univ. Leiden, 196a (1928), 1.

58. J. J. Lander. Physic. Rev., 74 (1948), 479.

59. J. Nystrom. Ark. Mat. Astr. Fysik, 34-A (1948), 1.

60. E. Edlund. Pogg. Ann., 140 (1870), 435.

61. G. Borelius. Ann. Phys., 52 (1917), 398.

62. G. Borelius. Ann. Phys., 56 (1918), 388.

63. G. K. Burgess, H. Scott. Bull. Bur. Stand., 14 (1918), 15.

64. C. C. Bidwell. Phys. Rev., 23 (1924), 357.

65. A. Durer. Z. Metallkunde, 30 (1939), 306.

66. W. F. Roser, H. F. Wensel. J. Research, 14 (1935), 247.

67. L. Holborn. Ann. Phys., 59 (1919), 145.

68. A. A. Rudnitskiy, Izv. Sektora platiny /Bull. of the Platinum Sector/ 27 (1952), 227.

69. A. A. Rudnitskiy, R. S. Polyakova, and I. I. Tyurin. Izv. Sektora platiny, 29 (1955), 184.

70. A. Mattiessen. Pogg. Ann., 103 (1858), 412.

71. W. Rohn. Z. Metallkunde, 16 (1924), 297.

72. H. Pelabon. Ann. Chim. Phys., 13 (1920), 169.

73. L. Holburn u. A. Day. Sitzungsber. Akad. Berlin (1899), 691.

74. L. Holburn u. A. Day. Ann. Phys., 2 (1900), 505.

75. F. M. Jaeger a. E. Rosenbohm. Proc. Acad. Amsterdam, 34 (1931), 808.

76. A. Goetz. Phys. Z., 25 (1924), 562.

77. G. Borelius, W. H. Keesom, C. H. Johansson, J. O. Linde. Comm. Phys. Lab. Univ., Leiden, 206-a (1930), 1; 217-d (1932), 1; 217-e (1932), 1; Supplement 70-A (1932), 1.

78. L. Landay and E. Lifshits. Statisticheskaya fizika /Statistical Physics/, Gostekhizdat 1951, 428.

79. V. K. Semenchenko, ZhFKh 26 (1952), 1337.

80. Ya. G. Dorfman, R. I. Yanus, K. V. Grigorov, and M. G. Chernikovskiy. ZhETF, 1, (1931), 155.

81. A. Schulze. Z. Metallkunde, 22 (1930), 308.

82. Ya. G. Dorfman and R. I. Yanus. ZhRFKhO, 60 (1928), 519.

83. Ya. G. Dorfman and I. K. Kikoin, ibid. 61 (1929), 159.

84. K. E. Grew. Phys. Rev., 41 (1932), 356.

85. A. W. Foster. Phil. Mag., 18 (1934), 470.

86. Cited from P. O. Obergoffer /Oberhoffer7, Tekhnicheskoye zheleze /Technical Iron/ GONTI, 1940.

87. A. A. Rudnitskiy, L. A. Pnteleymonov, V. V. Pimenova, and M. Ye. Berezkina, Vestnik MGU /Bull. Moscow State Univ./ No 3 (1952), 51.

88. A. A. Rudnitskiy, Izv. Sektora platiny, 27 (1952), 195.

89. N. A. Brilliantov, V. I. Lin'kov, P. G. Strekkov. Trudy Mos. Gos. in-ta mer i izmeritel'nikh priborov /Trans-Moscow State Inst. of Measures and Measuring Instruments/ 3 (1950), 3.

90. S. F. Zhemchuzhnyy, Materialy dlya izucheniya yestestven-nykh proizvoditel'nykh sil Rossii /Materials on the Study of the Natural Productive Forces of Russi/ 13 (1916), 1.

91. A. T. Grigor'yev, Izv. In-ta Platiny /News of the Platinum Inst./ 6 (1928), 178.

92. N. S. Kurnakov and N. I. Podkopayev, ibid. 7 (1929), 330.

93. V. A. Nemilov and A. T. Grigor'yev, ibid. 9 (1932), 113.

94. I. I. Chernyayev and A. M. Rubinshteyn, DAN SSSR (Trans. Acad. Sci. USSR) 8 (1945), 353.

95. R. J. Corruccini. J. Research, 47 (1951), 94.

96. V. A. Nemilov and A. A. Rudnitskiy. Izv. Sektora platiny 27 (1952), 187.

97. V. A. Nemilov, A. A. Rudnitskiy, and T. A. Vidusova, Izv. Sektora platiny 20 (1946), 225.

98. G. Grube u. R. Knabe. Z. Elektrochem., 42 (1936), 793.

99. G. Grube u. H. Kastner. Z. Elektrochem., 42 (1936), 156.

100. J. G. G. Connybear. Proc. Roy. Soc., 49 (1937), 29.

101. F. H. Schofield. Proc. Roy. Soc., 155 (1936), 301.

102. L. Holborn. Ann. Phys., 59 (1919), 145.

103. C. E. Mendehall a. L. R. Ingersoll. Phil. Mag., 15 (1908), 205.

104. E. T. Dixon. Phys. Rev., 38 (1931), 6.

105. F. M. Jeagera. J. E. Zanstra. Proc. Akad. Amsterdam, 34 (1931), 15.

106. E. T. Booth a. E. H. Dixon. Rev. Scient. Instr., 8 (1937), 381.

107. H. F. Wensel a. L. B. Tuckermann. Rev. Scient. Instr., 9 (1938), 237.

108. N. N. Tuturin. Prilozheniye termoelektricheskikh yavleniy k analizu metallicheskikh sistem splavov /Application of Thermoelectric Phenomena to the Analysis of Metallic Alloy Systems/ St. Petersburg 1909.

109. E. Rudolphi Z. anorg. Chem., 67 (1910), 65.

110. W. Haken. Ann. Phys., 32 (1910), 291.

111. M. W. Broniewski. Rev. Met., 7 (1910), 341.

112. W. Geibel. Z. anorg. Chem., 69 (1911), 38; 70 (1911), 240.

113. E. Sedstrom. Einige physikalische Eigenschaften metallischer Mischkristalle, Diss., Stockholm, 1924.

114. A. L. Norbury. Phil. Mag., 2 (1926), 1188.

115. V. A. Nemilov and N. M. Voronov. Izv. In-ta platiny 12 (1935), 27.

116. V. A. Nemilov, T. A. Vidusova, A. A. Rudnitskiy, and M. M. Putsykina, Izv. Sektora platiny 20 (1946), 176.

117. N. M. Voronov, ibid. 13 (1936), 145.

118. V. A. Nemilov and A. A. Rudnitskiy. Izv. AN SSSR /Bull. Acad. Sci. USSR/ seriya khim /Chemistry Series/ 1 (1937), 35.

119. V. A. Nemilov and A. A. Rudnitskiy. Izv. Sektora fiziko-khim. analiza /Bull. of the Sector of Physico-Chemical Analysis/ 14 (1941), 263.

120. ___ Izv. Sektora platiny, 21 (1948), 234.

121. ___ Ibid. 21 (1948), 239.

122. A. A. Rudnitskiy and R. S. Polyakova, ibid. <u>27</u> (1952), 223.

123. V. A. Nemilov, A. A. Rudnitskiy, and R. S. Polykova, ibid. <u>23</u> (1949), 102.

124. ___ ibid. <u>25</u> (1950), 138.

125. T. A. Vidusova, ibid. <u>28</u> (1954), 251.

126. V. A. Nemilov, A. A. Rudnitskiy, and R. S. Polyakova, ibid. <u>26</u> (1951), 16.

127. Ye. D. Devyatkova, Yu. P. Paslakovets, and L. S. Stil'-bans, ZhTF /Jl. Techn. Phys./ <u>22</u> (1952), 129.

128. E. Janecke. Metallurgie, 8 (1911), 599.

129. U. Raydt. Z anorg. Chem., 75 (1912), 58.

130. M. Khansen /Hansen/, Structura binarnykh splavov /Structure of Binary Alloys/. GONTI, Moscow, <u>1</u> (1941), 19.

131. E. Sedstrom. Ann. Phys., 59 (1919), 137.

132. W. Broniewsky, K. Weselowsky. C. R., 194 (1932), 2047.

133. Y. Schimizu. Sci. Rep. Tohoku Univ., 21 (1932), 829.

134. A. Olender. J. Am. Chem. Soc., 53 (1931), 3577.

135. L. W. Mc Keehan. Phys. Rev., 20 (1922), 424.

136. H. Weiss. Proc. Roy. Soc., 108 (1925), 652.

137. H. Yung. Z. Kristallographie, 64 (1926), 425.

138. S. Holgersson. Ann. Phys., 79 (1920), 42.

139. G. Sacksu. J. Weerts. Z. Physik, 60 (1930), 481.

140. V. G. Kuznetsov, Izv. Sektora platiny 20 (1946), 5.

141. G. Phragman. Fysick. Tidskr., 24 (1926), 40.

142. N. Norman a. B. E. Warren. J. Appl. Physics, 22 (1951), 483.

143. M. Khansen /Hansen/ Struktura binarnykh splavov, GONTI, M., 2 (1941), 964.

144. F. A. Schulze. Phys. Z., 12 (1911), 1028.

145. J. A. M. van Liempt. Rec. Trav. Chim. Pays-Bas, 45 (1926), 203.

146. G. Tamman u. H. J. Rocha. Festschr. zum 50-jahr. Bestehen der Platinschmelze. G. Siebert, Hanau, (1931), 309.

147. E. Vogt. Ann. Phys., 14 (1932), 1.

148. R. Ruer. Z. anorg. Chem., 51 (1906), 391.

149. W. Frenkel u. A. Stern. Z. anorg. Chem., 166 (1929), 164.

150. M. Khansen /Hansen/ Struktura binarnykh splavov. GONTI, M. 1 (1941), 247, 57.

151. S. Holgersson u. E. Sedstrom. Ann. Phys., 75 (1924), 143.

152. W. Stenzel u. J. Weerts. Festschr. zum 50-jahr. Bestehen d. Platinschmelze, G. Siebert, Hanau, 1931, 288.

153. G. Borelius. Ann. Phys., 53 (1917), 615.

154. J. Schniedermann. Ann. Phys., 13 (1932), 761.

155. R. Ruer. Z. anorg Chem., 51 (1906), 315.

156. Ye. Ya. Rode, Izv. Sektora platiny 13 (1936), 167.

157. L. W. Mc Keehan. Phys. Rev., 20 (1922), 424.

158. F. Krugeru. A. Sacklowski. Ann. Phys., 78 (1925), 72.

159. T. Erhard u. Schartel. Jahrbuch fur d. Berg- und Hutten-wesen in Sachsen, 17 (1879), 163.

160. F. Doerinckel. Z. anorg. Chem., 54 (1907), 333.

161. A. T. Grigor'yev. Izv. In-ta platiny 6 (1928), 184.

162. C. H. Johanssonu. J. O. Linde. Ann. Phys., 5 (1930), 762.

163. L. Nowack. Z. Metallkunde, 22 (1930), 97.

164. W. Stenzelu.J. Weerts. Festschr. zum 50-jahr. Bestehen d. Platinschmelze, G. Siebert, Hanau, 1931, 300.

165. C. G. Wictorin. Ann. Phys., 33 (1938), 509.

166. N. V. Ageev   Izv. AN SSSR, /Bull. Acad. Sci. USSR/ seriya khim. No 3(1940), 397.

167. G. Grube, A. Schneider u. U. Esch. Hereaus Festschrift, (1951), 20.

168. A. S. Darling, R. A. Miterna. J. C. Chaston. J. Inst. Met., 81 (1952), 125.

169. N. S. Kurnakov and V. A. Nemilov. Izv. In-ta platiny 4 (1926), 306.

170. C. H. Johansson u. J. O. Linde. Ann. Phys., 6 (1930), 4.

171. A. Schneider u. U. Esch. Z. Elektrochem., 49 (1943), 72.

172. A. A. Rudnitskiy, R. S. Polyakova, and I. I. Tyurin, Izv. Sektora platiny 29 (1955), 190.

173. V. A. Nemilov, A. A. Rudnitskiy, and R. S. Polyakova, Izv. Sektora platiny 25 (1950), 138.

174. E. A. Owena. J. J. Jones. Proc. Phys. Soc., 49 (1937), 587.

175. C. H. Johansson. Ann. Phys., 76 (1925), 445.

176. C. H. Johanssonu. J. O. Linde, Ann. Phys., 78 (1925), 439.

177. C. H. Johanssonu. J. O. Linde, Ann. Phys., 82 (1927), 449.

178. G. Borelius, C. H. Johanssonu. J. O. Linde. Ann. Phys., 86 (1928), 291.

179. J. O. Linde. Ann. Phys., 15 (1932), 249.

180. B. Svensson. Ann. Phys., 14 (1932), 699.

181. H. J. Seemann. Z. Metallkunde, 24 (1932), 299.

182. H. J. Seemann. Z. Phys., 84 (1933), 557; 88 (1934), 14.

183. R. Taylor. J. Inst. Met., 53 (1934), 255.

184. P. S. Belonogov, Metallurg /Metallurgist7 92 (1936).

185. F. W. Jones a. C. S. Sykes. J. Inst. Met., 65 (1939), 419.

186. W. Koster. Z. Metallkunde, 32 (1940), 145.

187. S. Sidorov, ZhETF, 16 (1946), 629 and 503.

188. V. A. Nemilov, A. A. Rudnitskiy, and R. S. Polyakova, Izv. Sektora platiny, 24 (1949), 26.

189. N. S. Kurnakov and V. A. Nemilov, Izv. In-ta platiny 8, (1931), 5.

190. J. O. Linde. Ann. Phys., 30 (1937), 151.

191. F. Weibke u. H. Matthes. Z. Elektrochem., 47 (1941), 421.

192. A. Schneideru. U. Esch. Z. Elektrochem., 50 (1944), 290.

193. N. S. Kurnakov, Vvedeniye v fiziko-chemicheskiy analiz
      /Introduction to Physico-Chemical Analysis/ Acad.
      Sci. USSR Press, 1940. ZhRFKhO, 50 (1918), 157.

194. B. Hume-Rothery, Structure of Metals and Alloys (Russ.
      Transl.) M., 1938.

195. I. I. Kornilov, DAN SSSR 73 (1950), 495.